MOLECULAR DIAGNOSTIC REPORTING OF HEPATITIS C INFECTION BY DATA ANALYSIS, TEST VALIDATION, QUALITY CONTROL AND CLINICAL STATE OF THE PATIENT

Thesis submitted to

UNIVERSITY OF CALICUT

Malappuram, Kerala, India.

For the degree of

Doctor of Philosophy in Biochemistry

(Faculty of Science)

BY

ANN MARY JOSEPH

Under the Guidance of

DR. JOSE JACOB, M.D.

AMALA CANCER RESEARCH CENTRE

Thrissur - 680 555,
Kerala, India

JUNE 2022

DECLARATION

I hereby declare that the thesis entitled 'MOLECULAR DIAGNOSTIC REPORTING OF HEPATITIS C INFECTION BY DATA ANALYSIS, TEST VALIDATION, QUALITY CONTROL AND CLINICAL STATE OF THE PATIENT' is based on the original research carried out by me at Amala Cancer Research Centre, Thrissur, Kerala under the guidance of Dr. Jose Jacob, M.D, Professor, Department of Biochemistry, Amala Cancer Research Centre, Thrissur, Kerala and no part thereof has been presented for the award of any other degree, diploma or other similar titles.

Place: Amala Nagar

Date: 27-06-2022 Ann Mary Joseph

ACKNOWLEDGEMENT

Thank God, you are my rock. My wish getting accomplished with the support of many people whom you arranged. No credit to be taken for myself. I wish to express my sincere gratitude to everyone who supported and encouraged me during these years.

My heartfelt gratitude to my Guide **Dr. Jose Jacob, M.D,** Professor, Dept. of Biochemistry, Amala Cancer Research Centre who provided me with his wisdom, compassion and encouragement at all times of need throughout this journey. Thank you for introducing me into this field.

I express my deep sense of gratitude to our Research Director, **Dr. V. Ramankutty** and to our former Research Director **Dr. Ramadasan Kuttan**, Amala Cancer Research Centre for providing me a platform to do my Ph.D here and for providing me all the facilities at the centre.

I express my heartfelt thanks to Director **Rev. Fr. Julious Arakkal** CMI, Amala Institute of Medical Sciences and Amala Cancer Research Centre for permitting me to carry out the work here.

I convey my sincere gratitude to Dr. Sindu P.C, M.D, Professor, Department of Biochemistry Amala Institute of Medical Sciences. I am highly indebted to my colleagues **Dr. Krishna K Yathi** who was instrumental in helping me reach this lab, grow and Dr. Nesheera K K for all the support and guidance.

I express my honest thankfulness to Dr. KK Janardhanan Dr. TD Babu, Dr. Achuthan CR, Dr. Suraj K, Dr. Manu Aryan, Professors, Department of Biochemistry, Amala Cancer Research Centre for their timely help.

I remember with gratitude and respect all my teachers and mentors throughout my studies especially Dr. Maitreyi S Rajala and Dr. Pradeep Kumar G for providing me with early career research experience.

I share my happiness with my lab members Ms. Hasnamol P T, Ms. Shaima Rashid and Ms. Sindhu P Vinod for your friendship and support.

I am grateful to all my colleagues at Clinical Biochemistry Lab, Amala Institute of Medical Sciences for all the help and support.

I am thankful to Mrs. Sunitha, and Mrs. Preetha C G, Ms. Sruthi PK and Mr. Pareeth CM and all students of Amala Cancer Research Centre for all the help and support provided, especially at times research meetings.

My family, the biggest support at all times and I am grateful for the never-ending love and support, K T Joseph, Molly Joseph, K T Baby, Mallika Baby and my siblings Sherin, Kishore, Bilson and Dr. Billcy. **Dr. Libison KB** who kept me going, tried to empower me to become a better humane and our children **Lian, Liam** and **Teresa** for the happy and tough times together.

Ann Mary Joseph

CONTENTS

LIST OF TABLES

LIST OF FIGURES

ABBREVIATIONS

aa	Amino acids
ALP	Alkaline Phosphatase
ALT	Alanine Amino Transferase
Anti-HCV	antibodies to hepatitis C Virus
AST	Aspartate aminotransferase
BLAST	Basic Local Alignment Search Tool
BLASTn	Nucleotide BLAST
BLASTp	Standard Protein BLAST
bp	Base Pair
C	Core
CDC	Centres for Disease Control and Prevention
CDC	Centres for Disease Control and Prevention
cDNA	complementary DNA
CHC	Chronic Hepatitis C
CI	confidence interval
CI	confidence interval
CIA	Chemiluminescence Immuno Assay
CLIA	Chemi Luminescent Immuno Assay
Cq	Quantification Cycle
Ct	Threshold cycle
CV	coefficient of variation
DAAs	Direct Acting Antivirals
E	Envelope
EB	Ethidium Bromide
EIA	Enhanced Immuno Assay
EIA	Enzyme Immuno Assay
EQA	External quality assessment
FAM	Flourescein Amidites/ 6-carboxyfluorescein
FASTA	Fast All
GT	Genotype
HBsAg	Hepatitis B Surface Antigen
HBV	Hepatitis B Virus
HCC	Hepatocellular Carcinoma

HCV	Hepatitis C Virus
HD	hemodilaysis
IC	Internal Control
IFN	interferon
IRES	Internal Ribosome Entry Site
ISs	International Standards
IU	International Units
IVDs	in vitro diagnostic devices
K-S	Kolmogorov – Smirnova
NAFLD	Non-Alcoholic Fatty Liver Disease
NANBH	Non A Non B Hepatitis
NCBI	National Centre for Biotechnology Information
NCR	Non Coding Region
NS	Non Structural
NS3/NS4A	non-structural protein 3/non-structural protein 4A
NS5B	non-structural protein 5B
nt	Nucleotide
NTR	Non Translated Region
ORF	Open Reading Frame
PBMCs	Peripheral-Blood Mononuclear Cells
PT	Proficiency Testing
PWID	people who inject drugs
QC	Quality Control
QCMD	Quality Control for Molecular Diagnostics
Q-Q-Plot	Quantile – Quantile plot
RBV	Ribavirin
RdRp	RNA Dependent RNA Polymerase
RLS	Resource Limited Setting
RNA	Ribo Nucleic Acid
ROX	6-carboxy-X rhodamine
RT PCR	Reverse Transcription Polymerase Chain Reaction
RT-qPCR	Reverse transcription quantitative Real Time PCR
S/CO	Signal-to-Cut Off
SD	Standard Deviation

SE	Standard Error
SVR	Sustained Viral Response
SVR12	sustained virological response at 12 weeks post-treatment
S-W	Shapiro – Wilk
TAMRA	6-carboxytetramethylrhodamine
UTR	Un Translated Region
WHO	World Health Organization

CHAPTER 1

GENERAL INTRODUCTION AND OVERVIEW

1.1. General Abstract

As most patients with hepatitis C virus (HCV) infection have no symptoms, diagnosis of HCV infection was done by screening for anti-HCV antibody, followed by confirmation of diagnosis by HCV RT-PCR of RNA isolated from plasma.

The plasma viral load in HCV infection was often very low in a large number of patients, leading to problems related to validation of qualitative RT-PCR, its sensitivity and the differentiation from quantitative RT-PCR. These issues were solved by developing decision criteria for performance and for validation of qualitative and quantitative RT-PCR.

Internal control (IC), made up of the reference gene PCR amplification system with fixed concentration of template and fluorescent probe, and present in the assay matrix of all HCV RT-PCR assay systems, was evaluated for detection of the preanalytical and analytical influences on the amplification systems.

The low viral load also led to increased preanalytical influences and decreased HCV RT-PCR performance. As these influences affected the quality of data generated by RT-PCR, criteria were developed to study the different aspects of preanalytical influences such as four parameter data analysis of RT-PCR amplification plots (using SigmaStat software), exponential amplification immediately above threshold (using LinRegPCR software) and preanalytical influence on calibrators. The most important preanalytical influence were due to tissue damaging condition and various drugs used in the patient. Tissue damaging conditions could increase nonspecific RNA isolated along with HCV RNA.

The antibody levels were also found to increase with viral load. The distribution pattern of anti-HCV antibody was found to be bimodal in both RT-PCR positive and RT-PCR negative samples. Antibody reactive RT-PCR negative samples may be considered as occult infection or due to antiviral treatment.

Sequence data analysis were performed in the PCR products by comparing with established reference sequences and reference sequences of

various HCV genotypes in the NCBI database. The 5'UTR region was found to be the most conserved region with a percent identity of sequence at around 96 – 100%. This region was used for diagnostic purpose. The Core E1 region was less conserved with a percent identity of 87 – 95%. A moderate number of RT-PCR done with Core E1 primers gave negative results with no PCR products. Even though the percent identity was high at 95% for NS5B, it was difficult to find a conserved stretch of sequence which led to difficulties in designing primers for consistent PCR performance.

The most common genotypes identified were genotype 1 and 3, and specific sequence data analysis was done for the 5'UTR region to differentiate the genotypes. The presence three conserved regions in 5'UTR region signifies the functional importance of the region, and required the secondary RNA structure and its entropy plot to be constructed.

As Core E1 and NS5B regions were translated regions the possible antigenic epitopes were analysed by the B-cell epitope prediction and Kolaskar and Tongaonkar antigenicity prediction methods.

Phylogenetic trees were constructed with the database of all the seven genotypes from the NCBI site, and analysed along with genotypes 1, 3 and 4 identified in our study. The three genotypes identified by us clustered with the respective reference sequence in the leaf and branches of the phylogenetic tree.

1.2. General Introduction

Large number of patients with hepatitis C virus (HCV) infection have no symptoms (Orland et al, 2001). Diagnosis of HCV infection was done by screening for anti-HCV antibody for selecting the patients with reactive levels of antibody (Ritcher et al, 2002), followed by confirmation of diagnosis by HCV RT-PCR of RNA isolated from plasma of the antibody reactive patients (Bukh et al, 1992; Barbara et al, 2009). The plasma viral load in HCV infection was often very low in a large number of patients (Glynn et al, 2005; Fytili et al, 2007), much below the validated calibration plots for quantitative PCR (RT-qPCR) assays. There were difficulties in interpretation of the antibody screening and RT-PCR assays arising out of the low anti-HCV antibody levels (Zer et al, 2009), low plasma viral load (Glynn et al, 2005; Fytili et al, 2007), spontaneous

resolution of infection (Bulteel et al, 2016; Hofer et al, 2003; Micallef et al, 2006), decreasing viral load and occult infection (Marco et al, 2009; Welker and Zeuzem, 2009; Carreno et al, 2008).

The concentration of the free hydrolysis probe of RT-PCR that give rise to the real-time fluorescence amplification plot, increase exponentially or doubling from the first cycle onwards. But fluorescence intensity reached the detectable level of the RT-PCR machine only after several cycles, near the quantification threshold (Cq) and was related to initial copy number of the template DNA (Kralik and Ricchi, 2017; Adams, 2006). As the initial copy number increased, with increase in the plasma viral load of HCV or concentration of the calibrator, the Cq decreased (Adams, 2006). The fluorescence intensity increase immediately above the threshold level would be exponential with an efficiency nearer to two for all validated calibrator concentrations (Ramakers et al, 2003; Ruijter et al, 2009).

This study examined the various preanalytical influences and performance of HCV RT-PCR to improve the sensitivity and specificity for diagnosis of HCV infection. Data analysis was also done on the sequences of the major PCR products of 5'UTR, Core E-1 and NS5B regions of the HCV genome.

1.2.1. Organisation of the thesis into nine chapters:

The nine chapters comprises of initial general chapters, followed by the result chapters. The initial general chapters, one to four were General Introduction, Objectives, Review of literature and Materials and methodology, respectively. There were five results chapters from chapter 5 to 9.

1.3. Objectives

1. Establishment of the methods for evaluation by data analysis, test validation, quality control and clinical state of the patient for Molecular Diagnostic reporting of Hepatitis C virus infection.
2. Use of these procedures for confirmatory diagnosis of hepatitis C virus infection, its plasma viral count determination and genotyping.

1.4. Materials and Methods

Institutional Ethics and Research Committee approvals were obtained.

Samples collected were a) EDTA-blood samples for plasma RNA isolation, followed by HCV RT-PCR; b) Blood samples in vacuum tubes with clot activator for serum anti-HCV antibody assays. Plasma and serum samples were prepared by centrifugation.

Sample collection from patients with **preanalytical influences** on samples due to tissues damaging conditions and due to the influence of drugs, were excluded from the RT-PCR assays, for two weeks or till the condition of the patient improved. All these preanalytical influences were overlooked in emergency cases. But in such patients the HCV RT-PCR data were examined for preanalytical influences.

RNA isolation was done with column chromatography method using reagents (QIAamp viral RNA mini kit), used immediately or stored at -80^{o}C in aliquots. **Real time HCV RT-PCR** was done using reagents (Artus HCV RG RT-PCR kit). The primers for diagnostic RT-PCR were targeted to 5'UTR conserved sequence (**Bukh, J, 1992, Hoffman, Q. Liu, 2011**).

Statistical calculations were done with SPSS, SigmaStat 4.0, Excel and Graphpad. The major molecular biology related **software used** were LinRegPCR software, phylogenyfronline for phylogenetic tree construction, Finch TV for Sequence analysis, iedb.org for epitope and antigenicity peptide prediction.

RESULTS CHAPTERS 5 TO 9

1.5. Chapter 5. Analysis of calibration plot, efficiency and individual amplification to differentiate between qualitative and quantitative HCV RT-PCR

1.5.1. ABSTRACT

Real-time RT-PCR may be quantitative or qualitative (David and Theo, 2006). Validated quantitative RT-PCR assay required an acceptable performance of calibrators and calibration plot for reporting the viral load in the patients' plasma. Validation for quantitative RT-PCR was done by the manufacturers of the assays (Qiagen, Germany). According to the clinical

diagnostic requirements, these assay performances were verified by the user for acceptable performance (Wallace and McCulloch, 2021). Hepatitis C virus (HCV) load in plasma were often below the validated RT-qPCR calibration plot concentrations. **The research problem** of this study was to define the lower limit of the selected quantitative RT-PCR assay with acceptable performance, and to differentiate the quantitative RT-PCR assays from the qualitative RT-PCR assays at lower plasma viral load. In this report, data analysis of RT-PCR amplification plots and calibration plots were done to define the performance characteristics of the higher Cq range of qualitative RT-PCR and to differentiate it from quantitative RT-PCR (RT-qPCR).

Patients reactive for anti-HCV antibody screening assays or exposed to HCV infection were selected for RT-PCR assay done with RNA isolated from plasma. Validated and diluted calibrator concentrations were used to construct calibration plots, and for data analysis along with patients' RT-PCR, using software packages.

Normalised fluorescence intensity (100%) and slope at inflection point (1.65 - 1.50) of the sigmoid fluorescence amplification plots were of acceptable performance for validated quantitative calibrators, but were decreased for diluted calibrators and for patients' sample with Cq greater than that of the 10 IU/µl validated calibrator (Cq >33.2) (Table 5.3). Calibration plot of validated calibrators had slope, efficiency and sensitivity of -3.471, 94% and 36.404, respectively, but the diluted calibrators showed decreased performance of -2.305, 171% and 35.52, respectively. Log-transformed exponential amplification plots analysed by LinRegPCR software, showed acceptable performance at the validated calibrator concentrations and decreased performance with diluted calibrators and patients' sample with Cq >33.2. The four-parameter validated qualitative RT-PCR Cq range was from 33.2 to 39.9. The 10 IU/µl calibrator was the reference point to differentiate between qualitative and quantitative RT-PCR. Decision-criteria were developed for establishing the range of validated qualitative RT-PCR performance, and to differentiate it from quantitative RT-PCR.

1.6. Chapter 6. Analysis of Internal Controls in the matrix of HCV RT-PCR assays showed analytical and pre-analytical influences independent of template concentrations

1.6.1. ABSTRACT

The negative RT-PCR results should truly represent the absence of PCR diagnostic targets. But false-negative results could occur from failure of one of the test steps of nucleic acid extraction, reverse transcription reaction and RT-PCR set up, or inhibitory substances in the samples. Efforts to control false-negative results were based on the addition of exogenous nucleic acids amplification system (the IC) to the RT-PCR reaction, so that the presence of any inhibitory substances (eg. heparin) in the samples or errors in test steps would also affect the amplification of the exogenous material (Lv et al, 2020). Therefore, the research problem in the present report was that the IC might be used to detect influences on the RT-PCR assay systems independent of HCV template concentrations.

Internal control (IC), made up of the reference gene PCR amplification system with fixed concentration of template and fluorescent probe, and present in the assay matrix of all HCV RT-PCR assay systems, was evaluated for detection of the preanalytical and analytical influences on the amplification systems. IC was added to patients' plasma RNA, calibrators, quality control (QC) RNA and non-template control (NTC). All IC additions were from the same lot for a set of calculations. The IC fluorescence emission of ROX dye at 610±5 nm, was independent of the HCV template amplification with FAM dye having emission at 510±5 nm. The average IC threshold cycle (Cq) was lowest for NTC (30.346), followed by the calibrators (31.425), and it was even higher for quality control samples (33.767) and the HCV infected patients' plasma RNA sample (33.017). The average %CV was the same for NTC, calibrators and QC sample. But was increased for patients' sample. The lowest average Cq in NTC might due to absence of HCV RT-PCR products, which were present in calibrators. The QC and patients' samples contained the PCR products, and in addition it contained the RNA from plasma which included the non-specific RNA. These PCR products might be the causes for the influence on IC Cq. The

patients' samples were from different patients', unlike that of QC sample and calibrators which were a single sample, contributing to higher average patients' %CV (Fig. 6.4A and B). The mean Cq difference between NTC and calibrators might be attributed to analytical influence, while that between the calibrator and patients' sample might be attributed to pre-analytical influences. Slope, normalised fluorescence intensity and efficiency decreases with decrease in viral load both in calibrators and with patient samples. when concentration is expressed as Cq, the relationship of Cq, fluorescence intensity and efficiency become inversely related.

1.7. Chapter 7. Hepatitis C Virus RT-PCR amplification data showed preanalytical influences of sample that can affect the RT-PCR diagnostic outcome

1.7.1. ABSTRACT

RT-PCR inhibition is detected by use of internal controls that use of house-keeping genes unrelated to the template in each assay (Maaroufi et al, 2006; Courtney et al, 1999). Contaminations are detected by use of non-template controls with each set of assays in a run (Espy et al, 2006). RT-PCR inhibition is caused typically in clinical samples by the influence of heme, hemin, hemolysed plasma sample (Byrnes, J. J et al, 1975; Levere et al, 1991; Panaccio and Lew, 1991), heparin (Satsangi et al, 1994). Common cause of RT-PCR inhibition is the inhibition of DNA polymerase and reverse transcriptase. Those negative influences were clinically excluded in this study by careful selection of samples that are unlikely to show RT-PCR inhibition, and by repetition of assays showing RT-PCR inhibition after decreasing the effect of these agents and conditions. Use of hypochlorite, UV light and biosafety cabinet to control contamination

Large number of third generation anti HCV antibody reactive results were found to be RT-PCR negative. The discrepancy between these results were analysed in this study. The variation in the internal control (IC) Cq and fluorescence intensity showed sample influences on the RT-PCR results. In this study, clinical cases selected and the assays were designed in such a way that the preanalytical influences may be observed directly in a particular case or

cases. Tissue damaging conditions were found to be a major cause of preanalytical variation. The first case was an HCV RT-PCR positive patient, who underwent extensive surgical procedures immediately after the positive RT-PCR. Within a few days after surgery, the RT-PCR results became negative (Fig. 7.1). The PCR product of the sample was analysed and was confirmed to produce the 272 bp PCR product of 5'UTR region before surgery. The preanalytical influences were also found to be influencing the calibration plot. When there were preanalytical influences on RT-PCR from patient sample, and when these assays were repeated after two weeks, these influences were found to be decreased resulting in decrease in Cq. There was one sample which was negative, became positive. These case studies demonstrated again that the preanalytical influences on HCV RT-PCR affected the diagnostic outcome of the patients.

1.8. Chapter 8. RT-PCR positive and negative samples that have reactive levels of anti-Hepatitis C virus antibody levels showed similar bimodal distribution and questions the validity of false positive reporting

1.8.1. ABSTRACT

Increasing the sensitivity of screening assays resulted in large increase in the detection of reactive levels of anti-HCV antibody in serum samples. The large increase in reactive screening assays reports and absence of symptoms in HCV infected individuals often lead to questions among clinicians about the usefulness of screening assay with high seroconversion detection rates, dumbed most reports as 'false reactive' (personal experience) and even attempted to raise the cut off levels of reactive anti-HCV antibody levels (Kamili et al, 2012) to match it with the cut off levels of absorbance or colour-based, second-generation EIA. This subjective and hypothetical method of branding reactive reports of screening assays with high seroconversion detection rates as 'false reactive' was examined in our laboratory and results are reported in this study.

We hypothesised that the large number of 'false reactive screening assay' reports were due to insensitivity of RT-PCR assays. As the plasma viral loads were low, the issue of lowering the limit of detection for assaying the viral loads

by RT-PCR was taken up. The sensitivity of RT-PCR was increased by controlling the preanalytical procedures of the assay that involves plasma sample collection, RNA isolation and cDNA preparation from plasma.

The reactive anti-HCV antibody concentrations may be RT-PCR positive or RT-PCR negative. Samples were collected after excluding patients with tissue damaging conditions and influence of drugs, as far as possible. RT-PCR assay was done after preanalytical control of samples to decrease non-specific influences, probably of nucleic acids and drugs, immediate isolation of RNA from EDTA-plasma. Distribution of the concentrations of anti-HCV reactive antibody were plotted as a histogram. There were two distribution clusters for anti-HCV antibody, the lower antibody cluster was between 1.0 and 15.0 and the higher antibody cluster was between 15.0 and 42 (Fig. 8.1). Each of the two reactive antibody clusters had HCV RT-PCR positive and negative groups (Fig. 8.2). The two antibody clusters in the antibody distribution of histogram were found to have both RT-PCR negative and positive samples, indicating that both clusters might have occult and positive HCV infection. These results questioned the large number of 'false reactivity' issue with the third generation anti-HCV antibody assays.

1.9. Chapter 9. Sequence and phylogenetic data analysis of HCV genotypes of 5'UTR, Core E1 and NS5B

1.9.1. ABSTRACT

Data analysis was also done on the sequences of the major PCR products of 5'UTR, Core E-1 and NS5B regions of the HCV genome. Phylogenetic tree was constructed using reference sequence from the seven genotypes and were aligned and compared with the HCV sequences submitted. Phylogeny was done for core E1 and NS5B regions too with the seven different reference sequences from NCBI database.

The **5'UTR region** is a highly conserved, 341 bp region with secondary RNA structure that has functional importance. **Graphic representation of 24 sequences** of this region showed >200 alignment score with reference sequence, and percent identity from 96 to 100% for genotype 1. Similar data was obtained for **genotype 3**, with percent identity from 95.57 to 99.57. The major genotypes

identified were 1 and 3, and the positions showing nucleotide differences were also studied (Table 9.5). There were highly conserved regions of 5'UTR with low entropy, and these sites were used for designing primers that were used for diagnostic purposes. The secondary structure of (5'UTR) showed several sites of stacking interactions between successive base pairs, and predicted energetically most stable structure.

Similar **sequence data analysis** was also done with **Core E1 region**. Six different sequences of **genotype 1** of Core E1 region were submitted to NCBI database and were found to have alignment score >200 and percent identity between 94.59 and 95.46. Due to lack of specific highly conserved sites, primer designing for both CE1 and NS5B were found to be more difficult and less productive. There was one sequence with **genotype 3a** with alignment score >200 and percent identity of 91.53. There were five sequences of core E1 matched with **genotype 3b** with alignment score >200 and percent identity 87.75 to 89.29. One sequence showed >200 alignment score with **genotype 4** with percent identity of 91.67.

Epitope prediction was done for **Core E1** using software (a) Bepipred Linear Epitope Prediction and (b) Kolaskar and Tongaonkar Antigenicity Predicted peptides. B-cell epitopes were used by the former and physicochemical properties were used for the latter. The secondary structure of core E1 were also analysed.

Similar analysis was done with **NS5B** but the PCR product and the data obtained were much less than the other two regions due to larger variations distributed in the NS5B region. There were only **two PCR products** amplified using various primers designed for NS5B. The secondary structure of core E1 and the possible three-dimensional tertiary distribution of the secondary structures were also analysed.

Phylogenetic tree was constructed using reference sequence from the seven genotypes of 5'UTR (Fig. 9.19). These reference sequences were aligned and compared with the HCV sequences submitted to NCBI from this study. Phylogenetic trees were also constructed for core E1 and NS5B regions with the different reference sequences from NCBI database.

CHAPTER 2
OBJECTIVES

1. Establishment of the methods for evaluation by data analysis, test validation, quality control and clinical state of the patient for Molecular Diagnostic reporting of Hepatitis C virus infection.
2. Use of these procedures for confirmatory diagnosis of hepatitis C virus infection, its plasma viral count determination and genotyping.

Description and the Methods to achieve the objectives

The above two objectives have been analysed in the five results chapters.

- Methods of Data analysis of RT-PCR fluorescence amplification plot (SigmaStat, LinRegPCR)
- Methods for Test validation of the RT-PCR assays by data analysis of quantitative and qualitative calibration plots, along with data analysis of qualitative and quantitative RT-PCR fluorescence amplification plots to report an assay as quantitative and qualitative.
- Methods for Quality Control in Molecular Diagnostic Assays:
- Data analysis for influences on RT-PCR: Methods were developed to identify analytical and preanalytical influences.
- Data analysis of anti-HCV antibody levels and distributions
- Sequence data analysis for information on conserved, low entropy, construction of secondary structure of proteins, and for genotype analysis.

CHAPTER 3

REVIEW OF LITERATURE

3.1. Hepatitis C Virus

Hepatitis C Virus, a human pathogen, first identified by Choo Q et al, 1989, is an enveloped, positive sense, single stranded hepatotropic RNA virus belongs to genus Hepacivirus and family Flaviviridae with a high degree of genetic heterogeneity. Hepatitis is the inflammatory disease of liver caused by Hepatitis C Virus (HCV). The HCV RNA contains a single large open reading frame (ORF) flanked by an untranslated region (UTR) at each end (5'UTR and 3'UTR), a genomic organization conserved among members of the Flaviviridae family. HCV infection affects more than 170 million people worldwide with acute infection being asymptomatic, may lead to chronic HCV infection. Globally, an estimated 58 million people live with chronic hepatitis C virus infection, with about 1.5 million new infections occurring per year (WHO, 2021). According to WHO estimates, in 2019 approximately 290,000 people died due to cirrhosis and hepatocellular carcinoma developed after HCV infection. Chronic HCV infection and cirrhosis is associated with development of hepatocellular carcinoma (Saito et al, 1990). The infection was primarily acquired through percutaneous and intravenous blood exposure, multiple use of needles and Injection Drug Use (IDU). Control of these procedures, such as use of disposable syringes and diagnostic testing, have had a protective effect.

3.1.1. Biochemistry of Hepatitis C Virus Infection

3.1.1.1. History

The specific diagnostic tests became available for Hepatitis A Virus (HAV) and Hepatitis B Virus (HBV) in 1970's and at that time post transfusion hepatitis was named as non-A non-B Hepatitis (NANBH) due to lack of serological markers (Alter MJ et al, 1982). The causative agent for NANBH was finally found in 1989 and which led to the characterisation of Hepatitis C Virus (Choo Q L et al, 1989). The development of sensitive screening assays revealed that most of the NANBH cases were due to HCV infection (Kuo G et al, 1989; Di Bisceglie AM et al, 1991). HCV is one of the major global causes of death and morbidity (Cooke GS, 2013). Most of the patients with acute hepatitis C infection progress to chronic HCV infection due to lack of effective diagnosis and treatment. Chronic hepatitis C resulted in liver fibrosis, cirrhosis, hepatic failure or hepatocellular carcinoma (Cooke GS, 2013; Ly KN et al, 2016). In 1989 HCV was identified, but until 1992, the blood for transfusion was not

screened for HCV. Therefore, earlier to 1992, the primary reason of infection was contaminated blood products (AASLD-IDSA, 2018; Smith BD et al, 2012).

WHO estimated that in 2015, 71 million were with chronic HCV infection worldwide and that 3,99,000 died from cirrhosis or Hepatocellular carcinoma caused by HCV infection. The World Health Assembly in May 2016, endorsed the Global Health Sector Strategy (GHSS) on viral hepatitis, which proposes to eliminate viral hepatitis as a public health threat by 2030 (90% reduction in incidence and 65% reduction in mortality). Elimination of viral hepatitis as a public health threat requires 90% of those infected to be diagnosed and 80% of those diagnosed to be treated (WHO, 2018).

Viral hepatitis caused 1.34 million deaths in 2015, introduction of direct-acting antivirals (DAAs) led to a sustained virological response (SVR) in greater than 90% of treated individuals (Feeney and Chung, 2014; Pawlotsky, 2014). DAAs are now recommended by the World Health Organization (WHO) and many other HCV treatment guidelines (WHO, 2016). DAAs not only improved SVR rates but simplified HCV management algorithms and now smaller health facilities manages HCV-infected individuals (Soriano, 2013). Despite the availability of effective treatment, most HCV-infected individuals remain undiagnosed and untreated (Papatheodoridis et al, 2014). Left untreated, approximately 15–30% of individuals with chronic HCV infection progress to cirrhosis, leading to end-stage liver disease and hepatocellular carcinoma (WHO, 2016; Lavanchy, 2009).

3.1.2. Transmission and Life Cycle of Virus

HCV is transmitted by intravenous, percutaneous or permucosal exposure to infectious blood or blood-derived body fluids (Thomas DL, 2013; Mohd Hanafiah K et al, 2013). 3-4 million people are infected with HCV every year (Lavanchy D, 2011).

The primary source of HCV transmission is through HCV infected blood and blood products, and the major mode of transmission is Injection drug use (IDU). First, the routes of transmission of HCV includes Persons who inject drugs (PWID) (Nelson PK et al, 2011), and has the highest risk of infection. Globally, the prevalence of HCV is 67% among PWID. Second, recipients of infected blood products or people who undergo invasive procedures in health-care settings with inadequate infection control practices (Shepard CW et al, 2005; Frank C et al, 2000; Singh S et al 2000, Marx MA et al, 2003; Lin CC et al, 2003; Saxena R et al, 1999; Candotti D et al, 2001; El-Zanaty

F et al, 2009). The risk of HCV infection depends upon the frequency of invasive medical procedures and level of infection-control practices. Third, HCV infected mother to child transmission (Thomas DL et al, 1998; Mast EE et al, 2005). This type of transmission risk is estimated to be 4–8% among mothers without HIV infection. The transmission risk is estimated to be high up-to 17-25% among mothers with HIV co-infection. Fourth, people with sexual partners who are HCV-infected (Terrault NA et al, 2013; Valadez JJ et al, 2013; Tseng YT et al, 2012; Price H et al, 2013). The risk in sexual transmission is high with co-infection of HIV. Fifth, Persons with HIV infection, in particular MSM (men having sex with men), are at increased risk of HCV infection through unprotected sex (Tohme et al, 2010; Karuru et al, 2005; Quaranta et al, 1994; Sherman et al, 2002; Rauch et al, 2005; D'Oliveira et al, 2005; Vandelli et al, 2004; Eyster et al, 1991; Taylor et al, 2012). Sixth, people who have used intranasal drugs (Scheinmann et al, 2007), non-injecting drug use (e.g., through sharing of inhalation equipment for cocaine) is associated with a higher risk of HCV infection. Seventh, People who have had tattoos or piercings (Jafari S et al, 2010). Tattoo recipients have higher prevalence of HCV compared with persons without. In industrialized countries, transmission occurs mainly between people who inject drugs; other mechanisms of HCV transmission include perinatal transmission, invasive medical and dental procedures, and rarely via sexual route. Mucous membrane exposures to blood also can result in transmission, although this route is less efficient. HCV can be detected in saliva, semen, breast milk, and other body fluids, although these body fluids are not believed to be efficient vehicles of transmission (Thomas et al, 2000; CDC, 2001).

The HCV life cycle is only partly understood and difficulties in establishing an in vitro model of replication and also the complex network of cell surface molecules that mediate viral entry have delayed our understanding of various molecular mechanisms involved (Maggi et al, 2017; Paul et al, 2014).

3.1.2.1. Role of Structural and Non-structural proteins in the Life Cycle of HCV

The structural proteins include the core, envelope glycoproteins E1 and E2, and the non-structural proteins include p7, viroporin and non-structural protein 2 (NS2); NS3 and NS4A, NS4B, NS5A, and NS5B. NS2 participate in virus assembly and release, NS3 and NS4A, the protease complex that is actively targeted by the protease inhibitor class of Direct Acting Antivirals (DAAs); NS4B, a membrane-associated protein that mediates virus host interactions; NS5A, a zinc binding and proline-rich hydrophilic phosphoprotein involved in HCV RNA replication and

targeted by NS5A inhibitor DAAs; and NS5B, the RNA-dependent RNA polymerase targeted by nucleoside and non-nucleoside polymerase inhibitor DAAs.

3.1.2.2. HCV Receptors

Life cycle of HCV is initiated by the attachment of virus to specific receptors present on the hepatocytes, like the high-density lipoprotein receptor, scavenger receptor class B type 1, tetraspanin CD81, tight junction protein claudin-1, and occluding for initiating the attachment step of HCV infection (Zhu YZ et al, 2014) and triggers receptor mediated endocytosis. Many receptors are proposed to act as receptors for mediating HCV binding and internalisation. The most extensively studied putative HCV receptor molecules is CD81 (Pileri et al, 1998). A candidate receptor for HCV is proposed to be scavenger receptor B type I (SR-BI) (Scarselli et al, 2002). Another proposed tissue-specific capture receptors for HCV in different cell types that may have a critical role in viral pathogenesis include dendritic cell-specific intercellular adhesion molecule-3-grabbing nonintegrin and the liver/lymph node-specific intercellular adhesion molecule-3 grabbing integrin (Gardner et al, 2003; Lozach et al, 2004; Lozach et al, 2003; Pohlmann et al, 2003). The asialoglycoprotein receptor is reported to mediate binding and internalization of structural HCV proteins, in a baculovirus expression system. It is possible that heparan sulfate proteoglycans (glycosaminoglycan expressed as cell surface molecule) serves as the initial docking site for HCV attachment and the virus is subsequently transferred to another high-affinity receptor triggering entry (Barth et al, 2003).

3.1.2.3. Cellular attachment of HCV virions and entry

HCV, an enveloped virus, envelope surrounds the nucleocapsid, it has multiple copies of a small basic protein (core or C), and the RNA genome. The HCV virion circulates in the bloodstream either as a free particle or surrounded by host low-density lipoproteins (Andre P et al, 2002), attaches onto the target cell membrane by sequential binding of various receptor molecules, and enters into the cell by a clathrin-mediated endocytosis process.

3.1.2.4. HCV cell entry mechanism and fusion

Soon after binding with receptor complex, virion receptor is internalised and nucleocapsid which contains single-stranded (ss), positive-sense RNA genome is released into the cytoplasm of a newly infected cell. Viral surface glycoproteins control the entry process that triggers the changes required for mediating fusion. The viral entry into cells is dependent on pH and through endocytosis (Agnello et al, 1999;

Bartosch et al, 2003b; Hsu et al, 2003). The low pH of the endocytic compartment presumably helps in the fusion of viral and cellular membranes.

The RNA genome is then directly translated at the rough endoplasmic reticulum (ER) in a single polyprotein precursor of about 3000 amino acid residues that is eventually cleaved by cellular and viral proteases into ten mature products (Andre P et al, 2002; Lohmann V, 2013). This genome serves multiple roles within the virus life cycle: first, as a messenger RNA (mRNA) for translation of the viral proteins; second as a template for RNA replication; and third, as a nascent genome packaged within new virus particles. The precursor polyprotein produced is then cleaved by cellular and viral proteases into structural and non-structural proteins. The viral genome replication is done by the viral replication complex that is associated with cellular membranes. The site of viral replication is cytoplasm where it synthesis of full-length negative-strand RNA intermediates. Progeny virions are assembled through the formation of cytoplasmic vesicles by budding through intracellular membranes. By exocytosis, mature virions are released to the extracellular compartment.

3.1.2.5. Replication

Genomic RNA is uncoated in the cytoplasm and it is used for translation of polyproteins and replication occurs in the cytoplasm. HCV RNA Replication of HCV RNA occur in the cytoplasm of virus-infected cells based on the studies on cytoplasmic localization of viral RNA (Gowans, 2000) and polymerase (Hwang et al, 1997; Selby et al, 1993). RNA is synthesized by a membrane-associated replication complex that includes the HCV RNA-dependent RNA polymerase (RdRP) NS5B, other viral non-structural proteins (NS3, NS4A, NS4B, and NS5A), and few cellular proteins (Bartenschlager et al, 1995; Lin et al, 1997; Tu et al, 1999). Replication happens inside the "replication complex" which contains the viral non-structural proteins and cellular proteins. Major non- structural protein involved in replication is NS5B along with NTPase/helicase domain of the NS3 protein. The NS3 protein has several functions important for viral replication, which includes RNA stimulated NTPase activity, binding and unwinding of RNA regions of extensive secondary structure. NS5A protein has a regulatory role in virus replication.

The positive-strand RNA genome act as a template for the synthesis of a negative-strand intermediate of replication during the initial step. In the next step, negative-strand RNA stands as a template to produce large number of strands with positive polarity. It will be subsequently used in polyprotein translation, synthesis of new intermediates of replication and packaging to form new virus particles

(Bartenschlager et al, 2004). The positive-strand RNA progeny is transcribed in a five to ten-fold in excess compared to negative-strand RNA. The Direct Acting Antivirals (DAAs) used for treatment of Hepatitis C infection are designed to inhibit NS5B RNA dependent RNA polymerase.

3.1.2.6. Release

New virions produced are assembled in an ER-derived compartment and released by exocytosis following a Golgi-dependent secretory pathway. During this process, the virus undergoes maturation and becomes surrounded by endogenous lipoproteins that are believed to help immune escape (Maggi F et al, 2017; Paul D et al, 2014). Binding to host lipoproteins and envelopes without clearly discernible surface features confer to HCV virion low buoyant density and a broad size range (40-80 nm diameter) (Paul D et al, 2014).

3.1.3. HCV Genome structure and organization

HCV is a single stranded, positive sense RNA of approx. 9.6Kb in length (Choo et al, 1991). Viral RNA has a single large ORF flanked on both sides with UTR which is a genomic organisation conserved among different Flaviviridae family members. HCV RNA is highly variable which resulted in 7 different genotypes and many subtypes of that due to high degree of genetic variability due to mutations occurring during viral replication. But the rate of mutation varies in different regions.

The ORF is flanked in 5' and 3' by untranslated regions (UTR) are the most conserved regions (Choo et al, 1991; Miller and Purcell, 1990; Muerhoff et al, 1995) that has an important role in polyprotein translation and RNA replication (Thurner et al, 2004). The HCV Viral genome undergo direct translation and produce a polyprotein. This polyprotein is cleaved by viral and cellular proteases, co and post-translationally into ten gene products. The N-terminal region of the polyprotein encodes the structural proteins that are incorporated into the virus particle: the capsid-forming ‘core’ protein and the glycoproteins, E1 and E2. The two thirds of C-terminal region of the polyprotein encode the non-structural proteins that includes p7, NS2, NS3, NS4A, NS5A and NS5B. By definition, the NS proteins are expressed in virus-infected cells but are not incorporated into virus particles; they serve to coordinate the intracellular aspects of HCV replication, including RNA synthesis, modulation of host defense mechanisms and virus assembly (Lindenbach, BD et al, 2013). The heterodimeric complex of NS3 and NS4A proteins, referred to as NS3-4A, contains a serine protease domain and an RNA helicase domain. The serine protease activity is responsible for cleaving the viral polyprotein and cellular antiviral signaling proteins,

thereby abrogating the induction of type I interferon in infected cells. The RNA helicase domain is responsible for unwinding double-stranded forms of the viral genome or clearing proteins from the genome during RNA replication (Morikawa K et al, 2011)

3.1.3.1. 5'UTR

The mutation rate varies significantly in the different regions of the HCV genome, of which the 5'UTR and the extreme end of the 3'UTR have the lowest sequence diversity among various genotypes and subtypes (Choo et al, 1991; Miller and Purcell, 1990; Muerhoff et al, 1995). The relatively conserved nature of these regions signifies their functional importance in the viral life cycle. The 5'UTR of the HCV genome is 341-nt long in most viral isolates. There is more than 90% sequence identity among different HCV genotypes, with some segments nearly identical among different strains (Bukh et al, 1992). The secondary and tertiary structures of this region are also largely conserved (Brown et al, 1992; Honda et al, 1999a; Honda et al, 1996a). The 5'UTR contains four highly domains which are structured, from I to IV, contains numerous stem-loops and a pseudoknot (Brown et al, 1992; Wang et al, 1995). Domains II, III and IV and first 12 to 30 nucleotides of the core coding region comprise the IRES (Honda et al, 1996).

Viral protein synthesis is initiated in a cap-independent manner by a highly conserved domain that acts as an internal ribosome entry site (IRES), largely located at the 5′ UTR (Tsukiyama-Kohara et al, 1992; Wang et al, 1993). The HCV 5′ untranslated region (5′UTR), responsible for the initiation of viral translation with the help of an internal ribosome entry site (IRES), which is known to contain specific nucleotide substitutions when cultured in infected lymphoid cells (Laskus T, 2000). Sequence variability in this region has important implications for structural organization and the function of the IRES element and could correlate with HCV RNA concentration (Barría et al, 2009).

5' UTR of HCV RNA is the most highly conserved region among all genotypes (Bukh et al, 1995; Simmonds, 2004; Bukh et al, 1992; Davidson et al, 1995) of the genome and thus has been used in most laboratories to develop sensitive detection assays, which includes qualitative and quantitative HCV RNA detection (Hijikata M, 1991) due to its high level of conservation and sensitivity. However, due to this high level of conservation, the 5'UTR is limited in its ability to discriminate genotype 6 from genotype 1 and subtypes within genotypes 1, 2, 3, 4, and 6. Genotype 6 variants

other than 6a and 6b show 5'UTR sequences identical or similar to those of type 1 and, as a consequence, cannot be differentiated (Chinchai T et al, 2003; Stuyver, L et al, 1996). A large number of subtypes that often share the same 5UTR sequence have been described (Cantaloube, J. F et al, 2006; Corbet, S et al, 2003). The inability to distinguish subtype 2c from subtype 2a in the 5UTR is a good example of this phenomenon. Furthermore, some of the genotype- specific motifs that were initially identified in the 5' UTR are no longer found to be conserved. For example, the G residue at position 243 of the 5' UTR, originally considered to be representative of subtype 1b, is found to occur in a relative proportion of subtype 1a viruses (Cantaloube, J. F et al, 2006; Chen, Z and KE Weck 2002; Corbet, S et al, 2003; Germer JJ et al,1999; Tamalet C et al, 2003).

3.1.3.2. IRES

Translation of the HCV genome, which lacks a 5' cap, depends on an internal ribosome entry site (IRES) within the 5' UTR. The HCV IRES binds 40S ribosomal subunits directly and avidly, bypassing the need for pre-initiation factors, and inducing an mRNA-bound conformation in the 40S subunit (Spahn et al, 2001). The IRES–40S complex then recruits eukaryotic initiation factor (eIF) 3 and the ternary complex of Met-tRNA–eIF2–GTP to form a non-canonical 48S intermediate, before a kinetically slow transition to the translationally active 80S complex (Ji H et al, 2004, Otto et al, 2004). The minimal sequence required for IRES activity is believed to include nucleotide sequences spanning nucleotides 42 through 356 (Honda M et al, 1996a; Honda M et al, 1996; Honda, M et al, 1999a; Reynolds, 1995; Reynolds 1996; Rijnbrand 1995).

3.1.3.3. 3' Un Translated Region (3' UTR)

The 3'UTR which is approximately 225 nucleotides, is organized into three regions from 5' to 3' direction, first, a variable region of approximately 30-40 nucleotides, second, a long poly(U)-poly (U/ UC) tract, and third, a highly conserved 3'-terminal stretch of 98 nucleotides that includes three stem-loop structures (Kolykhalov et al, 1996; Tanaka et al, 1995; Tanaka et al, 1996). The 3'UTR interacts with the RdRp and with two out of four stable stem-loop structures located at the 3' end of the NS5B-coding region (Cheng et al, 1999; Lee et al, 2004). The 3' region and the 52 upstream nucleotides of the poly(U/C) tract were found to be important for RNA replication, whereas the remaining part of the 3'UTR appears to promote viral

replication (Friebe and Bartenschlager, 2002; Ito and Lai, 1997; Yi and Lemon, 2003a; Yi and Lemon, 2003b).

3.1.4. Structure of Hepatitis C Virus

HCV particles are enveloped which have structural proteins in its capsid which covers the genetic material RNA. They derive their envelope from the endoplasmic reticulum of the host, which includes E1 and E2, viral glycoproteins that helps in binding and entry to the host. HCV is associated in serum with lipoproteins and termed as Lipo Viral Particles (LVPs) (Andre et al, 2002). HCV particles range in size from 40-80 nm in diameter due to its asymmetric shape and size.

3.1.4.1. HCV Proteins

The polyprotein undergoes co- and post-translational processing by cellular and viral proteases into ten viral proteins. The open reading frame (ORF) of HCV contains 9024 to 9111 nucleotides depending on the type of genotype. They comprise three structural proteins that build up the virion: Core, E1 and E2, and also seven nonstructural (NS) proteins functions in replication and assembly and F protein which results from a frameshift in the core coding region.

3.1.4.2. Structural Proteins

3.1.4.2.1. Core Protein

The Core protein of HCV is a highly basic RNA binding protein and it may form the viral capsid. It is a 23kDa ie, 191 amino acid protein. The core protein contains three distinct predicted domains: an N-terminal hydrophilic domain of 120 aa (domain D1), a C-terminal hydrophobic domain of about 50 aa (domain D2), and the last 20 or so aa that serve as a signal peptide for the downstream envelope protein E1 (Grakoui et al, 1993c; Harada et al, 1991; Santolini et al, 1994). Domain D1 contains numerous positive charges. It is principally involved in RNA binding and nuclear localization, as suggested by the presence of three predicted nuclear localization signals (NLS) (Chang et al, 1994; Suzuki et al, 1995; Suzuki et al, 2005). Domain D2 is responsible for core protein association with endoplasmic reticulum (ER) membranes, outer mitochondria membranes and lipid droplets (Schwer et al, 2004; Suzuki et al, 2005).

3.1.4.2.2. Envelope 1 and Envelope 2

The envelope glycoproteins E1 and E2, are important molecules of the HCV virion envelope and which is necessary for viral entry and fusion (Bartosch et al, 2003a; Nielsen et al, 2004). They have molecular weights of 33-35 and 70-72 kDa, respectively, and they assemble as noncovalent heterodimers (Deleersnyder et al,

1997). Envelope proteins are type I transmembrane glycoproteins, with N-terminal ectodomains, and a short C-terminal transmembrane domain. The envelope transmembrane domains are composed of hydrophobic amino acids in two stretches separated by a short polar region that contain fully conserved charged residues. They have many functions, which includes membrane anchoring, ER localization and heterodimer assembly (Cocquerel et al, 1998; Cocquerel et al, 2000). E2 plays an important role in the early stages of infection. Viral attachment may be initiated via E2 interaction components of the receptor complex (Flint and McKeating, 2000).

3.1.4.2.3. Frameshift Protein

The F (frameshift) protein or otherwise known as ARFP (alternate reading frame protein) is generated as a result of ribosomal frameshift (-2/+1) in the N-terminal core coding region of the polyprotein of HCV. Antibodies against peptides from the F protein were identified in chronically infected patients proved that the protein is produced during infection (Walewski et al, 2001). But, the exact translational mechanisms in the frequency and yield of the F protein during the different phases of HCV infection are not known. So, the activity of F protein in the HCV lifecycle remains inconclusive but it is proposed to be involved in viral persistence (Baril and Brakier-Gingras, 2005).

3.1.4.3. Non-Structural Proteins

3.1.4.3.1. P7

P7, which is a small integral membrane protein of only 63 amino acids (Carrere-Kremer et al, 2002). The two trans membrane domains organized in α-helices, connected by a cytoplasmic loop.

3.1.4.3.2. NS2

NS2 is a non-glycosylated transmembrane protein of 21-23 kDa. It has two internal signal sequences at amino acid positions 839-883 and 928-960, which is responsible for ER membrane association (Santolini et al, 1995; Yamaga and Ou, 2002). NS2, with the amino-terminal domain of the NS3 (NS2-3 protease), constitutes a zinc-dependent metalloprotease that cleaves NS2 and NS3 (Grakoui et al, 1993b; Grakoui et al, 1993c; Hijikata et al, 1993). NS2 is a short-lived protein does not have its protease activity after self-cleavage from NS3 and gets degraded by the proteasome in a phosphorylation-dependent manner by protein kinase casein kinase 2 (Franck et al, 2005).

3.1.4.3.3. NS3

NS3, which is a multi-functional protein has a serine protease domain in its N terminal and a helicase/NTPase domain in C-terminal. NS4A acts as a cofactor of NS3 protease activity. NS3-4A also has additional properties by its interaction with host cell pathways and proteins that are important in the lifecycle and pathogenesis of HCV infection. NS3-NS4A protease is one of the most known viral targets for anti-HCV therapeutics (Pawlotsky and McHutchison, 2004; Pawlotsky, 2006).

3.1.4.3.4. NS3-NS4A PROTEASE

The NS3-NS4A protease is also important in the HCV lifecycle. It cleaves HCV polyprotein at the NS3/NS4A, NS4A/NS4B, NS4B/NS5A and NS5A/ NS5B junctions. The central region of NS4A acts as a cofactor of NS3 serine protease activity, helping in its stabilization, localization at the ER membrane as well as cleavage dependent activation, particularly at the NS4B/NS5A junction (Bartenschlager et al, 1995; Lin et al, 1995; Tanji et al, 1995).

3.1.4.3.5. NS3 HELICASE-NTPASE

The NS3 helicase-NTPase domain consist of the 442 C-terminal amino acids of the NS3 protein is a member of the helicase superfamily-2. The NS3 helicase-NTPase has functions, including RNA-stimulated NTPase activity, RNA binding, and unwinding of RNA regions that has extensive secondary structure by coupling unwinding and NTP hydrolysis (Gwack et al, 1997; Tai et al, 1996). NS3 helicase has been suggested to translocate along the nucleic acid substrate by changing protein conformation during RNA replication, utilizing the energy of NTP hydrolysis.

3.1.4.3.6. NS4B

It is an integral membrane protein comprising of 261 amino acids with an ER or ER-derived membrane localization (Hugle et al, 2001; Lundin et al, 2003). At least four transmembrane domains and an N-terminal amphipathic helix that are responsible for membrane association in NS4B (Elazar et al, 2004; Hugle et al, 2001; Lundin et al, 2003). Out of many functions of NS4B, it acts as membrane anchor for the replication complex (Egger et al, 2002; Elazar et al, 2004). Other properties include inhibition of cellular syntheses (Florese et al, 2002; Kato et al, 2002), modulation of HCV NS5B RdRp activity (Piccininni et al, 2002), induction of interleukin 8 (Kadoya et al, 2005) and transformation of NIH3T3 cell lines (Park et al, 2000).

3.1.4.3.7. NS5A

NS5A, a phosphorylated zinc-metalloprotein of 56-58 kDa that probably plays an important role in virus replication and regulation of cellular pathways. The N-terminal region of NS5A contains an amphipathic α-helix important for membrane

localization in perinuclear membranes and for replication complex assembly (Brass et al, 2002; Elazar et al, 2003; Penin et al, 2004a). There are studies where HCV replicon RNA replication was inhibited by mutations in the NS5A sequence (Elazar et al, 2003) and abolished by alterations of the zinc-binding site (Tellinghuisen et al, 2004). Also, NS5A phosphorylation plays a key role in the viral lifecycle by regulating a switch from replication to assembly. NS5A can interact directly with NS5B, but the mechanism of how NS5A modulates the NS5B RdRp activity is not well known (Shimakami et al, 2004). In addition, NS5A also known to interact with a geranyl geranylated cellular protein (Wang et al, 2005a). This becomes important while considering the assembly of the viral replication complex that require geranyl geranylation of one or more host cell proteins (Ye et al, 2003). Multiple functions are assigned to NS5A based on its interactions with cellular proteins (Tellinghuisen and Rice, 2002). NS5A plays a role in interferon resistance by binding to and inhibiting PKR, which is an antiviral effector of interferon-α (Gale et al, 1998). NS5A also has transcriptional activation functions (Pellerin et al, 2004) and involved in the regulation of cell growth and cellular signalling pathways (Tan and Katze, 2001; Tellinghuisen and Rice, 2002). All these have to be confirmed by in vivo studies.

3.1.4.3.8. NS5B RNA-DEPENDENT RNA POLYMERASE

NS5B forms an α-helical trans membrane domain at C-terminal region that is responsible for post-translational targeting to the cytosolic side of the ER, protein domain which is functional is exposed (Moradpour et al, 2004; Schmidt-Mende et al, 2001). The crystal structure of NS5B reveals that the RdRp has a classical "fingers, palm and thumb" structure formed by its 530 N-terminal amino acids (Ago et al, 1999; Bressanelli et al, 1999; Lesburg et al, 1999). Interactions between the fingers and thumb subdomains resulted in completely encircled catalytic site which ensures synthesis of positive- and negative-strand HCV RNA (Lesburg et al, 1999). The RdRp is also another important target for the development of drugs against HCV (Di Marco et al, 2005; Pawlotsky and McHutchison, 2004; Pawlotsky, 2006). Interactions between NS5B and cellular components have also been reported. The NS5B C-terminus can interact with the N-terminus of hVAP-33, and the interaction may play a crucial role in the formation of the HCV replication complex (Gao et al, 2004; Schmidt-Mende et al, 2001). NS5B also reported to bind cyclophilin B, a cellular peptidyl-prolyl cis-trans isomerase that apparently regulates HCV replication through modulation of the RNA binding capacity of NS5B (Watashi et al, 2005).

3.1.5. HCV virion structure: The lipoviral particle

HCV particles are enveloped viruses containing core proteins forming a capsid around the viral genome. The envelope is derived from the host cell's endoplasmic reticulum (ER) upon biogenesis, and incorporates two separate viral glycoproteins, E1 and E2, which mediate binding and entry into the host cell. The most outstanding characteristic of HCV particles however, is that they are inextricably bound to serum lipoproteins as lipo viral particles (LVPs) (Andre et al, 2002).

3.1.6. Antibody to Hepatitis C Virus

HCV, which is a major public health concern does not have vaccine available so far and the immunity against HCV is not well understood. The critical gaps in understanding the correlating factors of protective HCV immunity remains a blockade in the design of anti-HCV vaccines and novel immunotherapeutic (Trucchi C et al, 2016). vaccination is considered the most effective means of eradicating viral infections (Walker CM et al, 2015), a prophylactic HCV vaccine is an urgent, unmet medical need (Hagan LM et al, 2013). Almost 20 – 40% spontaneous recovery in case of HCV infection (Thomas DL et al, 2009) suggests that induction of an efficient HCV-specific natural immunity can control the infection. Protection against persistent HCV infection is associated with a vigorous T-cell response (Cashman SB et al, 2014). However, the widely accepted key role is played by of neutralizing antibodies (nAbs) (Dustin LB et al, 2014; Walker CM, 2017). This point was proved by demonstrating that natural clearance correlates with the early development of nAbs (Osburn et al, 2014), and with nAbs that exhibit distinct epitope specificity (Ndongo N et al, 2010). The characterization of monoclonal HCV-neutralizing antibodies, combined with crystal structures of the HCV envelope protein E2, which is the target of most HCV-nAbs, has provided valuable information regarding the E2 antigenic landscape (Kong L et al, 2013; Khan AG et al, 2014). Recent studies have demonstrated that the early appearance of broadly neutralizing antibodies (bnAbs) is associated with spontaneous clearance (Osburn WO et al, 2014). Interestingly, bnAbs also protect against HCV infection in animal models (Morin TJ et al, 2012).

3.1.7. Viral Load

Treatment-naive persons with hepatitis C virus (HCV) infection usually have viral loads around 10^5–10^6 IU/mL (Zeuzem S et al, 1996; Fytili P et al, 2007; Barreiro P et al, 2015). Viral loads <400 000–800 000 IU/mL have been referred to as low viral loads (Zeuzem S et al, 2006; Hartwell D et al, 2011; Pearlman BL et al, 2014; Bulteel N et al, 2016) and have been associated with higher proportions of spontaneous viral clearance (Bulteel N et al, 2016; Scott JD et al, 2006), slower liver disease progression

(Ijaz B et al, 2011; Hisada M et al, 2005; Adinolfi LE et al, 2001), improved response to interferon-based treatment (Pearlman BL and Ehleben C, 2014; Zeuzem S et al, 2006), and more successful treatment of liver cancer (Shindoh J et al, 2013).

Viral loads <600 IU/mL (Fytili P et al, 2007) and <5000 IU/mL (Hoefs JC et al, 2012) have been referred to as "very low viral loads" (VLVLs). There is no much information regarding the prevalence of VLVL in HCV in treatment-naive persons. First time HCV antibody reactive samples have viral loads ≤3000 IU/ml in 3% of the samples tested. The sensitivity is low for HCV antigen testing to detect VLVL, the commercially available HCV antigen test had a detection limit of 3000 IU/mL (Freiman JM et al, 2016; Chevaliez S et al, 2011; Ottiger C et al, 2013).

3.1.8. Molecular Biology of Hepatitis C Virus and its Genotypes

Similar to that of other RNA viruses, HCV circulates in infected individuals as a population of closely related but diverse viral sequences which is referred to as quasispecies. Heterogeneity of the HCV genome is a consequence of mutations during viral replication, which is mainly due to the error-prone viral RNA polymerase and the lack of an associated repair mechanism. Different HCV isolates display significant nucleotide sequence variability depending on the genomic region. The E1 and E2 regions are highly variable, whereas the 5' UTR is the most conserved (Bukh J et al, 1995; Simmonds P, 2004; Bukh J et al, 1992, Hijikata, M, 1991; Weiner A J et al; 1991; Cha T A et al, 1991; Han J H et al, 1991).

Hepatitis C Virus infection can lead to acute and chronic Hepatitis which can progress to liver cirrhosis and HCC. There is substantial diversity in nucleotide sequence, with 68 - 79% overall sequence similarity among strains (Davis GL, 1999). The accumulation of mutations in the viral genome over time has led to the emergence of multiple HCV genotypes. Seven major genotypes (GTs) have been recognized to date, the complete genomes of which differ from each other by at least 30% at the nucleotide level (Simmonds P et al, 2005; Smith DB et al, 2014; Murphy DG et al, 2015; Bukh et al, 1993). Genotypes 1–4 and 6 contain multiple subtypes that typically differ by 15%–25% and display high genetic variability, whereas GT5 has 1 subtype identified (Smith DB et al; 2014). In 2006, a novel HCV GT was identified in a patient originating from the Democratic Republic of Congo, which was later classified as HCV GT7a with subsequent identification of GT7b (Smith DB et al, 2014; Murphy DG et al, 2015; Bukh et al, 1993; Schreiber J et al, 2016). High genetic variability is the cause of obstacle for vaccine development and also for effective antiviral therapy,

which is influenced by different viral strains. The efficiency of antiviral treatment is measured by the rate of sustained virological response (SVR) and genotype and subtype information is of higher clinical importance, which is defined as the rate of persistent viremia 24 weeks after the end of antiviral therapy, is greatly impacted by genotype and subtype distribution (Gower E et al, 2014).

HCV genotypes display different geographic distributions worldwide (Simmonds P et al; 2005). Determination of the HCV genotype is now part of medical practice for pre-treatment in patient management. Genotyping is also useful for investigating outbreaks of infections and for understanding the epidemiology and virological features of this virus. Several methods targeting different regions of the HCV genome have been used for assessing genotypes. The most accurate method is to sequence an appropriate coding region that is divergent enough to allow the discrimination of types and subtypes (Nolte FS, 2001; Pawlotsky JM, 2002). The three most studied regions are the core, E1, and NS5B (Bukh J et al, 1995).

HCV can be classified to seven major genotypes and 80 subtypes (Smith DB et al, 2014; Kuiken C and Simmonds P, 2009; Kato N, 2000). HCV genotypes show changes in patterns of geographical distribution and response to antiviral therapy. Variations in gene sequences is used to make subtypes (Kuiken C et al, 2008). Genotypes 1, 2, and 3 are distributed globally. In contrast, genotypes 4, 5, and 6 are more concentrated to specific regions. Genotype 4 and subtype 5a are mainly found in Middle Eastern countries and the northern part of South Africa, respectively. Genotype 6 is mainly found in China and Southeast Asia. The estimated prevalence of HCV infection in India is approximately 0.5%–2.0%, with GT3 being most common (Panigrahi AK et al, 1997, Das BR et al, 2002). Despite the low prevalence of HCV, India with its large population accounts for a significant proportion of the global HCV burden with approximately 12–18 million people infected (Dhiman RK, 2014). Significant variability in prevalence has been described across Indian geographical regions (Sievert W et al, 2011; Welzel TM et al, 2017). The State of Punjab in northwest India has among the highest rates of HCV infection in India, estimated to be between 3.2% and 5.2%, predominantly GT3 (Dhiman RK et al, 2016).

The genetic variation in Hepatitis C Virus (HCV) is due to accumulation of mutations due to the error prone nature of RdRp and long association of virus with human population (Smith DB et al, 1997). Recombinant HCV strains are described due to intra and inter-genotyping (Hedskog C et al, 2015).

Genotyping based on HCV 5'UTR is enough for clinical purpose as subtyping is not essential. The reliable and standard method to determine genotype and subtypes is sequencing and phylogenetic analysis using HCV NS5B region (Laperche S et al, 2005; Nakano T et al, 2012; Golemba MD et al, 2013). Sequencing of the HCV genes regions which are divergent enough to differentiate genotypes and subtypes is considered as most accurate method (Weck K, 2005; Smith DB et al, 2014).

Vaccine against HCV is not yet developed, but different treatment options and increased cure rates attained with the development of direct acting antivirals (DAA) (D'Ambrosio R et al, 2017). These DAA therapies are genotype specific although there are some pan-genotype HCV treatments available (Tong L et al, 2017; WHO, 2018). Therefore, genotyping is a crucial tool for the therapeutic management of HCV infection and diverse technological advances led to development of methods for genotype determination.

3.2. Clinical history of Hepatitis C Virus Infection

HCV causes inflammation and fibrosis in liver and may develop as a subclinical condition over years. Infection begins as acute and usually asymptomatic during early stages (Blackard J. T et al, 2008). In most untreated cases, long term infection progresses into chronic infections and gradually develops liver fibrosis which then leads to cirrhosis, liver damage, and hepatocellular carcinoma (HCC) (Hajarizadeh B et al, 2013). Persistent infection may rely on rapid turnover of virus and continuous cell-to-cell spread and lack of vigorous T-cell immune response to HCV antigens. The HCV turnover rate can be quite high with replication ranging between 10^{10} to 10^{12} virions per day, and a predicted viral half-life of 2 to 3 hours (Neumann AU et al, 1998).

3.2.1. Acute Hepatitis C infection

Acute hepatitis C infection is defined as the initial period of 6 months after acquiring the infection. The patient may not have clinical signs or symptoms of acute hepatitis. Most people clear acute HCV infection in 6 months. It is an early infection with HCV RNA detected and documented HCV antibody seroconversion. Acute infection of HCV is symptomatic or asymptomatic, most patients does not show any symptoms and recognised rarely. In symptomatic acute HCV infection, clinical features resemble that of other viral hepatitis. If symptoms develop this is usually seen within 4- 12 weeks after getting the infection, and may persist for 2-12 weeks. A

minority of those infected have self-limited disease, whereas the majority go on to persistent infection. In transfusion patients, 70-80% is reported to be asymptomatic (McCaughan GW et al, 1992). 20-30% people develop symptoms like malaise, weakness, anorexia and jaundice after 3-12 weeks after exposure to infection (Alter H.J et al; 2000, Thimme R, et al; 2001).

3.2.1.1. Clinical and serological features of Acute HCV infection

HCV RNA can be detected by RT-PCR within 1-2 weeks after initial exposure (Thimme R, et al; 2001, Farci P, et al; 1991). The level of HCV RNA rises rapidly during the first few weeks, and then peaks between 10^5 to 10^7 IU/ml, shortly before the peak of serum aminotransferase levels and onset of symptoms. In self-limited acute hepatitis C, symptoms can last several weeks and subside as ALT and HCV RNA levels decline. In 4-12 weeks after HV infection, patients may have liver cell injury results in elevation of serum ALT levels.

The antibody to HCV, as detected by enzyme immunoassay, becomes positive near the onset of symptoms, approximately 20- 150 (4-12 weeks) days after exposure, with a mean of 50 days (Alter MJ et al, 1992; Barrera JM et al, 1995; Hoofnagle JH, 1997). Window period is the time period from the start of HCV infection until seroconversion. Up to 30% of patients will test negative for anti-HCV at onset of their symptoms, making anti-HCV testing unreliable in diagnosis of acute infection (Farci P et al, 1991). Almost all patients eventually develop the antibody to HCV; however, titers can be low or undetectable in immunodeficient patients. The anti-HCV assay detects greater than 90% of HCV infections after the initial 3 months. A positive anti-HCV cannot differentiate between acute and chronic HCV infection

3.2.2. Chronic hepatitis C Infection

With about 130–170 million infections worldwide, nearly 3 percent of the world´s population is chronically infected with the hepatitis C virus (Lavanchy D, 2009; Shepard CW et al. 2005). 80 million people are living with chronic hepatitis C virus (HCV) infection worldwide (Mohd Hanafiah et al, 2013). Due to the chronic progression of the disease, patients are at increased risk to develop complications such as cirrhosis and hepatocellular carcinoma (Klevens RM et al, 2012). Chronic Hepatitis C infection is marked by the persistence of HCV RNA in the blood for at least 6 months after the onset of acute infection. HCV is self-limiting in only 15%-25% of patients in whom HCV RNA in the serum becomes undetectable and ALT levels return to normal.

Approximately, 75%-85% of infected patients do not clear the virus in 6 months, and leads to chronic hepatitis. Chronic hepatitis C is asymptomatic, most of the times discovered only by routine serologic or biochemical testing (Sievert et al, 2002; Teoh et al, 2004; Sherman et al, 2006).

In individuals with chronic hepatitis C, viral load and elevated serum alanine aminotransferase (ALT) levels may have clinical relevance (Beld M et al, 1998; Mateescu RB et al, 2006; Al-Quaiz MN et al, 2003). When parenchymal liver cells are damaged, aminotransferases leak from the liver into the blood, resulting in elevated levels of these enzymes in the bloodstream. The exact definition of the normal levels of serum ALT activity is crucial for screening and follow-up studies in hepatitis C infection (Mohamadnejad M et al, 2003; Prati D et al, 2002). It should be noted, however, that half of the untreated patients with chronic HCV infections display normal or minimally elevated serum ALT levels (Puoti C et al, 2000; Shiffman ML et al, 2006).

3.2.2.1. Progression to Liver Fibrosis

In persisting Hepatitis C virus infection, the rate of progression of liver fibrosis varies. The natural course of disease progression from chronic hepatitis C infection to cirrhosis, HCC, and death. The liver biopsy is the gold standard for the grading and staging of chronic hepatitis C. The activity of liver disease or grading is measured by the number of mononuclear inflammatory cells present in and around the portal areas, and by the number of dead or dying hepatocytes. Liver Fibrosis and stage of liver fibrosis (structural liver damage) is variable in chronic HCV infection. In mild cases, fibrosis is restricted to the portal and periportal areas. More changes are defined by the fibrosis that extends from one portal area to other which is also known as bridging fibrosis. Cirrhosis develops in approximately 10% to 15% of individuals with chronic HCV infection. There are other external and host factors that can increase the risk of liver disease progression. The major external risk factor is chronic alcohol use for the progression of chronic hepatitis C to cirrhosis and HCC.

3.2.2.2. Long Term Complications: Cirrhosis and HCC

The progression to cirrhosis in majority of cases is clinically silent, and some patients are not known to have hepatitis C unless they show any complications of end-stage liver disease or HCC. The complicating features of decompensated cirrhosis includes, development of ascites, upper gastrointestinal bleeding secondary to varices or portal hypertensive gastropathy, hepatorenal syndrome and hepatic encephalopathy.

Approximately, 10% - 20% of chronic HCV infections advance to end-stage liver disease over one or two decades. Extrahepatic manifestations can occur during chronic HCV infection or cirrhosis, but HCC appears to develop only after cirrhosis is established.

3.2.3. Spontaneous clearance of HCV infection

Hepatitis C virus (HCV) infection spontaneously clear in about 15–45% of infected individuals. There factors that influence spontaneous HCV clearance are unidentified. The two distinct outcomes of acute infection are spontaneous viral clearance and progression to chronic infection (55–85% of subjects) (J. M. Micallef et al, 2006; J. Grebely et al, 2006; NIH, 2002). Patients who clear HCV spontaneously are identified by testing reactive for antibody to HCV (anti-HCV), but absence of detectable HCV-RNA (Strader et al, 2004). In those who develop chronic infections (anti-HCV positive/HCV-RNA positive) progression to fibrosis, cirrhosis, end stage liver disease, and hepatocellular carcinoma can occur (NIH, 2002, L. B. Seeff, 2002; L. B. Seeff, 1997).

3.2.4. Occult HCV Infection

Occult hepatitis C virus (HCV) infection (OCI), is defined as the presence of HCV RNA in hepatocytes or peripheral blood mononuclear cells but HCV RNA is undetectable in the serum. The name was first described in 2004 (Castillo et al, 2005). There are two types of OCI, seronegative OCI where anti HCV antibody is reported to be negative and HCV RNA also reported as negative and, seropositive OCI where anti HCV antibody is positive and HCV RNA is reported to be negative. It is also called secondary occult HCV infection. Liver biopsy is the gold standard for the diagnosis of OCI by detecting HCV RNA in hepatocytes. But liver biopsy is not available in resource limited settings and it carries risks, like bleeding or inadvertent puncture of other organs. Therefore, most of the studies made the diagnosis of OCI by testing PBMCs. Diagnosing using PBMCs may underestimate the exact prevalence of OCI.

One of the studies provides suggestion regarding the absence of anti HCV antibodies and RNA in the serum is that a mutation impacts the virus encapsidation capacity or the formation and release of virions into blood circulation. This leads to low levels of viremia that are frequently below the detection range of assays.

HCV, being a positive stranded Virus, the replication requires the synthesis of a complementary strand of RNA, called the negative strand or antigenomic HCV RNA. It is assumed that the presence of the antigenomic HCV RNA strand in plasma indicates ongoing viral replication. 84% patients with OCI had antigenomic HCV

RNA strands present in their hepatocytes. In the follow-up study they investigated the PBMCs as sites of HCV viral replication in 18 patients with OCI (Castillo et al, 2005). While the liver is the main site of virus replication, it can also take place at extrahepatic sites, such as in the PBMCs. In that study, the antigenomic HCV RNA strand was present in 61% of the patients. This percentage of HCV replication in the PBMCs of patients with occult HCV infection was similar to that found in the PBMCs of patients with chronic hepatitis C. In addition, the ratio of HCV positive to negative strands in PBMCs was similar to the ratio for a virus replicating in vivo. These findings suggested that patients with OCI have ongoing viral replication.

3.3. Epidemiology

Hepatitis C Virus (HCV) infection seems to be endemic in many parts of the world, with an estimated gross prevalence of 3%. However, there are reported geographic and temporal variation in the incidence and prevalence of HCV infection. A prevalence data that is, with age-specific criteria, there are three distinct transmission patterns identified. In countries with the first pattern, most infections are found among persons 30-49 years old, indicating that the risk for HCV infection is greatest in the relatively recent past (10-30 years ago) and primarily affected young adults and injection drug use (IDU) is the predominant risk factor for HCV infection. In countries with the second pattern, most infections are found among older persons, consistent with the risk for HCV infection having been greatest in the distant past. In countries with the third pattern, high rates of infection are observed in all age groups, indicating an ongoing high risk for acquiring HCV infection. In countries with the second or third patterns, unsafe injections and contaminated equipment used in healthcare-related procedures appear to have played a predominant role in transmission. Much of the variability between regions can be explained by the frequency and extent to which different risk factors have contributed to the transmission of HCV. Because different strategies are required to interrupt different patterns of HCV transmission, determining the epidemiology of HCV infection in areas where that information has not yet been assessed is critical for developing appropriate prevention programs (Wasley A and Alter MJ, 2000).

3.4. Anti-Viral Treatment

A sustained virologic response (SVR) to antiviral therapy is defined by normal alanine aminotransferase (ALT) activity and negative HCV RNA detection in serum for 6 months after treatment withdrawal. The aim of antiviral treatment is long term

elimination of HCV from the blood which prevents progression of liver disease and reduces the risk of HCV associated complications. For a period of 10 years the standard care of HCV treatment was the combination of pegylated interferon-alpha (Peg-IFN) and the guanosine analog ribavirin (RBV). In 2011, first DAAs, the HCV NS3/4 protease inhibitors (PI) boceprevir and telaprevir were to be approved for the treatment of HCV genotype GT1 infection in combination with pegIFN/RBV. At this time the combination initiated a new era in the treatment of chronic hepatitis C and significantly improved sustained virologic response (SVR) rates. Based on large number of clinical trials, guidelines for response guided therapy (RGT) were established, focussed on the optimization of treatment duration and the prediction of treatment outcome on the basis of HCV RNA viral load monitoring and are applied during routine management with Peg-IFN/RBV and first-generation PI-based triple therapy regimens.

3.4.1. Interferon based treatment regimen

Subcutaneous injection of IFN-α thrice a week was just the treatment option until 1998. When the treatment was extended upto 48 weeks, the cure rate as only 15-20% (Carithers and Emerson, 1997; Poynard et al, 1996; Tine et al, 1991). Combination therapy of IFN-α and ribavirin during 24-48 weeks increased SVR rates to 30-40% (McHutchison et al, 1998), and it was found to be more effective (Manns et al, 2001). Half-life of IFN-α was improved by pegylation (addition of PEG) and so the dosage can be once a week. SVR rates in combination therapy is different in various genotypes, ~45 % for genotype 1 and up to 80 % for genotypes 2, 3, 5 and 6 (Antaki et al, 2010). But, IFN-α therapy came with many side-effects including flu-like symptoms, gastritis/gastroenteritis, pruritus, and even severe depression and suicidal ideation. The main adverse effect of ribavirin is hemolytic anemia. Taken together, these side-effects led 10 % to 20 % of all patients to withdraw prematurely from IFN-α and ribavirin combination therapy (Manns et al, 2006).

3.4.2. Direct Acting Antivirals (DAAs)

The commencement of direct-acting antivirals (DAAs) lead to sustained virological response (SVR) in more than 90% of all HCV infected individuals (Feeney ER et al, 2014; Pawlotsky JM, 2014). DAAs are now recommended by WHO and many other HCV treatment guidelines (WHO, 2014). DAAs will not only enhance SVR rates, but also make comprehensive HCV management algorithms and allow smaller health facilities to manage HCV-infected individuals (Soriano V et al, 2013).

HCV therapy partake a new beginning in 2011 when DAAs for Genotype 1 got approval. It includes boceprevir/ telaprevir which targets NS3-4A, oral administered. This was combined with IFN-α/ribavirin led to a triple therapy which improved viral cure upto 70%. The limitations for this included severe side effects and was available for Genotype 1 patients only (Bacon et al, 2011; Jacobson et al, 2011; Poordad et al, 2011; Zeuzem et al, 2011). By 2014-15 HCV therapy entered a new phase by the introduction of sofosbuvir (NS5B nucleotide analogue), daclatasvir/ledipasvir (NS5A inhibitors).

In 2014-2015 the second generation of oral DAAs completely revolutionized HCV therapy. Sofosbuvir (NS5B nucleotide analogue) and daclatasvir or ledipasvir (NS5A inhibitors) with or without ribavirin for 12 or 24 weeks attained SVRs upto 90 % and beyond. These new interferon-free all-oral regimens are well tolerated and present very few side effects (Afdhal et al, 2014a; Afdhal et al, 2014b; Sulkowski et al, 2014).

3.5. Diagnosis of HCV

3.5.1. Screening of Hepatitis C Virus Infection

Hepatitis C Virus exposure is identified by performing a screening assay for anti-HCV antibodies, though active viral infection is diagnosed by RT-PCR. The Laboratory diagnosis for the detection of HCV infection is primarily based on antibodies against recombinant HCV polypeptides in body fluids using enzyme immunoassays (EIAs) or chemiluminescence immunoassay (CIA) techniques. The diagnostic methods became available in 1990. Since the discovery of HCV (Choo, Q.-L, 1989), significant progress in the development of serologic tests for the detection of antibodies to HCV has been made. The HCV genome encodes a single long polyprotein of approximately 3011-3033 amino acids which is processed into structural and nonstructural proteins with the following gene order: 5'-C-E1-E2-p7-NS2-NS3-NS4A-NS4B-NS5A-NS5B-3' (Lindenbach and Rice, 2005). Three generations of screening EIAs are developed for the detection of antibodies against different epitopes of these proteins. The first-generation HCV EIAs (EIAs 1.0) was targeted to the Nonstructural region 4 (NS4) using c100-3 epitope (Kuo G, 1989). The sensitivity of these EIAs was low and false positive rate as high. The sensitivity and specificity were low with EIAs 1.0 (Alter HJ, 1992. The seroconversion in patients with acute HCV infection is not detected util 3 months or longer after infection (Van

der Poel CL et al, 1994). The second-generation assay (EIAs 2.0) in 1992, which is more sensitive and specific incorporated additional antigens from NS (C33c) and structural (c22-3) proteins. It can detect HCV antibodies in 20% more patients and 30 - 90 days earlier than EIAs 1.0 (Alter HJ, 1992). The window period for seroconversion came down from 16 weeks to 10 weeks by using EIAs 2.0 and it has 95% sensitivity. The third generation EIA (EIA 3.0) established in 1996 that added a fourth antigen (NS5) to those in EIAs 2.0 (Uyttendaele et al, 1994). EIA 3.0 detected antibodies an average of 26 days earlier in 5 of 21 individuals with transfusion-transmitted HCV (Barrera JM, 1995) and 97% sensitivity, which is slightly higher than EIAs 2.0 (Kao JH, 1996). These tests are based on four recombinant HCV antigens c22-3, c100-3 5-1-1 and c33c(Core, NS3, NS4 and NS5 sequences). It increases sensitivity and specificity, and also shortens the period to first detection of anti-HCV antibodies in the course of infection (Colin C et al, 2001). In third-generation assays, the HCV-antibody window period is approximately 58 days (Busch M P et al; 2005). In addition, false-positive results may occur in patients with autoimmune diseases and in neonates born from mothers with chronic HCV infection (Krajden M; 2000). The Ortho HCV 3.0 ELISA third-generation system with enhanced Sample Addition Verification (SAVe) is an anti-HCV test kit that contains three recombinant antigens: c22-3, c200 and NS5: the HCV recombinant protein c200 is encoded by the putative NS3 and NS4 regions of the HCV genome.

In developing countries like India, WHO recommends the use of 3rd generation HCV EIA kits. Several commercial kits which employ the structural and non-structural antigens i.e, core, E1, E2, NS3, NS4 and NS5 are in use. The 3rd generation kits are better than the previous versions with improved specificity and sensitivity. The use of EIA kits in India is limited as it requires expertise in handling and in developing countries like India where the health care resources are already burdened; it becomes very difficult to reach the people (Thakur V et al, 2003).

3.5.2. Polymerase Chain Reaction

3.5.2.1. Developmental History of real time RT-PCR

Molecular Biology technique that amplifies a particular sequence of deoxy ribonucleic acid (DNA) in vitro by a cycling process. DNA is separated into two strands and is incubated oligonucleotide primers and DNA polymerase (Kleppe et al, 1971). The term Polymerase chain reaction (PCR) was first used by Saiki et al, 1985. The difficulty in PCR applications due to the usage of thermolabile Klenow fragment

for amplification, which needed to be added to the reaction after each denaturation step. The crucial development which enabled routine usage of PCR was the introduction of thermostable polymerase from Thermus aquaticus (Saiki et al, 1988). This development together with the availability of thermal cyclers and chemical components, led to the use of PCR as the most important tool for the specific enzymatic amplification of DNA in vitro. The point at which the fluorescence intensity increases above the detectable level corresponds proportionally to the initial number of template DNA molecules in the sample. This point is called the quantification cycle (Cq) and allows determination of the absolute quantity of target DNA in the sample according to a calibration curve constructed of serially diluted standard samples with known concentrations or copy numbers (Yang and Rothman, 2004; Kubista et al, 2006; Bustin et al, 2009).

The other major milestone in PCR utilization was the introduction of the concept of monitoring DNA amplification in real time through monitoring of fluorescence (Holland et al, 1991; Higuchi et al, 1993). In real time PCR, fluorescence is measured after each cycle and the intensity of the fluorescent signal reflects the actual amount of DNA amplicons in the sample at that specific time. In initial cycles the fluorescence is too low to be distinguishable from the background. qPCR can also provide semi-quantitative results without standards but with controls used as a reference material. It this case, the observed results can be expressed as higher or lower multiples with reference to control. This application of qPCR has been extensively used for gene expressions studies (Bustin et al, 2009). There are two strategies developed in paralell for the real time visualization of amplified DNA fragments—non-specific fluorescent DNA dyes and fluorescently labelled oligonucleotide probes (Holland et al, 1991; Higuchi et al, 1993).

3.5.2.2. Conventional PCR

In conventional PCR the template DNA is mixed with DNA polymerase, nucleotides, and other components of the PCR. The DNA template obtained may be from pure cultures, clinical and diagnostic specimens, intact organisms, or environmental samples. If RNA is taken as the template, due to many biological and biochemical differences, first needs to be reverse transcribed to single stranded complementary DNA (cDNA). Thermocycling, which includes denaturation, annealing and extension is performed for a total of 30-45 cycles. In conventional PCR, gel electrophoresis is used to analyse the PCR reaction after it is completed. The PCR product is detected and identified by their size using Agarose Gel electrophoresis (end

point measurement). Conventional PCR is qualitative in nature, the result may be interpreted as negative or positive. This PCR product detection method is time consuming and laborious. These limitations led to the development of real-time PCR, which is also called quantitative PCR (qPCR) or kinetic PCR.

3.5.2.3. Reverse Transcription - PCR

Hepatitis C Virus, an RNA virus can be detected by Reverse Transcription Polymerase Chain Reaction (RT-PCR). RNA viruses (retroviruses) can transcribe their RNA into DNA using reverse transcriptase (RNA dependent DNA polymerase-RDRP) discovered in 1970 (Baltimore, 1970; Temin and Mizutani, 1970). RT-PCR was first described in 1987 (Powell et al, 1987). RT-PCR contains two enzymatic steps: production of a single-strand complementary DNA copy (cDNA) from reverse transcription of RNA, then amplification of the cDNA resulting from the reverse transcription. It may be completed in two separate reactions in two separate tubes (two-tube/two-enzyme), or as two separate reactions in a single tube (one-tube/one or two-enzyme). At least four different RT enzymes are commercially available, HIV-1 –RT from human immunodeficiency virus type 1, AMV –RT from avian myeloblastosis virus, M-MLV–RT from Moloney murine leukemia virus, and recombinant Thermus thermophilus polymerase rTth.

In RT-PCR assays there are many variables that could influence the final result: the yield of extracted RNA; the efficiency of reverse transcription (cDNA synthesis), the efficiency of the PCR amplification; the concentration of deoxyribonucleotide triphosphates (dNTPs), $MgCl_2$ concentration, primers, polymerase, and PCR temperature cycle scheme.

3.5.2.4. Real Time Polymerase Chain Reaction

Principle of real-time PCR is fluorescence probe-based monitoring detection technique which allows detection and documentation during the amplification process. Real-time PCR eliminates post-PCR processing of amplicons. This helps to increase throughput and decrease the chance for carryover contamination. The idea to monitor the PCR reaction in the thermal cycler as it progresses was first realized by Higuchi and colleagues (Higuchi et al, 1992). Reverse transcription (RT) that is followed by polymerase chain reaction (PCR), or RT-PCR is the most commonly used technique for the detection and quantification of various RNA types. The first practical, kinetic PCR technology, the 5'-nuclease assay, was established in 1993 by Higuchi and co-workers by combining exponential PCR amplification with the monitoring of newly

synthesized DNA in each PCR cycle (Higuchi et al, 1993; Heid et al, 1996). Earlier, the accumulation of PCR product could be visualized at each cycle by addition of ethidium bromide (EtBr) to the PCR and by continuously measuring the increase in EtBr intensity during amplification with a charge-coupled device camera (Higuchi et al, 1993). Few years later, commercial platforms were released on the market. The first was the Applied Biosystems ABI Prism 7700 Sequence Detection System, followed by the Idaho Technology LightCycler (Wittwer et al, 1997). There are two methods used to obtain a fluorescent signal from the PCR product. One method involves the use of DNA- specific intercalating dyes such as SYBR Green I to bind to double stranded DNA. The second method is to use fluorescent resonance energy transfer (or Förster resonance energy transfer (FRET)) (Didenko, 2001), FRET occurs by energy transfer between two fluorescent molecules that is donor to an acceptor fluorophore. These molecules are attached to primers, the PCR product or probes such as hydrolysis probes.

Real-time PCR is one of the most sensitive and accurate quantitative method available for gene expression analysis. It has been broadly applied to microarray verification, pathogen quantification, cancer quantification, transgenic copy number determination and drug therapy studies (Klein D, 2002; Bustin SA, 2000; Mocellin S et al, 2003; Mason G et al, 2002). A PCR has three phases, exponential phase, linear phase and plateau phase. The exponential phase is the initial segment in the PCR, in which product increases exponentially since the reagents are not limited. The linear phase is identified by a linear increase in product as PCR reagents become limiting. The PCR finally reach the plateau phase during later cycles due to exhaustion of some reagents but the amount of product will not change. Real-time PCR exploits the fact that the quantity of PCR products in exponential phase is in proportion to the quantity of initial template under ideal conditions (Heid CA et al, 1996). During the exponential phase PCR product will ideally double during each cycle if efficiency is perfect, i.e. 100%. It is possible to make the PCR amplification efficiency close to 100% in the exponential phases if there are optimal PCR conditions, primer characteristics, template purity, and amplicon lengths. Both genomic DNA and reverse transcribed cDNA can be used as templates for real-time PCR. The dynamics of PCR are typically observed through DNA binding dyes like SYBR green or DNA hybridization probes such as molecular beacons (Strategene) or Taqman probes (Applied Biosystems) (Bustin SA, 2000). The fundamental point of real-time PCR is a direct positive association between a dye with the number of amplicons. Plot of logarithm 2- based

transformed fluorescence signal versus cycle number will provide a linear range at which logarithm of fluorescence signal correlates with the original template amount. A baseline and a threshold can then be set for further analysis. The cycle at which the fluorescence rises above the threshold is defined as the threshold cycle, Ct or Quantification Cycle Cq or Crossing point Cp. The higher the starting copy number of the nucleic acid target, the sooner a significant increase in fluorescence will be observed. Amplification data measured as an increase in reporter fluorescence are collected in real time and are analysed by the detection system software. Real-time PCR data are quantified absolutely or relatively. Absolute quantification utilise an internal or external calibration curve to calculate the initial template copy number. In cases where exact copy number to be determined, absolute quantification is important, however, relative quantification is adequate for most physiological and pathological studies. Relative quantification relies on the comparison between expression of a target gene with a reference gene and the expression of same gene in target sample versus reference samples (Pfaffl, 2001).

3.5.2.5. Confirmation of Diagnosis by HCV RT-PCTR

The Polymerase Chain Reaction (PCR) is a rapid and powerful technique for the in vitro amplification of DNA (Mullis et al. 1986). Quantitative nucleic acid testing is very important in making clinical decisions in case of antiviral therapy, and the method used is real time PCR based assay (Drexler JF et al, 2009; Cobb BR et al, 2011).

Detection of Hepatitis C Viral RNA is done by Reverse Transcriptase Polymerase Chain Reaction (RT-PCR) which includes amplification and detection techniques. This method adopted is very sensitive and specific. RT-PCR is of two types, quantitative RT-PCR (qRT-PCR) and qualitative RT-PCR. Quantitative RT-PCR is used in quantitation of mRNA. Real-time PCR is the ability to monitor the progress of the PCR as it occurs. Data is collected throughout the PCR process rather than at the end of the PCR process. In real-time PCR, reactions are characterized by the point in time during cycling when amplification of a target is first detected rather than the amount of target accumulated after a fixed number of cycles.

3.5.3. Limit of Detection/ quantification

In a diagnostic procedure, the critical performance characteristics is related to the lowest amount of analyte detected and quantified. Limit of detection (LoD) and limit of quantification (LoQ) are the parameters that describe these properties. The

Clinical Laboratory Standards Institute (CLSI), defines LoD as the lowest amount of analyte in a sample that can be detected with 95% probability compared to blank, although perhaps not quantified as an exact value (CLSI, 2004). CLSI defines LoQ as the lowest amount of measurand in a sample that can be quantitatively determined with acceptable precision and stated, accepted accuracy, under stated experimental conditions.

3.5.4. MIQE guidelines

MIQE guidelines provide guidance for researchers, reviewers and editors to measure the technical quality of the scientific work established for qPCR (Bustin et al, 2009; Huggett et al, 2013). MIQE represents a set of guidelines that describe the minimum information necessary for evaluating qPCR experiments and give a clear framework from which to conduct validated and reliable quantitative PCR experiments. The purpose of it is to support experimental transparency, promote consistent, comparable, valid and therefore reliable quantitative results. The optimization and validation of the absolute or relative quantification strategies is one major point of the MIQE guidelines with the objective of increasing the credibility of results and helping to insure the integrity of scientific work, with major focus on biological relevance (Bustin et al, 2013; Dijkstra et al, 2014; Dooms et al, 2014; Remans et al, 2014). The two strategies that is performed in quantitative RT-PCR, the concentrations of genes or viral templates may be calculated by absolute or relative quantification.

3.5.5. Absolute Quantification

In absolute quantification the PCR data to input copy number is calculated using a calibration (or standard) curve. Therefore, this calibration curve is used to determine the concentration of the unknown analyte. It is referred to as absolute quantification and would be better to be defined as ‘calibration quantification’. This is because, in this context, the word ‘absolute’ is misleading, as the concentration of the field sample in fact is measured ‘relative’ to the concentrations of the standard samples used in the calibration curve (Svec et al, 2015). The reliability of an absolute real-time RT-PCR assay depends on the condition of same amplification efficiencies for both the native target and the calibration curve in RT reaction and qPCR (Souaze et al, 1996; Pfaffl, 2001; Pfaffl et al, 2002). In absolute quantification approach, a stable standard RNA material is required and it is used to generate the calibration curve, it must have a known concentration. When correctly applied, the calibration curve is

highly reproducible and allows the generation of highly specific, sensitive and reproducible data (Bustin, 2000; Pfaffl et al, 2002; Rutledge and Côté, 2003; Svec et al, 2015).

The external calibration curve model has to be thoroughly validated, as the accuracy, sensitivity, reproducibility and the range of quantification depends entirely on the accuracy of the standards used. There are several difficulties associated with production of an RNA standard. The standard RNA design, synthesis, determination of exact concentration and assured stability over long storage times is not straightforward. At low concentrations, RNA is highly sensitive to degradation and therefore, needs storing in a good buffer, an RNAse free environment and responsible handling by the personnel. The stability of RNA standard material of low concentration (e.g. lower than 100 molecules) is particularly critical for high reproducibility (Reiter et al, 2011). The low template copy input in the assay results in higher than in the range of higher copy number (Pfaffl and Hageleit, 2001; Rasmussen, 2001). At very low copy numbers, under 20 copies per tube, the random variation due to sampling error (Poisson's error law) becomes significant (Peccoud and Jacob, 1996; Rasmussen, 2001). But it is exactly in this variable region that target quantification is of high interest for molecular diagnostics eg., detect RNA viruses or bacteria at low plasma concentrations, early after infection, or to quantify rare transcripts in limited sample material.

The dynamic range of the calibration curve can be up to seven orders of magnitude from 10^1 to 10^8 standard molecules, but at least five 10-fold dilutions may be used depending on the stability of the used RNA standard material (Pfaffl and Hageleit, 2001; Fronhoffs et al, 2002; Reiter et al, 2011). A suitable RNA standard material, commercially synthesized RNA may be used or in vitro transcribed RNA, recombinant RNA, universal standard/reference material or alternatively a transcriptome with known concentration of the mRNA or microRNA transcript of interest (Pfaffl and Hageleit, 2001; Cronin et al, 2004).

A significant drawback associated with RNA based calibration curves is that they are subject to the variability of the reverse transcription reaction (RT), which increases the variability of the calibration curve especially at low concentrations (Reiter et al, 2011). Another problem when using an RNA quantification procedure is due to the impact of RNA secondary structure. In contrast to naturally occurring RNA, isolated from biological samples, artificial RNA standard material is highly homogeneous, uniform in length and sequence motifs. Natural biological samples

contain a high percentage of sub-fractions, e.g., ribosomal RNA (rRNA 85-90%), transfer RNA (tRNA ~ 5-10%), messenger RNA (mRNA ~ 1-5%) and various families of noncoding RNAs eg., microRNA, piRNA, siRNA, snRNA, snoRNA, long non-coding RNAs (~ 1-5%). Varying RNA subfractions have an influence on the cDNA synthesis rate and consequently on the validity of the calibration curves but in an unknown manner.

Absolute quantification with external RNA standards requires careful, time-consuming optimization of its precision (by using technical replicates in the same PCR run, reported as intra-assay variation) and reproducibility (using technical replicates in separate PCR runs, reported inter-assay variation) in order to understand the limitations within the given application and fulfil the MIQE guidelines (Pfaffl and Hageleit, 2001; Reiter et al, 2011).

3.5.6. qPCR Equations

The possibilities of qPCR in quantification of viruses, we need to understand the mathematical principle of this method. PCR is an exponential process where the nucleic acid template theoretically doubles after each cycle, if the efficiency is 100%.

$Nn = N0 \times (1 + E)^n$ Equation- 1

Where, N_n is the number of PCR amplicons after n cycles, N_0 is the initial number of template copies in the sample, E is the PCR efficiency that can assume values in the range from 0 to 1 (0–100%) and n is number of cycles. In a scenario where there is initially one copy of the template in the reaction and PCR efficiency is 100%, it is possible to simplify the equation as follows:

$Nn = 2^n$ Equation -2

A calibration curve with 10 fold dilutions if used gives a difference in Cq values between two ten fold serial dilutions may be expressed as

$10= 2^n$ Equation - 3

Then n= 3.322, if this value when used in Eqn (1) is the starting point and the equation is

$E = 10^{-(1/n)} - 1$ Equation - 4

If n= 3.22, Efficiency is 1, 100%

PCR efficiency is therefore a significant factor for the quantification of the target DNA in unknown samples. The reliability of the calibration curve in enabling

quantification is then determined by the spacing of the serial dilutions. If the Log_{10} of the concentration or copy number of each standard is plotted against its C_q value, the E can be derived from the regression equation describing the linear function

$y = kx + c$ Equation - 5

Where x and y, the concentration or amount of target and C_q values respectively, characterize the coordinates in the plot, k is the regression coefficient or slope and c is the intercept. The intercept shows the C_q value when one copy would be theoretically detected (Kubista et al, 2006; Johnson et al, 2013). The concentration or amount of target nucleic acid in unknown samples is then calculated according to the C_q value through Equation (5).

From the definitions above it is evident that C_q values are instrumental readings, and must be recalculated to values with specific units, e.g, copies of organism, ng of DNA, various concentrations, etc, (Bustin et al, 2009; Johnson et al, 2013). However, referral to C_q values in scientific papers is widespread and interpretations based on C_q values can lead to misleading conclusions. Concentrations in qPCR are expressed in the logarithmic scale and C_q differences between 10-fold serial dilutions are theoretically always 3.322 cycles. Therefore, although the numerical difference between C_q 20 and 35 is rather negligible, the difference in real numbers (copies, ng) is almost five orders of magnitude (Log_{10}).

This feature must be reflected in the subsequent calculations. For example, the coefficient of variation (CV, ratio between standard deviation and mean) calculated from the C_q values and real numbers results in profoundly different results. The same applies for any statistical tests where C_q values are used, even for cases where the logarithm of C_q values is used for the normalization of data before the statistical evaluation. The correct procedure should include initial recalculation to real numbers followed by logarithmic transformation.

3.5.7. Factors affect RT-qPCR

Factors that influence RT-PCR assay and that include the quality of extracted RNA, the efficiency of reverse transcription (cDNA synthesis), the efficiency of the PCR amplification, the concentration of deoxyribonucleotide triphosphates (dNTPs), MgCl2 concentration, primers, polymerase, and PCR temperature cycling conditions. The purity of the probe is also important. Mistakes during synthesis or mishandling (eg. exposure to light, possibly also freezing and thawing) can adversely affect probe function.

3.5.7.1. Hydrolysis Probes (TaqMan probes)

The real-time PCR system is based on the detection and quantification of a fluorescent reporter (Heid et al, 1996). Hydrolysis probes are one of the main fluorescence monitoring systems for DNA amplification. They are oligonucleotides (single stranded DNA that contain a fluorescent dye, commonly on the 5´ nucleotide (6-carboxyfluorescein (FAM)), and a quenching dye (6-carboxytetramethylrhodamine (TAMRA)), or ([4-((4- (dimethylamino) phenyl) azo) benzoic acid ester] (DABCYL)), typically located on the 3´nucleotide or attached to a thymidine in a middle position of the probe sequence. The 3´ nucleotide is phosphate to prevent it from being extended as an amplicon by the DNA polymerase. The quencher dye quenches the fluorescence emitted by the reporter. Hydrolysis probes are designed to anneal to an internal region of the PCR substrate, between the two PCR primers. During PCR, when the polymerase replicates a template on which a TaqMan probe is bound, the 5´-3´ exonuclease activity of the polymerase degrades the probe (Holland et al, 1991), resulting in the separation of the reporter and the quencher dye and therefore an increase in reporter fluorescence emission. The probe melting temperature (Tm) should be 5-10 ºC greater than that of the primers. The GC content of the probe should be in the 30-80% range, there should be no Gs at the 5´end, and the probe sequence should not overlap with the primer regions. During the early PCR cycles, the background signal in the well is used to determine the baseline fluorescence across the entire reaction. A fluorescence threshold can be set above the baseline. Fluorescence values are detected during every cycle and plotted against cycle number.

3.5.7.2. Terminology in real-time RT-PCR

Baseline of the real-time PCR applies to the signal produced during the initial cycles of PCR, usually 3-15 cycles, where there is little change in fluorescent signal. The baseline phase contains all the amplification that is below the level of detection of the real-time instrument. Signal is not detectable, but exponential amplification happens during these cycles. Exponential phase contains the earliest signal detected from the PCR, where amplification happens in exponential rate. The number of cycles in this phase depends on the initial template concentration and the quality of the real-time pcr assay.

Threshold in a real-time PCR is the signal level above the baseline and sufficiently low to be within the exponential phase of the amplification curve. The

threshold is the line whose intersection with the amplification plot determines the CT. The analysis softwares adjust the threshold so that a standard curve will have the highest R^2. Quantification threshold (Cq) or Threshold cycle (Ct) is the fractional cycle number at which the fluorescent signal of the reaction crosses the threshold.

Controls should be included to monitor contamination and sensitivity of the assay. No Template Controls (NTCs) should be included in every assay. These controls make sure that the assay does not have contamination. The presence of a PCR inhibitor in the reaction mixture will produce a higher CT value and use of internal controls help to monitor that.

Standard Curve helps to determine reaction efficiency by constructing a standard curve prepared by serial dilution of known calibrator concentration. In this, Cq is plotted on the y-axis and logarithm_{10} concentration is plotted on the x-axis. A standard curve using a known standard concentration should result in a slope, coefficient of determination (R^2) and y-intercept that demonstrate good efficiency, accuracy and sensitivity. E may be derived from a standard curve using the following formula: E = 10(–1/S)-1. E equals the amplification efficiency and S is the slope of the standard curve (which should be a negative slope). The slope should be -3.3 (-3.1 to -3.6), which corresponds to 100% efficiency. The sample concentrations should be within the linear range of the standard curve.

Correlation coefficient R, which is used to analyze a standard curve (ten-fold dilutions plotted against Ct values) obtained by linear regression analysis. It should be ≥0.99 for a good amplification, that reflets the linearity of the standard curve. The values range between zero and –1 for negative correlation and zero and +1 for positive correlations. $\mathbf{R^2}$ coefficient, that is R-squared (also called coefficient of determination). This coefficient only takes values between zero and +1. R2 is used to assess the fit of the standard curve to the data points plotted. The closer the value to 1, the better the fit.

Y-intercept, corresponds to theoretical limit of detection and is useful in comparing different amplification systems and targets used in amplification. Y-intercept is an indication of the sensitivity of the assay and how accurately the template has been quantified. An assay can have an apparently acceptable efficiency of 95–100% but if the y-intercept is substantially higher than 37 or lower than 33, it indicates that the amount of template is not correctly determined. In the case of a high y-

intercept, deterioration of the template may have occurred. Degradation of template is a common result of too many freeze–thaw cycles of the standard or storing the template at too low a concentration without a carrier.

Exponential phase determines the amplification rate on the basis of fluorescence increase. Amplification efficiency is calculated by direct methods, based on either a dilution method or by indirect methods, where the efficiency calculation is based on its fit to a mathematical model, that may be sigmoidal, logistic models or an exponential curve fitting.

In dilution method which is a direct method, the amplification rate is calculated on the basis of a linear regression slope of a dilution series. Efficiency (E) is determined based on equation, $E = 10^{-1/slope}$ (Higuchi et al, 1993; Rasmussen, 2001). In this method, the efficiency ranges from E = 1.60 to values over 2 (Souaze et al, 1996).

In indirect method, efficiency calculation is done from the fluorescence increase in the exponential phase of fluorescence amplification plot in logarithm scale. Fitting can be done visually or more reliably by software applications like LinRegPCR (Ramakers et al, 2003) or DART-PCR (Peirson et al, 2003). The linear regression plot that is drawn from at least four data points, the slope that is calculated from these data points represents the PCR efficiency. So this method is more or less arbitrary and dependent on the selected data points. Resulting efficiencies range between E = 1.45, and E = 1.90, and it seems more realistic. This efficiency calculation method might be good estimator for the 'real efficiency,' because data evaluation is made exclusively in exponential phase.

In **Sigmoidal or logistic curve fit**, efficiency calculation is based on all fluorescence data points from cycle 1 to last cycle (Tichopad et al, 2003; Liu and Saint, 2002; Rutledge, 2004). The benefit of this models is that all data points are included in the calculation process and no background subtraction is necessary. The efficiency will be calculated at the point of inflexion, at absolute maximum fluorescence increase. In the four-parametric sigmoid model equation, $F = Yo + \frac{a}{1+e^{-\left(\frac{X-Xo}{b}\right)}}$ x is the cycle number, f(x) is the computed function of the fluorescence in cycle number x, y0 is the background fluorescence, a is the difference between maximal fluorescence reached at plateau phase and background fluorescence , e is the natural logarithm base, x0 is the co-ordinate of the first derivative maximum of the model or inflection point of the

curve, and b describes the slope at x0 in the log–linear phase (Tichopad et al, 2004). The slope derived by the sigmoidal or logistic models cannot be direct comparison with the real PCR efficiency. The major advantages of this method are that it is easy to perform, is a good estimator for the maximum curve slope with high correlation between replicates ($r > 0.99$) and the algorithm can easily implemented in analysis software. The resulting efficiencies are comparable to the latter method and range from 1.35 to 1.65.

Normalization is an essential part of a reliable qPCR assay as this process controls for changes that can happen in extraction yield, reverse-transcription yield, and efficiency of amplification, thus enabling comparison. The utilisation of reference genes as internal controls is the most common method for normalizing cellular mRNA data. The use of reference genes is commonly accepted as the most appropriate normalization strategy (Hugget J et al, 2005). Normalization involves reporting the ratios of the mRNA concentrations of the genes of interest to those of the reference genes. Normalization with multiple reference genes is preferred. In normalization a control gene that is expressed at a constant level is used to normalize the gene expression results for variable template amount or quality. The incorporation of multiple housekeeping genes that are most suitable for the target tissue is the best way for normalization. In real-time quantitative reverse transcription polymerase chain reaction (qRT-PCR), the specificity, wide dynamic range and ease-of-use made it a method of choice for quantification of RNA. Data normalization is an essential component of the qRT-PCR analysis process, and is the key for accurate qRT-PCR measurement. Genes used for normalization is referred as reference genes. Reference genes represent the most common method for normalizing qRT-PCR data. This targets RNAs that are constitutively expressed, and whose expression does not differ between the experimental and control groups, that can report any variation that occurs due to an error during the experiment. Theoretically, reference genes are ideal as they are subject to all the variation that affects the gene of interest. The problem occurs when a reference gene is used without validation. Reference genes (previously termed housekeeping genes) such as GAPDH (glyceraldehyde-3-phosphate dehydrogenase) are historical carry-overs from RNA measurement techniques that generate more qualitative results

3.5.7.3. qPCR Calibration plot data analysis

Quantitative reverse transcription-polymerase chain reaction (RT-qPCR) has been proven to be the most sensitive method for the quantification of HCV RNA in blood and is used to confirm chronic HCV infection as well as evaluate treatment response to antiviral therapy (Choo Q L et al, 1989; Clarke B, 1997; World Health Organization, 2017).

Calibration curve method is the most accurate method for the efficiency calculation in qPCR (Svec D et al, 2015), and is required in the MIQE guidelines: "Calibration curves for each quantified target must be included with the submitted manuscript, slopes and y intercepts derived from these calibration curves must be included with the publication" (Bustin SA et al, 2009). The calibration curve is made by using serially diluted known nucleic acid concentration and plotting the quantification cycle (Cq) values on the y-axis against the logarithm of the sample concentrations on the x-axis. The efficiency (E) is estimated from the slope of this curve using the classical formula E = 10–1/slope – 1.

There are several other methods developed to estimate qPCR efficiency from single curves and to improve qPCR precision, such as the PCR-Miner (Zhao S and Fernald RD, 2005), LinRegPCR (Rao X et al, 2013), sigmoidal fitting (Spiess AN et al, 2008) and others. All these methods are based on the principle on determining the same basic parameters (called Fq, Cq and E) and "all calculate a target quantity using an efficiency value and a Cq value" (Rujiter JM et al, 2013).

To make the quantitation of HCV RNA comparable among the different assays, the National Institute for Biological Standards and Controls (NIBSC) and the World Health Organization (WHO) developed and certified a uniform standard for measuring HCV RNA in international units (IU) (Pawlotsky, J. M et al, 2000).

3.5.7.4. PCR efficiency determination

The raw PCR data which is not baseline corrected are used in the analysis. Baseline correction was carried out with a baseline trend based on a selection of early cycles of study. The PCR efficiency for each individual sample was derived from the slope of the regression line fitted to a subset of baseline-corrected data points in the log-linear phase using LinRegPCR (Ramakers C et al, 2003).

Serial dilution method to determine a mean PCR efficiency is a common practice for the calculation of mean PCR Efficiency, it is calculated from the slope of the serial dilution standards using the equation E = 10[1−slope]. This results in values

ranging from E = 1.0 (minimum value) to E = 2.0 (theoretical maximum and optimum efficiency) (Higuchi et al, 1993; Rasmussen, 2001).

3.5.7.5. Single run PCR efficiency determination based on all cycle data:

Efficiency determination based on complex modelling of the fluorescence data using sigmoidal or logistic algorithms. This method can be applied to each single reactions and therefore each sample can be analyzed individually. The advantage of this model is that all fluorescence data points are included in the calculation process and no background subtraction is necessary (Liu & Saint, 2002; Tichopad et al, 2003). The derived efficiency values obtained after applying mathematical modelling algorithms range between 1.7 and 1.9 and so are not directly comparable to those from the serial dilution method. This difference might be due to the sigmoidal or logistic fitting procedure and could reflect a single biological sample rather than an average estimate between various replicates and dilutions.

3.5.7.6. LinRegPCR

LinRegPCR is a program for the analysis of real time RT-PCR Data. The program uses non-baseline corrected data, performs a baseline correction on each sample separately, determines a window-of-linearity and then uses linear regression analysis to fit a straight line through the PCR data set (Rujiter et al, 2009). From this line the PCR efficiency of each individual sample is calculated. The mean PCR efficiency per amplicon and the Ct value per sample are used to calculate a starting concentration per sample, expressed in arbitrary fluorescence units. Data input and output are through an Excel spreadsheet.

3.5.8. Interpretation of qPCR result

The quantification of nucleic acid concentration in the sample is done by comparing the Cq of the sample with the Cq of different concentrations of standards in the same run or a calibration curve derived using the same lot of reagents. The precision of real-time PCR quantification depends on the quality of the standard curve. The chances of error in quantitative real-time PCR are the measurement threshold, inaccuracy during sample preparation and pipetting mistakes. If the sample contains inhibitors, or if the probe has fluorescence decrease, absence of amplification, erroneously high Ct values or low signal strength may occur. The accuracy of quantitative real-time PCR is also dependent on changes in PCR efficiency. The expected slope for 100% PCR efficiency is 3.3 cycles per tenfold concentration

difference. Real-time PCR results are dependent on the optimal master mix reagents, since the amount of the fluorescent signal can be affected by the correct amount of polymerase, the optimal concentration of dNTPs, MgCl2, primer and probe.

Fluorescence data analysis is usually carried out using the software available in the qPCR machine. qPCR machine subtracts the baseline fluorescence, set a Cq based on threshold cycle, that is the number of cycles required to reach the threshold cycle (Bustin et al, 2009). PCR Efficiency is derived from the standard curve (Rasmussen, 2001). There are several methods available to analyse amplification curves (Ramakers et al, 2003; Zhao and Fernald, 2005; Tichopad et al, 2003; Peirson et al, 2003; Lievens et al, 2012; Rutledge and Stewart, 2008; Spiess et al, 2008; Ruijter et al, 2009). Calibration Plot was prepared for each lot of RT-PCR reagent and its Data analysis was done was done to calculate PCR Efficiency and slope of the plot.

RT-PCR fluorescence Amplification Plot Data analysis with the four parameter characteristics of the sigmoid plot was analysed for each amplification plot. The four parameter characteristics of the 10 IU/µl standard from a high efficiency calibration plot sample was done. Data analysis of other HCV concentrations and influences on them by the sample were done when required.

The test contains an internal control (IC), which is added to each test sample before processing to monitor the integrity of sample processing and amplification and thereby eliminate false negative results. The IC is an RNA transcript with primer regions identical to those of the HCV target and a unique probe region. Second, the TaqMan HCV quantitative test uses standards calibrated in, and thus reports results in, international units (IU)/ml. The IU is defined by a standard solution prepared from a clinical specimen that, by international agreement, is defined as containing 100,000 IU/ml. As other test developers adopt the IU/ml as a unit of measurement, comparisons of assay sensitivity, dynamic range, and precision will be possible.

3.5.9. Data Analysis and Reporting

Data analysis of qPCR is important in reporting a valid result. A standard curve using a defined template provide slope, coefficient of determination (R^2) and y-intercept that demonstrate good efficiency, accuracy and sensitivity. The baseline and threshold should be properly set. The amplification curves should demonstrate exponential amplification and be within the detection limits of the instrument. Quality controls are included to check for contamination and sensitivity of the assay.

The Cq (Ct) is defined as the cycle when sample fluorescence exceeds a chosen threshold which is above baseline fluorescence. The reporter signal is normalized to a reference dye by dividing the raw fluorescence of the reporter by the fluorescence of the passive reference, to compensate for minor well-to-well variation. This value is referred to as the Rn, the normalized reporter signal. When the background value has been subtracted from the Rn, then this value is referred to as delta (Δ) Rn, the normalized fluorescence value corrected for the background. XY plots with the log template amount as the x value and the cycle threshold (Ct) as the y value. A line representing the best fit is calculated for a standard curve using the least squares method of linear regression: $y = m x + b$ where y = Ct, m = slope, x = log10 template amount, and b = y-intercept. The coefficient of determination, r^2 should also be noted. Assay efficiency is based on the slope of the line, calculated by the formula: Efficiency = [10 (–1/slope)] – 1.

Efficiency is primarily an indication of how well the PCR reaction has proceeded. The integrity of the data fit to the theoretical line is described by the R^2. This is a measure of the accuracy of the dilutions and precision of pipetting. The y-intercept is an indication of the sensitivity of the assay and how accurately the template has been quantified.

A perfect assay would have a slope of –3.32 (100% efficiency), a y-intercept between 33 and 37 cycles and an r2 of 1.00. The slope of the line increases (becomes more negative), the efficiency decreases, the y-intercept increases and the sensitivity of the assay suffers because more starting copies are needed before the detection limit is reached or more cycles are required to detect the same number of template molecules.

3.5.9.1. Four parameter sigmoid model qPCR data analysis

In comparison with linear quantitation methods, sigmoidal models are developed for non-linear fitting of the RT-PCR data, very commonly using Boltzmann or logistic sigmoidal function (Tichopad A et al, 2003; Liu W et al, 2002; Rutledge RG, 2004). The advantage of non-linear fitting is that PCR efficiency is not a constant but a variable that changes during cycles of PCR, with maximum efficiency in the exponential phase of the reaction and which declines in later cycles of the reaction when reagents get depleted, thus leading to the sigmoidal curvature. In non-linear fitting, calculation of threshold fluorescence, cycle-dependent efficiency (E_{cyc}) and estimation of the starting template amount (F_0) is possible. The sigmoidal

qPCR models are four-parameter models that define ground fluorescence, slope at inflection point, difference between maximum fluorescence and groung fluorescence and Cq at inflection point. These parameters of logistic curves describe the qPCR data usually well and supersede other models like Gompertz and Chapman (Zhao S et al, 2005).

PCR data can be fitted with the four-parameter model, which suggests symmetry in the upper and lower part of the curve, that results in the similar curvature on both sides of the inflection point. The two problems posed in that situation is firstly, it is not clear that qPCR curves can be assumed to be symmetric. Secondly, which is important for the quantification aspect, is that fitting four-parameter models with symmetry as an inherent constraint onto asymmetric data will consequently lead to suboptimal fits and suboptimal estimation of parameters (Van der Graaf PH et al, 1999).

The effect of application of logistic and also log logistic five-parameter models to qPCR data, in which the fifth parameter takes a possible asymmetrical structure of the data. Asymmetry of the lower and upper part of the sigmoidal curve (in respect to the inflection point) is the main feature that discriminates the five-parameter models from the four-parameter models. When four-parameter sigmoidal models are fitted onto many datasets, the fitted curves are not optimal at the different phases of an amplification curve. The fifth parameter have large impact on the sigmoidal curvature of the fit. The use of the five-parameter models is better as asymmetry of qPCR data seems to be an inherent characteristic and absolutely symmetric qPCR data rarely occur. The efficiency estimation and reproducibility using five-parameter models are significantly better than four-parameter models.

3.5.10. Verification/ Validation

The term verification is defined as confirmation through the provision of objective evidence, that specified requirements have been fulfilled by FDA and ISO (Code of Federal Regulations. 2010; International Organization for Standardization, 2007). This term is used by CLIA specifically to relate to confirmation that the laboratory using a test can replicate the manufacturer's performance claims when the test is used according to the package insert.

The term validation used by FDA and ISO is defined as confirmation by examination and provision of objective evidence that the particular requirements for a

specific intended use can be consistently fulfilled (Code of Federal Regulations. 2010; International Organization for Standardization. 2007). The World Health Organization (WHO) defines validation as “the action (or process) of proving that a procedure, process, system equipment or method used works as expected and achieves the intended result” (CLSI, 2008).

The information that should be recorded includes identity of the analyte, purpose of the examination and goals for performance, performance requirements (detection limit; quantification limit; linearity; sensitivity; measurement precision, including measurement repeatability and reproducibility; and selectivity/specificity, including interfering substances and robustness), specimen type, required equipment and materials, calibration procedures, step-by-step instructions for performing the examinations, quality control procedures, interferences, calculations, measurement uncertainty, reference intervals, reportable interval, alert/critical values, test interpretation, safety precautions, and potential sources of variation. In addition, for each validation study, acceptance/ rejection criteria, results obtained, control and calibration procedures, data analysis, performance characteristics determined, comparison of results with other methods, factors influencing results, carryover when applicable, and interferences or cross reactivity should be reported (International Organization for Standardization, 2007; Westgard JO, 2008).

Performance specifications for laboratory-developed tests must be established for the following characteristics: accuracy, precision, analytical sensitivity, analytical specificity to include interfering substances, reportable range, reference intervals (normal values), and any other characteristics required for test performance (Code of Federal Regulations, 2009).

3.5.11. Reportable range

CLIA uses the term “reportable range” to refer to the span of test result values over which the laboratory can establish or verify the accuracy of the instrument or test system measurement response. Laboratories may quantitatively report only results that fall within the reportable range. Reportable range and other terms, such as measuring interval, analytical measurement range (AMR), and linear range, are used interchangeably to refer to the same performance characteristic of quantitative assays (CLSI, 2003; Westgard, 2008). In practice, it is common to refer to the “linear range,” and laboratories generally use a linearity experiment to determine the reportable range

for a test (CLSI, 2003; Westgard, 2008). It is not mandatory that a method provide a linear response, but a linear response is desirable since test results that are in the linear range are considered to be directly proportional to the concentration of the analyte in the test samples (CLSI, 2003; Westgard, 2008). The boundaries of the reportable range are the lowest and highest analyte concentrations that generate results that are reliably produced by a test method without dilution of the specimen (CLSI, 2003). The lower limit must also be clinically relevant and acceptable for clinical use (CLSI, 2004). The lower limit of linearity is frequently referred to as the lower limit of quantification (LLOQ) and the upper limit of linearity as the upper limit of quantification (ULOQ). The upper limit of linearity may be restricted by the highest available concentration in a sample or by the saturation of the signal generated by the instrument.

3.5.12. Precision

The term "precision" refers to how well a given measurement can be reproduced when a test is applied repeatedly to multiple aliquots of a single homogeneous sample (FDA, 2001). Precision is defined as the "closeness of agreement between independent test/measurement results obtained under stipulated conditions" (IOS, 2006). When considering precision, it is important to remember that a measurement may be very precise (replicates have the same result) but not very accurate (the real value is much different). The ideal assay is both precise and accurate. Precision (also referred to as random analytical error) is related entirely to random error caused by factors that vary during normal operation of the assay

3.6. Quality Control

The concepts of Quality Assurance (QA) and Quality Management (QM) where first introduced in Laboratory by Belk and Sunderman in the late 1940s/early 1950s in an effort to help reduce the high number of diagnostic errors observed in relation to the handling and testing of patient specimens which ultimately could have an impact on patient care. Quality Management System (QMS) which is entitled to support the whole diagnostic process that is, preanalytical, post analytical and also the verification, validation and implementation phases of the diagnostic assays used within the molecular biology laboratory.

By the execution of quality principles, new quality term is introduced into clinical virology in recent years is Total Quality Management (TQM). In the clinical virology laboratory, TQM provides a different description for the incorporation of all

quality parameters and development of quality culture followed by all laboratory personnel. Then the aim of the laboratory transforms to, not only to provide correct results, but also ensures that the appropriate test is performed on the appropriate specimen, the accurate result is obtained and interpreted, and provided to the right patient within a meaningful time frame and using the errorfree procedures. The laboratory should ensure confidentiality, the safety of the patient, and also provide a mechanism for continuously monitoring and improving of the diagnostic service.

Clinical molecular biology laboratories and the testing services are required to be accredited which helps the clinical laboratory to exhibit the competence and reliability of the services provided to everyone in the healthcare environment and to doctors who routinely utilize the testing service. Clinical molecular Biology laboratories gain accreditation to the Internationally recognized standard ISO 15189, developed specifically for the medical laboratories involved in laboratory testing and examination. In some countries, laboratories are accredited to the national regulatory framework. The quality management requirements of ISO 15189 are also aligned to those in ISO 9001 which provides a basic standard and quality language across diverse industry sectors.

Quality Management System (QMS) covers all the policies, documented processes, procedures, and records used in order to deliver the diagnostic testing service to the patient under its defined scope of accreditation. Quality Management Documentation used in QMS include the Quality Manual or Services Manual which stipulate the laboratory's quality policy and objectives. It includes the quality control measures and internal quality assurance procedures the laboratory undertakes, as well as the external quality assessment (EQA) schemes, the laboratory is adhered to.

The procedural documents including standard operating procedures (SOPs), equipment operating procedures (EOPs), which describes in detail about specific laboratory activity or how an equipment is to be used, who is authorized to do, also when and where that activity is to be performed or equipment used.

For setting the standards for health systems globally, WHO established internationally accepted reference materials, e.g., international standards (ISs) for nucleic acid testing. The ISs are measurement standards with defined concentrations of specific analytes that enable the comparison of results among different assays and different laboratories. These reference materials initially were prepared from viremic

plasma donations (reflecting the type of sample being tested) and freeze-dried. WHO ISs representing complex biological materials, the WHO took the approach of adopting international units (IU); IU have been used to define potencies of all ISs for Nucleic Acid based assays. An international working group on standardization of genomic amplification techniques (SoGAT) was established in 1995, on behalf of the WHO, and has since been coordinated by the National Institute for Biological Standards and Control (NIBSC) (United Kingdom).

International standards are measurement standards and are assigned an internationally agreed unitage in IU (WHO, 2006). WHO ISs are considered the highest-order, international, conventional calibrators, in accordance with ISO guidelines (Code of federal regulations, 2010). The principal uses of ISs are for the calibration of secondary standards, traceable in IU, and for the evaluation of critical assay parameters such as analytical sensitivities and quantification range, including upper and lower limits of quantification. The preparation and calibration of secondary standards are described in detail (Code of federal regulations, 2010; World Health Organization, 2017).

qPCR has a very significant part in molecular diagnostics due to its ease of use, sensitivity, specificity and lower turnaround time. The qPCR assay kits are calibrated with world Health Organisation (WHO) reference standards and National Institute for Biological Standards and Control (NIBSC) standards and proficiency testing is done with Quality control for Molecular Diagnostics (QCMD).

The essential components include nucleic acid extraction systems, internal controls for quality check during isolation, calibrator standards with known concentrations to evaluate the result, qPCR mix, primer-probe mix and quantitation standards. The reporting scale is in international unit per ml (IU/ml), which gives a more precise and accurate result. The assay performance is made better with adequate sample storage, preparation of high-quality nucleic acids, good quality reverse transcription primers and probes and correct for statistical data analysis. For the exceptional performance of a molecular diagnostic laboratory, the sample extraction, separated pre and post PCR analysis areas that maintains unidirectional workflow. The lab should be on regular cleaning and fumigation procedures that helps to prevent cross contamination. The lab must be strictly using biosafety level 2 cabinets, calibrated pipettes, aerosol barrier tips. Appropriate room temperatures and sample storage

facilities are crucial for maintaining proper quality control. The lab personnel responsible must be trained in GLP practices.

Good quality sample used for nucleic acid extraction is crucial in quality management and to obtain optimal results. Inappropriate sample storage can increase chance of inhibition, other microbial contamination and nucleic acid degradation.

Quality management and quality assurance (QA) program is composed of quality control (QC), external quality assessment (EQA), standard operating procedure (SOP) and competency assessment (CA). It is regulated by certification processes like ISO 15189 (ISO15189, 2012). QC focuses on the intrinsic performances of tests in laboratory, reviewing the performance (specificity & sensitivity), regular maintenance of all used materials, the constant quality of reagents, negative and positives controls (Arora DR, 2004). QC is insufficient (Bartlett RC et al, 1994), especially because they do not include pre- and post-analytical steps (Kalra J, 2004; West J et al, 2017; Plebani M, 2006).

EQA, which includes external and proficiency testing (PT) with samples sent by reference nodal laboratories to be analyzed and described (Arora DR, 2004). Audits give an idea about the structural dysfunctions and possible points of improvement. Both external audits and PT provide valuable information on the better functioning of the laboratories but are limited by their rare occurrence.

PT has shown several limitations which can only partially evaluate the pre- and post-analytical steps (Shahangian, 1998); for example, PT samples that come in modified forms (e.g. dried, synthetically produced, pre-treated as with serum samples instead of whole blood), can prevent their inclusion into normal lines of sample handling. PT is not available for all the different tests offered in laboratories (Greub et al, 2016). It has been shown that their recognition as EQA can lead to falsely reassuring results because of the extra caution given in their processing (Reilly et al, 1999; Boone et al, 1982); indeed, samples labeled as EQA were shown to provide more reliable results than EQA submitted blindly (Kumasaka et al, 2001). Competency assessment (CA) identifies the ability of the laboratory personnel to complete their work effectively, in good adequacy with SOP.

3.6.1. Preanalytical Conditions in Sample collection

Blood and its components, serum and plasma are among the most common samples received in molecular laboratories. Most of the samples obtained may contain

anticoagulants, therefore awareness about the possible confounding effects of each anticoagulant and selection of the proper one has a very important role in ensuring the accuracy of reports. Anticoagulants used may adversely affect the analytical results. There are some reports implying that heparin, if not completely removed during extraction, can inhibit enzyme-based molecular tests (Beutler et al, 1990; Al-Soud and Radstrom, 2001; Schrader et al, 2012). It has been shown that even low concentrations of heparin may suppress DNA amplification although the inhibition of heparin on PCR using large amounts of DNA may be not significant (Bonger et al, 2010; Yokota et al, 1999; Neumaier et al, 1998). But there are other studies that disagree with the effect of heparin as a significant inhibitor of PCR reaction for intracellular RNA. Overall, it is recommended to avoid usage of a heparinized sample as much as possible in molecular assays, but in certain situations such as only one sample or emergency states, a heparinized sample may not be rejected.

3.6.2. Quality Management in Molecular Diagnostics

3.6.2.1. Sample storage

Transportation and storage have a very significant role in the quality of the clinical specimen and therefore the accuracy and outcome of the laboratory result. The diagnostic assays require strict conditions of sample collection, transportation, storage, and processing because of the unstable nature of viral nucleic acids (Jose M et al, 2005), especially viral RNAs (D Candotti et al, 2003). Storage Conditions of samples may affect the stability of nucleic acids and its ability to detect viral nucleic acid, especially at lower viral concentrations. Instability of viral nucleic acids are due to decay mechanisms. Due to the conserved nature of 5′-untranslated region (5′-UTR) (B. Hoffman et al, 2011) of hepatitis C virus (HCV) it is used as targets in many commercial HCV RNA detection kits. But, 5′-UTR undergo unique decay mechanisms due to its secondary structure. The 5′-UTR includes a region of the HCV internal ribosome entry site element (D. Pineiro et al, 2012), which can be hybridized with the liver-specific microRNA (miR-122), to unlock and switch the 5′-UTR to an open structure (R. Diaz-Toledano et al, 2009), and the RNA secondary structure can also melt with increasing temperatures to an open conformation (F. Narberhaus et al, 2006). The opened conformation induces the exposure of the 5′ end of the 5′-UTR to exonuclease-mediated degradation (Y. Li et al, 2013). The HCV 5′-UTR strand can fold into several stem–loop secondary structures (N. Beguiristain,

2005), and the loop structures are more sensitive to cleavage by endonuclease than are the stem structures (R.M. Smith et al, 2002). As described in the previous paragraph, the 5′-UTR of HCV RNA is prone to cleavage into short pieces of different lengths (Y. Li et al, 2013; R.M. Smith et al, 2002). So, there are chances of RNA cleavage during sample collection, handling and storage which may lead to decreased sensitivity in detection and may give a false negative result using the diagnostic assay kits.

3.6.3. Molecular Diagnostics Reporting

The investigation of HCV diagnosis starts with serological assays for detecting antibodies to HCV followed by molecular assays for detecting HCV RNA. Initial diagnosis of HCV infection is classically done by serologic methods either by determining anti HCV antibody by EIAs or by immunoblot assays and by determining the presence of HCV RNA. The introduction of simple rapid immunoassays has significantly reduced the risk of HCV transmission, but concern remains for patients in high-risk groups (Clemens JM et al, 1992; Somi MH et al, 2014; Nafishah A et al, 2014; Atrah HI et al, 1995). Studies have shown that false negative results in rapid tests might arise in patients who are severely immunocompromised such as those co-infected with HIV (van der Helm J et al, 2013), in patients on hemodialysis, IDUs, thalassaemic. So, molecular detection by reverse transcription polymerase chain reaction (RT-PCR) remains the best method for proper diagnosis.

Testing algorithm for laboratories that provide anti-HCV testing is that they should perform initial screening with an FDA-licensed or approved anti-HCV test according to the manufacturer's instructions. If the screening test is non-reactive, samples can be reported as non-reactive for anti-HCV antibody. If the screening-test is reactive, samples require supplemental serologic or nucleic acid testing according to the testing algorithm. They can opt for supplemental testing 1) based on screening-test reactive s/co ratios, or 2) on all specimens with screening-test reactive results. For screening-test reactive samples that require supplemental testing, the anti-HCV result should not be reported until the results from the supplemental tests are available.

Certain situations exist in which the HCV RNA result can be negative in persons with active HCV infection. As the titre of anti-HCV increases during acute infection, the titre of HCV RNA declines (Busch MP et al, 2000). Thus, HCV RNA is not detectable in certain persons during the acute phase of their hepatitis C, but this finding can be transient and chronic infection can develop. In addition, intermittent

HCV RNA positivity has been observed among persons with chronic HCV infection (Alter MJ et al, 1992; Thomas DL et al, 2000; Larghi A et al, 2002). Therefore, in the absence of additional clinical information, the significance of a single negative HCV RNA result is unknown, and the need for further medical evaluation is determined by verifying anti-HCV status.

A negative HCV RNA result also can indicate resolved infection. Among anti-HCV positive persons who acquired their HCV infection as older adults (aged >45 years), 15% - 25% apparently resolve their infection; this proportion is higher (40% - 45%) among anti-HCV positive persons who acquired their infection as children or younger adults (Alter HJ et al, 2000). To determine if HCV infection has resolved, a negative HCV RNA result should be demonstrated on multiple occasions; however, such follow-up testing is indicated only in persons with serologically confirmed anti-HCV positive results.

3.6.4. Internal Controls

The internal control (IC) is a second heterologous amplification system to identify possible PCR inhibition. Internal control is a nontarget DNA sequence present in the same sample assay matrix, which is coamplified along with the target sequence. In a PCR without an IC, a negative amplification results mean that there is no target sequence present in the reaction. But it can be due to the reaction inhibition/ due to malfunction of thermal cycler/ incorrect PCR mixture/ poor DNA polymerase activity/ or the presence of inhibitory substances in the sample matrix (Radstrom et al, 2003).

3.6.5. Clinical Bioinformatics in Molecular Diagnosis

Direct DNA sequencing (Sanger et al, 1977) is a relatively inexpensive and routine procedure in molecular biology. DNA sequence data are used to identify organisms, genes or mutations, or to confirm laboratory testing. Comparing sequence data from one or more samples to each other and to a known “reference” alignment is a standard procedure. Evolutionary relationships between samples are elucidated by phylogenetic analyses, which typically involve DNA sequences from many organisms of interest, and from many related samples for comparison. In 1979, the Los Alamos Sequence Database was established by Walter Goad (Kanehisa et al, 1984). With support from the National Institutes of Health, this database was expanded in 1982 and renamed “GenBank” (Bilofsky et al. 1986). Since 1982, the number of nucleotides in GenBank doubles approximately every 18 months (Benson et al. 2015). The

International Nucleotide Sequence Database Collaboration (INSDC) (Karsch-Mizrachi et al. 2012) is a collection of three publicly available nucleotide (DNA or RNA) sequence databases, which synchronize data daily. The collection consists of the DNA Data Bank of Japan (DDBJ, located in Japan), the European Molecular Biology Laboratory (EMBL, located in the United Kingdom) and GenBank (located in the United States of America). Researchers share sequence data with the academic community by submitting sequences to these public databases. This is generally a requirement when sequences are included in their research publication. In addition to nucleotide sequence data, various additional data fields are included with sequence submissions. These fields include the name of the organism from which the sequence data originated, the names of the authors or researchers, a draft publication title, co-ordinates of any coding regions within the sequence, and the date of the submission. If coding regions are specified, the resulting protein translation is stored in the database automatically. Although sequence data submitted to the databases is checked for integrity, no checks are performed on text submitted into the free-form text fields, such as the "Author" or "Note" fields. Data are submitted and extracted from the database in a flat, plain text ("ASCII") file format. Sequence data are typically extracted from the database by issuing a query to the database via the database web-site. Results are displayed on the web-site and can be downloaded in various file formats. As data have been submitted over many years, during which time, sequencing and computing techniques have evolved and improved, the reliability and accuracy of these data can vary. Thus, unavoidable artefacts, errors and inconsistencies may be present in the data.

3.7. Primer design and synthesis

HCV RNA sequence amplification from cDNA synthesised by reverse transcription and Polymerase Chain Reaction (PCR) is the method available to detect HCV viral infection (Weiner et al, 1990; Kato et al, 1990; Zonaro et al, 1991; Garson et al, 1990). But due to the genetic heterogeneity in different genotypes and subtypes (Okamoto et al, 1990; Takamizawa et al, 1991; Hijikata et al, 1990; Enomoto et al, 1990) may lead to false negative result during Reverse Transcription Polymerase Chain Reaction due to primer and template mismatch. So the primers were designed from the conserved regions of HCV genome (Miller and Purcell, 1990; Kubo et al, 1989; Bukh et al; 1991). Thus primer selection becomes an important factor in the sensitive and specific detection of HCV RNA (Table 3.1).

Primer 5.0 is used to predict potential primers from nucleic acid sequences from the HCV database. Primers are designed for 3 regions, UTR most conserved region, Core E1 structural region and NS5B region non-structural region. Good primer and probe design is a prerequisite for qPCR. Complete or partial genomes from GenBank for the target sequences are first aligned using BLAST, and by using reference sequence as query (http://www.ncbi.nlm.nih.gov/blast/). Areas of sequence conservation are identified, and the degree of representativity for all sequences in the alignment, or selected groups included in the alignment. The positions of highly conserved stretches were selected for primers and probes All primers and probes were designed after evaluation using the on-line software Oligo Analyzer 3.0. (http://www.idtdna.com/analyzer/Applications/OligoAnalyzer/) When designing the oligonucleotide, primer and probe self- and inter complementarity should be avoided. Especially, complementarity of the probe to the 3´ end of the primer should be avoided. The primer 3´ ends should be free from repetitive sequences and highly degenerate sequences. The stability of the interaction between oligonucleotides (primers and probe) and a complementary target determines the melting temperature (Tm), which is the temperature at which 50% of a given oligonucleotide is hybridized. The Tm of oligonucleotides depends on length and GC content. The latter ideally should be between 40-70%. Tm as determined using oligo analyzer 3.0 was used as an initial guide. Primers were designed with the goal of minimizing the free energy (åG) of primer-primer and primer-probe interactions.

3.7.1. NCBI sequence submission

3.7.1.1. GenBank

GenBank (Benson DA et al, 2013) is a comprehensive public database of nucleotide sequences and supporting bibliographic and biological annotation. GenBank is built and distributed by the National Center for Biotechnology Information (NCBI), a center within the National Library of Medicine at the National Institutes of Health, was created in 1988 to develop information systems for molecular biology (Sayers EW et al,2020).

NCBI receives data from three sources: direct submissions from researchers, national and international collaborations or agreements with data providers and research consortia, and internal curation efforts. The U.S. Patent and Trademark Office also contributes sequences from issued patents. GenBank participates with the

European Molecular Biology Laboratory Nucleotide Sequence Database (EMBL-Bank), part of the European Nucleotide Archive (ENA) (Leinonen R et al, 2011; Amid C et al, 2019), and the DNA Data Bank of Japan (DDBJ) (Kaminuma E et al, 2011; Ogasawara O et al, 2020) as a partner in the International Nucleotide Sequence Database Collaboration (INSDC) (Karsch-Mizrachi I et al, 2018). The INSDC partners exchange data daily to ensure that a uniform and comprehensive collection of sequence information is available worldwide. NCBI makes the GenBank data available at no cost over the Internet, through FTP and a wide range of web-based retrieval and analysis services (NCBI, 2013). Details about direct submission processes are available from the NCBI Submit page www.ncbi.nlm.nih.gov/home/submit.shtml) and from the resource home pages (e.g. the GenBank page, www.ncbi.nlm.nih.gov/genbank/).

3.7.1.2. Sequence identifiers and accession numbers

Each GenBank record, consisting of both a sequence and its annotations, is assigned a unique identifier called an accession number that is shared across the three collaborating databases (GenBank, DDBJ, EMBL-Bank). The accession number appears on the ACCESSION line of a GenBank record and remains constant over the lifetime of the record, even when there is a change to the sequence or annotation.

3.8. Genotyping and Phylogenetic Analysis

Phylogenetic analysis has been used to distinguish viral genotypes and/or subtypes from each other, and for subtyping newly isolated strains by comparing them to existing alignments and trees. However, phylogenetic analysis often cannot distinguish between inter-subtype recombinants and new subtypes, as both can branch out between clusters in a similar way. To reveal the mosaic organization of recombinant viruses, new methods that process the genotype in segments along a sequence were designed (Siepel et al, 1995; Salminen et al, 1995; Lole et al, 1999). These methods rely upon multiple alignments of a query sequence and the reference sequences of known viral subtypes. However, the high variability of viral genomes often makes it impossible to align viral sequences automatically. In these cases, the alignments have to be done laboriously by hand.

3.8.1. Phylogenetic reconstruction methods

The numerous phylogenetic reconstruction methods, two algorithms most often used in population genetics, unweighted pair group mean analysis and neighbour-joining (Saitou & Nei, 1987) algorithms.

3.8.1.1. UPGMA

UPGMA, or unweighted pair-group method with arithmetic means, is one of the most widely used and simplest methods of topological reconstruction. Computer simulations suggest that this method performs poorly when the evolutionary rates are not constant, i.e. if we cannot assume a constant molecular clock. The UPGMA method was described in 1973 for constructing taxonomic phenograms. Advantages of this method is that, it is extremely fast and since it averages out the branch lengths, it diminishes associated errors.

3.8.1.2. Neighbour-joining (NJ)

NJ method is one of the minimum evolution methods (Cavalli-Sforza & Edwards, 1967), where the tree with the smallest sum of branch lengths is found. The minimum evolution algorithm originally described is computationally intensive, since it searches the minimum branch length tree among all possible trees. Obviously, the number of possible trees increases with the number of OTUs, and rapidly reaches a number impossible to compute. For this reason, Saitou and Nei in 1987 proposed a heuristic algorithm for this minimum evolution tree and called it neighbour-joining, where the minimum evolution principle is implicit on each step of the algorithm, producing a single bifurcating tree. The neighbour-joining algorithm starts with a star-tree topology and sequentially chooses the pair of OTUs (or neighbours) that minimise the total length of the tree. This process is continued until the tree is completely resolved. It has been shown to perform quite well (that is, it recovers the correct tree most of the time), when unbiased distances are used. Tests of tree reliability Bootstrap test Any given data set, regardless of its phylogenetic signal content, will yield a tree. Thus, one has to be extremely careful when drawing conclusions simply based on a tree. For this reason, various statistical tests have been developed in order to provide estimates of the reliability of phylogenetic trees. The most commonly used statistical test in phylogenies is the bootstrap developed by Efron in 1982. The bootstrap technique uses resampling with replacement and was developed for phylogenetic studies by Felsenstein (1985). In this case the total number of residues is drawn with replacement and all sites have the same probability of being sampled. Since it is a

replacement technique, some sites will be sampled more than once, whereas others will not be sampled.

3.9. Statistics in Molecular Diagnosis

Statistical analysis was performed with SPSS statistical software version 14.0 (SPSS Inc, Chicago, IL, USA) for Windows® and a P-value <0.05 was considered as significantly different. The $\chi 2$-test was used for statistical analysis of non-parametric data. SPSS is the most popular quantitative analysis software program used by social scientists. Made and sold by IBM, it is comprehensive, flexible, and can be used with almost any type of data file. However, it is especially useful for analyzing large-scale survey data. It can be used to generate tabulated reports, charts, and plots of distributions and trends, as well as generate descriptive statistics such as means, medians, modes and frequencies in addition to more complex statistical analyses like regression models. SPSS provides a user interface that makes it easy and intuitive for all levels of users. With menus and dialogue boxes, you can perform analyses without having to write command syntax, like in other programs. It is also simple and easy to enter and edit data directly into the program. There are a few drawbacks, however, which might not make it the best program for some researchers. For example, there is a limit on the number of cases you can analyze. It is also difficult to account for weights, strata and group effects with SPSS.

Measures of Central Tendency, Average measures that describe the central aspects of a data are called averages. An average summarizes all the characteristics of entire mass of data. Most of the items of the series are clustered around the average, so it is called as measure of central tendency. **Arithmetic mean** which is the sum of all the observations divided by the number of observation

Mean = sum of all the observations/ Total number of observations

Median is the value of the middle item of a given series of data arranged in ascending or descending order of magnitude.

Median = value of the item (n + 1)/ 2

Mode is the most frequently occurring value in a sample. A sample with a single mode is referred as unimodal. If it has two mode it is called as bimodal and more modes as polymodal or multimodal. If no mode, it is no modal sample.

A **measure of dispersion** (also called measure of variation, scatter, spread) is to describe the extent of scattering of items around a measure of central tendency. Different types of measure of dispersion used here. **Range** is the minimum and maximum value of the given series of data (Gurumani, 2005). **Standard deviation** is defined as the square root of the arithmetic mean of the squared deviation of the various items from the mean. The mean squared deviation is called the variance. Therefore, the square root of variance is the standard deviation.

Coefficient of variation (CV) is also known as relative standard deviation (RSD). It is a measure of dispersion of a probability distribution or frequency distribution. CV is defined as the ratio of standard deviation to the mean and is expressed in percentage. I t is widely used in analytical chemistry to express the precision and repeatability of an assay.

95% Confidence Interval of Mean is a range of values which can be confident including the true values. A confidence interval for the estimated mean extends either side of the mean by a multiple of the standard error. 95% confidence interval was calculated by multiplying standard error by 1.96 and then identifying the range by adding and subtracting the value from mean.

Frequency Graphs, Histogram is the graphical representation of continuous frequency distribution. The X-axis has the true class intervals, and the Y-axis, the frequencies. The bars are of equal width indicating that the class- intervals are of equal width. The height of the bar is proportional to the respective frequency. Therefore, it may be said that the area (length ×breadth) of each bar is equal to the total of all the frequencies.

Scatter diagram is an easy and simple method for studying correlation between two variables. If X and Y are pairs of variables, the values of the variable X are marked in the X – axis and the values of variable Y are marked in the Y axis. A point is plotted against each value of X and the corresponding Y value. A swarm of dots is obtained, and this is called the scatter diagram. From this scatter diagram we can understand about the correlation between the variables whether it is positive correlation or negative correlation.

3.10. Secondary and Tertiary Structure Prediction

3.10.1. RNA secondary structure prediction

RNAfold web server programme was used to predict the secondary RNA structure of 5'UTR region. The MFE structure of an RNA sequence is the secondary structure that contributes a minimum of free energy. The structure prediction is done using a loop-based energy model and the dynamic programming algorithm (Zuker et al, 1981).

3.10.2. Protein structure prediction

The Phyre2 (**P**rotein **H**omology/analog**Y** **R**ecognition **E**ngine V 2.0) Protein Fold recognition server is used for protein structure prediction (Kelley LA et al, 2015). Phyre2 is a set of tools available on the web to predict and analyze protein structure, function and mutations. The focus of Phyre2 is to provide biologists with a simple and intuitive interface to state-of-the-art protein bioinformatics tools. Some of the most widely used web servers for protein modeling are Phyre2, i-TASSER8, Swiss-Model9, HHpred10, PSI-BLAST–based secondary structure prediction (PSIPRED)11, Robetta12 and Raptor13. I

3.10.3. Bepipred-1.0 Linear Epitope and Kolaskar and Tongaonkar antigenicity scale Prediction

BepiPred predicts the location of linear B-cell epitopes using a combination of a hidden Markov model and a propensity scale method. The residues with scores above the threshold are predicted to be part of an epitope (Larsen et al, 2006). A semi-empirical method which makes use of physicochemical properties of amino acid residues and their frequencies of occurrence in experimentally known segmental epitopes was developed to predict antigenic determinants on proteins (Kolaskar et al, 1990).

3.11. Machines

3.11.1. Biosafety Level 2 Thermofischer scientific

HCV is considered a Biosafety Level 2 (BSL-2) virus, according to the Biosafety in Microbiological and Biomedical Laboratories manual published by the Centers for Disease Control and Prevention. A Class II biological safety cabinet (BSC) is a ventilated containment device found in laboratories around the world. BSCs are used in many applications, including cell culture, pharmaceutical, clinical and microbiological work. Due to the critical nature accomplished inside these commonly

used laboratory products, BSCs are regulated through rigorous standards and compliance. Engineered controls are built into the design of BSCs providing protection to the operator, product and environment.

For a B2 BSC, the air is pulled in at the front aperture creating an air barrier that gives the operator protection. Air is also pulled from an opening at the top of the cabinet that supplies the downflow fans with air. Then the air goes through a HEPA filter and is 100% exhausted through a dedicated duct with an exhaust fan motor. The air is then released into the atmosphere. The purpose of this is to remove toxic vapors that are generated in the cabinet with no recirculation within the BSC. Airflow through a B2 is 100% externally exhausted which means the air that is drawn into the cabinet is 100% exhausted into the atmosphere. None of the air drawn into the B2 for either inflow or downflow is recycled within the airflow system. This is where an A2 differs as it does recycle a portion of its air after filtration – approximately 60% to 70%.

3.11.2. Rotor Gene Q 5plex HRM, Qiagen, Germany

Rotor Gene Q, which enables high precision real-time PCR, end point PCR and high-resolution melt (HRM) analysis. The machine is very well suited for gene expression analysis, genotyping, pathogen detection.

3.11.2.1. Thermal performance of Rotor Gene Q

The sophisticated heating and cooling design helped to obtain optimal thermal and optical uniformity between samples which help in optimal reaction condition and precise analysis. During the run samples are spun continuously at 400 rpm which helps to prevent condensation, removes air bubbles and do not pellet nucleic acid. So, samples need not be spun initially. Heating and cooling of samples happens in a low mass air oven, heating achieved by nickel-chrome element in the lid and cooled by venting the air out through the top of the chamber while ambient air is blown up through the base.

3.11.2.2. Optical system

There are 6 excitation sources and 6 detection filters combined with a short, fixed optical path, the Rotor-Gene Q can be used for multiplex PCR reactions, ensuring minimum fluorescence variability between samples and eliminating the need for calibration or compensation (Table 3.2). Samples are excited from the bottom of the chamber by a light-emitting diode. Energy is transmitted through the thin walls at the base of the tube. Emitted fluorescence passes through emission filters on the side of

the chamber and is then collected by a photomultiplier. The fixed optical path ensures consistent excitation for every sample, which means that there is no need to use a passive internal reference dye such as ROX.

Of the two quantification strategies, absolute and relative, we use the former with external standard plot. qRT–PCR was done with Artus HCV RG RT-PCR kit (Qiagen, Germany) based on Taqman probes by One step RT-PCR on Rotor-Gene Q instrument. Passive reference dye (ROX/Fluorescein) (6 Carboxy-X Rhodamine) for correction / normalisation of fluorescence was not required in Rotor gene Q instrument as there was no difference in fluorescence excitation, emission, and detection between reaction vessels. Master mix is prepared from Hep. C Virus Master A (12 µl) and Hep. C Virus Master B (18 µl) with internal control (2 µl). Add 30 µl of this mix into PCR tube and 20 µl of eluted sample RNA. Correspondingly any one of the Quantitation standards and negative control (Water, PCR grade) was pipetted into other tubes. PCR tubes were placed on the locking ring, enter the details and temperature was optimised at 50 °C. The cycling conditions were entered as 50°C for 30 minutes when the reverse transcription took place, 95°C for 15 minute for initial denaturation, 95°C for 30s, 50°C for 60 s and 72°C for 30s repeated for 50 cycles. After completion of the run, data analysis was done.

3.11.3. Agarose Gel Electrophoresis

Agarose gel electrophoresis is widely used for qualitative analysis of nucleic acid fragments after Polymerase Chain Reaction. The agarose-based technique provides a broad separation range of nucleic acid molecules based on size and charge. During RNA electrophoresis, negatively-charged RNA migrates through the gel towards the anode. The length of RNA molecule determines the migration time. But, secondary structure formation of RNA due to intramolecular base pairing, may delay migration. So, it is recommended to do RNA electrophoresis under denaturing conditions. For detection, RNA within the gel is stained with ethidium bromide or a highly sensitive fluorescent dye (e.g. SYBR Green II or SYBR Gold). These intercalating dyes fluoresce when exposed to light. Ethidium bromide which is a potential mutagen, carcinogen, and teratogen require safety precautions and safety during disposal of these hazardous waste. SYBR-based dyes are more sensitive and less harmful alternative of ethidium bromide. The stained gels are viewed with a transilluminator. A transilluminator system may also include image capture devices,

such as a digital or Polaroid camera, which allow an image of the gel to be taken or printed for further analysis using specific gel analysis software (Sambrook et al, 1989).

3.11.3.1. Gel Documentation

The products of PCR reaction are analysed using Agarose Gel Electrophoresis in which the amplified target sequence can be visualised and the approximate length of the amplified fragment can be detected. There are several methods to detect the amplified nucleic acid fragments like autoradiography, fluorescent dyes or silver staining.

After the separation is complete, the gel is exposed to light of a suitable wavelength; the light emitted by the dye molecules is either viewed directly or captured by image-recording device. As in fluorescent events, the light emitted by the dye is of a longer wavelength than that used to excite the dye. The dye/DNA complex often exhibits enhanced fluorescence relative to the unbound dye, a property of the dye that also leads to greater sensitivity. In recent years the development of more-sensitive fluorescent dyes has been spurred by the rising costs associated with handling radiolabeled nucleic acids. There have also been improvements in imaging devices. Whereas using photographic film and an ultraviolet lightbox was previously the only way to record the images of fluorescently stained gels, charge-coupled device (CCD) cameras now offer greater sensitivity than film, and a number of very sensitive dedicated fluorescent imagers are also available. A serious objection to the use of fluorescent dyes for nucleic acid detection is that they represent a safety hazard and must be handled and disposed of accordingly. It should come as no surprise that molecules exhibiting a high affinity for DNA should have the potential to interfere with DNA function: Most dyes used for detecting nucleic acids are mutagens and are either suspected or confirmed carcinogens. Because it is simple to use and is sufficiently sensitive for most routine procedures, ethidium bromide has long been the standard fluorescent dye for staining nucleic acids in gels. Agarose gels are most conveniently cast and run with buffers already containing the dye at a concentration of 0.5 µg/ml. Ethidium bromide is an intercalating dye: The planar molecule fits with high affinity between adjacent base pairs in the double helix of dsDNA, but it also binds ssDNA and RNA. If dye is included in the gel and running buffer, the progress of the separation can be monitored during electrophoresis by using a handheld UV lamp, but ethidium bromide–stained gels are most commonly viewed by placing them

on an ultraviolet lightbox. The image can be recorded using either a conventional or a CCD camera.

Fig. 3.1. Structure of Hepatitis C Virus

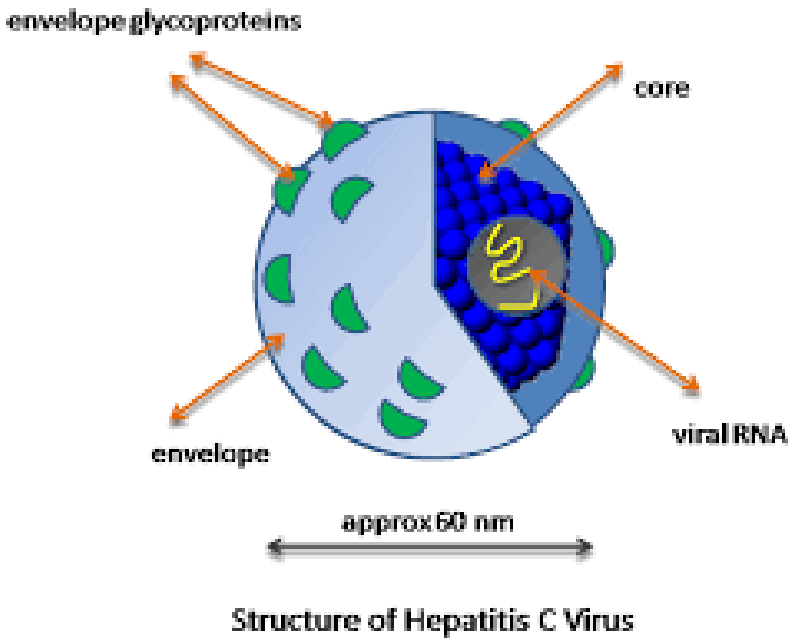

Fig. 3.2. HCV genome and polyprotein (Abdel-Hakeem et al, 2014)

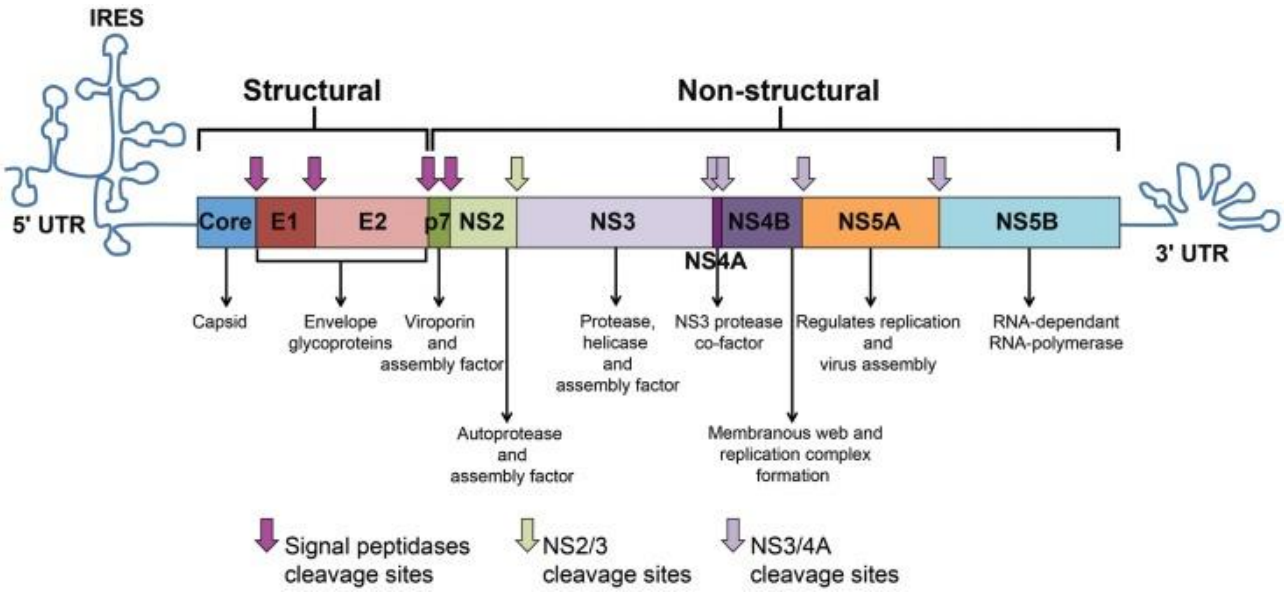

Fig. 3.3. HCV antigenic regions used in serological assays. E, envelope; NS, nonstructural protein; a.a., amino acid sequence of recombinant protein or synthetic peptide antigen. b, Ortho HCV ELISA (version 3.0; Ortho-Clinical Diagnostics, Inc.). c, Chiron RIBA HCV strip immunoassay (SIA; version 3.0; Chiron Corporation). d, p, synthetic peptide. e, Abbott HCV EIA (version 2.0; Abbott Laboratories).

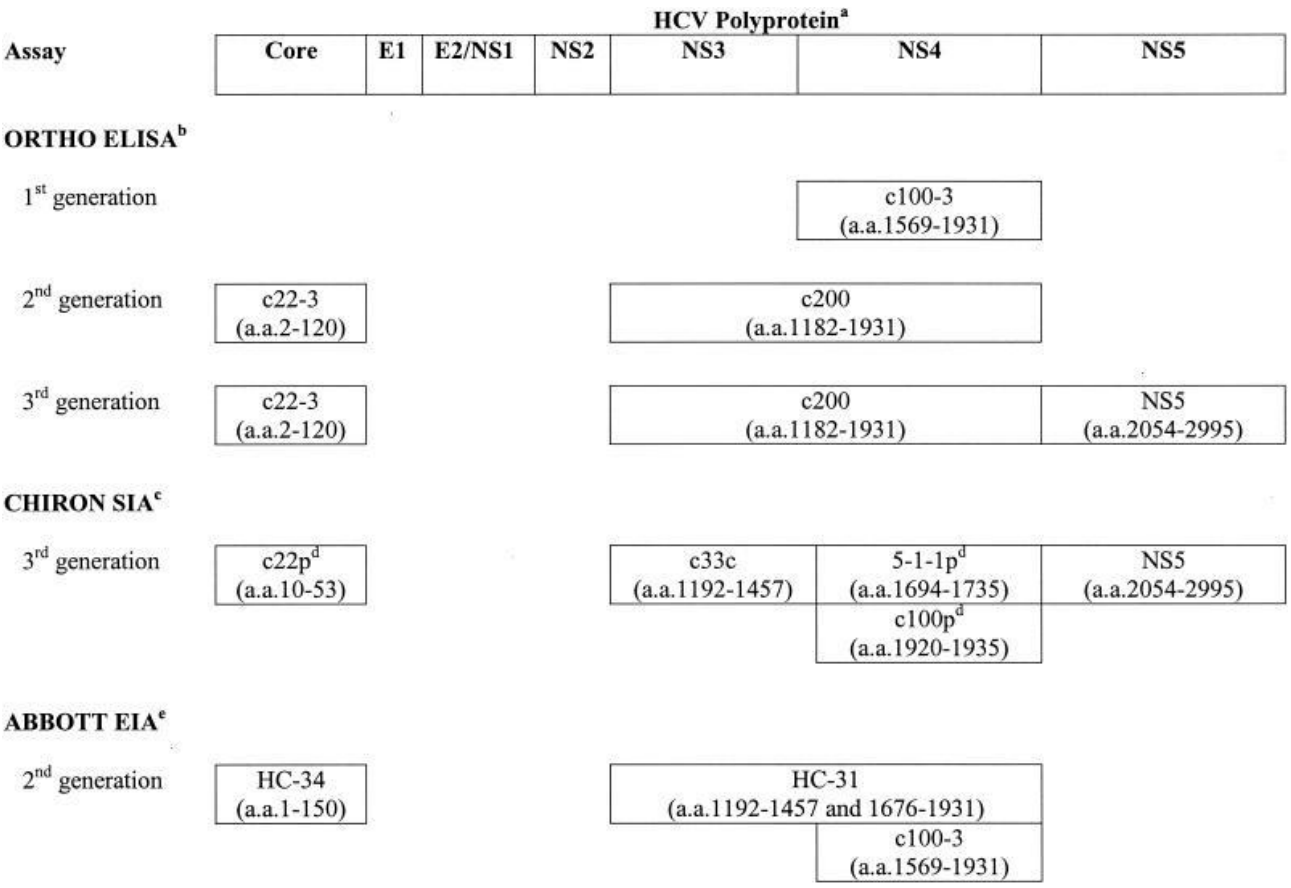

Table 3.1. Size of PCR products with the sequence of primers used in this study

Region	5'UTR	Core E1	NS5B
Length	272 bp	494 bp	263 bp
Forward Primer (5' - 3')	ACTGTCTTCACGCAGAAAGCGTCTAGCCAT	GCAACAGGGAACCTTCCTGGTTGCTC	CATCATGGCCAAGAACGAGG
Reverse Primer (5' - 3')	GGGTGCTTGCGAGTGCCCCGGGAGGTCTCG	TGATGATGAACTGGTCCCCTAC	GTATGATACCCGCTGTTTTG

Table 3.2. Excitation wavelengths, fluorescent probe sources and detection filters in the optical system of Rotor Gene Q

Channel	Excitation (nm)	Detection (nm)	Examples of fluorophores
Blue	365±20	460±20	Marina Blue, Edans Bothell Blue, Alexa Fluor 350, AMCA-X
Green	470±10	510±5	FAM, SYBR Green I, Fluorescein, EvaGreen, Alexa Fluor 488
Yellow	530±5	557±5	JO, VIC, HE, TET, CAL Fluor Gold 540, Yakima Yellow
Orange	585±5	610±5	ROX, CAL Fluor Red 610, Cy3.5, Texas Red, Alexa Fluor 568
Red	625±10	660±10	Cy5, Quasar 670, LightCycler Red640, Alexa Fluor 633
Crimson	680±5	712 highpass	Quasar 705, LightCycler Red705, Alexa Fluor 680
HRM	460±20	510±5	SYBR Green I, SYTO9, LC Green, LC Green Plus+, EvaGreen

CHAPTER 4

MATERIALS AND METHODS

4.1. Study setting, study population and Research Design

The present study was done at Department of Biochemistry, Clinical Biochemistry Laboratory, Amala Institute of Medical Sciences, Thrissur from March, 2017 to March, 2022. The **study population** was the Anti-HCV antibody reactive or clinically suspected patients or patients at risk of contracting hepatitis C virus (HCV) infection selected from Thrissur District, Kerala, India. From this study population**,** EDTA-treated blood samples were obtained for RT-PCR, qualitative or quantitative PCR and genotyping at the Molecular Diagnostic Laboratory at Amala Institute of Medical Sciences, Thrissur, Kerala state, India.

This is an **observational cross-sectional study** (chapters 5, 7, 8, 9) and **observational control study** (chapter 6) of real-time RT-PCR for HCV in RNA isolated from plasma of individuals who were reactive for anti-HCV antibody by the screening immunochemistry assay or suspected to have contacted HCV infection. The control samples used to study the influence were internal controls, quality controls, calibrators/ positive controls and NTC. The study was approved by the **Institutional Research and Ethics Committees** for the research project proposal to DST-SERB, New Delhi from Krishna K Yathi with Jose Jacob as Mentor (Ref. AIMSIEC/37/2017 latter dated 18-05-2017), and for the research proposal for PhD registration of Ann Mary Joseph with Jose Jacob as Guide to Calicut University (AIMSIEC/16/2017 dated 17-01-2017). The DST-SERB project was also approved by IBSC (**Institutional Biosafety Committee**) under Department of Biotechnology (DBT) guidelines dated 27th October 2017. Participants were approached directly by the investigators. The research program and the method of blood sample collection and assay were described to the participants. After including the participants by clinical and preanalytical evaluation, **informed written consents** were obtained and blood samples were collected.

4.1.1. Samples used for RT-PCR (n=1104)

The serum and plasma samples analysed in this study were obtained from the Central Laboratory, and from the In-Patient Departments (IPDs) of Amala Institute of Medical Sciences. A total of 1104 plasma samples were analysed for HCV RT-PCR.

4.2. Selection of participants, Inclusion and Exclusion criteria

The inclusion and exclusion criteria for sample collection and selection of RT-PCR cases for study were related to the preanalytical condition of the patient. Patients with acute tissue damaging diseases such as severe acute infections, accidents (crush injury), surgery and patients undergoing chemotherapy were found to influence the samples for RT-PCR. Samples from patients with chronic inflammation, abscesses and in autoimmune disorders were also found to influence RT-PCR (Satsangi J et al, 1994; Byrnes JJ et al, 1975). These preanalytical conditions were avoided as far as possible, or sample collection was delayed till the disease state subside or was overcome. Blood samples from heparinised patients, eg. dialysis and cardiology patients, were delayed for up to a day or two, or till the next injection of heparin and drugs. Sample collection was avoided soon after intravenous injections of drugs, and in such patients, samples were taken immediately before the next intravenous injection. In all emergency and other unavoidable circumstances, all the above preanalytical criteria were overlooked, but the results of RT-PCR were analysed for analytical or preanalytical influences. The samples included in the study (antibody screening, RT-PCR and nucleic acid sequencing) were from (a) those with reactive or borderline reactive screening tests for anti-HCV antibody above the cut off limits, (b) cases with abnormal liver function, (c) those suspected with HCV infection, such as from blood transfusions, and (d) all those who were suspected to be in the window period of antibody formation.

4.3. Sample collection

4.3.1. Sample collection and preparation for anti-HCV antibody assay

Blood samples were collected in vacuum tubes with clot activator (red capped, 4 ml), mixed, allowed to clot for 10 minutes, centrifuged at 3000 rpm for 5 minutes in a table top centrifuge, serum was separated, and clear serum samples without haemolysis, jaundice, cloudiness and clot particles were screened for the anti-HCV antibody with third generation enzyme immunoassays, against recombinant epitopes of NS5, c22-3, c200 antigens, having high sero-conversion detection rates (Bukh et al, 1992; aHCV reagent pack procedure manual, 2005). The enzyme immuno-assay

detection method was enhanced chemiluminescence methods (Vitros ECi, Ortho Clinical diagnostics, USA).

4.3.2. Sample collection and preparation for RT-PCR

Blood sample was taken with 2-4 ml EDTA-vacutainers (purple-capped), centrifuged at 3000 rpm for 15 minutes in a table-top centrifuge. Sample was collected from individuals after describing the details of the project in vernacular language, the patient information sheet and then getting the signature in the consent form. Plasma sample without haemolysis, jaundice, cloudiness and without clot particles was separated and used for RNA isolation and immediately followed by HCV RT-PCR. Plasma and RNA samples were stored immediately at -80^{0}C, in aliquots.

When screening assays showed anti-HCV antibody levels above cut off limit, quantitative_or qualitative RT-PCR was done for confirming the diagnosis of HCV infection.

4.4. Sample size calculation

Adequacy of sample size for calibrators, quality control samples and for evaluating performance characteristic were based on sample mean and standard deviations (SD) using the equation (nMaster 2.0 software),

$$n = \frac{Z^2_{1-\frac{\alpha}{2}} \text{ X } SD^2}{D^2 \text{ X } \mu^2} \qquad \text{Equation-1}$$

where, D = relative precision (10%); μ = mean; $Z\ 1-\alpha/2$ = desired confidence interval 95% (1.96); n = sample number. For each method of **qualitative evaluation**, we require a minimum sample size of three for **reproducibility** after standardisation. The minimum sample size required for **inter-assay and intra-assay internal controls and quality controls** was fifteen for each. As the SD was very low for calibrators, internal controls and quality control samples, the sample number required was very low. But as a routine practice for validated calibrators sample number, n ≥5, internal control ≥15, quality control ≥15. The variation in the sample number were due to availability of reagents in each lot.

4.5. Anti-HCV antibody Screening assay

The VITROS anti-HCV assay was performed using the VITROS anti-HCV reagent pack, VITROS Immunodiagnostic Products, and anti-HCV calibrator on the VITROS ECi Immunodiagnostic system. Mix samples, calibrator and controls by inversion and bring to 15-30^{O}C before use. The VITROS Anti-HCV assay uses 20 µl sample. An immunometric technique was used which involved a two-stage reaction. In the first stage, HCV antibody present in the sample bound with HCV recombinant antigens coated on the wells. Unbound sample was removed by washing. In the second stage, horseradish peroxidase (HRP) labelled antibody conjugate (mouse monoclonal anti-human IgG) binds to any human IgG captured on the well in the first stage. Unbound conjugate was removed by washing.

A reagent containing luminogenic substrates (a luminol derivative and a peracid salt) and an electron transfer agent, was added to the wells (Summers M et al, 1995). The HRP in the bound conjugate catalyses the oxidation of the luminol derivative, producing light. The electron transfer agent increased the level and duration of the light produced. The light signals were read by enhanced chemiluminescence method by VITROS ECi. The amount of HRP conjugate bound was indicative of the level of anti-HCV antibody present in the sample.

Screening for anti-HCV antibody was done in serum samples using enzyme immunoassays with high sero-conversion detection rates (aHCV reagent pack procedure manual, 2005). The assay was performed in Vitros ECi immunochemistry autoanalyser (Vitros ECi, Ortho Clinical diagnostics, USA) using enhanced chemiluminescence method. When screening assay showed reactivity above the cut off limit, real-time RT-PCR was done for confirming the diagnosis of HCV infection. HCV RT-PCR was done directly, without reactivity to antibody screening assay, in individuals frequently exposed to HCV infection, such as patients on dialysis or repeated blood transfusion. This was done to cover the long window period of HCV infection.

The calibration of the VITROS Anti-HCV test was traceable to an in-house reference calibrator of the manufacturer, which has been assigned values to optimize the clinical sensitivity and specificity of the performance.

4.5.1. Specimen Collection and Preparation - VITROS Anti HCV assay principle

Serum sample was the specimen recommended for the assay. Samples was kept in stoppered containers to avoid cross contamination and evaporation. Disposable tips may be used for samples if manual pipetting was required. Precautions were taken to avoid splashing, aerosol formation or cross contamination. Samples were stored at 22^0C up to 8 hours, if the test was not completed within that time, refrigerate the samples at 2-8^0C. If the sample testing needs shipment and needs more time for testing, the sample was frozen at or below -20^0C. Freeze-thawing of samples was not recommended as it might cause analyte deterioration. Specimens and controls should be handled as if infectious, using standard safe laboratory practices such as mentioned in CLSI Document M29-A. Thoroughly clean and disinfect all work surfaces with a freshly prepared solution of 0.5% sodium hypochlorite in deionized or distilled water.

4.5.2. Calculation of the reactivity and Interpretation of anti-HCV antibody reactivity

Results are automatically calculated by the VITROS Immunodiagnostic and VITROS Integrated Systems. Results may be interpreted from VITROS Anti HCV test upon completion of all testing steps required in the testing algorithm. If the VITROS Anti-HCV Test Result, signal/cutoff was <0.90, it might be interpreted as non-reactive, and the patient was presumed to be not infected with HCV. If the test result is ≥1.00 may be interpreted as reactive for anti-HCV antibody. If the reactivity was 0.90 to 0.99, the it was considered as indeterminate reactivity. CDC recommendations were followed for supplemental testing. Citrated plasma has been shown to lower the signal/cutoff values in some anti-HCV reactive samples.

Calculation of the reactivity of anti-HCV antibody **as a normalized signal**, relative to the cut off value (signal/cut off). During the calibration process, a lot-specific parameter was used to determine a valid stored cut off value for the VITROS Immunodiagnostic and VITROS Integrated Systems. Result = Signal for test sample / Cut off value

4.5.3. Calculation of frequency distribution

Calculation of frequency distribution of sample per unit chemiluminescence signal range (c) divided by sample number (n). Calculation of anti-HCV antibody reactivity per unit chemiluminescence signal (r) was by dividing the sample number by the chemiluminescence signal range, which gives the sample number per unit chemiluminescence range (r, r=n/c). The frequency distribution of the sample per unit chemiluminescence signal will be r/total sample number (N) (Table 8.3).

4.6. HCV RNA Viral Genome Extraction

When screening assays showed anti-HCV antibody levels above cut off limit, RT-PCR was done for confirming the diagnosis of HCV infection. 4 ml of EDTA blood sample was taken from the patient using EDTA-vacutainers, centrifuged and plasma sample, without hemolysis, jaundice, cloudiness and without clot formation was used for RNA isolation.

RNA may be isolated in bulk and in small quantity by manual methods. The first step in RNA isolation was the lysis of the cell using buffers or reagents containing chaotropic reagents (guanidinium isothiocyanate, guanidinium chloride, sodium dodecyl sulphate (SDS), sarcosyl, urea, phenol or chloroform). Denaturation and inactivation of RNases achieved by phenol and chloroform. RNA can be separated from other cellular components by adding chloroform and centrifuging the solution. This separated the solution into two phases, organic and aqueous phases. The aqueous phase contains RNA. RNA was often recovered from the aqueous phase using isopropyl alcohol or absolute ethanol by precipitation.

4.6.1. Chromatographic method for total RNA extraction.

Plasma was processed with a QIAamp Viral RNA Mini Kit (QIAGEN, USA) for RNA isolation. HCV RNA viral genome was extracted from 140 µl plasma separated from EDTA-treated blood collected in EDTA-vacutainers to which 560 µl Buffer AVL (viral lysis buffer) and 5.6 µl carrier RNA were added into a 1.5 ml microcentrifuge tube. Mixed by pulse-vortexing for 15s. Incubate at room temperature (15–25°C) for 10 minutes. Briefly centrifuge the tube to remove drops from the inside of the lid. Add

560 µl ethanol (96–100%) to the sample, and mix by pulse-vortexing for 15 seconds. After mixing, briefly centrifuge the tube to remove drops from inside the lid.

Carefully apply 630 µl of the solution (maximum capacity of column) to the QIAamp Mini column (in a 2 ml collection tube) without wetting the rim. Close the cap, and centrifuge at 6000 x g (8000 rpm) for 1 minute. Place the QIAamp Mini spin column into a second clean 2 ml collection tube (provided), and discard the tube containing the earlier filtrate. Carefully open the QIAamp Mini column, add the remaining of the prepared sample solution and repeat it again to complete removal of the solution in the column. In the next washing step, open the QIAamp mini column, add 500 µl Buffer AW1. Close the cap and centrifuge at 6000 x g (8000 rpm) for 1 minute. Place the column in a clean 2 ml collection tube and discard the tube containing filtrate. Carefully open the QIAamp Mini column, and add 500 µl Buffer AW2 for the second washing step. Close the cap and centrifuge at full speed (20,000 x g; 14,000 rpm) for 3 minutes. Place the column in mew collection tube and centrifuge at full speed for 1 minute to eliminate any chance of AW2 buffer carryover. The washing step was followed by elution in 60 µl Buffer AVE, after one minute of incubation at room temperature, the column was centrifuged at 6000 x g (8000 rpm) for 1 minute. Eluted RNA was stored at -80°C.

4.7. HCV RT-qPCR

HCV quantitative assay was used to determine the number of international units of HCV RNA per millilitre of serum or plasma (IU/mL) in known HCV positive patients. Recently, real time RT-PCR based detection systems have become widely available and were considered as the detection method of choice. The advantages of this technique were that they had a very low limit of detection, and have a broad dynamic range of amplification, thus improving the analytical limit of detection (LOD) of quantitative RT-PCR to 10 IU/mL, and linear quantification up to 10^7-10^8 IU/mL (Hawkins A et al, 1997; Beld M et al, 2002).

RT-PCR inhibition was evaluated by internal controls added to the patients' sample during RNA isolation, during of RT-PCR assay, to the

calibration standards during a run with test sample or standard. **Internal control** (IC) contains a second heterologous amplification system, an unrelated reference gene, **(a) to identify the possible PCR inhibition** in the assays of any HCV template amplification **(b) to monitor assay performance independent of target sequence** in the same assay tubes as the standards, quality control assays and in the HCV patients' sample assay tubes. The fluorescence detection system in the IC was using ROX dye (Channel A fluorescence detection during annealing step) with a fluorescence emission in Orange (excitation at 585 nm, detector at 610 nm). This fluorescence is different from that used for HCV target, 5'UTR, Taqman probe. PCR inhibition is seen by the decrease in maximum fluorescence intensity of more than 10%, with or without increase in Cq of internal control which was around 32 cycles.

Positive Controls and Non-Template Control of the RT-PCR assay: With every patient's sample assay set, there was, in addition, assay tubes for **(a) positive control and/or calibrator** with known template concentrations, **b) and/or quality control (QC) sample assay tube** with HCV target sequence of about 10 IU/µl, and **(c) a Non-Template Control (NTC)** in other assay tubes.

The above assay sets were done to: **(a) monitor the threshold cycle values (Ct or Cq) values of known concentrations of viral load, (b) as a reference for importing and interpreting calibration plot and (c) to calculate initial template concentrations or viral load of the patients' sample.**

The data of Cq and viral load will be used to calculate %CV, z value or the log difference of viral load. These control standards, especially the 10 IU/µl standard, **were also used for studying the influence of the isolated preanalytical sample RNA. NTC** was used along with the sample to get the blank data, and also to catch aerosol contamination.

4.7.1. Delayed Amplification and Theoretical Basis of the term:

It is a term that we have used in this study to define an amplification of RT-PCR in an assay from patients sample where with Cq values of assays often exceed the $\log_{10}$ zero concentration calibration point; Calibration

points being in the $\log_{10}$ scale, antilog of zero calibration plot value was concentration at 1 IU/µl (428 IU/ml of plasma; 535 HCV copies/ml of plasma) of the initial HCV template concentration. As viral load beyond the zero calibration on the x-axis or even 10 IU/µl was found to be significantly influenced by sample characteristics, quantitation was not considered beyond this point. All RT-PCR amplifications beyond this point was verified by PCR product electrophoresis and some of them were also sequenced. The typical Cq value corresponding to 1 IU/µl point was about 35.5 to 36.

4.7.2. Internal Control, Quality Control and Assay Validation of Qualitative and quantitative RT-PCR

Internal controls were used in the assay medium of RT-PCR to find out PCR inhibition and was commonly caused by heparin and other drugs. When there was PCR inhibition (fluorescence intensity less than 90%), there was a negative influence RT-PCR Cq result and the value of the quantitative RT-PCR results were not valid. Internal controls were also used to calculate the %CV of the Cq values.

Quality control: There were no quality control reagents or external quality control reagents of HCV RNA for low viral load from 40 IU/ml to 5,000 IU/ml of plasma available in the market till February, 2020. Therefore, we **made our own quality control HCV reagents from validated samples with low viral load**. Cq <36 was considered for quantitative analysis and Cq >36 was considered only for qualitative analysis. **Quality control reagents** for **very low viral load (100 IU/ml of plasma)** was available in the market (Qnostics, UK) from February, 2020. Quality Control was done with samples that have known concentrations of HCV virus made from samples with low, medium and high concentrations. The %CV of Cq and virus concentrations were estimated from the data.

Internal validation of qualitative RT-PCR was done using PCR product electrophoresis to confirm the size of the expected PCR product. If the PCR product was of the expected size (256 bp) and if there were no other bands, then the qualitative RT-PCR was validated (Fig. 1). RT-PCR samples with Cq values above about 36 was considered only as qualitative RT-PCR.

NTC was also kept along with the sample to get the zero-calibration data during calibration. It was also used along with all patient's samples to detect aerosol contamination.

4.7.3. External Quality Control and External Assay Validation methods

External quantitative RT-PCR quality control was done by **inter laboratory comparisons (ILC) with another NABL accredited laboratory. When** ILC showed a log viral load concentration of <0.5 between the two concentrations (Table 1), it was acceptable performance.

External qualitative validation of RT-PCR: Primers were designed and synthesised, PCR was done and PCR products, after electrophoresis, were sequenced for external sequence comparisons with external database (NCBI) in the external qualitative validation of an RT-PCR assay. Often our PCR products had over 90% sequence homology with NCBI database for 5'UTR sequence and Core/E1.

4.7.4. Analytical Sensitivity of Calibration Plots and Sample Assays

Analytical sensitivity of Calibration plot was calculated from the RT-PCR done after repeated dilution of the 10 IU/µl standard. Analytical sensitivity of Quantitative RT-PCR was identified from the linear calibration plot data analysis, and the four-parameter data analysis of the sample RT-PCR fluorescence amplification data. Even in the linear calibration plot range, when the influence on maximum fluorescence intensity was <10% (fluorescence decrease <10%), it was quantitative RT-PCR and when the influence was >10%, it was qualitative RT-PCR.

4.7.5. Case studies of pre analytical sample influences on HCV RT-PCR amplification

Various pre analytical conditions of the patients were found to be influencing RT-PCR. To study these conditions, the influence of defined pre analytical states of the patient or pre analytical variables on RT-PCR amplification of the calibrator standards were studied.

4.8. Organisation of work and its Flow Sequence

4.8.1. Organisation of study: A. Types of assays and the assay matrix components

The HCV RT-PCR was organized with reference to the **four types of assay tubes**: NTC or blank, calibrators or positive control, QCs and patients' sample. HCV and IC templates with their respective fluorescent probes were in the same assay matrix but with different excitation and emission wavelengths, and detection channels. Total volume of 128 µl of reagents were prepared and 30 µl was distributed into the four types of assay tubes so that concentration of the fluorescent probes was same in each assay tube. If there were more than one of each assay type then the total volume of reagents was increased in multiples of 30 µl.

4.8.2. Organisation of study: B. Differentiating Analytical and Preanalytical influences

The components of RT-PCR assay that would influence the amplification system by themselves might be considered as the following: (i) RT-PCR amplification products of reference gene in IC; (ii) RT-PCR amplification products of HCV template; (iii) RT-PCR influences of non-specific RNA and the possible influences of amplification products of non-specific RNA, and (iv) varying RNA isolated from plasma of different patients might influence the Cq of IC causing higher variations.

The NTC is influenced by (i); the calibrators by (i+ii); the QC samples by (i+ii+iii); the patients' sample might be influenced by (i + ii + iii + iv).

The analytical and pre-analytical influences could be differentiated on the following principles:

a) **The analytical influences** might be considered as the differences in the performance of Cq of ICs in the calibrators and NTC:

- Analytical Bias = mean Cq of calibrator ICs – mean Cq of NTC ICs
- Analytical imprecision = %CV of calibrator ICs – %CV of NTC ICs

b) **The preanalytical influences** might be considered as the differences in the performance of ICs in plasma RNA (patients' sample or QC sample) and the calibrators.

- Pre analytical Bias = mean Cq of ICs in patients' sample – mean Cq of ICs in calibrator
- Pre analytical imprecision = %CV of ICs in patients' sample – %CV of ICs in calibrator

4.9. Types of Samples Collected

(a) Samples **Non-Reactive** for Anti-HCV antibody in **Screening Assay** (anti-HCV antibody below a cut-off <0.90 or negative).

(b) Samples with **Indeterminate Reactivity** for Anti-HCV antibody in **Screening assay** (anti-HCV antibody between 0.90 - 0.99).

(c) Samples **Reactive** for Anti-HCV antibody in **Screening assay** (anti-HCV antibody above a cut-off ≥1.0 or positive).

(d) Samples **Reactive** for Anti-HCV antibody and **PCR Positive**

(e) Samples **Reactive** for Anti-HCV antibody and **PCR negative**

(f) Exposure (or high risk) group for HCV infection (Dialysis patients): Samples Non-Reactive for anti-HCV antibody (≤0.89) but **PCR positive**

(g) Exposure group (Dialysis patients): Antibody reactive or non-reactive but **PCR negative.**

4.9.1. Various Anti-HCV antibody distributions groups

Statistical studies on the distribution of anti-HCV antibody in sample that were reactive or non-reactive for HCV were studied by histogram and X-Y scatter. The samples were further partitioned into those that RT-PCR positive and negative. Samples were also partitioned according to the distribution groups.

4.9.2. Exposure groups

Exposure groups were those who are likely to be often exposed to HCV infection, such as dialysis patients, patients receiving frequent blood transfusions, etc. In this study, we have chosen dialysis patients.

4.10. Quality Management

First-party (Qiagen, Germany) or third-party (Qnostics, UK, supplied by Randox, UK) quality control (QC) reagents were used for QC assays with each set of HCV RT-PCR of patients' RNA. The performance values

(mean±SD, 95% CI of mean and %CV) for QC were calculated. Internal controls of HCV RT-PCR Positive samples (High, Medium and Low viral load samples). **Internal Controls** or ICs with reference genes were added to the matrix of each assay tube, including calibrators and patients' sample.

4.10.1. Periodic Schedule of Quality Control programs

4.10.1.1. Set A. Daily Quality control program with every set of assays

Assay tube 1: 10 IU/µl assay tube as standard and as a **positive control**.

Assay tube 2: NTC to monitor contamination and as a blank run for zero calibration point. Instead of NTC, a **negative control** with RNA isolated from a healthy plasma sample may be used.

Assay tube 3 set: Assay of patients' RNA isolated from plasma samples may be one or many more.

Additionally, a 4th assay tube of an **QC sample with known viral load** may be used along with this assay. This reagent may be used once a week.

Therefore, for every assay set, there will be a minimum of three and a maximum of five assay tubes, when there is one patient's sample. There will be additional tubes for every additional patient's sample.

4.10.1.2. Set B. Daily Internal Control (IC) with every assay tube

Internal Control reagents are added during RNA isolation of all assays, and in the assay tubes of 10 IU/µl standard and the NTC. Ct of the Internal Control amplification plots were used to calculate the %CV. The %CV was also calculated from the Internal Control PCR relative fluorescence amplification intensity. An acceptable %CV should not decrease more than 10% when there is no PCR inhibition. Decrease more than 10% or variation >0.5 log difference or greater than 2 Z values of the mean of the variation are considered unacceptable and root cause analysis should be done and corrected.

4.10.1.3. Weekly/monthly Quality Control Program according to sample size

The quality control programs were done once a week/month according to sample number. If there was one sample per day, quality control was done once a month and in addition whenever there was lot change and after all calibrations.

4.10.1.4. Set C. Intra assay variability or **Repeatability** was done once in three months on a **particular predetermined day** with a minimum of five sets of assay tubes as single or as duplicates containing 10 IU/µl standard for every lot of assays. Intra assay variability or Repeatability was calculated as %CV from the Ct and from log concentrations obtained from the calibration plot and/or with the imported calibration plot of Ct of the 10 IU/µl standard.

4.10.1.5. Set D. Inter assay variability or **Reproducibility** may be continuous or discontinuous. Discontinuous QC was preferred, as QC was done once or twice a week with a minimum of five days, with one or duplicate assay tube for each day containing 10 IU/µl standard. For every lot of assay reagent, a single lot of QC reagent was used. Inter assay variability or Reproducibility was calculated as %CV from the Ct values or from log concentrations of template obtained from calibration plot with the Ct of the QC reagent or of the positive control which was 10 IU/µl standard.

4.10.1.6. Set E. Inter-Batch or -Lot variability. When the reagent batch or lot is changed, split sample assays are done with the last sample of the previous lot. The previous or old lot reagent and the new lot reagent are used for split sample analysis. When the patient's sample is not available, 10 IU/µl standard may be used. Inter-Batch or -Lot variability is expressed as the difference in log concentrations obtained as log IU/µl from the Ct and calibration plot

4.10.1.7. Set F. External QC or Inter laboratory comparisons: These were done at **3 monthly intervals** for inter lab comparisons (ILCs) **with a NABL accredited laboratory.**

4.10.2. %CV (% Coefficient of Variation) of Ct values (amplification cycles) and Initial PCR target concentrations:

The %CV (% Coefficient of Variation) of the above parameters were calculated from **internal controls, HCV standards, quality control samples, external controls** (standard concentration of 10 IU/µl) and RT-PCR amplification data analysis (especially slope of amplification plot and maximum fluorescence). These were analysed for understanding the quality of the assay systems.

4.10.3. Influence of preanalytical conditions of the patient on RT-PCR

Various preanalytical conditions of the patients were found to be influencing RT-PCR. To study these conditions, RNA isolated from patients with defined preanalytical conditions were studied for their influence on various RT-PCR amplification systems: (a) the influence of defined preanalytical states of the patient or preanalytical variables on RT-PCR amplification of the 10 and 1 IU/µl calibrator standards were studied. (b) On RNA isolated from one HCV infected patient with low plasma viral load; (c) On RNA isolated from a second HCV infected patient with moderate plasma viral load. (d) On internal control containing house-keeping gene target sequence. (e) Influence of PCR inhibition on Internal Controls containing house-keeping genes on the HCV sample amplification in patients who are HCV RT-PCR positive and negative.

Controlling the preanalytical variables improves the sensitivity of detection of the low viral load: RT-PCR amplification data analysis and preanalytical control of the clinical condition of patient for sample collection could improve the RT-PCR sensitivity for HCV load.

4.11. Equations and Definitions

4.11.1. Adequacy of sample size for calibrators, quality control samples and for evaluating performance characteristic were based on sample mean and standard deviations (SD) using the equation (nMaster 2.0 software),

$$n = \frac{Z^2_{1-\frac{\alpha}{2}} \text{ X } SD^2}{D^2 \text{ X } \mu^2} \qquad \text{Equation-1}$$

where, D = relative precision (10%); μ = mean; $Z\,1-\alpha/2$ = desired confidence interval 95% (1.96); n = sample number.

4.11.2. Four parameter data analysis of the sigmoid fluorescence amplification plot was done using the equation

$$F = Yo + \frac{a}{1+e^{-\left(\frac{X-Xo}{b}\right)}} \qquad \text{Equation-2}$$

F was the value of function computed (fluorescence at cycle X), Y_0 was the ground fluorescence, 'a' was the difference between maximal fluorescence acquired in the run and the ground fluorescence, e was the natural logarithm base, X was Cq or cycle number, X_0 was the cycle number at the inflexion point of the sigmoid curve and b described the slope of curve at inflection point. The fluorescence intensity 'a' and slope b had also been measured manually.

4.11.3. Calculation of Efficiency from the linear calibration plot was done using the equation,

Efficiency, $E = -1 + 10^{\frac{-1}{slope}}$ Equation-3

4.11.4. Calculation of Efficiency, E of individual HCV RT-PCR exponential fluorescence amplification. Log transformation was done to convert the exponential amplification to a linear plot using LinRegPCR software. Baseline correction was carried out with a baseline trend based on early cycles. PCR efficiency for individual RT-PCR was derived by equation-4 from the slope of the regression line fitted to baseline corrected data points in the log-linear phase.

Efficiency, $E = 10^{slope}$ Equation-4

Linear part was extended to the Y-axis to obtain the initial theoretical fluorescence intensity which in turn is related to the concentration of the hydrolysed probe.

4.11.5. Calculation of plasma viral load from Cq obtained by real time RT-PCR of HCV infected plasma sample, and converted to concentration of the template from the calibration plot.

$$\text{Viral load (IU/ml of plasma)} = \frac{\text{(Patients' result Cq as IU/µl from calibration plot) x Elution Volume (60 µl)}}{\text{Sample Volume (0.14 ml)}}$$

Equation-5

4.12. Statistical Data Analysis

Biostatistical methods used in this study are defined and described below (Reffenberg, 2012; Gurumani, 2005; Altman, 1991). Statistical data analysis was done mainly by SPSS. Statistical analysis and estimation of the data generated by the screening anti-HCV antibody assay and from the RT-PCR fluorescence amplification data were done. SPSS used for calculating distribution characteristics such as the mean, median, mode, range, standard deviation, interquartile range, S.E of mean, 95% confidence interval, X-Y scatter plots, Histogram, Distribution frequency, t tests, correlations, etc.

Measures of Central Tendency, Average measures that describe the central aspects of a data are called averages. An average summarizes all the characteristics of entire mass of data. Most of the items of the series are clustered around the average, so it is called as measure of central tendency. **Arithmetic mean** is the sum of all the observations divided by the number of observations

Mean = sum of all the observations/ Total number of observations

Median is the value of the middle item of a given series of data arranged in ascending or descending order of magnitude.

Median = value of the item (n + 1) / 2

Mode is the most frequently occurring value in a sample. A sample with a single mode is referred as unimodal. If it has two mode it is called as bimodal and more modes as polymodal or multimodal. If no mode, it is no modal sample.

A **measure of dispersion** (also called measure of variation, scatter, spread) is to describe the extent of scattering of items around a measure of central tendency. Different types of measure of dispersion used here. **Range** is the minimum and maximum value of the given series of data (Gurumani,

2005). **Standard deviation** is defined as the square root of the arithmetic mean of the squared deviation of the various items from the mean. The mean squared deviation is called the variance. Therefore, the square root of variance is the standard deviation.

Coefficient of variation (CV) is also known as relative standard deviation (RSD). It is a measure of dispersion of a probability distribution or frequency distribution. CV is defined as the ratio of standard deviation to the mean and is expressed as percentage. It is widely used in analytical chemistry to express the precision/bias, and repeatability of an assay.

95% Confidence Interval of Mean is a range of values which can be confident including the true values. A confidence interval for the estimated mean extends to either sides of the mean by a multiple of the standard error. 95% confidence interval was calculated by multiplying standard error by 1.96 and then identifying the range by adding and subtracting the value from mean.

Frequency Graphs: Histogram is the graphical representation of continuous frequency distribution. The X-axis has the true class intervals, and the Y-axis, the frequencies. The bars are of equal width indicating that the class- intervals are of equal width. The height of the bar is proportional to the respective frequency. Therefore, it may be said that the area (length × breadth) of each bar is equal to the total of all the frequencies.

X-Y Scatter diagram is an easy and simple method for studying correlation between two variables. If X and Y are pairs of variables, the values of the variable X are marked in the X – axis and the values of variable Y are marked in the Y axis. A point is plotted against each value of X and the corresponding Y value. A swarm of dots is obtained, and this is called the scatter diagram. From this scatter diagram we can understand about the correlation between the variables whether it is positive correlation or negative correlation.

4.13. Software applications used in this study

4.13.1. SYSTAT and SigmaStat software

The four-parameter data analysis was done for the calibrators, diluted calibrator and different patient samples using SigmaStat software. SigmaStat is an easy-to-use, wizard-based statistical software package designed to guide users through every step of the analysis and perform powerful statistical analysis.

4.13.2. LinRegPCR

The LinRegPCR program reads data from an Excel spreadsheet. Therefore, the data have to be exported from your PCR apparatus and imported into Excel. Real-time PCR apparatus enable the export of the fluorescence data per cycle into a text file format. The exported data have to be corrected for the background but not be corrected for the fluorescence baseline. LinRegPCR estimates this baseline per sample and does a baseline subtraction.

4.13.2.1. LinRegPCR programme to calculate Individual sample efficiency

The background was exported, from the qPCR system to Excel in LinReg format but not the baseline-corrected data. Baseline is determined and the baseline correction for all sample is done by the LinRegPCR programme and a common window-of-linearity is determined for all samples. The program then sets the fluorescence threshold at one cycle below the upper limit of this window. Define grouping of samples per amplicon if needed: manually edit the amplicon group assignment. The program sets a window-of-linearity per amplicon group and sets the fluorescence threshold for each group. The individual samples are checked if needed and correct the baseline in individual samples. Adjust the window-of-linearity for an amplicon group or an individual sample. - export graphs to clipboard (click the right mouse button on a graph). The results can be saved to Excel.

4.13.3. Levey Jennings Plot

Quality control study using Levey-Jenning’s plot was sone by QIMacros, which is an excel add-on software. Levey Jennings (LJ Plot) is the common representation of quality control (bias and imprecision) and to evaluate the quality control results. Quality control results are added to the

plot with time (days / frequency). When the QC showed a stable performance, the mean value line represents the expected target value and the Standard Deviation (SD- 1SD, 2SD, 3SD) lines represent the expected imprecision. Assuming a Gaussian distribution, of imprecision, we expect approximately 99.72% (within ± 3SD), 0.28% (outside ± 3SD), 95.44% (within ±2SD), 4.56% (outside±2SD), 68.26% (within±1SD) and 31.74% (outside±1SD).

4.13.4. HCV sequence database and PCR Primer design

Good primer design is one of the major parameters in a Polymerase Chain Reaction. In Real Time PCR the amplicon length should be 50-150 bp in length. Primer should be in the length of 18-24 nucleotides. Primers designed should be specific and be free of internal secondary structures. Compatible annealing temperatures in primer pairs, approximately 50% GC and GC rich 3'end enhances the annealing. For primer designing, primer design software programs such as Oligoperfect designer, Primer Express software or Primer 3 software may be used.

Primers were synthesised for 3 regions - UTR, Core/E1 and NS5B. Primer 3 software is used to check for designing optimal primers for amplification of different regions of HCV genome. Amplification of HCV RNA sequences by reverse transcription and cDNA Polymerase chain reaction. HCV RNA isolation and Reverse transcription to make cDNA is done using Thermo Verso cDNA synthesis kit at 45^0C for 30 min in Thermal cycler (Applied Biosystem, Veriti model). The pair of primers should hybridise to the sequence and amplify the NS5B region. The primers should correspond to the site in NS5B region. The phylogenetic analysis was done with all the amplified NS5B sequences by the pairs of primers with known NS5B sequences.

4.13.4.1. Primer synthesis for 5'UTR

Appropriately validated primers are important in determining the specificity, sensitivity and robustness of a PCR reaction. Primers were synthesised from the conserved region of HCV. The 5' untranslated region (5'UTR) of HCV is the most conserved region. That is the reason for selecting 5'UTR as target by commercial RNA detection kits. The 5'-UTR

contains many stem and loop structures. Primer selection is done mainly from the stem part and try to avoid loop structures. The sequences near the 5' end of the 5'-UTR are susceptible to cleavage by 5'-3' exonucleases. 5'UTR sequences of Genotypes 1-7 were aligned and primer was selected from the conserved region. Because the base-pairing structures of the 5'-UTR might open at increasing temperatures.

4.13.5. NCBI database

The database of nucleotides with a large collection of complete or partial sequences from several sources including GenBank, RefSeq, TPA and Protein Data Bank. These sequence data provide information for biomedical researchers for further studies and discoveries in the field. Basic Local Alignment Search Tool (BLAST) finds regions of similarity between biological sequences. The program compares nucleotide or protein sequences to sequence databases and calculates the statistical significance (Zhang Z et al; 2000).

BLASTn or otherwise known as nucleotide BLAST is used to compare one or more nucleotide query sequences to a reference nucleotide sequence or a database of similar nucleotide sequences. This helps to determine the evolutionary relationships among different organisms.

BLASTx or translated nucleotide sequence searched against protein sequences compares nucleotide query sequence translated to six reading frames which gives six protein sequences against the protein database. As BLASTx translates the query sequence in all six reading frames, it provides combined significance statistics for hits to different frames. It is very useful when the reading frame of the query sequence is unknown or it contains errors that may lead to frame shifts or other coding errors. So BLASTx is the first analysis performed with a newly determined nucleotide sequence.

tBLASTn, protein sequence searched against translated nucleotide sequences is used to compare protein query sequence against the six-frame translations nucleotide sequences database. tBLASTn is beneficial for finding homologous protein coding regions in unannotated nucleotide sequences. Expressed sequence tags (ESTs) are short, single-read cDNA sequences. As ESTs have no annotated coding sequences, there are no corresponding protein translations in the BLAST protein databases. So

tBLASTn search is the only way to find potential coding regions at the protein level.

BLASTp (Protein BLAST) compares one or more protein query sequences to a subject protein sequence or a database of protein sequences. It is useful in identification of a protein sequence.

Maximum Score is the highest alignment score calculated from the scores provided for matched nucleotides and penalties for mismatches and gaps. **Total Score** is the sum of alignment scores of all segments from the reference sequence. **Query Coverage is** the percent of the query length that is covered in the aligned sequences.

Expect Value is the number of alignments expected by chance with the calculated score. The expect value is a default sorting metric for significant alignments. The E value should be very close to zero. **Identity** is the highest percent identity for a set of aligned segments to the reference sequence.

Accession Length is the number of nucleotides or amino acids in the result sequence identified by the accession number.

Accession number is a unique identifier assigned to records in the NCBI databases.

4.13.6. Phylogenetic Analysis

The analysis was performed on the Phylogeny.fr platform and sequences were aligned with MUSCLE configured for highest accuracy, after alignment, ambiguous regions (i.e. containing gaps and/or poorly aligned) were removed with Gblocks. The phylogenetic tree was reconstructed using the Maximum Likelihood method implemented in the PhyML program and graphically represented and edited. Finally, the phylogenetic tree was constructed with TreeDyn.

RNAfold, web server programme, was used to predict the secondary RNA structure of 5'UTR region. The sequences are pasted or uploaded and click 'proceed' to generate minimum free energy (MFE) structure. The MFE structure of an RNA sequence is the secondary structure that contributes a minimum of free energy. The structure prediction is done using a loop-based energy model and the dynamic programming algorithm (Zuker et al, 1981).

Centroid structure of an RNA sequence is the secondary structure with minimal base pair distance to all other secondary structures in the Boltzmann ensemble.

4.13.7. Protein Data Bank (PDB)

Biomolecules are hierarchical structures as proteins are composed of linear chains of amino acids that very often fold into compact subunits which then can associate into higher level assemblies with other proteins, small molecule ligands, and water or other solvent molecules. Biomolecules in the Protein Data Bank (PDB) archive are organized and represented using this hierarchy to simplify searching and exploration. Four levels of hierarchy are commonly used: Entry, Entity, Instance, and Assembly: An ENTRY is all data pertaining to a particular structure deposited in the PDB and is designated with a 4-character alphanumeric identifier called the PDB identifier or PDB ID. An ENTITY is a chemically unique molecule that may be polymeric, such as a protein chain or a DNA strand, or non-polymeric, such as a soluble ligand. Some entries may even have branched polymeric entities, such as oligosaccharides. An INSTANCE is a particular occurrence of an ENTITY. An ENTRY may contain multiple INSTANCES of an ENTITY, for example, many copies of a protein chain in a homo oligomeric protein. An ASSEMBLY is a biologically relevant group of one or more INSTANCES of one or more ENTITIES that are associated with each other to form a stable complex and/or perform a function (https://www.rcsb.org/docs/general-help/organization-of-3d-structures-in-the-protein-data-bank#definitions).

4.13.8. Protein structure prediction

The Phyre^2 (Protein Homology/analogY Recognition Engine V 2.0) Protein Fold recognition server was used for protein structure prediction (Kelley LA et al, 2015). Phyre2 is a suite of tools available as online software to predict and analyze protein structure, function and mutations. Phyre2 provides biologists with a simple and intuitive interface to state-of-the-art protein bioinformatics tools. Some of the most widely used web servers for protein modelling are Phyre2, i-TASSER8, Swiss-Model9, HHpred10, PSI-BLAST–based secondary structure prediction (PSIPRED)11, Robetta12 and Raptor13. I.

4.13.8.1. Phyre^2 Procedure

Sequence is submitted in Phyre^2 home page (http://www.sbg.bio.ic.ac.uk/phyre2). E-mail address to be given and the results are mailed to the given address on completion. There are options that can be added. Copy and paste the amino acid sequence into the form provided. To submit the sequence, click the 'Phyre Search' button. On clicking the button, the user will be taken to a job monitoring page that is automatically updated every 30 s. This page shows a progress bar for the job, information on the job and an estimate of the time it will take.

The core method of Phyre^2 for generating a 3D model of a protein sequence is composed of **four underlying technical stages**. **The first stage** is to gather homologous sequences and determine an evolutionary profile for the query that captures the residue preferences at each position. **The second stage** is the fold library scanning. The profile calculated in stage 1, together with the predicted secondary structure, is converted to a hidden Markov model (HMM). This HMM is then scanned using HMM-HMM matching against a precompiled database of HMMs of known structure known as the fold library. **The third stage** includes loop modelling. This library is constructed by a complete fragmentation of the structure database, followed by structural clustering. **The fourth stage** is the side chain placement. Side chain fitting to the backbone generated in third stage involves a fast graph-based technique and a side chain rotamer library to place side chains in their most probable rotamer while avoiding steric clashes. This technique is ~80% accurate if the backbone is correct.

4.13.9. SOPMA

Significant improvements in protein secondary structure prediction by consensus prediction from multiple alignments done using self optimized prediction method (SOPMA) (Geourjon and Deleage, 1995).

4.13.10. DNA sequencing and Sequence analysis

The specific amplified PCR products of 5'UTR, Core E1 and NS5B is sent for sequencing using Sangers method at Aggregenome sequencing Cochin. Chromatograms are checked for the sharpness of peak using FinchTV and analysed for mutation and Heterogeneity. The genotype was

determined by analysing the sequences using Bioedit and the sequences are submitted at NCBI.

Basic Local Alignment Search Tool (BLAST) finds regions of similarity between biological sequences. The program compares nucleotide or protein sequences to sequence databases and calculates the statistical significance (Zhang Z et al; 2000). Sequences are aligned using **ClustalW** (Larkin MA et al; 2007). Determination of taxonomic group of unaligned reads. To determine the taxonomic group of the unaligned reads and possible presence of unexpected HCV genotypes, analysis was conducted using the NCBI BLAST 2.2.28. A random subset of 50,000 of reads that did not align to HCV from each sample was aligned to the NCBI nucleotide (nt) database. The BLAST output was sorted into taxonomic groups using a script. Phylogenetic analysis of full-length HCV genome sequences. The generated full-genome sequences were aligned using Clustal W. In addition, to study the genetic similarity of these sequences to previously described full-length sequences, the 5 most genetically similar sequences for each the full-length sequence of each sample were included in the alignment, as determined by nucleotide BLAST (http://blast.ncbi.nlm.nih .gov/Blast.cgi). The alignment was cut into E1/E2, NS3/4A, NS5A, and NS5B genes. **Neighbor-joining phylogenetic trees** were inferred in MEGA 5.2 using the Tajima-Nei model and gamma-distributed rates among sites (0.5). The confidence of the branches was assessed by the bootstrap test using 500 replicates. The phylogenetic trees were visualized using FigTree version 1.3.1 (http://tree.bio.ed.ac.uk/).

4.14. Gel electrophoresis

The amplified viral nucleic acid sample was mixed with loading buffer and loaded on Agarose gel (1.5%) stained with Ethidium bromide. This was added to respective wells, PCR product is electrophoresed at 100V for 30-60 minutes and viewed on gel documentation. Agarose gel was prepared with 1X Tris Acetate EDTA (TAE) buffer. The amplified PCR product was analysed by gel electrophoresis, migration is dependent on the size of the PCR product.

Chapter 5

Analysis of calibration plot, efficiency and individual amplification to differentiate between qualitative and quantitative HCV RT-PCR

5.1. ABSTRACT

Background: Hepatitis C virus (HCV) load in plasma were often below the validated RT-qPCR calibration plot concentrations. In this report, data analysis of RT-PCR amplification plots and calibration plots were done to define the performance characteristics of the higher Cq range of qualitative RT-PCR and to differentiate it from RT-qPCR.

Methods: Patients reactive for anti-HCV antibody screening assays or exposed to HCV infection were selected for RT-PCR assay done with RNA isolated from plasma. Validated and diluted calibrator concentrations were used to construct calibration plots, and for data analysis along with patients' RT-PCR, using software packages.

Results: Normalised fluorescence intensity (100%) and slope at inflection point (1.65 - 1.50) of the sigmoid fluorescence amplification plots were of acceptable performance for validated quantitative calibrators, but were decreased for diluted calibrators and for patients' sample with Cq greater than that of the 10 IU/µl validated calibrator (Cq >33.2). Calibration plot of validated calibrators had slope, efficiency and sensitivity of -3.471, 94% and 36.404, respectively, but the diluted calibrators showed decreased performance of -2.305, 171% and 35.52, respectively. Log-transformed exponential amplification plots analysed by LinRegPCR software, showed acceptable performance at the validated calibrator concentrations and decreased performance with diluted calibrators and patients' sample with Cq >33.2. The four-parameter validated qualitative RT-PCR Cq range was from 33.2 to 39.9. The 10 IU/µl calibrator was the reference point to differentiate between qualitative and quantitative RT-PCR.

Conclusions: Decision-criteria were developed for establishing the range of validated qualitative RT-PCR performance, and to differentiate it from quantitative RT-PCR.

5.2. INTRODUCTION

Large number of patients with hepatitis C virus (HCV) infection have no symptoms (Orland et al, 2001). Diagnosis of HCV infection was done by screening for anti-HCV antibody for selecting the patients with reactive levels of antibody (Ritcher et al, 2002), followed by confirmation of diagnosis by HCV

RT-PCR of RNA isolated from plasma of the antibody reactive patients (Bukh et al, 1992; Barbara et al, 2009). The plasma viral load in HCV infection was often very low in a large number of patients (Glynn et al, 2005; Fytili et al, 2007), much below the validated calibration plots for quantitative PCR (RT-qPCR) assays. There were difficulties in interpretation of the antibody screening and RT-PCR assays arising out of the low anti-HCV antibody levels (Zer et al, 2009), low plasma viral load (Glynn et al, 2005; Fytili et al, 2007), spontaneous resolution of infection (Bulteel et al, 2016; Hofer et al, 2003; Micallef et al, 2006), decreasing viral load and occult infection (Di Marco et al, 2009; Welker and Zeuzem, 2009; Carreno V et al, 2008).

Real-time RT-PCR may be quantitative or qualitative (David and Theo, 2006). Validated quantitative RT-PCR assay required an acceptable performance of calibrator RT-PCR and calibration plot for reporting the viral load in the patients' plasma. Validation for quantitative RT-PCR was done by the manufacturers of the assays, and the assay performance were given in the procedure manual associated with the reagent pack. According to the clinical diagnostic requirements, these assay performances were verified by the user for acceptable performance (Wallace and McCulloch, 2021). In this study, the verified assay performance of quantitative RT-PCR required for HCV infection were described. Therefore, the first research problem of this study was to define the lower limit of the selected quantitative RT-PCR assay with acceptable performance. This would help in differentiating the quantitative RT-PCR assays from the qualitative RT-PCR assays at lower plasma viral load. The lower concentrations of calibrators were made by diluting the lowest validated calibrator.

The second research problem of this study was to determine the threshold cycle or Cq range of the validated qualitative RT-PCR assays. A qualitative RT-PCR assay reported that the assay was positive or negative for HCV RT-PCR, but would not contain the plasma viral load. There might be a comment in the report on the Cq to give an approximate and relative indication of the viral load. Validation of qualitative RT-PCR was not done by the manufacturer, as this required to define the acceptable qualitative performance characteristics of the RT-PCR fluorescence amplification plots and calibration

plots. This was done in this study. The diluted concentrations of calibrators and patients' samples were used to identify the lower and upper limit of qualitative template concentration or Cq of qualitative RT-PCR.

The concentration of the free hydrolysis probe of RT-PCR that give rise to the real-time fluorescence amplification plot, increase exponentially or doubling from the first cycle onwards. But fluorescence intensity reached the detectable level of the RT-PCR machine only after several cycles, near the quantification threshold (Cq) and was related to initial copy number of the template DNA (Kralik and Ricchi, 2017; Adams, 2006). As the initial copy number increased, with increase in the plasma viral load of HCV or concentration of the calibrator, the Cq decreased (Adams, 2006). The fluorescence intensity increase immediately above the threshold level would be exponential with an efficiency nearer to two for all validated calibrator concentrations (Ramakers et al, 2003; Ruijter et al, 2009).

Three research hypotheses were proposed to differentiate between qualitative and quantitative RT-PCR, and to validate the qualitative RT-PCR Cq range. (a) The first hypothesis was that these can be done by graphical observations and by four parameter data analysis of the sigmoidal fluorescence amplification plot of calibrators, diluted calibrators and patients' RNA sample. (b) The second hypothesis was that data analysis of the linear calibration plots of validated calibrators and diluted calibrators could be used to achieve these goals for quantitative and qualitative RT-PCR. (c) Finally, the log transformation of the initial exponential fluorescence amplification plot might be used to calculate the efficiency, E of individual amplification plots. The E value can used to validate the qualitative and quantitative RT-PCR. (d) Sequencing of the PCR product was done to validate the PCR product of a qualitative PCR as the sequence from the 5'UTR region of HCV.

A final decision-criteria had been proposed in this study for making a clinical report of an HCV RT-PCR assay as qualitative or quantitative. Decision criteria for validation of qualitative RT-PCR is given under Table 5.6.

5.3. Aspects of the original objectives discussed in this chapter

1. Establishment of the methods for evaluation by data analysis, test validation, quality control and clinical state of the patient for Molecular Diagnostic reporting of Hepatitis C infection.

2. Use of these procedures for confirmatory diagnosis of hepatitis C infection, its plasma viral count determination and genotyping.

The following research problems were addressed in this chapter for part-fulfilment of the above two main objectives.

Research problem 1- Define the lower limit of quantitative RT-PCR calibration plot and differentiate quantitative RT-PCR from qualitative RT-PCR.

Research problem 2- To determine the Cq range of qualitative RT-PCR.

5.4. MATERIALS AND METHODS

This is an **observational cross-sectional study** of real-time RT-PCR for HCV in RNA isolated from plasma of individuals who were reactive for anti-HCV antibody by the screening immunochemistry assay or suspected to have contacted HCV infection. **Study population** included the patients from whom EDTA-treated blood samples were obtained for RT-PCR at Amala Institute of Medical Sciences, Thrissur, Kerala state, India. The study was conducted from June 2017 to November 2021.

The study was approved by the **Institutional Research and Ethics Committees** for the research project proposal to DST-SERB, New Delhi from Krishna K Yathi with Jose Jacob as Mentor (Ref. AIMSIEC/37/2017 latter dated 18-05-2017), and for the research proposal for PhD registration of Ann Mary Joseph with Jose Jacob as Guide to Calicut University (AIMSIEC/16/2017 dated 17-01-2017). The DST-SERB project was also approved by IBSC (**Institutional Biosafety Committee**) under Department of Biotechnology (DBT) guidelines dated 27th October 2017. Participants were approached directly by the investigators. The research program and the method of blood sample collection and assay were described to the participants. After including the participants by clinical and preanalytical evaluation, **informed written consents** were obtained and blood samples were collected.

5.4.1. Organisation of the Study

a) Selecting patients' reactive to **anti-HCV antibody screening assays,** and those **exposed to HCV infection** for RT-PCR.
b) **Blood sample collection** in EDTA tubes after taking the **preanalytical precautions**, followed by centrifugation to **separate plasma**.
c) **RNA isolation** was done immediately after plasma preparation.
d) **Setting the real-time RT-PCR machine** for cycling number, temperatures and durations.
e) **RT-PCR** of validated HCV calibrators and diluted calibrators; **Construction of the calibration plots**.
f) **Data analysis of calibrator** fluorescence amplification plots and calibration plots for acceptable performance.
g) **HCV RT-PCR of RNA isolated from patients'** plasma sample.
h) Data analysis of patients' HCV fluorescence amplification plots to **report as quantitative or qualitative RT-PCR.**
i) **HCV PCR product sequence analysis** to validate the PCR product of a qualitative PCR from as that from particular region of the HCV genome (Table 9.30).

5.4.2. Sample Collection and Anti-HCV antibody Screening assay

Blood samples were collected in vacuum tubes with clot activator, allowed to clot for 10 minutes, centrifuged at 3000 rpm for 5 minutes in a table top centrifuge, serum was separated, and clear serum samples were screened for the anti-HCV antibody with third generation enzyme immunoassays (Ritcher, 2002; Ortho Clinical Diagnostics). The assay was performed in Vitros ECi immunochemistry autoanalyser (Ortho Clinical Diagnostics, USA) using enhanced chemiluminescence method. Refer Details 4.5 and 3.5.1.

5.4.3. Inclusion and Exclusion criteria, Preanalytical influences, Sample collection for RT-PCR

Inclusion criteria were reactivity to anti-HCV antibody and exposure to HCV infection and suspected exposure to HCV infection. There were many preanalytical states that influence RT-PCR (Refer Chapter 7). These conditions were documented with the sample. Refer Details 4.2 Exclusion criteria were related to the preanalytical condition of the patient, such as acute tissue

damaging disease conditions, patients on chemotherapy and who were heparinised were found to influence the RT-PCR (Byrnes et al, 1975; Akane et al, 1994; Al Soud et al, 2001; Burkardt, 2000; Radstorm et al, 2004; Yedidag et al, 1996). These conditions were avoided as far as possible. In all emergency and other unavoidable circumstances, all the above preanalytical criteria were overlooked, but the results of RT-PCR were analysed for influences.

Blood sample was taken with 4 ml EDTA-vacutainers, centrifuged at 3000 rpm for 15 minutes in a table top centrifuge. Plasma sample without haemolysis, jaundice, cloudiness and without clot particles was separated (WHO, 2002) and used for RNA isolation and HCV RT-PCR. Plasma and RNA samples were stored immediately at -20^{o}C and -80^{0}C, respectively, in aliquots. Refer Details 4.3.2

5.4.4. Sample size calculation

Estimation of sample size based on sample mean and SD (nMaster 2.0 software for sample number calculation). Refer Details 4.4.

5.4.5. RNA Isolation

HCV viral RNA Isolation was done by chromatography method from plasma with a QIAamp Viral RNA Mini Kit (Qiagen, Germany). Plasma (140 µl) was added to AVL buffer with carrier RNA (Qiagen, Germany), kept for 10 minute, 560 µl of >96% ethanol was added, and then passed through QIAamp mini column (Qiagen, Germany) to bind nucleic acids. Unbound material was washed out twice by microcentrifugation at 8,000 rpm for 1 minute and 14,000 rpm for 3 minutes. RNA was eluted with 60 µl elution buffer. Eluted RNA was assayed immediately and stored in aliquots at -80°C (QIAamp viral RNA mini handbook). Refer Details 4.6.

5.4.6. Setting of the RT-PCR machine

HCV RT-PCR cycling conditions were entered in the machine as 50°C for 30 minutes for reverse transcription, 95°C for 15 minutes for initial denaturation, cycling involves denaturation at 95°C for 30s, primer annealing at 50°C for 60s and extension at 72°C for 30s repeated for 50 cycles. Fluorescence was measured at 50°C in each cycle at different wavelengths according to the probe (artus HCV RG RT-PCR Kit Handbook).

5.4.7. HCV RT-PCR of validated and diluted calibrators, construction of the calibration plot

Assaying for RT-PCR fluorescence amplification plots was done with the four validated calibrators and two diluted calibrators. Each assay set would contain the different calibrator concentrations, blank, and the internal controls with reference gene in the assay matrix in each tube.

A calibration plot was constructed with the log concentration of the four validated calibrators from 10 IU/µl, 100 IU/µl, 1,000 IU/µl and 10,000 IU/µl and Non-Template Control (NTC or blank) versus Cq. A separate calibration plot of the diluted calibrators was constructed with $1/10^{th}$ and $1/100^{th}$ dilutions of 10 IU/µl calibrator, and blank. The second plot was used to identify the range of the qualitative RT-PCR scale. Calibration plot was prepared for each lot of RT-PCR reagent. The plot was analysed for slope and efficiency (artus HCV RG RT-PCR Kit Handbook).

The performance characteristics and data analysis of calibration plots were given in the Results Section.

5.4.8. HCV RT-PCR of RNA isolated from patients' plasma

RNA isolated from patients' plasma were assayed along with one validated calibrator, blank (or NTC), quality control, and internal control with reference gene in the assay matrix of each tube. External quality assurance programs were also performed. RT-PCR was done using Artus HCV RG RT-PCR kit (Qiagen, Germany) based on hydrolysis probes by One step RT-PCR on Rotor-Gene Q instrument. Master mix was prepared from Hep. C Virus Master A (12 µl) and Hep. C Virus Master B (18 µl) with internal control (2 µl). Add 30 µl of this mix into PCR tube and 20 µl of eluted sample RNA, quantitation standards and non-template control (NTC) to respective tubes (artus HCV RG RT-PCR Kit Handbook).

5.4.9. Equations and Definitions

Cq or CT was the quantification cycle or threshold cycle number where the amplification plot crossed the threshold. The threshold level was kept at 0.05 fraction of the total fluorescence intensity above the baseline.

Four Parameter Data analysis was done using the equation**.** Refer Details 4.11.2 and 3.5.9.1.

Validated calibrators were reagents that have real-time RT-PCR quantitative template concentrations with performance characteristics that were within the acceptable limits (refer Results section) set for the reagent for quantitation of the patients Cq values. In this study, the performance characteristics were set by the company (Qiagen, Germany) who validated the calibration standards, 10 IU/µl, 100 IU/µl, 1000 IU/µl, and 10000 IU/µl for quantitation of the patients' Cq values. These validated standards were **traceable** to the reference standard at the National Institute for Biological Standards and Control (NIBSC, UK) which coordinated the traceability studies on behalf of WHO.

Verified calibrators were the calibration standards that were found by the user to have the acceptable performance characteristics, and validated by the manufacturer for a set of calibrator concentrations (Qiagen, Germany).

Normalised 100% fluorescence intensity was the fluorescence intensity set for the validated HCV real-time RT-PCR calibrators, which was used to calculate the relative fluorescence intensities of the diluted calibrators and the patients' samples with Cq nearest to one of the validated calibrator concentrations. **As an example,** (a) for a diluted calibrator concentration of 1 IU/µl with Cq of 35.23 and 'a' of 21.7366 would have the 10 IU/µl validated calibrator with Cq of 33.19 and 'a' of 21.9323 as the reference 100% fluorescence intensity; (b) for an HCV infected patient's RNA with Cq of 30.09 and 'a' of 21.6422, the reference 100% fluorescence intensity was the 100 IU/µl calibrator with a Cq of 30.22 and 'a' of 25.3965. These were the examples taken from Table 5.2 where 'a' was the normalised fluorescence intensity.

Test samples may be a diluted calibrator concentration or a patient sample.

Calculation of Efficiency from the linear calibration plot was done using the equation,

Efficiency, $E = -1 + 10^{\frac{-1}{slope}}$ Refer Details 4.11.3 and 3.5.6.

5.4.10. Calculation of Efficiency, E of individual real-time HCV RT-PCR exponential fluorescence amplification.

Log transformation was done to convert the exponential amplification to a linear plot using LinRegPCR software. The slope from the linear regression line was calculated and efficiency was derived by the equation.

Efficiency, $E = 10^{slope}$ Refer Details 4.11.4.

Equation for calculation of plasma viral load from Cq obtained by real time RT-PCR of HCV infected plasma sample, and converted to concentration of the template from the calibration plot.

$$\text{Viral load (IU/ml of plasma)} = \frac{\text{(Patients' result Cq as IU/µl from calibration plot) x Elution Volume (60 µl)}}{\text{Sample Volume (0.14 ml)}}$$

Refer Details 4.11.5.

RT-PCR was Reverse Transcriptase-Polymerase Chain Reaction of both quantitative and qualitative PCR. **RT-qPCR** was Reverse Transcriptase-Polymerase Chain Reaction of quantitative PCR.

5.4.11. Quality Management and Assay Traceability

Quality control (QC) assays were done with each set of HCV RT-PCR assay with patients' RNA. The first party QC reagents were from Qiagen, Germany. The third-party QC reagents were from Qnostics, UK, supplied by Randox, UK. Standard deviation Index or SDI was calculated from Cq of QC reagents. When SDI was <2.0, it was considered as acceptable performance. Our SDI values were 0.7275 for first-party QC reagents, and 0.94 for the third-party reagents. If there was unacceptable SDI data, measures were taken to set right errors in machine functioning, reagents, storage or calibrations. The performance values (mean±SD and %CV) for quality control samples were 36.662±1.084, and 2.955 (n = 15). These data showed high level of RT-PCR quality.

External Quality Assessment: Log plasma viral load data and its mean or median difference was used for external quality assessment by VIROEQAS, CMC, Vellore, and by inter-laboratory comparison with an NABL, India

accredited laboratory. Typical log-median difference values obtained with the former was 0.20 and 0.40, and acceptable performance was between -0.50 to 0.50. The log-mean difference values obtained for the eight interlaboratory comparisons ranged from 0.10 to 0.442, and all these were in the acceptable range of -0.50 to 0.50. Interlaboratory comparisons were also done by calculating Z score, which showed the deviation within the acceptable ±2 Z score or standard deviations from the mean value.

Internal Controls with reference genes were added to the matrix of each assay tube, including calibrators and patients' sample. The performance values (mean±SD and %CV) for internal control were 31.707±0.739 and 2.33 (n = 30).

Traceability of the calibrators were to the reference standards at NIBSC (Ref. 'Validated Calibrators' above). Performance characteristics of calibration plots and their RT-PCR fluorescence amplification plot data are given under Results Section. The HCV RT-PCR assay had a validated limit of detection 34 IU/ml of plasma (artus HCV RG RT-PCR Kit Handbook).

5.4.12. Statistical analysis and Software

Fluorescence data and Cq were from Rotor-Gene Q software 2.3.1.49 (Qiagen), X-Y scatter plot was constructed, its trendline, correlation coefficient (R), and coefficient of determinations (R^2) were calculated by SPSS software. SigmaStat 4.0 was used for data analysis of sigmoid amplification plot (Systat Software, Inc, San Jose, USA). LinRegPCR program version 2020.2 was used for log transformation, calculation of slope and efficiency determination of the initial exponential fluorescence amplification of individual plots (Rujiter et al, 2009). Microsoft Excel was used as a medium for data transfer and common statistical calculations.

5.5. RESULTS

5.5.1. Graphical observations of the Sigmoid Fluorescence Amplification plots of Calibrators and Diluted Calibrators

RT-PCR fluorescence amplification plots with the four validated calibration concentrations, 10,000 IU/µl, 1,000 IU/µl, 100 IU/µl, and 10 IU/µl

(Qiagen, Germany) were performed. Graphical observations of the four-parameters (Equation-2) of the fluorescence amplification plots of calibrators were as follows: All four validated calibrators showed a typical sigmoid plot with an exponential increase immediately above the baseline fluorescence (Y_0), increasing to a maximum slope at the inflection point (b), followed by plateauing and reaching the maximum fluorescence (Fmax - Y_0 = 'a') which was considered as the 100% normalised fluorescence intensity, used also as the reference fluorescence intensity for comparisons (Fig. 5.1A). Yo was nearly the same for all samples. In this study, the normalisation to 100% fluorescence intensity of the validated calibrators, was done for calculations of the relative normalised fluorescence intensities of the diluted calibrators and the patients' samples with Cq nearest to the validated calibrator concentration. The sigmoid fluorescence amplification plot was near symmetrical at the inflection point. The Cq decreased with an increase in the concentration of the calibrator. The NTC showed no amplification or Cq value as it did not cross the threshold (Fig. 5.1A).

The repeated one-tenth dilutions of calibrators at 1 IU/µl and 0.1 IU/µl showed a decreased normalised fluorescence intensity, compared to the 100% fluorescence intensity of the 10 IU/µl validated calibrator and a decreased slope at the inflection point (Fig. 5.1A).

5.5.2. Data analysis of Linear Calibration Plots of Validated and Diluted Calibrators

RT-qPCR calibration plot of log concentration of calibrators against Cq, and its associated calibration data are given in the box (Fig. 5.1B). The coefficient of correlation, R or r, was 0.99963, and R^2, the coefficient of determination was 0.99925 (99.925%). The slope of the linear calibration plot, M was -3.471, which reflected a good PCR efficiency E of 0.94 (or expressed as 94%) with maximum efficiency of 1.0 (E, calculated from slope with equation-3). The Y-intercept, B was 36.404, the theoretical Cq obtained with 1 IU/µl of the calibrator template ($\log_{10}$ 1 = 0), and was considered as the sensitivity of the calibration plot (Fig. 5.1B). These results indicated good performance characteristics of the calibration plot.

The calibration plot with 10 IU/µl and its diluted concentrations, was constructed by plotting the log concentration against Cq (Fig. 5.1C). The slope

of the linear plot at -2.305, had decreased numerical value (less steep). The Y-intercept, B was 35.52, and was decreased (Fig. 5.1C). The R = 0.9924 and R^2 = 0.9849 (or 98.49%) were decreased. The efficiency calculated from the slope was 171% which was unacceptable (>110%) due to the unacceptable calibrator slope (<-3.10). The lower numerical value of the slope indicates lower efficiency which resulted from an increased Cq value for a particular concentration (Fig. 5.1C). These results indicated that the diluted calibrator concentrations had decreased performance characteristics for a calibration plot.

Bias/Uncertainty and analytical variation (%CV) of Cq obtained from RT-PCR of validated calibrators and diluted calibrators were presented as the mean± SD, 95% CI of mean and %CV (n = 6). The 95% CI of mean of diluted calibrators were overlapping, indicating increased variations. The %CV of validated calibrators ranged from 1.49 to 2.53, and that for the diluted calibrators were 2.087 to 3.169 (Table 5.1). Although the diluted calibrator %CV was higher, both were within the acceptable analytical performance of <7%.

5.5.3. Graphical observations of sigmoid fluorescence amplification plots of RNA from patients' plasma

Graphical observations of patients' plasma HCV RNA RT-PCR fluorescence amplification plots at high viral load (Cq <30) with Cq of 24.27 (Fig. 5.2A) and at medium viral load (Cq of 30 to 33.20) with Cq at 30.85 (Fig. 5.2B) showed near 100% normalised fluorescence intensities and good slope at inflection point when compared with the related validated calibrator at 100 IU/µl and 10 IU/µl.

At low plasma viral load (Cq >33.2), the slope decreased to 0.906 and fluorescence intensity decreased to near one-third (33%) (Fig. 5.2C) and can be also appreciated graphically. These results from the patients' RNA RT-PCR at Cq higher and lower than of the 10 IU/µl validated calibrator Cq of 33.19 (Fig. 5.2) confirmed that there was a decreased performance characteristic at Cq >33.2.

5.5.4. Data Analysis of four-parameter sigmoid fluorescence amplification plots of Calibrators and Diluted Calibrators

The graphical description of the sigmoid amplification was given in Fig. 1A. The four parameters of the sigmoid amplification plots were further analysed by SigmaStat software by the sigmoidal or logistic curve fit model (Table 5.2; Equation-2) for validating the sigmoid amplification plot. The numerical values obtained by this model might not be exactly comparable with the graphical description in Fig. 5.1A; Fig. 5.2A to 5.2C, and its data measured manually later in Table 5.3. The normalised fluorescence intensity and slope at the inflection point were the two of the four parameters that were found to be markedly decreased in the diluted calibrator range. The fluorescence intensity and slope of the diluted calibrators decreased ('a' = 21.7366 and 15.386; b = 1.8399 and 1.8921), respectively, when compared to the nearest validated calibrator (10 IU/µl), which showed 100% fluorescence intensity and slope ('a' = 21.9323; b = 1.9498). These two parameters were selected for differentiating quantitative and qualitative RT-PCR.

5.5.5. Data analysis of four-parameter sigmoid amplification plots of **RNA from patients' plasma**

The fluorescence intensity decreased sharply in the patient sample at Cq >33.2, but the slope did not show decrease upto Cq of 36.0 and at Cq >36.0 there was a significant decrease in slope. Therefore, the slope at inflexion point appears to be less influenced by Cq 33.2.to 36 in the patient sample. Yo, was the ground fluorescence which was nearly the same for all samples (Table 5.2).

5.5.6. There was a good relationship between the LinRegPCR software data with graphically observed data at various concentrations and Cq

Slope, Efficiency, and fluorescence intensity of Calibrators and Diluted Calibrators: The individual exponential fluorescence amplification plots of the validated calibrators were log-transformed and plotted against cycle number using LinRegPCR software (Fig. 5.3A). The slope of the initial linear part was measured (0.297 to 0.260) and PCR efficiency, E was calculated (1.98 to 1.82) from the slope (Table 5.3). This efficiency of the validated calibrators was within the acceptable efficiency range (2.0 – 1.80) of good amplification plots. The observed fluorescence intensity (100%) and manually measured slopes (1.65 – 1.50) were also in the acceptable range.

The diluted calibrators showed decreased slope (0.243 and 0.230), fluorescence intensity (89% and 78%), and E (1.75 and 1.7) (Table 5.3). The

manually measured slope also decreased to (1.477 and 1.08). Therefore, from these data the 10 IU/µl calibrator concentration and its corresponding Cq at 33.2 could be considered the point of differentiation of the quantitative and qualitative RT-PCR. The diluted calibrator concentration of 0.1 IU/µl was the limit of detection, as further dilutions did not give fluorescence amplification. Therefore, the validated qualitative RT-PCR range was from 10 to 0.10 IU/µl.

Slope, Efficiency, and fluorescence intensity of RNA from patients' plasma: The LinRegPCR software data of patients' plasma at high viral load (Cq <30) showed an efficiency 1.98 to 1.80 and samples with medium viral load (Cq 30 to 33.20) showed an efficiency of 1.708 to 1.797 (Table 5.4, Fig. 5.3B to 5.3D). These values nearly correspond with the validated calibrator efficiency range and good performance characteristics. At low plasma viral load (Cq >33.20), the slopes decreased to 0.238 and 0.173, and efficiency decreased to 1.728 and 1.489 (Table 5.4). Similarly, the manually measured normalised fluorescence intensity and slope at inflection point decreased at Cq >33.2. Again, confirming that the Cq of 33.2 was the cut off between quantitative and qualitative RT-PCR in patients' sample.

5.5.7. X-Y scatter, trendline and correlations of parameters associated with RT-PCR fluorescence amplification plots

Log concentration of diluted calibrators versus Cq at inflection point showed a negative correlation, R = 0.940 (Fig. 5.4A). The coefficient of determination, R^2 of linear and quadratic trendlines 0.883 and 0.943, respectively.

Log concentration of diluted calibrators versus slope at inflection point showed a positive and linear correlation, R = 0.866 (Fig. 5.4B). The linear and quadratic trendlines were nearly overlapping with a coefficient of determination, R^2 = 0.778 and 0.790, respectively, confirming that the relationship was linear.

Diluted Calibrator Cq versus normalised fluorescence intensity showed a negative correlation, R = -0.840 (Fig. 5.4C). The R^2 of linear and quadratic trendlines were nearly overlapping with 0.688 and 0.69, respectively, confirming the negative, linear relationship.

Log concentration of diluted calibrators versus efficiency, E of the individual fluorescence amplification was plotted. E was calculated from the slope of the log-transformed fluorescence amplification using LinRegPCR software (Fig. 5.4D). E of qPCR amplification was nearer to 2.0 with the validated 10 IU/µl calibrator indicating near doubling of the template with every cycle. As the concentration increased there was an increase in E resulting in a positive correlation. The R^2 for linear and quadratic trendlines were 0.491 and 0.639, respectively, indicating a marked increase with the quadratic trendline.

Cq of patient's HCV RNA versus Slope at inflection point demonstrated a negative hyperbolic, quadratic relationship. The R^2 for linear and quadratic trendlines are 0.681 and 0.731 respectively, thereby showing an increase in R^2 with the quadratic trendline (Fig. 5.5A).

Cq of patient's HCV RNA versus normalised fluorescence intensity showed a negative relationship (Fig. 5.5B). The relative fluorescence intensity was obtained with reference to a validated 10 IU/µl calibrator as the 100% fluorescence intensity. The R^2 calculated for the linear and quadratic trendline were closer at 0.703 and 0.742, respectively.

Cq of HCV RNA from patients' sample versus efficiency of individual fluorescence amplification plots calculated by LinRegPCR software (Fig. 5.5C). There was a decrease in efficiency with the increase in Cq. The R^2 calculated for linear and quadratic trendline were 0.384 and 0.473 indicating a negative hyperbolic relationship between Cq and E.

5.5.8. Decision criteria for determining the range of qualitative real-time RT-PCR

A. The graphical observations and the manually measured data from fluorescence amplification plots were found to be the most useful method for determining the range of Cq for qualitative RT-PCR of the patients' sample. Fluorescence Intensity, slope and Cq at the recommended levels will be a quantitative RT-PCR. When the fluorescence Intensity and slope were decreased, and Cq was increased to values greater than the Cq of 10 IU/µl validated calibrator, then it would be a qualitative RT-PCR. The Cq in this study

was 33.2, but might vary from assay to assay. Therefore, 10 IU/µl validated calibrator should be kept with each set of patients' samples as reference for determination of the cut off of quantitative and qualitative RT-PCR reporting (Table 5.6).

B. Four-parameter numerical data from SigmaStat software was suited for validation of the sigmoid amplification data, especially with Cq >39 and to establish the highest Cq of the qualitative RT-PCR. The highest Cq with validated amplification data was 39.9 (Table 5.2). But the four-parameter data could not be compared accurately with the graphical observations and the manually measured data (Fig. 5.1A; Fig. 5.3A to 5.3D; Table 5.3 and 5.4). There were some variations in the patients' data Cq, 'a', and b, which were not matching well with the 10 IU/µl calibrator data. This was because the SigmaStat software analysed the sigmoid fluorescence amplifications by the sigmoidal or logistic curve fit model for validating the sigmoid characteristics of the amplification plot. Fluorescence intensity and slope comparisons were more reliable with the graphical observations.

C. LinRegPCR software log-transforms the exponential fluorescence amplification above the threshold to a linear plot, slope of which was measured and efficiency was calculated from it using Equation-4. There was an acceptable slope and E for quantitative RT-PCR which was decreased in qualitative RT-PCR and the cut-off calibrator concentration was 10 IU/µl calibrator concentration which corresponded to Cq of 33.2. The data from LinRegPCR software matched well with (a) the manually measured data at all concentrations or Cq of quantitative and qualitative RT-PCR. (b) Data from LinRegPCR software and manually measured data matched well between the calibrator data and patients' data (Table 5.3, 5.4 and Table 5.6A and 5.6C). The slope of this linear plot can be extended to the Y-axis for obtaining the initial theoretical fluorescence intensity, which was also related to the concentration of the fluorescent probe released.

D. Data analysis of Calibration plots should be in the acceptable range of slope, efficiency and sensitivity for reporting a quantitative and qualitative RT-PCR. If the values were outside this range, patient's RT-PCR was

unacceptable. This problem can be solved by recalibration or by using fresh calibrators (Fig. 5.1B, 5.1C and Table 5.6D).

5.5.9. Reporting of Quantitative and Qualitative RT-PCR

The cut-off level for differentiating quantitative and qualitative RT-PCR was 10 IU/µl calibrator concentration, with Cq 33.2 in our assay and might vary a little in different assays. Therefore, this reference calibrator may be used in all HCV RT-PCR assays.

The range of qualitative RT-PCR was from 10.0 to 0.10 IU/µl calibrator concentrations with Cq of 33.2 to the SigmaStat validated Cq of 39.9 (Table 5.2).

Quantitative RT-PCR report included the plasma viral load, if the result fulfilled the quantitative decision criteria (Table 5.6). Cq from patient's RNA RT-PCR (Fig. 5.4) was converted to the corresponding calibrator concentrations from the calibration plot (Fig. 5.1B), and then converted to plasma viral load using equation-5.

Qualitative RT-PCR report would contain a positive or negative RT-PCR statement. The report may be supplemented with the Cq, and comments on the range of Cq for qualitative RT-PCR (Table 5.6).

5.5.10. Comments on Efficiency

The efficiency calculation by LinRegPCR software was used to determine the quantitative and qualitative range of individual RT-PCR amplifications (Fig. 5.3A to 5.3D; Table 5.3 and Table 5.6C). RT-PCR amplification plot increased exponentially above the threshold line, doubling with every cycle with an efficiency nearer to 2.0, as calculated by LinRegPCR software and equation-4 (Ramakers C et al, 2003). When the efficiency was lower, the template concentration increased by a factor which was less than 2.0. The PCR efficiency at each cycle of RT-PCR could be influenced by primer concentrations and availability at that cycle, inappropriate primer binding, mutations in the primer binding sites on the template and PCR inhibitors (David and Theo, 2006; Life technologies).

The second type of efficiency, calculated from the slope of calibration plot using equation-3, determined whether all the RT-PCR assays, quantitative and qualitative, done with the reagents and calibration data were acceptable or not. There was a relationship between slope, efficiency and sensitivity of the assay in the calibration plot (Fig. 5.1B, 5.1C and Table 5.6D). When the y-intercept increased and the sensitivity of the assay suffered because more of the starting copies were needed before the detection limit was reached. Deterioration of the template, resulting from too many freeze–thaw cycles or storing the template at too low concentrations without a carrier (Adams, 2006). Solution was root cause analysis and recalibration with appropriate fresh reagents.

5.5.11. Comments on X-Y scatter with multiple data points

All results from Fig. 5.1 to Fig. 5.3 were with single data points. The X-Y scatter diagram were used to confirm that similar results were obtained with multiple data points. In most instances the changes in the direction of scatter happened approximately at Cq >33.20, which was the Cq of the validated 10 IU/µl calibrator (Fig. 5.4A to 5.4D). The observations with the calibrators were nearly reproducible with the patients' sample Cq at >33.2 (Fig. 5.5A to 5.5C).

The multiple data points required the calculation of R and R^2. The R^2 for the different X-Y scatter of calibrators ranged from 0.790 to 0.639 indicating fairly good correlation and that 79.0 to 63.9% of the data fit the regression model for the multiple calibrators at each concentration. For the patients sample the R^2 ranged from 0.731 to 0.639, showing close similarity between the correlations of the calibration data and patients' data.

5.6. DISCUSSION

During reporting, the cut-off level for differentiating quantitative and qualitative RT-PCR was 10 IU/µl calibrator concentration, with Cq 33.2 in this report, and might vary little in other laboratories. As the highest four-parameter SigmaStat validated patients' Cq was 39.9 (Table 5.2), the Cq range for reporting validated qualitative RT-PCR was from 33.2 to 39.9.

The report of quantitative RT-PCR included the plasma viral load, if the result fulfilled the quantitative decision criteria. The qualitative RT-PCR report would contain a positive or negative statement. This report may be

supplemented with the Cq, and comments on the range of Cq for qualitative RT-PCR (Table 5.6).

The validated calibrator RT-PCR amplification plot increased exponentially above the threshold line, doubling with every cycle with an efficiency nearer to 2.0, as calculated by LinRegPCR software and equation-4 (Ramakers, 2003). When the efficiency was lower, the template concentration increased by a factor which was much less than 2.0. The PCR efficiency at each cycle of RT-PCR could be influenced by primer concentrations and availability at that cycle, inappropriate primer binding, mutations in the primer binding sites on the template and PCR inhibitors (David and Theo, 2006).

There was a relationship between slope, efficiency and sensitivity calculated from the calibration plot (Fig. 5.1, C and Table 5.6D). These criteria determined whether all the RT-PCR assays, quantitative and qualitative, done with the RT-PCR reagents and calibration data were reportable or not. Deterioration of the template from too many freeze–thaw cycles, storing the template without a carrier (Adams, 2006) and reagent degradation affected calibration plots. Root cause analysis should be done, followed by recalibration with appropriate reagents or calibrators.

All results, except those in X-Y scatter (Fig. 5.4) and Table 5.3, were with single data points. The data from X-Y scatter diagrams and Table 5.3, confirmed that similar results were obtained with multiple data points. The changes in the direction of scatter happened approximately at Cq >33.20, which was the Cq of the validated 10 IU/µl calibrator (Supplemental Fig. 2, A to C). The observations with the calibrators were nearly reproducible with the patients' sample Cq at >33.2 (Fig. 5.5). The high R^2 for the different X-Y scatter of diluted calibrators and patient sample indicated fairly good correlations and data fit for the regression model between them in the qualitative RT-PCR range.

5.7. CONCLUSIONS

In this study data analysis of calibration plot and HCV RT-PCR fluorescence amplification plots were analysed to differentiate between qualitative and quantitative RT-PCR and to establish validation criteria for

qualitative RT-PCR. In qualitative RT-PCR, the fluorescence intensity and slope at inflection point were decreased in qualitative PCR. The lower analytical limit of quantitative PCR calibration plot was at 10 IU/µl calibrator concentration which was equivalent to Cq of about 33. The calibration plot of qualitative RT-PCR concentrations showed unacceptable performance outside the acceptable limits: Cq range 33.2 to 39.9; slope at inflection point from 1.50 – 1.08; four-parameter slope at inflection point ≤1.90; log fluorescence intensity slope <0.255 and efficiency <1.80; calibration plot slope >-3.1 or <-3.6, efficiency >110% and < 90% and acceptable calibration sensitivity 33 – 37.

Fig. 5.1. Construction of RT-PCR calibration plots with validated and diluted calibrators of HCV 5'UTR templates. 1A. Seven RT-PCR plots of cycle number versus normalised fluorescence amplification. Of these, four were validated concentrations of calibrators at 10,000 IU/µl, 1000 IU/µl, 100 IU/µl, 10 IU/µl (from left to right), with the two diluted concentrations 1 IU/µl, 0.1 IU/µl (5th and 6th plots from left), and NTC or blank below the 0.05 threshold line. **1B and 1C:** Calibration plots constructed with log concentration versus threshold cycle (Cq or CT) of the validated (B) and diluted (C) concentrations. **Calibration plot data are given in the box:** where R is coefficient of correlation, R^2 is coefficient of determination, M is slope, B is Y-intercept Cq at log 1 IU/µl = 0.0 on the x-axis, E is efficiency.

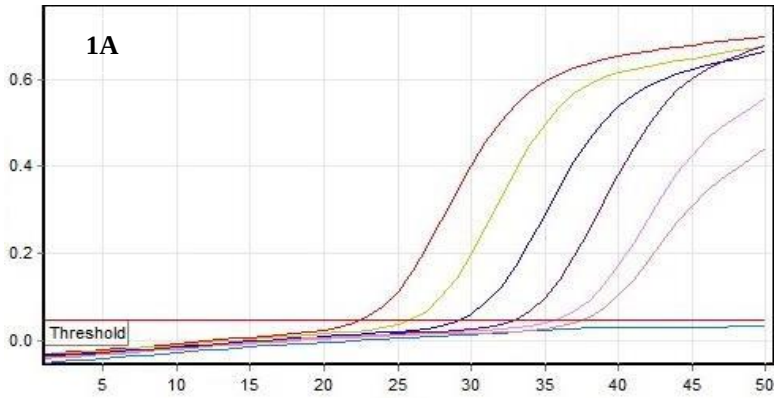

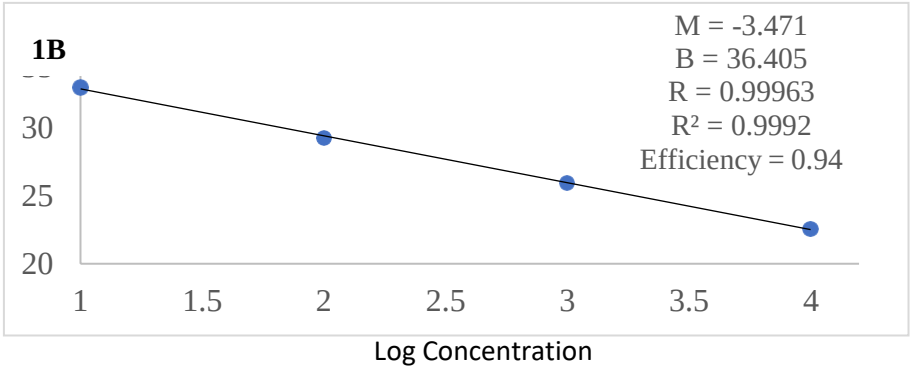

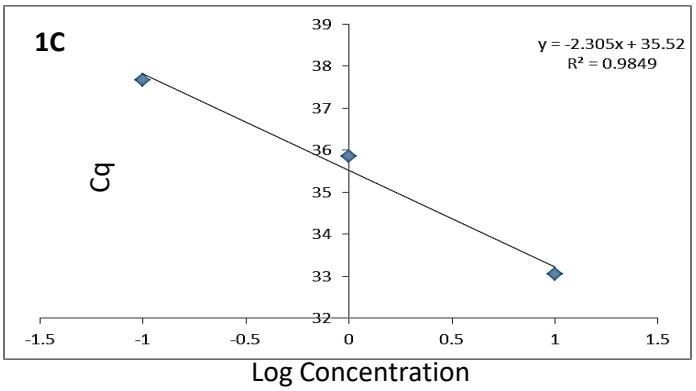

Table 5.1. Analytical bias/imprecision and performance of Cq from calibratorconcentrations.

Calibrators (IU/µl) (n = 6)	Mean±SD	95% CI of mean	%CV
10,000	22.937±0.44	22.47 – 23.40	1.92
1000	26.29±0.664	25.59 – 26.99	2.53
100	30.118±0.45	29.65 – 30.59	1.49
10	33.615±0.61	32.98 – 34.26	1.81
1	36.747±0.77	35.94 – 37.55	2.09
0.1	38.22±1.21	36.95 – 39.49	3.17
0.01	0.00	0.00	0.00

Fig. 5.2. RT-PCR fluorescence amplification plots of HCV 5'UTR templates in RNA isolated from patients' plasma. Three assay sets, each with one plot of validated calibrator (100 IU/µl in 2A, and 10 IU/µl in 2B and 2C) at 100% fluorescence intensity, one plot with high (2A, Cq = 24.27), medium (2B, Cq = 30.85), and low (2C, Cq = 37.14) viral load of HCV RNA isolated from plasma samples, and one NTC.

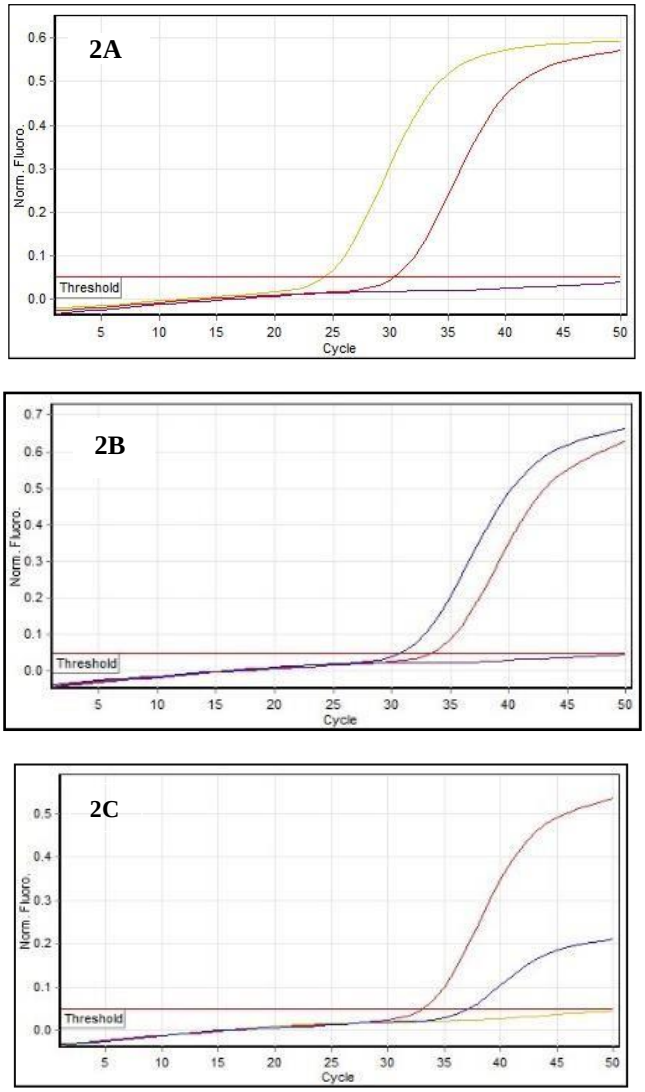

Table 5.2. Comparison of the four-parameters (Equation-2) of the sigmoid fluorescence amplification plots of calibrators and patients' sample using SigmaStat software. F was the fluorescence at cycles X, Y_0 was the ground fluorescence, a is the difference between maximal and the ground fluorescence, X was Cq, X_0 was threshold cycle at inflexion point and b was maximum slope at inflection point.

Calibrator IU/µl or patient Cq range	'a'	b	Xo	Yo	X	F
A. HCV calibrator data						
10,000	**28.3457**	**2.5488**	**31.0893**	**8.1441**	**23.52**	**9.52**
1000	**27.0062**	**2.0575**	**34.1316**	**8.3177**	**27.04**	**9.15**
100	**25.3965**	**2.1379**	**37.4121**	**8.2899**	**30.22**	**9.14**
10	**21.9323**	**1.9498**	**39.8055**	**8.3354**	**33.19**	**9.05**
1	**21.7366**	**1.8399**	**41.6766**	**8.2320**	**35.23**	**9.01**
0.1	**15.386**	**1.8921**	**43.7597**	**8.3823**	**37.77**	**8.87**
B. HCV plasma RNA data						
<30	**30.7911**	**2.7254**	**28.4913**	**7.4396**	**20.11**	**8.79**
	30.2908	**2.0366**	**32.6106**	**7.7446**	**24.77**	**8.37**
30-33	**21.6422**	**2.1516**	**35.9496**	**7.2092**	**30.09**	**8.54**
	19.9231	**2.1437**	**38.7092**	**7.9987**	**32.9**	**9.54**
33-36	**17.0118**	**1.9566**	**39.9054**	**8.1662**	**35.08**	**9.50**
	11.532	**2.1081**	**41.2883**	**8.2021**	**35.61**	**8.93**
36-39	**7.2049**	**1.8377**	**39.1442**	**8.2958**	**36.66**	**9.77**
	7.8317	**1.6209**	**41.1921**	**8.3832**	**38.57**	**9.67**
>39	**7.6439**	**1.6506**	**41.9932**	**8.2528**	**39.5**	**9.63**
	6.958	**1.6796**	**41.3865**	**7.7825**	**39.9**	**9.24**

Fig. 5.3. Log transformed fluorescence amplification plot from LinRegPCR software. Cycle number versus log fluorescence amplification plots of HCV RT-PCR were constructed using LinRegPCR software and analysed for slope of the linear part from which efficiency was calculated. **3A.** The six calibration plots in Fig-**3A;** The patients' plasma HCV RNA sample with high (**3B**), medium (**3C**), and low (**3D**) viral loads with one validated calibrator (10 IU/µl) in each set from Fig-3B to D.

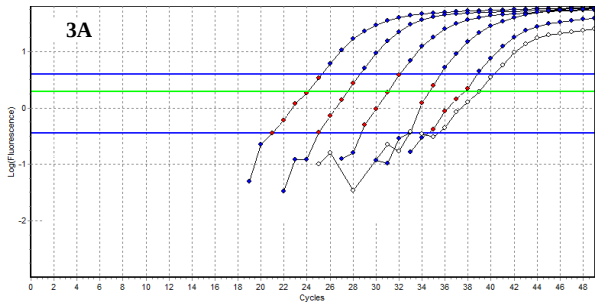

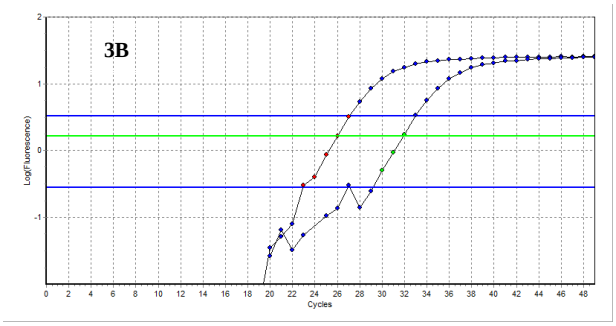

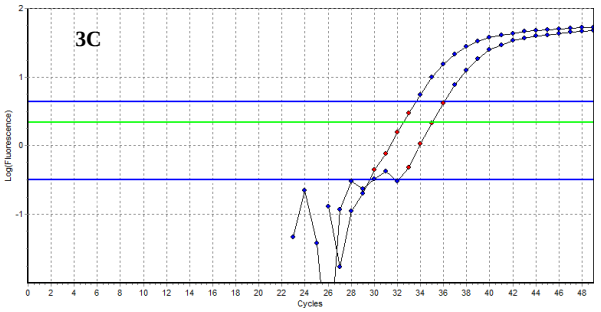

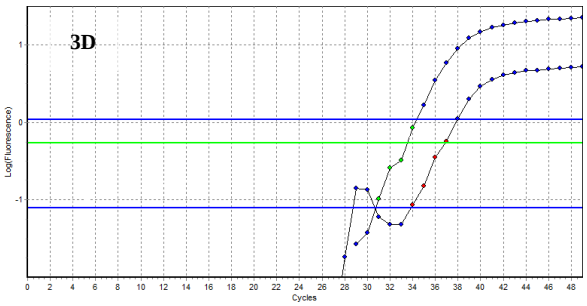

Table 5.3. Comparison of fluorescence amplification plot data of calibrators from LinRegPCR software with manually measured data. Comparison of RT-PCR data of plots of cycle number versus log fluorescence amplification plots of **HCV validated calibrators and diluted calibrators** using LinRegPCR software. Concentrations of calibrator viral load, IU/µl, were also converted to plasma viral load, IU/ml. E was efficiency calculated from slope.

IU/µl calibrator / IU/ml plasma	**Cq**	**LinRegPCR software**		**Manually measured**	
		E	**Slope**	**Normalised fluorescence intensity**	**Slope at inflection point, b**
HCV RT-PCR of calibrator data					
10^4 / 4.28×10^6	23.52	1.98	0.297	100	1.647
10^3 / 4.28×10^5	27.03	1.923	0.284	100	1.614
10^2 / 4.28×10^4	30.08	1.821	0.260	100	1.566
10^1 / 4.28×10^3	33.19	1.9	0.2787	100	1.571
1 / 4.28×10^2	35.8	1.75	0.243	89	1.477
0.1 / 4.28×10^1	37.74	1.7	0.230	78	1.08

Table 5.4. Comparison of fluorescence amplification plot data of patients RNA from LinRegPCR software with manually measured data. Comparison of real time RT-PCR data of plots of cycle number versus log fluorescence amplification plots of **HCV patients' plasma RNA sample** using LinRegPCR software. Concentrations of calibrator viral load, IU/µl, were also converted to plasma viral load, IU/ml (Ref. 'Methods' section). E was efficiency.

IU/µl calibrator / IU/ml plasma	**Cq**	**LinRegPCR software**		**Manually measured**	
		E	**Slope**	**Normalised fluorescence intensity**	**Slope at inflection point, b**
HCV RT-PCR of plasma RNA data					
1.25×10^5 / 5.34×10^7	20.16	1.998	0.301	100	1.7
2.27×10^3 / 9.71×10^5	24.77	1.8	0.255	100	1.66
5.5×10^1 / 2.35×10^4	30.85	1.708	0.232	100	1.54
4.4×10^1 / 1.88×10^4	32.9	1.797	0.255	90	1.58
--	37.23	1.728	0.238	55	0.928
--	38.21	1.489	0.173	40	0.553

Fig. 5.4. X-Y scatter, trendline and correlations of parameters of HCV RT-PCR. Correlations of concentrations or Cq of diluted calibrators, 10 IU/µl calibrator (A to D) with parameters of RT-PCR fluorescence amplification. **4A.**Log diluted calibrator concentrations versus Cq, **4B.** Log diluted calibratorconcentration versus slope at inflection point, **4C.** Cq versus normalised fluorescenceintensity compared to 100% fluorescence of 10 IU/µl validated calibrator. **4D.** Log diluted calibrator concentrations versus efficiency of individual fluorescenceamplification (from LinRegPCR).

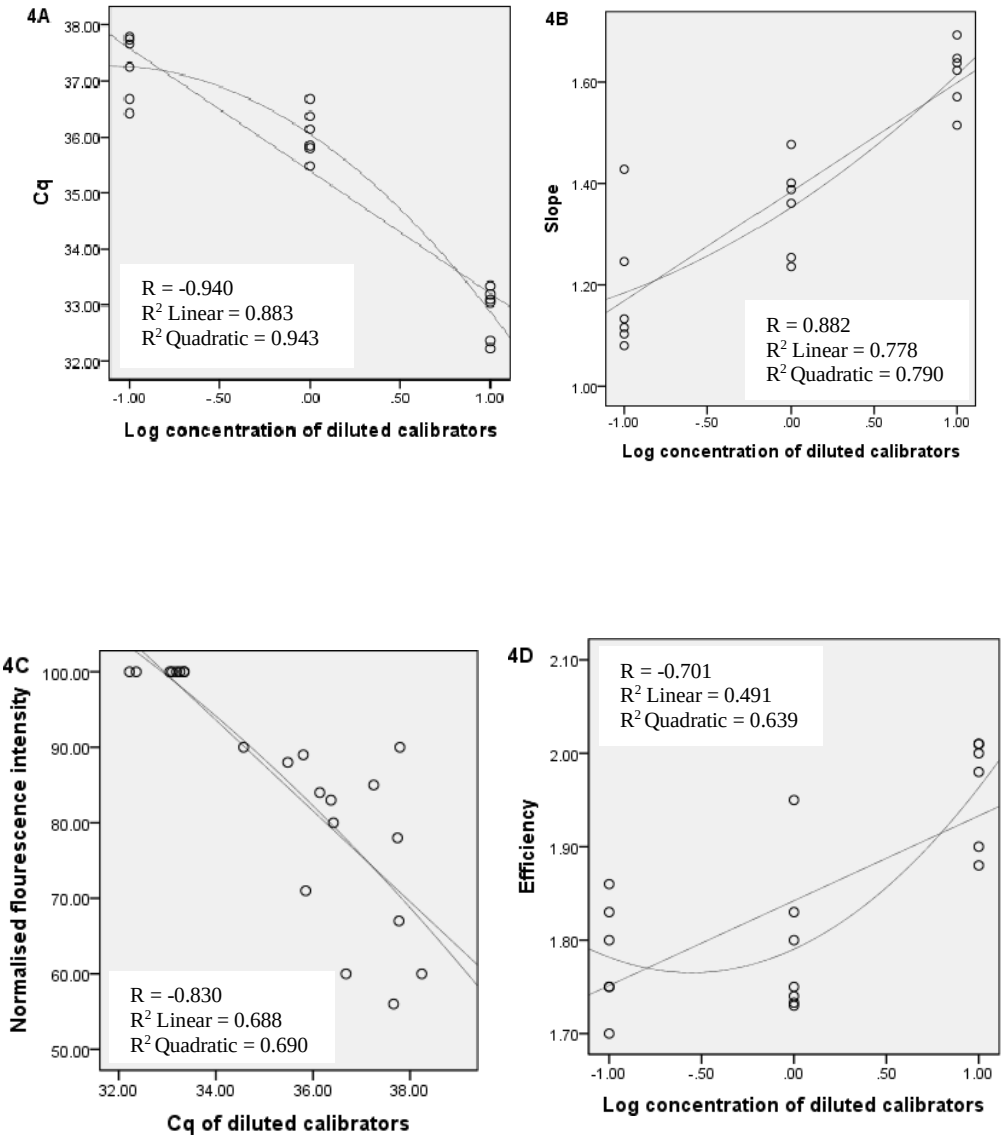

Fig. 5.5. X-Y scatter, trendline and corelations of parameters of HCV RT-PCR of plasma samples. 5A. Cq versus slope at the inflection point. **5B.** Cq versus normalised fluorescence intensity, **5C**. Cq versus efficiency of individual fluorescence amplification (from LinRegPCR).

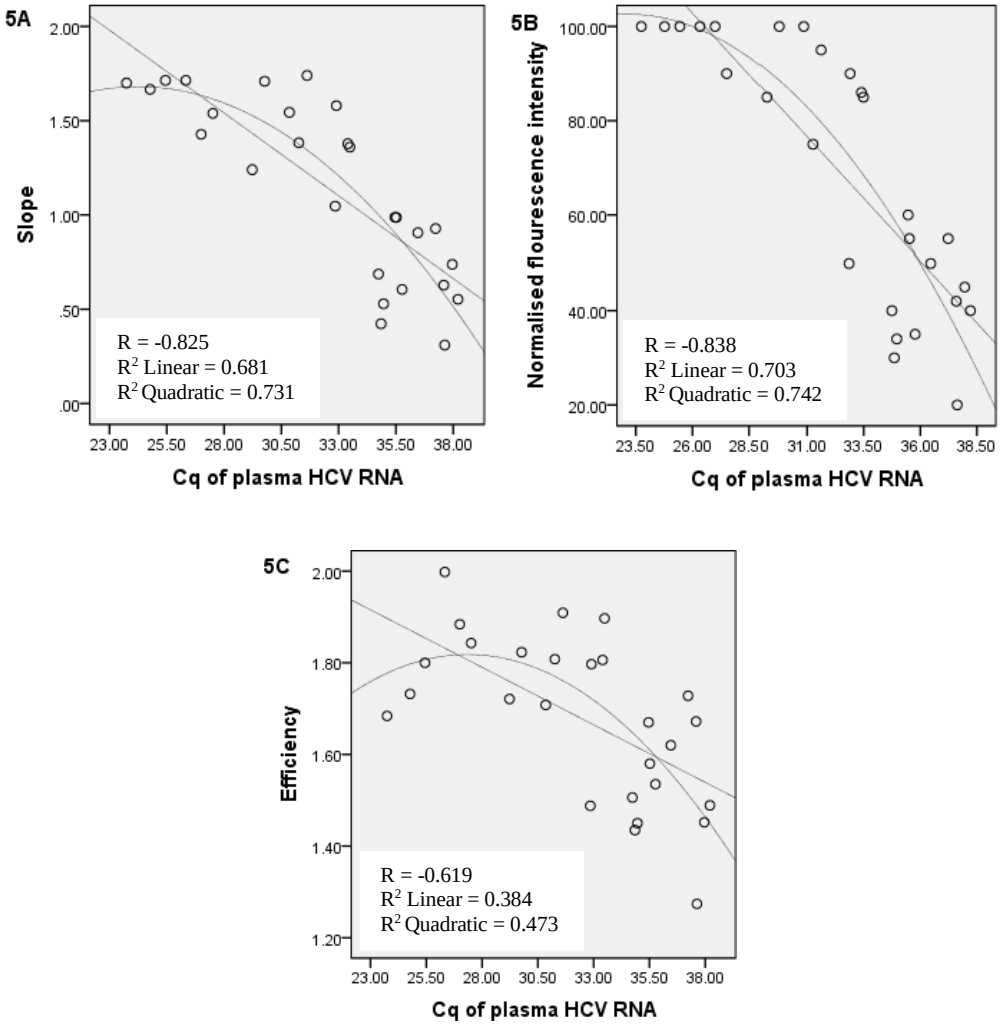

Table 5.5. Validation by qualitative PCR using gene specific primers of HCV plasma samples having sigmoid amplification plot in RT-PCR with Cq > 35.5.

Sl. No	Sample	Amplified/ Not Amplified	NCBI Accession No.	Cq
1	Case 619	Amplified	MW281561	36.85
2	Case 218	Amplified	MT258412	37.63
3	Case 216	Amplified	MW281560	35.5
4	Case 194	Amplified	MW970035	36.37
5	Case 23	Amplified	KX455813	36.1
6	Case 566	Amplified	MW970030	36.99
7	Case 561	Amplified	No Result	37.45
8	Case 562	Amplified	No Result	37.55

Fig. 5.6. The agarose gel electrophoresis and Gel documentation of 100 bp DNA ladder (1), PCR product 5'UTR (2) and Core E1(3) region and NTC (4)

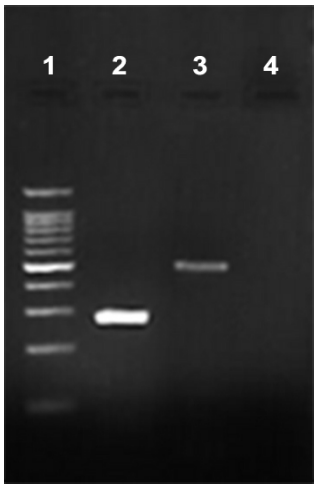

Table 5.6. Decision criteria for differentiation quantitative and qualitative real time RT-PCR. Data from the fluorescence amplification plots by (a) visual observation, (b) calibration plots, (c) four-parameter data from SigmaStat, (d) log fluorescence intensity from LinRegPCR and refer chapter 9 for (e) sequence analysis.

Parameter	Quantitative range	Qualitative range	Sources of the Data and Comments
A. Graphical observation from fluorescence amplification plot			
Normalised fluorescence intensity, 'a'	Near 100%	<90%	Manually measured; Data from Fig. 5.1 and Table 5.3
Slope at inflection point, b	1.65 – 1.50	1.50 – 1.08	Manually measured; Data from Fig. 5.1 and Table 5.3
Cq or Concentration of Calibrator	<33.20 or >10 IU/µl	33.20 to 39.90 or <10 IU/µl	Data from Fig. 8.1, Table 5.1. 10 IU/µl calibrator may be used as a reference data point in RT-PCR assays
B. Four-parameter data from calibrators and plasma RNA by SigmaStat software			
Fluorescence intensity (normalised), 'a'	28.35 – 21.93 (100%)	21.74 – 15.39 (decreased)	Data from Table 5.2
Slope at inflection point, b	2.55 – 1.95 (100%)	≤1.90 (decreased)	Data from Table 5.2
C. Log fluorescence intensity from LinRegPCR software			
Slope	0.301 - 0.255	<0.255	Data from Fig. 5.3. and Table 5.3
Efficiency, E	2.0 – 1.80	<1.80	Data from Fig. 5.3. and Table 5.3
D. Data analysis of Calibration plots			
Slope, M	-3.1 to -3.6	>-3.1 or <-3.6 (outside numerical value of 3.1 to 3.6)	Data from Fig. 5.1B
Efficiency	110% - 90%	>110% and < 90%	Data from Fig. 5.1B
Acceptable calibration Sensitivity, Cq at 1 IU/µl	33 – 37	33 – 37	<33 or >37 unacceptable calibration plot sensitivity.
%CV of calibrator and diluted calibrator, Cq	<7%	<7%	>7% Unacceptable calibrator RT-PCR Cq performance. Data from Table 5.1.

Chapter 6

Analysis of Internal Controls in the matrix of HCV RT-PCR assays showed analytical and pre-analytical influences independent of template concentrations

6.1. ABSTRACT

Internal control (IC), made up of the reference gene PCR amplification system with fixed concentration of template and fluorescent probe, and present in the assay matrix of all HCV RT-PCR assay systems, was evaluated for detection of the preanalytical and analytical influences on the amplification systems. IC was added to patients' plasma RNA, calibrators, quality control (QC) RNA and non-template control (NTC). All IC additions were from the same lot for a set of calculations. The IC fluorescence emission of ROX dye at 610±5 nm, was independent of the HCV template amplification with FAM dye having emission at 510±5 nm. The average IC threshold cycle (Cq) was lowest for NTC (30.346), followed by the calibrators (31.425), and it was even higher for quality control samples (33.767) and the HCV infected patients' plasma RNA sample (33.017). The average %CV was the same for NTC, calibrators and QC sample. But was increased for patients' sample. The lowest average Cq in NTC might due to absence of HCV RT-PCR products, which were present in calibrators. The QC and patients' samples contained the PCR products, and in addition it contained the RNA from plasma which included the non-specific RNA. These PCR products might be the causes for the influence on IC Cq. The patients' samples were from different patients', unlike that of QC sample and calibrators which were a single sample, contributing to higher average patients' %CV. The mean Cq difference between NTC and calibrators might be attributed to analytical influence, while that between the calibrator and patients' sample might be attributed to pre-analytical influences. Slope, normalised fluorescence intensity and efficiency decreases with decrease in viral load both in calibrators and with patient samples. when concentration is expressed as Cq, the relationship of Cq, fluorescence intensity and efficiency become inversely related.

6.2. INTRODUCTION

The plasma viral load in hepatitis C virus (HCV) infection was often found to be very low in a large number of patients (Glynn et al, 2005; Fytili et al, 2007), much below the validated calibration plots for quantitative PCR (RT-qPCR) (artus HCV RG RT-PCR Kit Handbook, 2012). As large number of patients with HCV infection have no symptoms (Orland et al, 2001), diagnosis of HCV infection was done by screening for anti-HCV antibody, followed by selecting the patients with reactive levels of antibody (Ritcher, 2002) for confirmation of diagnosis by HCV RT-PCR of RNA isolated from plasma (Bukh et al, 1992; Barbara et al, 2009). Most patients with HCV have very low anti-HCV antibody levels and low viral loads (Fytili et al, 2007; Zer et al, 2009). In practice, when the signal level decreases, the errors become more prominent and influence the signals. Similarly, preanalytical influences are prominent when template or viral concentrations are low, as in HCV RT-PCR, and these influences, whenever possible, may be decreased by selecting patients without tissue damaging conditions such are surgery, crush injury, abscess, chronic ulcers, such as diabetic foot and in autoimmune diseases. The pre-analytical and analytical influence are least evident when the HCV template concentrations were high, especially at Cq <33 (Joseph et al, 2022 and chapter 5).

The negative RT-PCR results should truly represent the absence of PCR diagnostic targets. But false-negative results could occur from failure of one of the test steps of nucleic acid extraction, reverse transcription reaction and RT-PCR set up, or inhibitory substances in the samples. Efforts to control false-negative results were based on the addition of exogenous nucleic acids amplification system (the IC) to the RT-PCR reaction, so that the presence of any inhibitory substances (e.g., heparin) in the samples or errors in test steps would also affect the amplification of the exogenous material (Zambenedetti et al, 2017). Therefore, the research problem in the present report was that the IC might be used to detect influences on the RT-PCR assay systems independent of HCV template concentrations.

As HCV RT-PCR Cq value was varying in patients' sample according to viral load, it could not be used for studying the analytical and preanalytical influences. Internal Control (IC) RT-PCR amplification system with fixed concentration of reference gene template, with the ROX dye, present in the assay matrix, could be used to analyse the various influences independent of the HCV template amplification. ICs were added to patients' sample, calibrators, quality control (QC) samples and into the non-template control (NTC). Due to these reasons, IC could be used to study the preanalytical and analytical influences on the RT-PCR amplification. This was the research hypothesis of this report.

6.3. Aspects of the original objectives addressed in this chapter

1. Establishment of the methods for evaluation by data analysis, test validation, quality control and clinical state of the patient for Molecular Diagnostic reporting of Hepatitis C infection.
2. Use of these procedures for confirmatory diagnosis of hepatitis C infection, its plasma viral count determination and genotyping.

The following research problems were addressed in this chapter for part-fulfilment of the above two main objectives.

Part of the objective of this study was to evaluate the influence of the 'clinical state of the patient' on the HCV RT-PCR assay system, especially when the viral load in patients were low or very low. The research problem in the present report was to evaluate the use of the fixed concentration of IC to detect the sample influences on the RT-PCR assay systems, independent of HCV template concentrations, which vary from patient to patient.

6.4. MATERIALS AND METHODS

The study design was observational, control study of ICs in real-time RT-PCR for HCV of RNA isolated from plasma of individuals who were reactive for anti-HCV antibody or suspected to have contacted HCV infection.

6.4.1. Sample Collection and Anti-HCV antibody Screening assay

Blood samples were collected in vacuum tubes with clot activator (red capped, 4 ml), mixed, allowed to clot for 10 minutes, centrifuged at 3000 rpm for 5 minutes in a table top centrifuge, serum was separated, and clear serum samples without haemolysis, jaundice, cloudiness and clot particles were screened for the anti-HCV antibody with third generation enzyme immunoassays. The assay was performed in Vitros ECi immunochemistry autoanalyser (Ortho Clinical Diagnostics, USA) using enhanced chemiluminescence method. When screening assay showed reactivity above the cut off limit, RT-PCR was done for confirming the diagnosis of HCV infection. HCV RT-PCR was done directly, without reactivity to antibody screening assay, in individuals frequently exposed to HCV infection, such as patients on dialysis or repeated blood transfusion. This was done to cover the long window period of HCV infection.

6.4.2. Inclusion and Exclusion criteria, Preanalytical influences, Sample collection for RT-PCR

Inclusion criteria were reactivity to anti-HCV antibody and exposure to HCV infection. Exclusion criteria were related to the preanalytical condition of the patient, such as acute tissue damaging disease conditions, patients on chemotherapy and who were heparinised were found to influence the RT-PCR (Byrnes et al, 1975; Akane et al, 1994; Al Soud et al, 2001; Burkardt, 2000; Radstorm et al, 2004; Yedidag et al, 1996). These conditions were avoided as far as possible. In all emergency and other unavoidable circumstances, all the above preanalytical criteria were overlooked, but the results of RT-PCR were analysed for influences. Other inclusion criteria were reactivity to anti-HCV antibody and exposure to HCV infection. Refer Details 4.2

Blood sample was taken with 4 ml EDTA-vacutainers, centrifuged at 3000 rpm for 15 minutes in a table top centrifuge. Plasma sample without haemolysis, jaundice, cloudiness and without clot particles was separated (WHO, 2002) and used for RNA isolation and HCV RT-PCR. Plasma and RNA samples were stored immediately at -20^{o}C and -80^{0}C, respectively, in aliquots. Refer Details 4.3.2

6.4.3. Organisation of study: A. Types of assays and the assay matrix components

The study was organized with reference to the four types of assays, NTC, calibrators, QCs and patients' sample (Table 6.1). HCV and IC templates with their respective fluorescent probes were in the same assay matrix but with different excitation and emission wavelengths, and detection channels. Total volume of 128 µl of reagents were prepared and 30 µl was distributed into the four types of assay tubes so that concentration of the fluorescent probes was same in each assay tube. If there were more than one of each assay type then the total volume of reagents was increased in multiples of 30 µl.

6.4.4. Organisation of study: B. Differentiating Analytical and Preanalytical influences

The components of RT-PCR assay that would influence the amplification system might be considered as the following: (1) RT-PCR amplification products of reference gene in IC; (2) RT-PCR amplification products of HCV template; (3) RT-PCR influences of non-specific RNA and the possible influences of amplification products of non-specific RNA, and (4) varying RNA isolated from plasma of different patients might influence the Cq of IC causing higher variations.

The NTC is influenced by (1); the calibrators by (1+2); the QC samples by (1+2+3); the patients' sample might be influenced by (1+2+3+4).

The analytical and pre-analytical influences could be differentiated on the following principles:

a) The analytical influences might be considered as the differences in the performance of Cq of ICs in the calibrators and NTC:
- Analytical Bias = mean Cq of calibrator ICs – mean Cq of NTC ICs
- Analytical imprecision = %CV of calibrator ICs – %CV of NTC ICs

b) The preanalytical influences might be considered as the differences in the performance of ICs in plasma RNA (patients' sample or QC sample) and the calibrators.

- Pre analytical Bias = mean Cq of ICs in patients' sample – mean Cq of ICs in calibrator
- Pre analytical imprecision = %CV of ICs in patients' sample – %CV of ICs in calibrator

HCV viral RNA isolation was done by chromatography method from plasma with QIAamp Viral RNA Mini Kit (Qiagen, Germany). Plasma (140 µl) was added to AVL buffer with carrier RNA, precipitated with ethanol, passed through QIAamp mini column. Unbound material was washed out. RNA was eluted with 60 µl elution buffer. Eluted RNA was assayed immediately and stored in aliquots at -80°C.

6.4.5. HCV RT-PCR of RNA isolated from patients' plasma

HCV RT-PCR was done using RNA isolated from plasma or QC sample, along with one validated calibrator, blank (NTC) and IC with reference gene in the assay matrix (Table 6.1), according to manufacturer's instructions.

Equation for conversion of IU/µl of calibrator to IU/ml of plasma sample is given below. Calculation of plasma viral load from Cq obtained by real time RT-PCR of HCV infected plasma sample, and converted to concentration of the template from the calibration plot.

$$\textbf{Viral load (IU/ml of plasma)} = \frac{\textbf{(Patients' result Cq as IU/µl from calibration plot) x Elution Volume (60 µl)}}{\textbf{Sample Volume (0.14 ml)}}$$

6.4.6. Quality Control Reagents

First-party (Qiagen, Germany) or third-party (Qnostics, UK, supplied by Randox, UK) quality control (QC) reagents were used for QC assays with each set of HCV RT-PCR of patients' RNA. The third-party controls were from a quality control reagent supplier and there were of three reagents, plasma samples of QC-1, QC-2 (genotype 1) and QC-3 (genotype 3) samples. The first-party controls were the validated calibrators of the reagent manufacturer. The performance values (mean±SD, 95% CI of mean and %CV) for QC samples were calculated and given under results. NTC contained all the assay mix including IC,

except the HCV 5'UTR template. The second party QC samples were prepared by the user laboratory from HCV RT-PCR positive samples, typically immediately after calibrating with fresh calibrators and QC reagents.

Internal Control (IC) with reference genes were added to the assay matrix of NTC, calibrators, QCs and patients' samples. IC fluorescence probe ROX (6-carboxy-X-rhodamine) was with excitation 585±5 nm and detection 610±5 nm. The hydrolysis probe in the test sample was Fluorescein amidites (FAM) and which has an excitation 470±10 nm and emission wavelength and detection at 510±5nm.

Calibrators, Of the four validated calibrators supplied by the manufacturer (Qiagen) S3 (100 IU/µl) and S4 (10 IU/µl) were used in this study. Traceability of the validated calibrators were to the reference standard at the National Institute for Biological Standards and Control (NIBSC, UK) which coordinated the traceability studies on behalf of WHO.

6.4.7. Levey-Jennings Plot

Levey-Jennings (L-J) plot is the common representation of quality control (bias and imprecision) and is done to evaluate the QC results. The QC results from the same lot of QC reagents were added to the plot with time (daily or with varying frequency). When the QC showed a stable performance, the mean value line represented the expected target value and the Standard Deviations (1 SD, 2 SD, 3 SD) lines represented the expected imprecision. Assuming a Gaussian distribution, of imprecision, we expect approximately 99.72% within ±3SD, 0.28% outside ±3SD, 95.44% within ±2SD, 4.56% outside ±2SD, 68.26% within ±1SD and 31.74% outside ±1SD. These data should be differentiated from the QC rules and events data, where 1_{1S} represented the single data points between ±1SD and ±2SD, and 1_{2S} event represented two consecutive data points between ±1SD and ±2SD.

All other details of Methodology were described under Chapter 4 where the general 'Methodology' was given.

6.5. RESULTS

6.5.1. HCV RT-PCR amplification plots of various assay systems and their internal controls

Organisation of the study with reference to the four types of assays, the fluorescent probes of HCV and ICs in the assay matrix. Total volume of 128 µl of reagents were prepared and 30 µl was distributed into the four types of assay tubes so that concentrations of the fluorescent probes were same in each assay tube where Ex. is excitation, Em. is emission (Table 6.1).

Amplification plots of calibrators, QC reagents, patient sample and NTC were plotted to evaluate the amplification, Cq and fluorescence intensity. In the QC-1 sample, the Cq was 34.09, the fluorescence intensity and slope at inflection point were decreased when compared with the samples having lower Cq (or higher template concentration). NTC, as expected, was below the threshold line. The validated calibrators S3 (100 IU/µl), S4 (10 IU/µl) and the patient sample (Cq = 25.81) showed amplification plots that had good RT-PCR amplification and slope at inflection point (Fig. 6.1A).

The ICs of all the five RT-PCR assays in Fig. 6.1A were evaluated for their Cq and fluorescence intensity. The IC of NTC had the lowest Cq of 30.04. The patient's sample showed the maximum increase in Cq of 32.58 and was higher than that of S3 and S4 calibrators (30.31 to 30.88). The Cq of QC-1 sample which had the same sample matrix of plasma as the patient's sample was intermediate between calibrators and patient sample (Fig. 6.1B).

6.5.2. HCV RT-PCR calibration plot data analysis of diluted calibrators

The calibration plot was constructed with log concentration versus Cq and the slopes between each concentration points were measured. From 100 IU/µl to 10 IU/µl, the slope was -3.76; from 10 IU/µl to 1 IU/µl the slope was -2.8 and from 1 IU/µl to 0.1 IU/µl, the slope was -1.81 (Fig. 6.2).

The numerical slopes were found to decrease with decrease in concentration.

The calibration plots were also constructed with multiple data points (n=7) for each concentration from 100 IU/µl to 0.1 IU/µl. The mean and SD of these 7 data points were calculated and plotted (Fig. 6.3). The mean of each data points were connected to measure the slope between each concentration points (Bold line in Fig. 6.3). The numerical value of slope decreased from 3.87 to 1.542. The average slope was also measured by constructing a straight-line calibration graph through the different data points. The mean value of average slope decreased at -2.7687. the Y-intercept was 36.043 at 1 IU/µl. The coefficient of determination (R^2) was very high 0.9754. These results indicated that the slope of the calibration plot decreased with decrease in concentration below 10 IU/µl, indicating the lack of acceptability of the calibration plot below 10 IU/µl.

6.5.3. Influence of various assay systems on the Internal Control threshold cycle, Cq

The performance characteristics of Cq of quality control samples of various assay systems were studied (Table 6.2A). The performance characteristics of Cq of IC of various assay systems (Table 6.2B) were evaluated. The IC of NTC (n = 6) showed the lowest mean Cq of 30.346 and the variation, as expressed by % CV 1.3, was low. The mean Cq of calibrators, which were used as first party control reagents, was found to be 31.425 (S4) and 30.92 (S3), and were higher than that obtained by IC in NTC. The ICs in QC-1 was even higher with mean Cq of 33.767 with %CV of 1.52 (Table 6.2B). IC of QC-2 and QC-3 were also increased at 31.563 and 31.663, respectively. Similarly, the mean Cq of IC was also increased in the second party quality control reagents. These results indicated that the assay matrix of the plasma sample can influence the Cq and cause an increase in the mean Cq value.

The influence of RT-PCR products and patient RNA on Cq of IC were analysed by plotting the mean Cq of IC from various HCV RT-PCR assays and controls. The mean IC Cq of patient sample with Cq 30 – 36 (n

= 6) was 32.42, patient sample with Cq >36 (n = 6) was 33.053, and that in patient sample with Cq <30 (n = 6) was 32.2 (Fig. 6.4A). The Cq was lowest for IC of NTC and the Cq increased sequentially for IC of calibrator, QC reagents and in patients' sample (Fig. 6.4A).

Similarly, the average %CV of Cq from IC of NTC, calibrators, QC reagents and patient samples were found to be similar, unlike that seen with mean Cq. But the %CV was markedly increased in the patient's sample (Fig. 6.4B). The results indicated that, even though the mean Cq increased sequentially, the variation was increased only in the different patients' sample.

6.5.4. Analytical variation of calibrators and diluted calibrators

The performance characteristics of the calibrators and diluted calibrators at various concentrations were evaluated by calculating the Mean, SD, 95% CI and %CV of the Cq value at various concentrations. The %CV ranged from 1.359 to 2.006 from 10,000 to 1 IU/µl (Table 6.3). At 0.1 IU/µl the %CV suddenly increased to 2.913.

The %CV of the calibrator concentration converted to concentration of IU/ml of the calibrator was found to have a higher %CV range. This was due to the log scale of concentration used in the previous calculation of %CV of Cq. The %CV ranged from 23.723 to 28.391 from 10,000 IU/µl to 100 IU/µl. At 10 IU/µl and 1 IU/µl the %CV were 41.138 and 43.774 respectively (Table 6.3). The %CV was found to increase with calibrator concentration from 10 IU/µl downwards.

6.5.5. X-Y scatter of Cq or concentration versus various RT-PCR parameters

X-Y scatter diagram were plotted with calibrator concentrations or Cq of calibrators against various RT-PCR parameters such as slope, normalized fluorescence intensity and efficiency. The concentration and Cq of calibration at 100 IU/µl and 10 IU/µl had similar slope, fluorescence intensity and efficiency (Fig. 6.5). These results confirmed that there are validated calibrators with acceptable performance. But at diluted calibrator concentration of 1 IU/µl and 0.1 IU/µl, the performance of these RT-PCR

parameters decreased with decrease in concentration. The R^2 for slope and normalized fluorescence intensity were found to have a quadratic, than a linear relationship. This resulted from the decrease in performance at lower concentration. But as concentration decreased, decrease in efficiency was linear (Fig. 6.5).

Similar data as above for calibrators was also collected for patient sample. RT-PCR parameter of slope, fluorescence intensity and efficiency were compared with Cq of patient sample by use of X-Y scatter diagram. All scatter diagrams showed a linear decrease in slope, fluorescence intensity and efficiency with increase in Cq of HCV in patients plasma sample. This decrease was evident from Cq around 29 to 38.5 (Fig. 6.6). These results indicate that there is influence on RT-PCR amplification by patient plasma sample even at relatively higher concentration of HCV template in the plasma. The Cq of 10 IU/µl calibrator, which is the borderline of quantitative and qualitative RT-PCR, was the point at which the performance decreased in the calibrators. But in patient sample, the performance started decreasing even from a Cq of 29. This is the major difference between X-Y scatter of calibrators and patients' plasma sample.

6.5.6. Four parameter data analysis

The sigmoid fluorescence amplification plot characteristic might be analysed by the four parameters as represented by 'a' (difference between maximum and ground florescence), 'b' (slope at inflection point) and Y_0 (ground fluorescence). Of these four parameters, 'a' was found to decrease when the concentration falls below that of the validated calibrators. The fluorescence intensity decreased sequentially at 1 IU/µl and 0.1 IU/µl. The slope did not show noticeable variation (Table 6.4). These differences in the observed slope of the sigmoid amplification and slope calculated from SigmaStat curve fit model, were due to calculations related to the curve fit model. Therefore, these characteristics are better suited for validation of a qualitative RT-PCR amplification plot. The maximum Cq observed was 40.17 and the sigmoid characteristics of

fluorescence intensity, slope at infection point X_0 and Y_0 were preserved. Therefore, from these results the limit of detection in terms Cq was 40.17.

The difference between the Cq at threshold level and the Cq at the inflection point (X_0 - X) have been identified as other criteria to evaluate the sigmoid characteristic of the fluorescence amplification plot (Table 6.4 and Fig. 6.7). As the slope decreases, the X_0 – X increases, further decrease in slope, the X_0 – X was found to further increase to much lower levels. The quadratic trendline R^2 was found to be 0.408 and indicates the observed trendline. The peak difference of X_0 – X was found to be at Cq of 36.00.

6.5.7. Validation of Cq and sigmoid amplification plot of calibrators and patient sample with SigmaStat

The influences of the patient's sample on HCV RT-PCR amplification plot when analysed by SigmaStat software was found to show large variations. The fluorescence intensity change 'a' from Cq of 33 – 36 was found to vary significantly from 4.2005 - 19.923 (Table 6.5). The slope at inflection point was found to vary significantly from 1.7868 - 7.7637. There was also moderate variation from Cq 36 – 39. The fluorescence intensity 'a' was found to vary from 1.6 to 9.09. the slope at inflection point was found to vary from 1.6307 - 12.3918 (Table 6.4, details are described under Table 6.5). From these variations it appears that fluorescence intensity variations were higher at 33-36 Cq than at 36 - 39 Cq. But, the slope at an inflection point 'b' may vary higher at 36-39 Cq.

The value of X_0 – X was found to decrease in patient sample with increase in Cq from 34 - 39 (Fig. 6.8). But with calibrator the X_0 – X was lower at Cq 33, then increased to a peak at Cq 36 and then decreased. It shows that in patient sample the X_0 – X was higher at Cq 34 in patient sample than for calibrator at Cq 33. So, these results indicate that there is influence on sigmoid amplification plot in patient sample.

The %CV of calibrators and patient sample were found to be very similar with %CV of 2.56 and 2.8 respectively (Table 6. 6). Therefore, at these ranges, the influence on Cq was much less but the amplification plot

above the threshold had strong influence on fluorescence intensity and slope. In the calibrators, the %CV for ‘a’ and ‘b’ were 15.34 and 15.16 respectively which were quite high. But in the patient samples, these values were at 51.34 and 62.17 respectively. Therefore, in the patient sample showed major influence on the variation in the amplification plot above the threshold value (Table 6.6). These results indicate that upto threshold line, RT-PCR amplification and Cq appears to be more constant in the calibrator and patient sample. But above the threshold, the fluorescence intensity and slope showed major influences in the patient sample and moderate influence with calibrators.

The experimental amplification above and below the threshold line might be converted to the linear scale by log transformation using LinRegPCR software. The exponential amplification above the threshold is characteristic of RT-PCR. This feature has been evaluated in Fig 6.8 and Fig. 6.9. The calibrators at low concentration have been used to perform the evaluation. There is a characteristic linear LinRegPCR plot for the high template concentration of calibrators (10,000 IU/ml, Cq 23.43) with a linear plot having 6 points. The 1 IU/µl, 0.1 IU/µl and 0.05 IU/µl calibrator also have a linear LinRegPCR plot with more than 4 points in the linear scale (Fig. 6.9A and B).

When the graphical evaluation of LinRegPCR plot of patient sample with low viral load were analysed, it was observed that a Cq of 37.14, gave more than 4 linear points (Fig. 6.10A). But as the Cq increased to 37.91 and 39.78 the linearity of the points were found to be moderately or severely affected in the respective plots (Fig. 6.10B and C). Therefore, the LinRegPCR plot of exponential amplification may not validate the patient sample with Cq 39.78. Similarly, there were issues with patient sample with Cq of 38.13 which showed only two linear points in the LinRegPCR plot (Fig. 6.10D). Similarly, at Cq of 39.12 also the linearity of the LinRegPCR plot showed three points (Fig. 6.10E).

These results indicate that above Cq 39 validation of the sigmoid amplification with LinRegPCR plot was difficult.

6.5.8. Levey-Jennings Plot of Internal Controls from various assay systems

When the L-J plot of ICs of various samples were analysed, there were large number single events between ±1SD and ±2SD. The number decreased to 3 events between ±2SD and ±3SD, and further decreased to 1 event outside ±3SD (Table 6.7).

The total number of events outside ±1SD for NTC was 10 (8+2) and the total number of samples were 30. Therefore, 33.3 % of the events were outside ±1SD, which was very close to the expected events, 31.74%. Similarly, the IC Cq values for calibrator S4, QC-1 and patient RNA were calculated.

a) Percentage of events outside the ±1SD for NTC, calibrator S4 (Fig. 6.11) and QC-1 (Fig. 6.12) are 33.33%, 36.67% and 40%, respectively. There were no events outside ±2SD for the above.

b) Percentage of events outside the ±1SD for HCV patients' RNA with Cq <30, Cq 30 – 36, Cq >36 were 22.22%, 16.66% and 20.69%, respectively. Percentage of events outside the ±2SD for patients' samples with Cq <30, Cq 30 – 36, Cq >36 were 3.7%, 8.33% and 0%, respectively. But percentage of events outside ±3SD for Cq >36 was 3.45% (Fig. 6.13).

These results indicate that the number of events outside ±2SD and ±3SD were more in patients' samples.

The assays given in the L-J plot were analysed for their bias and imprecision by calculating the mean and SD. The mean and %CV of performance of Cq of ICs in the environment of assay matrix of NTC, calibrators (first party QC), QC-1 and patient sample were analysed. The NTC had the lowest mean Cq, followed by the calibrator. The patients' sample and QC-1 showed the higher mean Cq. The patients' sample had high %CV. The %CV was much lower for NTC, calibrator and QC-1.

The Levey Jennings plot shows percentage of events outside the ±1SD for NTC is 33.33% (Fig. 6. 11)

The Levey Jennings plot constructed with the third-party quality control reagents (Qnostics) with a given concentration of 100 IU/ml showed variation within the acceptable levels. The assay matrix was serum, even though the initial variation was higher than the later data, they were all within the acceptable limits. The mean and SD were 36.662±1.0836 (Fig. 6. 11 and Table 6.7).

The Levey Jennings plot constructed with the first party quality control reagents (Qiagen) with a given concentration of 10 IU/µl are within the acceptable levels. The variation was limited as the matrix of the assay is not serum sample, they were all within the acceptable limits. The mean and SD were 32.9716±0.453 with a %CV of 1.375 (Fig. 6. 10 and Table 6.7).

The internal control of the above third-party quality control data gave a Levey Jennings Plot with all data within acceptable limits (Fig. 6.12). These results indicate the excellent performance of the quality control data within the serum matrix.

The internal control data also showed consistent variation with acceptable data and without outliers of the ±3SD. As these are first party internal controls, the variation was limited as the matrix of the assay is not serum sample. These results indicate the dependable data of the first party internal control (Fig. 6. 10).

Internal controls are sequences unrelated to the template that is amplified, but functions in the same matrix of amplification. Therefore, Internal Controls monitor the influences of various agents, especially drugs and nonspecific RNA contamination on the amplification system. Most commonly affected components by drugs are the enzymes of the amplification system. Nonspecific RNA consumes the primers and affect amplification.

The Levey Jennings Plot of Internal Control with patient sample amplification Cq<30, indicating relatively high Hepatitis C viral load showed predominantly fluctuations of imprecision and there was no systematic error seen. There were two samples above ±2 Standard

Deviation and 3 samples outside ±2 Standard Deviation. All these samples decreased in their variation and were below ±1 Standard Deviation or crossed the mean line. There was no amplification with Cq outside ±3 Standard Deviation. The fluctuation above ±2 Standard Deviation was sustained only for one day. None of the samples retained their position for more than one day (Fig. 6. 12).

To study the influence on Internal Controls with lower Hepatitis C Viral load plasma samples between Cq 30 and 36, the Levey Jennings was plotted (n=24). In this plot also none of the samples were outside ±3 Standard Deviation and the few samples that were outside ±2 Standard Deviation were imprecision errors. These results in this Fig.6.12B showed good performance of RT-PCR without any systematic error. The %CVA were 6.4 and 2.3 indicating mostly precision errors and almost no bias (Table 6.7).

At very low plasma viral load of Hepatitis C Virus the Standard Deviation showed 1.41 indicating low general influence on the Internal Control. But one sample was further analysed as a case study (Fig. 6. 12C and Table 6.7).

6.5.9. Quality Management in **Real Time PCR**

Intra assay (repeatability on the same day) and inter lot comparison with First party QC reagents (Qiagen). SDI = mean difference / SD of the previous lot. Intra Assay %CV was low at 0.85%, Inter Assay of the previous lot was high at 1.7% and the new lot of reagents gave a %CV of 1.01%. The Inter Assay CV of the previous lot and new lot was higher than the intra Assay CV. The %CV of the new lot was lower than that of the previous lot. This probably may be due to the fresh reagents of the new lot (Table 6.8).

The Internal Controls of the first party reagents used in Table 6.8 was evaluated for their %CV of the Internal Controls. Internal Controls are quality control reagents of unrelated genes in the matrix of the same assay. The intra assay CV was low at 0.68%, the inter assay %CV in the previous lot of reagents was 1.788% and the %CV in the new lot was 1.352 (Table 6.9). The variation was higher for the inter assay when compared with intra

assay. The %CV of the previous lot was higher when compared to the new lot. This is due to fresh reagents in the new lot. This data from the first party quality control in Table 6.2 and Table 6.3 indicate almost very little influence or variation between the intra assay data, previous lot and the new lot data. Therefore, the quality of these results was highly satisfactory.

6.6. DISCUSSION

RT-PCR influences were typically observed in the test sample amplification when the template or viral load was very low. But it might be assumed that there were preanalytical and analytical influences even when the viral loads were high. When the template or viral loads were high, the early rise in fluorescence intensity and the lower Cq value may not make the analytical and preanalytical influences prominent enough for observation. The influences were visible only when the Cq values were >33 or the template concentrations was <10 IU/µl. These observations might be due to (a) the larger number of cycles required for the low concentration of non-specific RNA from plasma to influence the RT-PCR amplification plots, and b) the influences of PCR products on the RT-PCR amplifications. The influence of PCR products from template amplification should be seen in all amplification plots at all concentrations of the template, except in NTC.

In the case of patient sample, Cq varies from sample to sample from high to low Cq and, therefore, Cq of patients' sample cannot be used for studying the influences on Cq. But IC concentrations were same in all assays for a particular lot of reagents. Due to these reasons, the variations in Cq of IC were evaluated to study the analytical and preanalytical influences. All data given in the present report were reproduced with a single lot of IC reagent.

We might consider analytical influences as the ones caused by the PCR amplification products of HCV template RNA. The preanalytical influences may be considered as the influences of components in the plasma sample that were isolated along with HCV RNA. These co-isolates of HCV RNA might probably be contaminating RNA or might be DNA.

Such contaminating nucleic acids were increased in tissue damaging conditions which were exclusion criteria for sample collection, except in emergencies. If such samples were not excluded, the influences of contaminating RNA might be much more. Drugs commonly affected enzymes of RT-PCR (Yedidag et al, 1996). Non-specific RNA and their non-specific amplification products also might consume the primers and affect amplification.

The most analytical and preanalytical influences might be considered to be least in NTC, where the only amplification product was that from the reference gene. Therefore, as expected, the analytical influences were the lowest leading to the lowest IC mean Cq and low %CV (Table 6.2B and Fig. 6.4). In the first party control samples were the calibrators of HCV, commonly the S4 or 10 IU/µl calibrator. Therefore, the preanalytical influence of plasma samples were absent. But in the third-party and second-party control RNA was isolated from plasma and preanalytical influences would be more evident.

The influences on the Cq were seen as an increase in mean Cq value (Fig. 6.4A). Patients' sample showed greater %CV, as the plasma RNA samples were isolated from different patients (Table 6.2 and Fig. 6.4). NTC which has no preanalytical and least analytical influence has least mean Cq, followed by first party controls (calibrators), then third party controls and then followed by highest mean Cq of IC in patient sample. But the Cq variation, represented as %CV, remained fairly constant in all samples, except in the patients' sample where the variation markedly increased (Fig. 6.4B). The high %CV of patients' RNA might be due the sample collection from different patients and there was no repetition with the same sample as with calibrator and QC samples.

6.7. CONCLUSIONS

IC was added to HCV RT-PCR assays with patients' plasma RNA, calibrators, QC RNA and NTC. All IC additions were from the same lot for a set of calculations. The IC fluorescence emission of ROX dye at 610±5 nm, was independent of the HCV template amplification with FAM

dye having emission at 510±5 nm. The average IC Cq was lowest for NTC, followed by the calibrators, QC samples and the HCV infected patients' plasma RNA sample. The average %CV was the same for NTC, calibrators and QC sample, but was increased for patients' sample. The results showed that the analytical influences might be due to HCV RT-PCR products which could be attributed to the IC Cq difference between the calibrator and NTC. The preanalytical influences might be contributed by IC Cq difference between patients' (or QC) sample, and the calibrator. QC and patients' sample contained non-specific RNA from plasma which might contribute to the pre-analytical influences. The patients' samples were from different patients' contributing to higher average patients' %CV, unlike that of QC sample and calibrators which were a single sample.

Slope, normalised fluorescence intensity and efficiency decreases with decrease in viral load both in calibrators and with patient samples. when concentration is expressed as Cq, the relationship of Cq, fluorescence intensity and efficiency become inversely related.

Table 6.1. Organisation of the study with reference to the four types of assays, the fluorescent probes of HCV and ICs in the assay matrix.

Reagents	**Different RT-PCR Assays**				**Total volume µl**
	NTC µl	**Calibrators µl**	**QC RNA µl**	**Test RNA µl**	
Reagent A + B, with HCV probe FAM Ex. = 470±10, Em./detection = 510±5	12 + 8	12 + 18	12 + 18	12 +18	48 + 72 = 120
IC, with its probe ROX, Ex. = 585±5 nm, Em. = 610±5nm	2	2	2	2	8
Total volume of reagents used	30	30	30	30	128 µl
Template RNA / RNase free water	20 µl water	20 µl RNA	20 µl RNA	20 µl RNA	---

Fig. 6.1. HCV RT-PCR amplification plots **(A)** and IC amplification plots **(B)** of calibrators, QC RNA, patient's plasma RNA and no template control (NTC). The threshold cycles (Cq) are given in the box.

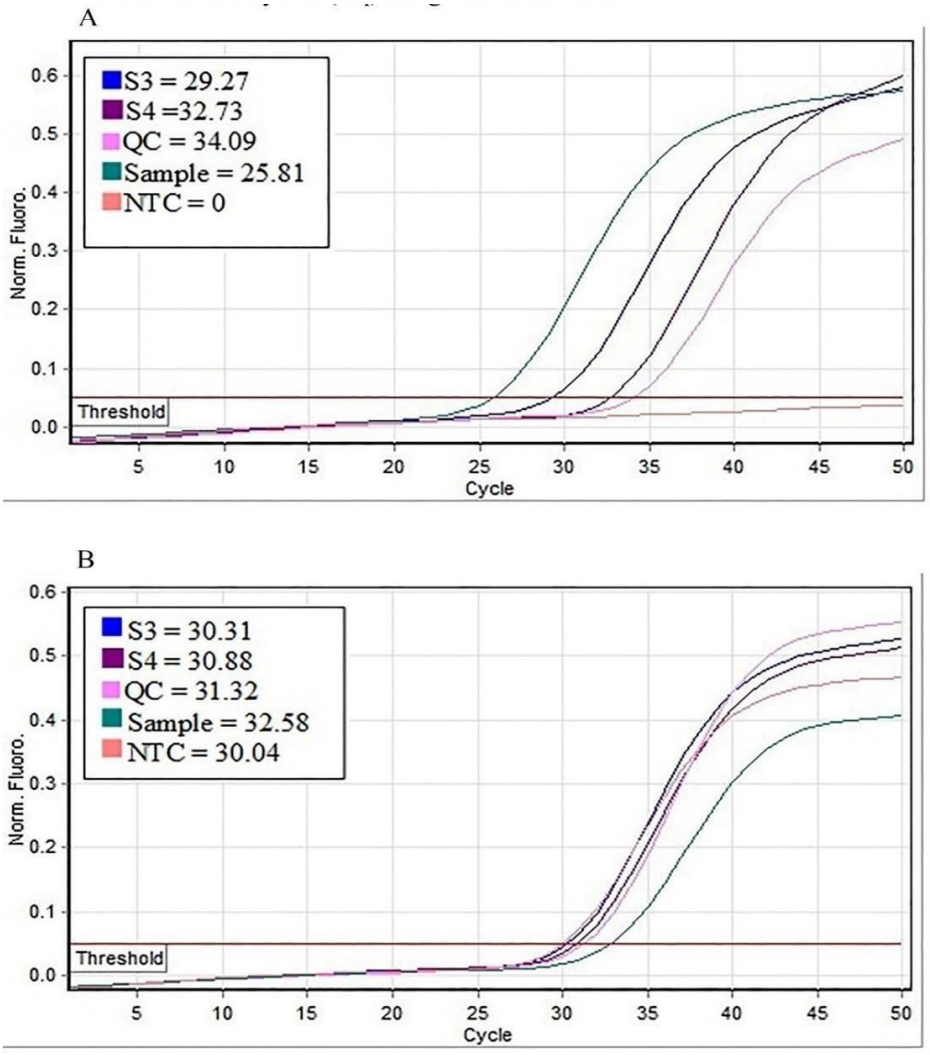

Fig. 6.2. Slopes of sections of calibration plot of log concentration versus Cq.

Plot of log 100 IU/µl to log 0.1 IU/µl (2.0 to -1.0) versus Cq. Slopes of sections of the calibration plot are given in Box.

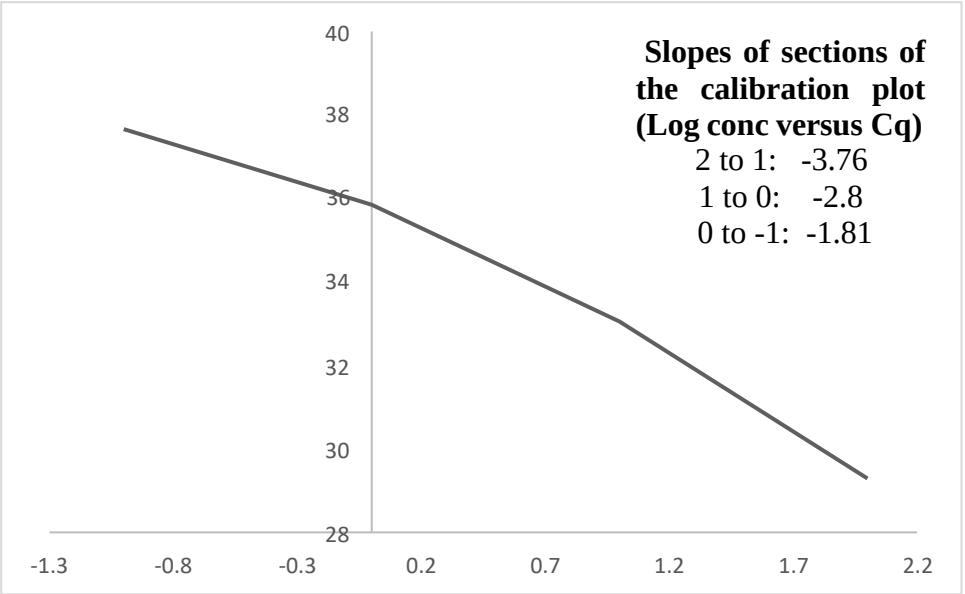

Fig. 6.3. Correlation coefficient and coefficient of determination of calibration plot of multiple data points, variation of slopes at low concentrations of calibration plots with multiple data points.

Mean and SD of Cq of calibration points from 100 IU/µl to 0.1 IU/µl (n = 7)

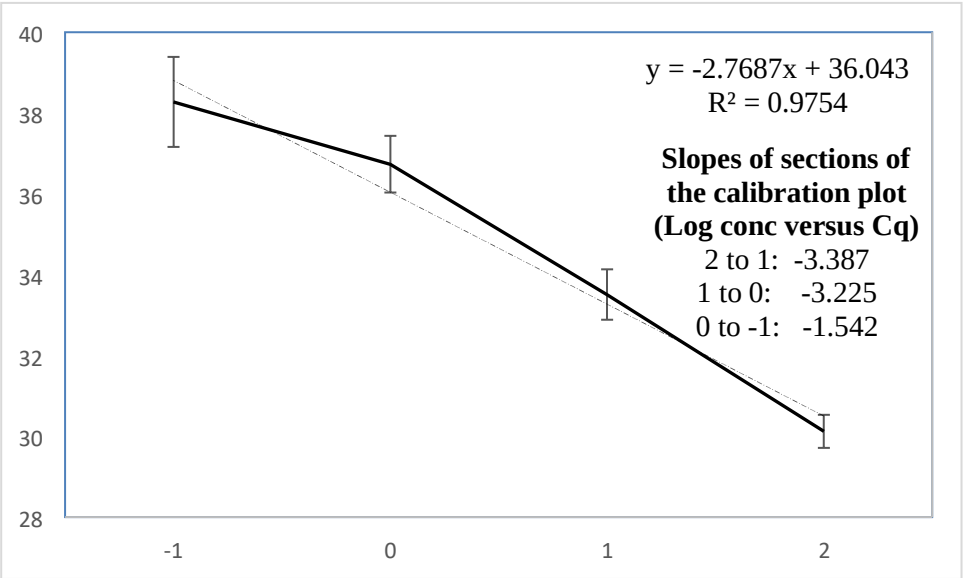

Table 6.2. Performance of the Cq of quality control (QC) samples (n = 6) (A) and their internal controls (IC) (B). Third-party control plasma (Randox, Quality reagent provider), second party plasma (prepared by user laboratory), first-party control reagent is calibrator (Qiagen, manufacturer of reagents) and internal controls were included in the matrix of the assays (Qiagen, manufacturer).

Control samples	Mean±SD	95% CI	%CV
Third party HCV control plasma, n = 6 (Qnostics, Randox, QC provider)			
QC-1	31.255±0.878	30.332 – 32.177	2.81
QC-2	33.71±0.27	33.423 – 33.993	0.805
QC-3	36.962±0.723	36.202 – 37.721	1.96
Second party control plasma, n = 6 (user defined)			
Control plasma with Cq 36	36.537±1.00	35.483 – 37.590	2.74
Control plasma with Cq 31	31.232±0.366	30.848 – 31.616	1.17
First party controls, n = 6 (calibrators from Qiagen, reagent manufacturer)			
S4 (4280 IU/ml)	32.832±0.570	32.233 – 33.430	1.73

Table 6.2B. Performance of the IC Cq in different assay systems. The same calibrators and QC samples were used to calculate mean±SD of six assays. Patient's samples were from six different patients.

Control samples	Mean±SD	95% CI	%CV
IC in NTC	30.346±0.395	29.932 – 30.761	1.3
IC in third party HCV control plasma, n = 6 (Qnostics, Randox, QC provider)			
IC of QC-1	33.767±0.498	32.31 – 33.23	1.52
IC of QC-2	31.563±0.334	31.212 – 31.914	1.05
IC of QC-3	31.663±0.355	31.290 – 32.036	1.12
IC in second party control plasma, n = 6 (user defined)			
IC in control plasma with Cq 36	33.017±0.816	32.16 – 33.873	2.47
IC in control plasma with Cq 31	32.303±1.05	31.19 – 33.41	3.27
IC in first party controls, n = 6 (calibrators from Qiagen, reagent manufacturer)			
IC in S4 (4280 IU/ml)	31.425±0.485	30.92 – 31.93	1.54
IC in S3 (42800 IU/ml)	30.92±0.38	30.52 – 31.32	1.23
IC in patients' sample, n = 6 (from 6 different patients)			
Patients' sample with Cq <30	32.2±1.373	30.76 – 33.64	4.26
Patients' sample with Cq 30 – 36	32.42±0.833	31.54 – 33.29	2.57
Patients' sample with Cq >36	33.053±1.051	31.95 – 34.16	3.18

Fig. 6.4. IC mean Cq **(A)** and average %CV **(B)** of NTC, calibrator, QC samples and patients' samples (n = 6).

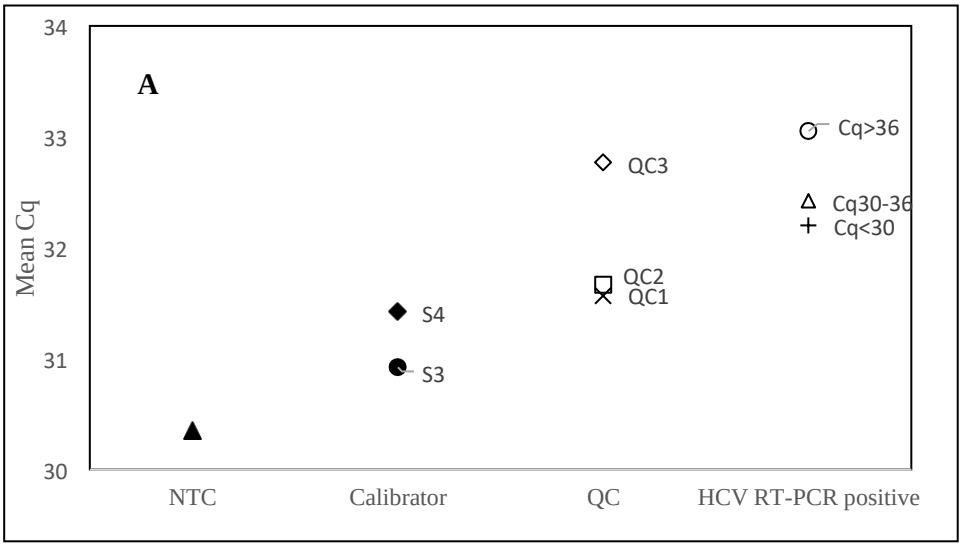

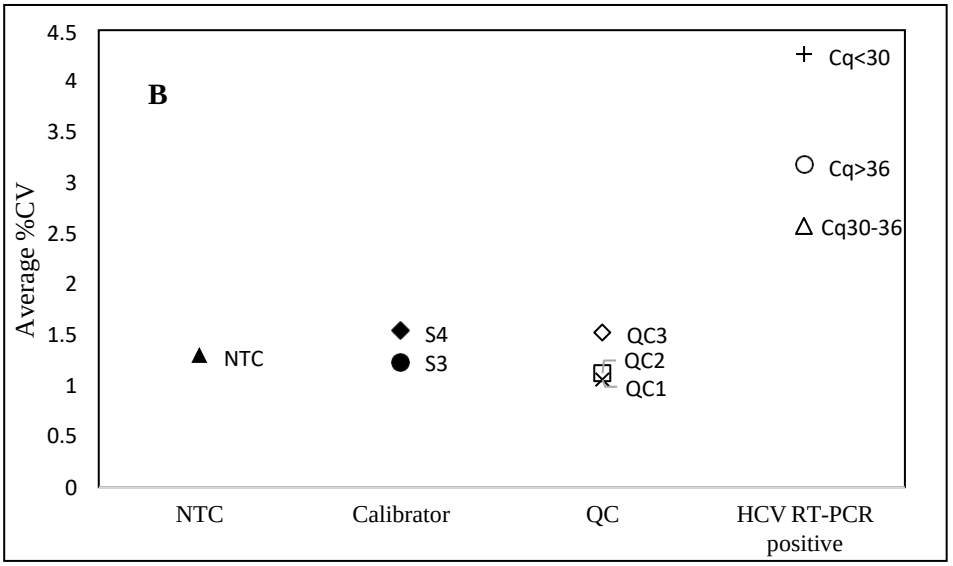

Table 6.3. Analytical variation (%CV) of Cq and plasma viral load at various calibrator concentrations.

Concentration	Cq			Viral Load		
	Mean±SD	95% CI	%CV	Mean±SD	95% CI of Mean	%CV
10^4 IU/µl	22.951 ±0.404	22.577 – 23.325	1.7622	3,114,365.57 ±738835.27	2,431,056-3,797,674	23.72
10^3 IU/µl	26.334 ±0.528	25.845 – 26.823	2.006	362855.86 ±126148.11	246,188 – 479,523	34.76
100 IU/µl	30.12 ±0.409	29.741 – 30.498	1.359	33625.86 ±9546.66	24796 – 42455	28.39
10 IU/µl	33.507 ±0.626	32.928 – 34.085	1.867	3559.14 ±1464.19	2204 – 4913	41.14
1 IU/µl	36.733 ±0.701	36.084 – 37.381	1.909	446.5714 ±195.48	265 – 627	43.77
0.1 IU/µl	38.274 ±1.115	37.243 – 39.305	2.913	----	----	

Fig. 6.5. X-Y scatter of RT-PCR parameters of calibrators. Log concentration of calibrators from 100 IU/µl to 0.1 IU/µl (2.0 to 0.1) or Cq versus RT-PCR parameters, Slope at inflection point (A), Normalised fluorescence intensity (B), Efficiency (C).

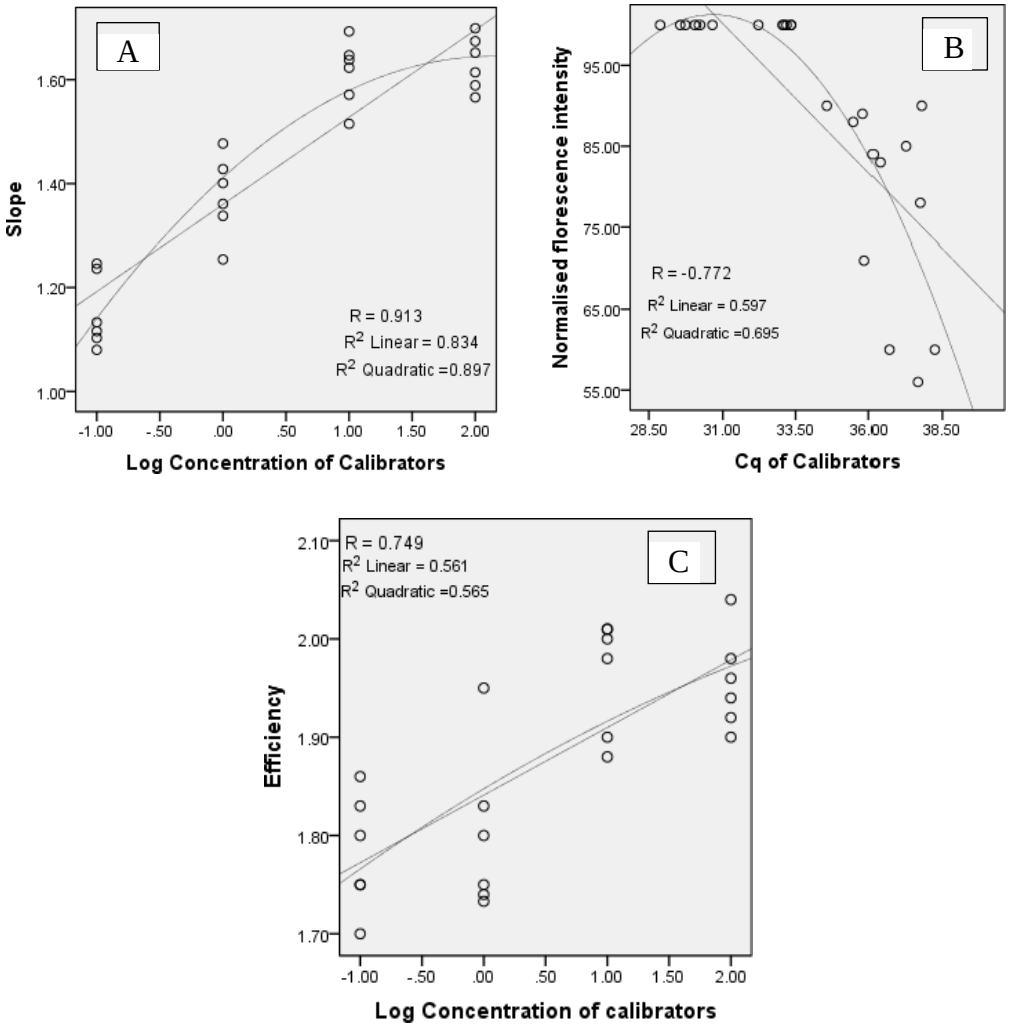

Fig. 6.6. X-Y scatter of RT-PCR parameters of HCV plasma sample, Cq of patients' RNA from plasma versus different RT-PCR parameters like Slope at inflection point (A), Normalised fluorescence intensity (B), and Efficiency (C).

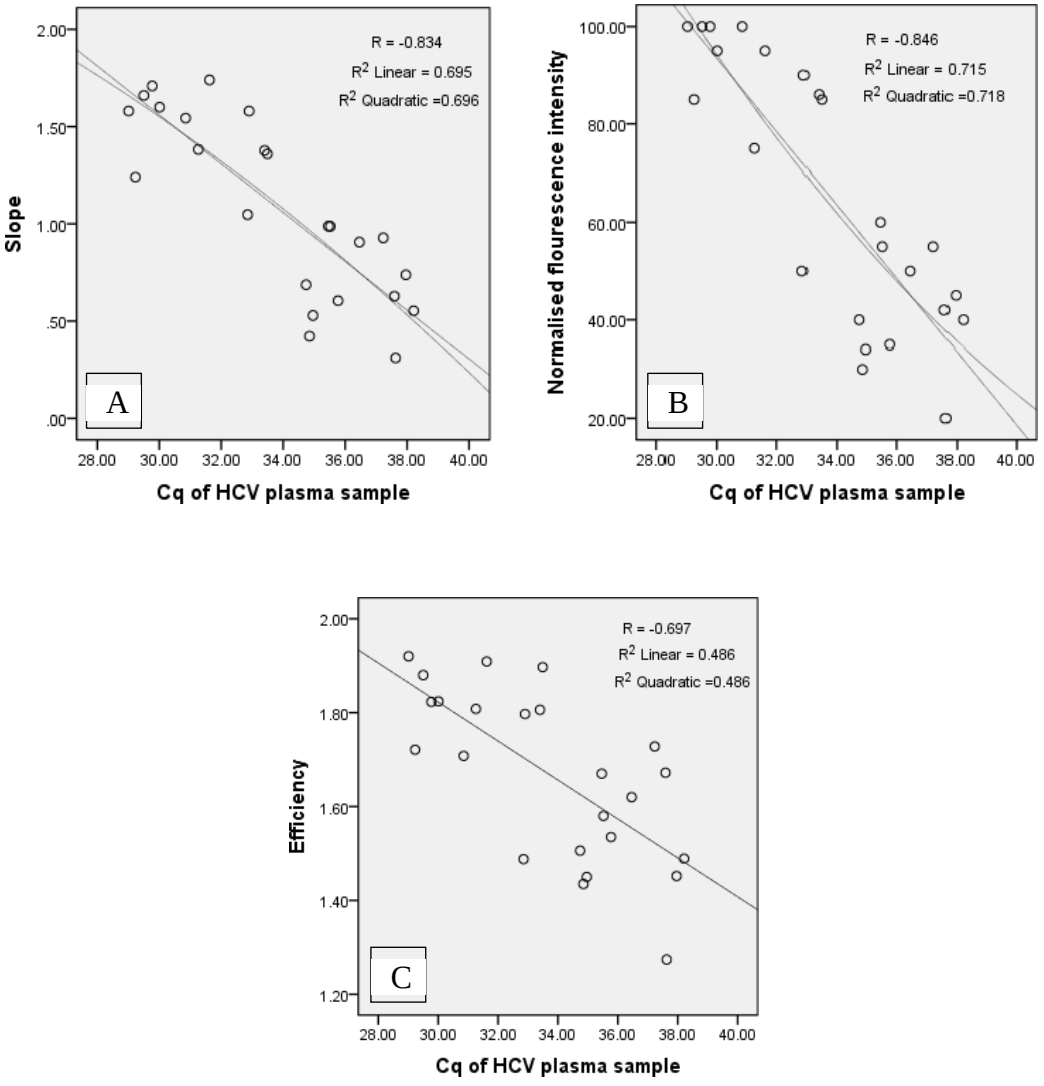

Table 6.4. Comparison of the four-parameters of the RT-PCR sigmoid fluorescence amplification plots of HCV calibrators using SigmaStat software. F was the fluorescence at cycle X (Cq), Y_0 was the ground fluorescence, 'a' is the difference between maximal and the ground fluorescence, X was Cq, X_0 was the Cq at inflexion point and b was maximum slope.

Calibrator (IU/µl)	'a'	b	Xo	Yo	X	F	Xo - X
10	20.2729	2.0773	39.206	6.70759	32.22	7.386	6.99
10	24.2112	1.886	39.3375	8.7895	34.01	10.14	5.33
10	25.7811	2.0937	40.8141	8.3233	33.5	9.1	7.31
10	22.3656	1.8933	39.6428	8.4653	33.08	9.1427	6.56
10	20.5581	1.90359	38.6846	9.7144	32.62	10.53	6.06
10	22.9024	1.7344	40.6231	9.9603	34.28	10.536	6.34
10	22.7419	1.9684	39.7613	9.2306	33.14	9.9912	6.62
1	39.8446	1.8714	43.2541	14.7843	35.85	15.532	7.4
1	24.9178	2.2649	42.3836	6.74036	34.57	7.5071	7.81
1	17.3473	2.1951	41.9194	6.17212	34.72	6.8013	7.2
0.1	25.7495	1.827	43.7719	14.1018	37.66	14.978	6.11
0.1	25.445	2.2399	44.4289	6.75031	36.42	7.4433	8.01
0.1	17.1645	2.3965	44.8964	5.84132	37.19	6.5035	7.71
0.1	9.14513	2.7113	46.4256	4.70418	38.95	5.249	7.48
0.1	13.7538	1.9777	45.8297	5.03577	38.7	5.399	7.13
0.05	6.9934	2.0562	43.6005	5.02263	39.84	5.99	3.76
0.05	15.7508	2.1484	45.9363	5.487	40.17	6.4938	5.77
0.05	11.2654	2.0350	44.6149	5.28223	39.75	6.2273	4.86

Fig. 6.7. X or Cq plotted with Xo – X of calibrators and diluted calibrators.

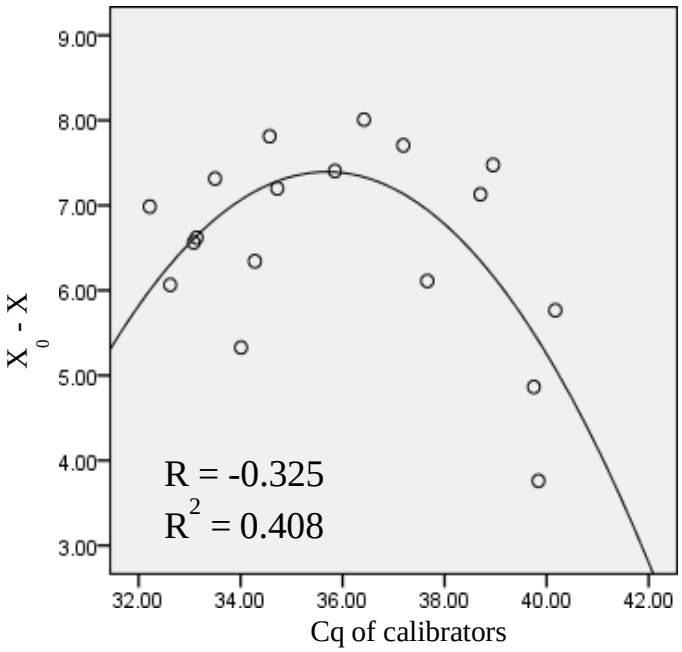

Table 6.5. Comparison of the four parameters (Equation-2) of the real-time RT-PCR sigmoid fluorescence amplification plots of patients' plasma RNA sample using SigmaStat software.

Cq range	'a'	b	Xo	Yo	X	F	X0 - X
33 – 36	19.7335	1.7868	39.485	8.6092	33.24	9.19	6.25
	19.9231	2.1437	38.7092	7.9987	33.4	9.5429	5.31
	6.2332	3.0930	37.853	7.9781	33.46	9.1911	4.39
	6.7297	7.7637	39.99	8.6503	34.48	10.868	5.51
	20.81	2.0906	40.1808	8.3098	34.85	9.8	5.33
	4.2005	4.2727	37.6852	7.8341	34.85	9.262	2.84
	17.0118	1.9566	39.9054	8.1662	35.08	9.5	4.83
	11.532	2.1081	41.2883	8.2021	35.61	8.9327	5.68
	13.5604	2.1493	40.4807	13.7133	35.67	15.02	4.81
	6.3929	2.2452	39.4484	9.0441	35.81	10.0997	3.64
36 – 39	6.3427	2.2418	40.0264	8.6966	36.28	9.7	3.75
	4.3266	6.8956	39.5365	8.4301	36.51	10.126	3.03
	7.2049	1.8377	39.1442	8.2958	36.66	9.77	2.48
	7.7843	1.6716	39.0451	8.4786	36.78	10.07	2.27
	5.8827	1.8412	40.2013	8.2049	36.85	9.02	3.35
	6.2262	1.8718	40.5925	8.2203	36.85	8.96	3.74
	4.1829	12.3918	40.0081	7.9246	36.87	9.7526	3.14
	5.5715	1.9175	40.47	8.0580	37.14	8.892	3.33
	4.3103	3.2391	40.3466	7.5208	37.33	8.739	3.02
	6.2442	2.0325	41.2297	8.2172	37.59	9.11	3.64
	7.6439	1.6506	41.9932	8.2528	37.98	9.63	4.01
	5.4055	2.7313	42.193	7.924	38.31	8.974	3.88
	7.8317	1.6209	41.1921	8.3832	38.57	9.67	2.62
	5.9012	2.4028	42.2238	8.8128	38.68	9.91	3.54
	5.7768	2.302	40.1261	8.5370	38.81	10.621	1.32
	8.3422	1.8583	41.7302	8.1171	38.9	9.6	2.83
	6.958	1.8796	41.3865	7.7825	38.9	9.24	2.49
	4.8305	3.0474	41.8397	7.9073	38.21	9.8228	3.63
	4.4859	2.2255	41.5375	7.9289	38.70	9.7889	2.84
>39	3.0937	3.0001	40.6234	7.7645	39.12	9.8309	1.5
	6.6398	1.8374	41.1432	8.1708	39.25	9.9171	1.89

Fig. 6.8. X plotted with Xo – X of HCV plasma samples with low viral load.

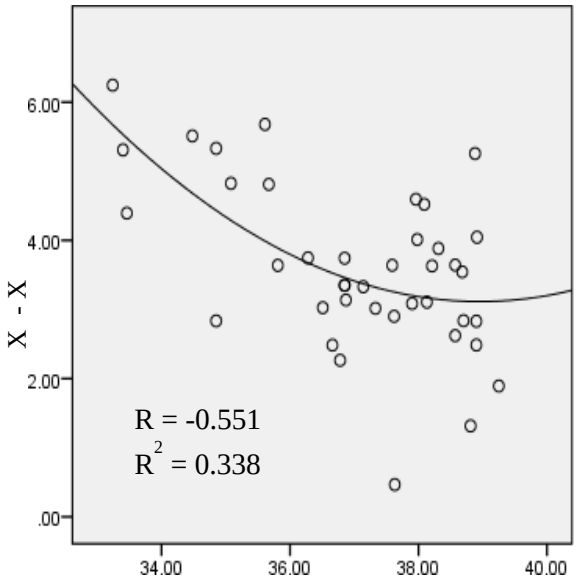

Cq of HCV plasma samples with low viral load

Table 6.6. Comparison of the selected parameters of the real-time RT-PCR sigmoid fluorescence amplification plots of calibrators and patients' plasma RNA sample using SigmaStat software

	Mean±SD	95% CI	%CV
Calibrators, Cq at 10 and 1 IU/µl or Cq 33 - 36 (n = 10)			
Cq	33.648±0.863	33.03 – 34.265	2.56
a	21.642±3.321	19.265 – 24.017	15.34
b	2.088±0.3167	1.862 – 2.315	15.16
Patients' Samples with Cq from 33 to 36 (n = 10)			
Cq	34.645±0.9757	33.947 – 35.343	2.8
a	12.613±6.4766	7.979 – 17.245	51.34
b	2.961±1.841	1.6437 – 4.2782	62.17

Fig. 6.9. Graphical evaluation of amplification plots of calibrators at low template concentrations with LinRegPCR. Calibrators at 10 IU/µl for comparison with low template concentration at 0.10 IU/µl and 0.05 IU/µl.

Fig. 6.9A

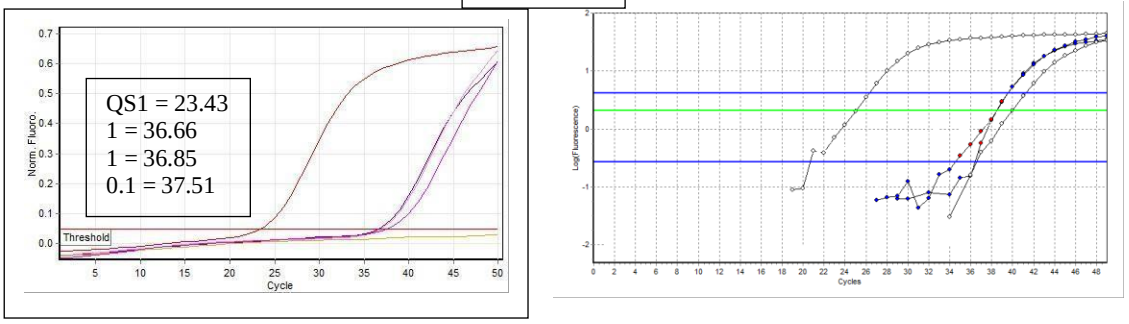

Fig. 6.9B

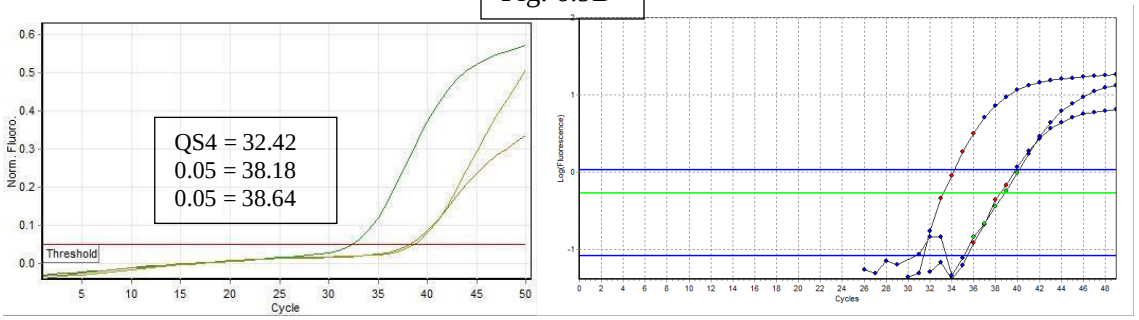

Fig. 6.10. Graphical evaluation of amplification plots of patients' sample at low plasma viral load. Calibrators are for comparison with patients' amplification plot

Fig. 6.10A

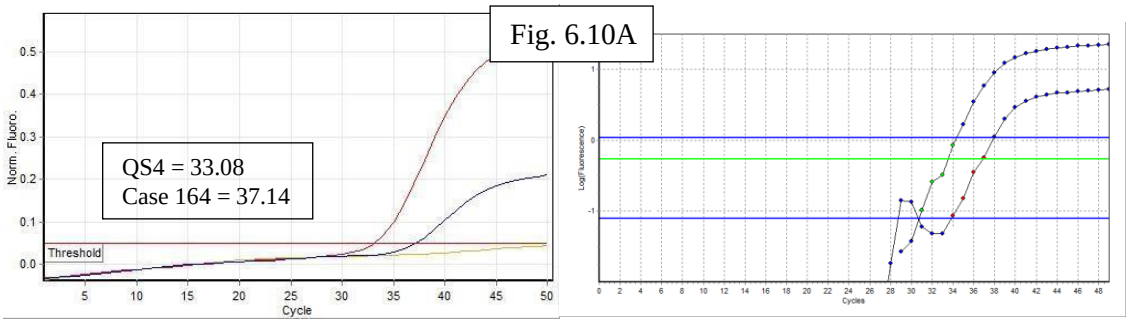

Fig. 6.10B

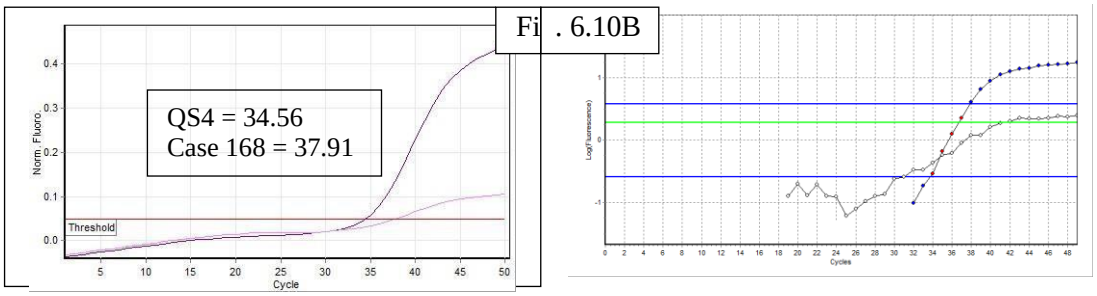

Fig. 6.10C

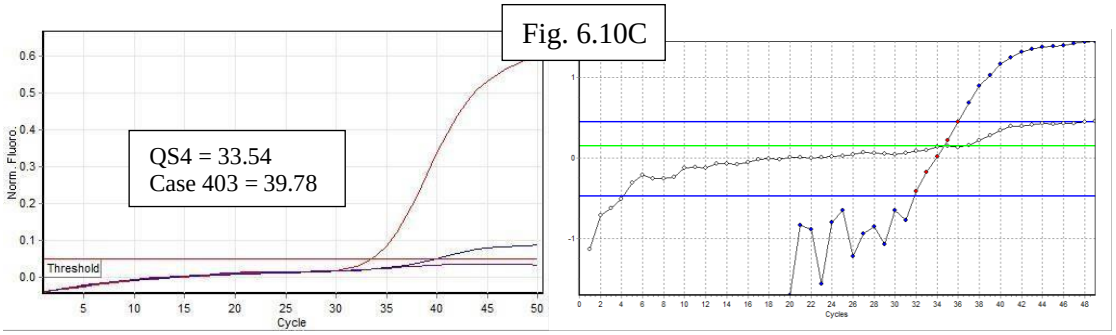

Fig. 6.10D

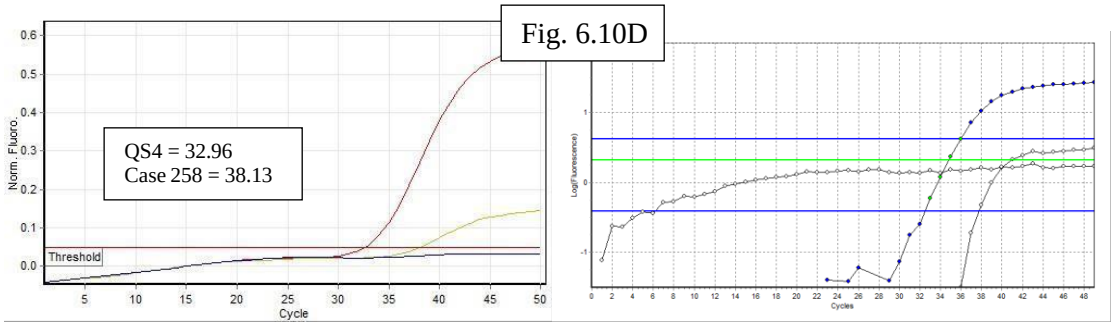

Fig. 6.10E

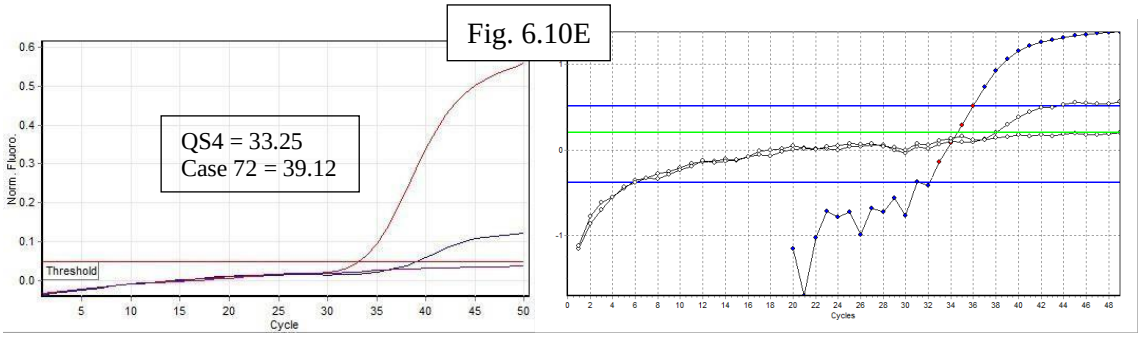

Fig. 6.11. Levey Jennings Plot of IC Cq from NTC (A) and IC Cq from S4 (B) with n = 30. UCL and LCL are upper and lower control limits at ±3SD.

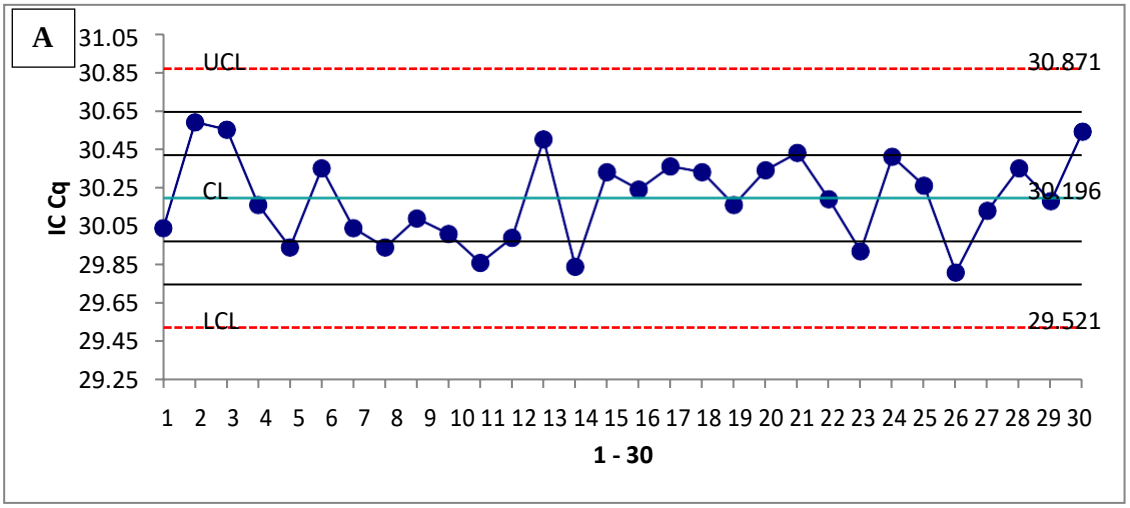

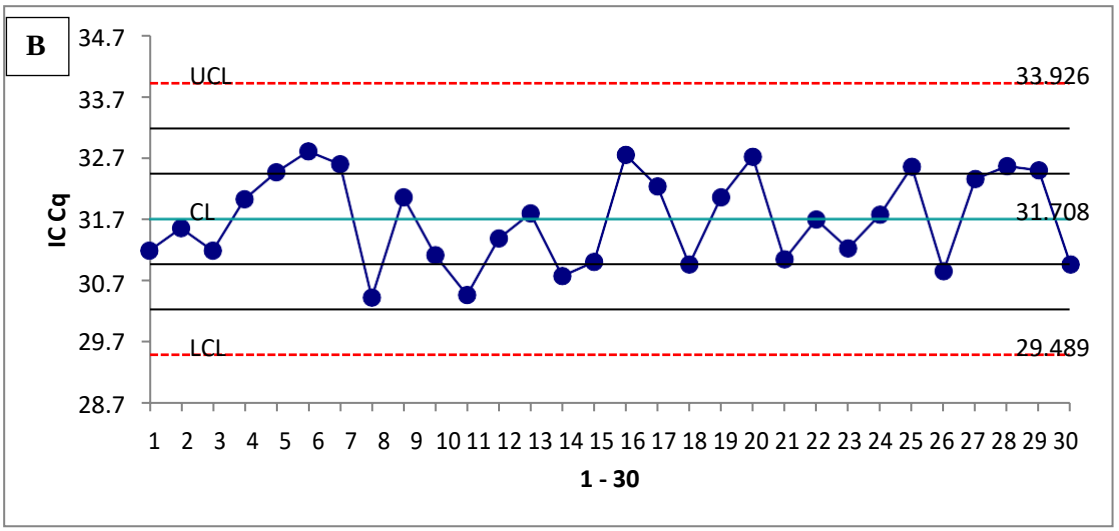

Fig. 6.12. Levey Jennings plot of IC Cq from HCV QC-1 sample (n = 15).

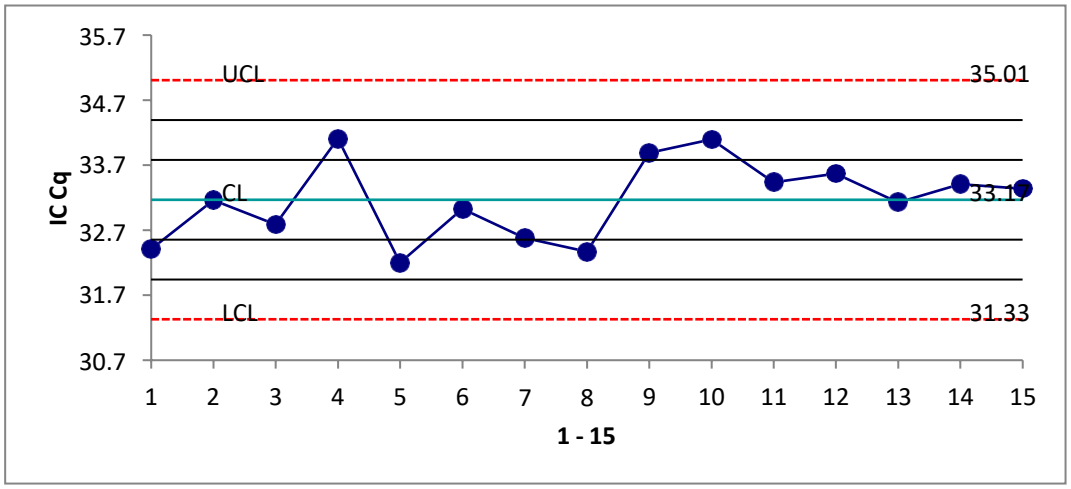

Fig. 6.13. Levey Jennings plot of IC Cq from patient's plasma with Cq < 30, n = 27 (A), Cq 30 - 36, n = 24 (B) and Cq > 36.0, n = 29 (C).

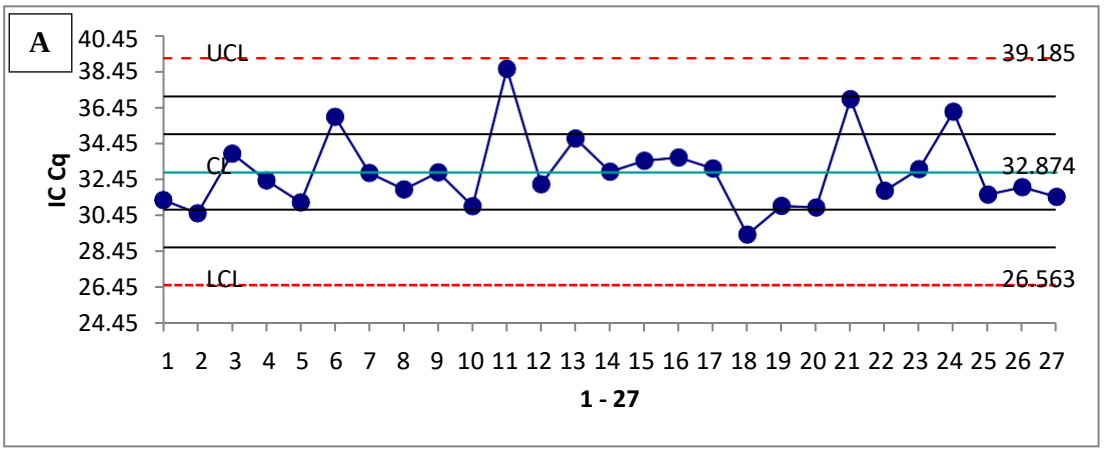

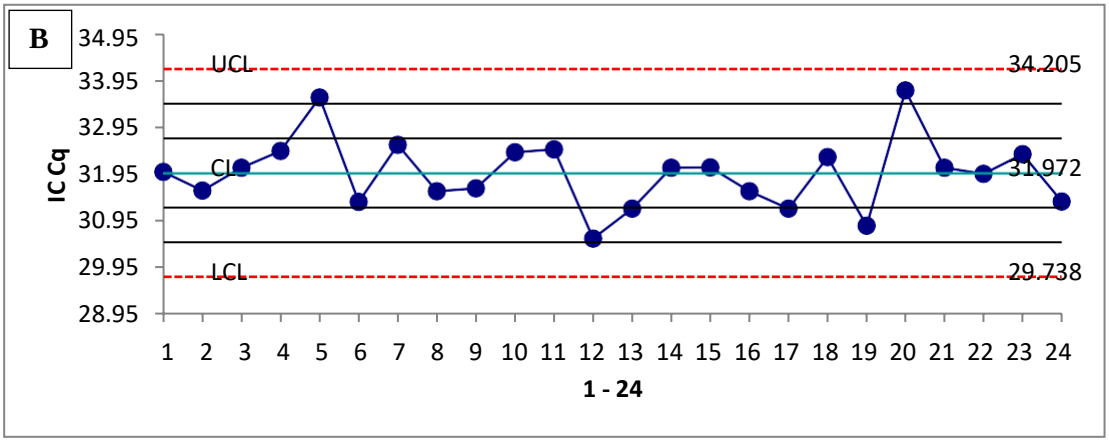

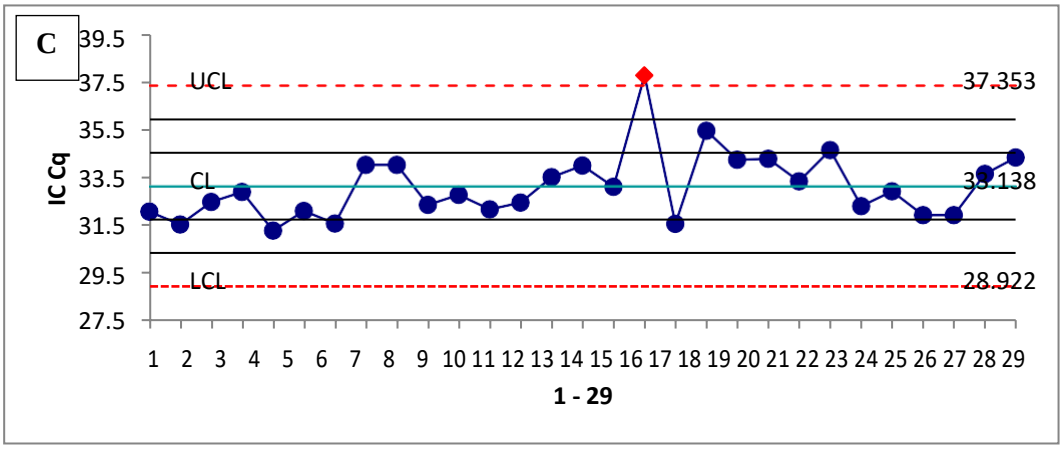

Table 6.7. The summary of the Levey Jennings plot data of IC Cq in NTC, calibrators, QC and patient samples given in Fig. 3 – 5. 1_{1S} indicates the number of events between ±1SD and ±2SD. 1_{2S} will mean the number of events between ±2SD and ±3SD. 1_{3S} will mean the number of events outside ±3SD.

	NTC (n = 30)	**Calibrator S4 (n = 30)**	**QC 1 (n = 15)**	**Patient RNA, Cq<30 (n = 27)**	**Patient RNA, Cq,30-36 (n = 24)**	**Patient sample, Cq>36 (n = 29)**
Mean±SD	30.19±0.23	31.71±0.74	33.17±0.61	32.87±2.10	31.97±0.74	33.14±1.41
95% CI	30.11 – 30.28	31.43 – 31.98	32.83 – 33.51	32.041 – 33.71	31.66 – 32.29	32.60 – 33.67
%CV	0.75	2.33	1.85	6.39	2.33	4.24
QC rules	**QC events**					
1_{1S}	8	7	4	5	2	5
1_{2S}	-	-	-	1	2	-
1_{3S}	-	-	-	-	-	1
2_{1S}	1	2	1	-	-	-
2_{2S}	-	-	-	-	-	-
2_{3S}	-	-	-	-	-	-

Table 6.8. Intra assay and inter lot comparison with First party QC reagents (Qiagen).

	Intra Assay (Repeatability on the same day)	**Inter Lot**	
		Previous Lot	**New Lot**
Mean± SD	32.728±0.277	32.884±0.558	33.29±0.336
%CV	0.85%	1.7%	1.01%
		SDI	0.72759

Table 6.9. Internal Control in the assay matrix of first party quality control

	Intra Assay on same day	**Inter Lot, Inter Assay**	
		Previous Lot	**New Lot**
Mean± SD	30.376±0.208	31.902±0.570	31.712±0.429
%CV	0.68%	1.7879	1.3516
		SDI	0.333

Chapter 7

Hepatitis C Virus RT-PCR amplification data showed preanalytical influences of sample that can affect the RT-PCR diagnostic outcome

7.1. ABSTRACT

Large number of third generation anti HCV antibody reactive results were found to be RT-PCR negative. The discrepancy between these results were analysed in this study. The variation in the internal control (IC) Cq and fluorescence intensity showed sample influences on the RT-PCR results in an earlier chapter. In this study, clinical cases selected and the assays were designed in such a way that the preanalytical influences may be observed directly in a particular case or cases. Tissue damaging conditions were found to be a major cause of preanalytical variation. The first case was an HCV RT-PCR positive patient, who underwent extensive surgical procedures immediately after the positive RT-PCR. Within a few days after surgery, the RT-PCR results became negative. The PCR product of the sample was analysed and was confirmed to produce the 272 bp PCR product of 5'UTR region before surgery. The preanalytical influences were also found to be influencing the calibration plot. When there were preanalytical influences on RT-PCR from patient sample, and when these assays were repeated after two weeks, these influences were found to be decreased resulting in decrease in Cq. There was one sample which was negative, became positive. These case studies demonstrated again that the preanalytical influences on HCV RT-PCR affected the diagnostic outcome of the patients.

7.2. INTRODUCTION

There are diagnostic issues with Hepatitis C Virus infection, where large number of patients have no clinical symptoms (Orland JR et al, 2001), low anti-HCV antibody levels (Zer Y et al, 2009), relatively low plasma viral load (Barbara H et al, 2009; Simone A et al, 2005), spontaneous resolution of HCV infection (Bulteel N 2016; Hofer H et al, 2003; Micallef J M et al, 2006) and there are issues resulting from occult HCV infection (De Marco L et al 2009; Welker and Zeuzem, 2009, Carren˜o V et al, 2008**).** Also, there were interpretation issues with the second and third generation anti HCV antibody screening assay results, and concerns related to the guidelines proposed by Centre for Disease Control and Prevention (CDC) and WHO (Alter J, 2003 for CDC, Barrera et al, 1995; WHO, 2001). The WHO-

defined diagnostic criteria for HCV infection recommends a third-generation screening assay followed by confirmatory RT-PCR assay (WHO, 2001, Barrera, J. M, 1995). As RT-PCR is a confirmatory test for diagnosis of HCV infection, a wrong diagnostic outcome has serious consequences. The diagnostic difficulties arising from the above discussed clinical aspects of HCV infection were due to problems arising from (i) the sensitivity and specificity of laboratory assays, (ii) clinical interpretation of laboratory reports with large number of suspected 'false reactive' results from third generation anti-HCV antibody screening assays and (iii) the follow up of clinical cases of HCV infection which are affected by spontaneous resolution of infection and due to occult infection, (iv) Long duration of RT-PCR negative results from patients under anti-retroviral treatment.

Of the four above-defined problems, the issues related to sensitivity and specificity of RT-PCR and clinical interpretation of laboratory reports were taken up for in this study. The basic concepts of RT-PCR data analysis were applied to analyse the influence of the HCV infected clinical plasma samples. The data analysed were RT-PCR fluorescence amplification and calibration plot data, along with PCR product and its sequence to understand the clinical sample influence on sensitivity of RT-PCR.

The methods that might be used for data analysis were rate of exponential fluorescence amplification (Ramakers et al, 2003; Ruijter et al, 2009), sigmoid amplification plot data analysis (Tichopad et al, 2003; Pfaffl, 2006), calibration plot data analysis (artus HCV Procedure manual), fluorescence amplification efficiency calculated from these data, PCR product size and product sequence.

Therefore, the research problem of this study was to understand the influence of RNA isolated from plasma of patients on HCV RT-PCR assay, especially when viral load is low.

There are influences on the four parameter amplification data of patient's sample (Spiess et al, 2008, Tichopad A et al, 2003). After initiation of RT-PCR into diagnostic assays, the two controls used were non-template control (NTC) and internal control (IC). NTC assay is done in a separate assay tube along with the test and the standard assay tubes to detect PCR

contamination from PCR products or from target sequences (Espy MJ, et al, 2006). IC is done in all the assay tubes by use of a heterologous amplification system, unrelated to the target test sequence to detect RT-PCR inhibition (Maaroufi Y et al, 2006), which is commonly seen in presence of drugs or haemolysis (Satsangi, J et al, 1994, Byrnes, J. J et al, 1975).

Graphical observation of the RT-PCR fluorescence amplification plot showed the possibility of influences on fluorescence intensity and slope at inflection point of the amplification plot. These observations resulted in a systematic search for patients' samples or cases to demonstrate the sample influences.

RT-PCR inhibition is detected by use of internal controls that use of house-keeping genes unrelated to the template in each assay (Maaroufi et al, 2006). Contaminations are detected by use of non-template controls with each set of assays in a run (Espy et al, 2006). RT-PCR inhibition is caused typically in clinical samples by the influence of heme, hemin, hemolysed plasma sample (Byrnes, J. J et al, 1975), heparin (Satsangi et al, 1994). Common cause of RT-PCR inhibition is the inhibition of DNA polymerase and reverse transcriptase. Those negative influences were clinically excluded in this study by careful selection of samples that are unlikely to show RT-PCR inhibition, and by repetition of assays showing RT-PCR inhibition after decreasing the effect of these agents and conditions. Use of hypochlorite, UV light and biosafety cabinet to control contamination

The primers for diagnostic RT-PCR are commonly targeted to 5'UTR conserved sequence (Bukh, J, 1992, Hoffman, Q. Liu, 2011).

The above reports and our preliminary observations lead to the following **research questions**: Are the RT-PCR assays sensitive enough to detect the low viral counts of HCV? Are there any interferences that affect RT-PCR assay, especially at low plasma viral load of HCV, affecting the outcome of the assay? Can there be methods that can be designed to improve the sensitivity of RT-PCR and detect the interferences on RT-PCR? This observation also raises the suspicion of sensitivity of RT-PCR. Is it possible that the large number of "false reactivity" in the screening assays associated

with low circulating anti HCV antibodies may be the consequence of insufficient sensitivity of detection of low plasma HCV viral load by RT-PCR? The low reactive anti HCV antibody levels or concentrations are detected by immunochemistry auto analysers having enhanced chemiluminescence method of signal detection. Is it right to remove an antigenic epitope from the anti-HCV antibody screening assays before demonstration of cross-reactive antibodies and is it an answer to the former research question?

The research hypothesis of the study was that there are HCV patients sample influence on low viral load RT-PCR assays that might give negative result. These negative results from RT-PCR may be the cause of false reactive antibody assays from the reactive results of third generation antibody assays. This was analysed in the study by evaluating the sample influences on RT-PCR.

7.3. ORIGINAL OBJECTIVES

1. Establishment of the methods for evaluation by data analysis, test validation, quality control and clinical state of the patient for Molecular Diagnostic reporting of Hepatitis C infection.
2. Use of these procedures for confirmatory diagnosis of hepatitis C infection, its plasma viral count determination and genotyping.

7.3.1. Aspects of the original objectives addressed in this chapter

The following research problems were addressed in this chapter for part-fulfilment of the above two main objectives.

The research problem of this study was to understand the preanalytical influence of RNA isolated from plasma of patients on HCV RT-PCR assay, especially when viral load is low.

HCV RT-PCR assay sensitivity was discussed under Chapter 5. The preanalytical influence in low viral load were also discussed in Chapter 5. In this study, cases were selected to evaluate the preanalytical influences on the diagnostic outcome of HCV RT-PCR. Also, studies were done to overcome these influences.

7.4. MATERIALS AND METHODS

7.4.1. Sample Collection and Anti-HCV antibody Screening assay

Blood samples were collected in vacuum tubes with clot activator (red capped, 4 ml), mixed, allowed to clot for 10 minutes, centrifuged at 3000 rpm for 5 minutes in a table top centrifuge, serum was separated, and clear serum samples were screened for the anti-HCV antibody with third generation enzyme immunoassays. When screening assay showed reactivity above the cut off limit, RT-PCR was done for confirming the diagnosis of HCV infection. HCV RT-PCR was done directly, without reactivity to antibody screening assay, in individuals frequently exposed to HCV infection, such as patients on dialysis or repeated blood transfusion. This was done to cover the long window period of HCV infection. Refer Details 4.5 and 3.5.1.

7.4.2. Inclusion and Exclusion criteria

Inclusion criteria were reactivity to anti-HCV antibody and exposure to HCV infection. **Exclusion criteria** were related to the **preanalytical condition** of the patient, such as acute tissue damaging disease conditions, patients on chemotherapy and who were heparinised were found to influence the RT-PCR. These conditions were avoided as far as possible. Sample collection was delayed till the condition subsides or was overcome, up to a day or two for heparinised patients, or sample was collected before the next intravenous injection. In all emergency and other unavoidable circumstances, all the above preanalytical criteria were overlooked, but the results of RT-PCR were analysed for influences.

7.4.3. Sample Collection for RT-PCR:

When screening assays showed anti-HCV antibody levels above cut off limit, **Quantitative RT-PCR was done for confirming the diagnosis of HCV infection**. 4 ml of EDTA blood sample was taken from the patient using EDTA-vacutainers, centrifuged and plasma sample, without hemolysis, jaundice, cloudiness and without clot formation was used for RNA isolation. In the later part of the study preanalytical variables were also taken into consideration before collecting samples for HCV RT-PCR. Plasma and RNA samples were stored immediately at -20^{o}C and -80^{0}C, respectively, in aliquots. Refer Details 4.3.2

7.4.4. Calculation of viral load in plasma

Calculation of plasma viral load from Cq obtained by real time RT-PCR of HCV infected plasma sample, and converted to concentration of the template from the calibration plot.

$$\text{Viral load (IU/ml of plasma)} = \frac{(\text{Patients' result Cq as IU/µl from calibration plot}) \times \text{Elution Volume (60 µl)}}{\text{Sample Volume (0.14 ml)}}$$

Refer Details 4.11.5.

7.4.5. The two cases and their diagnostic criteria

Case 1. Low viral load HCV positive with late amplification (Cq 36.51). CA rectum, underwent surgery, HCV RT PCR done before, immediately after and 4 days after surgery.

Case 2. HCV PCR negative, ovarian cancer, underwent surgery, Sample taken before surgery, immediately after surgery, and 4 days after surgery. For study of the influence of these samples on QS4 (1.0 and 0.5 IU/µl.

7.4.6. RNA Isolation

HCV viral RNA Isolation was done from 140 µl plasma processed with a QIAamp Viral RNA Mini Kit (QIAGEN, USA) according to manufacturer's instructions and eluted in 60 µl Elution Buffer. Eluted RNA was stored at -20°C. Refer Details 4.6.

7.4.7. RT-PCR of HCV

Each assay or a set of assays were done in Triplicates, with test sample or several (patients') sample, a standard with a known template concentration (or calibrator) and a non-template control or NTC without template (blank sample). RT PCR was done using Artus HCV RG RT-PCR kit (Qiagen, Germany) based on Taqman probes by One step RT-PCR on Rotor-Gene Q instrument. Master mix is prepared from Hep. C Virus Master A (12 µl) and Hep. C Virus Master B (18 µl) with internal control (2 µl). Add 30 µl of this mix into PCR tube and 20 µl of eluted sample RNA, quantitation standards and Non template control. The cycling conditions were entered as 50°C for 30 minutes when the reverse transcription took place, 95°C for 15 minutes for initial denaturation, 95°C for 30s, 50°C for 60 s and 72°C for 30s repeated for 50 cycles. Fluorescence was measured at 50°C at each cycle.

7.4.8. Four Parameter Data analysis

Four parameter data analysis done using the equation given in

$$f = y_0 + \frac{a}{1 + e^{-\left(\frac{x - x_0}{b}\right)}}$$

Refer Details 4.11.2 and 3.5.9.1.

7.4.9. Statistical Analysis

Fluorescence data and Cq were from Rotor-Gene Q software 2.3.1.49 (Qiagen), X-Y scatter plot, its trendline, correlation coefficient (R), and coefficient of determinations (R^2) were done by SPSS software. SigmaStat 4.0 was used for data analysis of sigmoid amplification plot (Systat Software, Inc, San Jose, USA). LinRegPCR program version 2020.2 was used for log transformation, calculation of slope and efficiency of the initial exponential fluorescence amplification of individual plots (Rujiter et al, 2009). Microsoft Excel was used as a medium for data transfer and common statistical calculations.

7.4.10. Method validation

5'UTR primers selected (Bukh et al, 1992) used to amplify the fragment and validated by sequencing from Aggregenome, Cochin. NCBI

accession number obtained for 5'UTR was MT258412. Validation was required as we did the qualitative PCR.

7.4.11. External Quality Control or External Assay Validation methods

External quantitative RT-PCR quality control was done by interlaboratory comparisons with a NABL, India accredited laboratory. Interlaboratory comparisons showed the z value of the deviation within ±2 z value or standard deviations from the mean value and the required difference between the log viral load concentration was <0.5.

All other details of Methodology were described under Chapter 4 where the general 'Methodology' was given.

7.5. RESULTS

7.5.1. Observation of preanalytical influence on RT-PCR in Case No. 1

After RNA isolation, RT-PCR was done on an HCV infected plasma sample of a patient with carcinoma rectum (Fig. 7.1). RT-PCR fluorescence amplification before surgery showed a Cq value of 36.51 (Fig.7.1A) which increased to a Cq of 37.45 two hours after surgery (Fig. 7.1B). But RT-PCR done three days after surgery, gave a negative result, indicating absence of HCV or viral load below detection limit (Fig. 7.1C). The standard plot of 10 IU/µl corresponds to a calculated plasma viral load of 4280 IU/ml of plasma. The calculated viral load of the plasma sample before surgery was 428 IU/ml, 2 hours after surgery was 390 IU/ml and 3 days after surgery was negative (Table 7.1). These results indicated that after surgery there was a decrease in calculated plasma viral load, and the outcome 3 days after surgery was a negative RT-PCR result, indicating preanalytical influence on the outcome of RT-PCR result.

As the viral load in Case No. 1 was very low, the presence of HCV in plasma sample and the 5'UTR specific PCR product (272 bp) was internally validated by synthesising primers for 5'UTR region (Bukh et al; 1992) followed by agarose gel electrophoresis for molecular size determination (Fig. 7.2). The assay method was externally validated by sequencing the internally validated PCR product using Sanger's method and

submitting the sequence to NCBI. At NCBI, the BLAST analysis showed 100% homology with 5'UTR region and identified as genotype 1 of HCV with Accession No. MT258412.

7.5.2. Calibration plot extended to concentrations below the limit of quantitative RT-PCR

The calibration plot for quantitative RT-PCR validated by the reagent manufacturer (Artus HCV RG RT-PCR Kit of Qiagen, Germany) was from 10^1 IU/µl to 10^4 IU/µl of 5'UTR template concentration in the calibrator reagent. The 10^1 IU/µl calibrator was serially diluted 1 in 10 to give 1 IU/µl and 0.1 IU/µl. Six assays were done with each of the calibrator concentration. The mean of log calibrator concentrations versus mean±SD of Cq were plotted (Fig. 7.3).

The %CV of Cq values of six sets of each calibration concentrations obtained from 10^4 to 10^{-1} IU/µl are 1.81%, 1.489%, 2.525%, 1.92%, 2.087% and 3.169%, respectively. These results indicated very good RT-PCR calibrator performance till 1 IU/µl calibrator concentration. But the variation increased to 3.169% at 10^{-1} IU/µl. The calibration plot constructed from the above mean values gave an $R^2 = 0.996$, slope = -3.098 and PCR efficiency = 1.1 indicating good calibrator performance.

The Standard Deviation of Cq values of six sets of each calibration concentrations obtained from 10^4 to 10^{-1} IU/µl are 0.4409, 0.664, 0.4484, 0.6099, 0.767 and 1.211, respectively These results indicated that the standard deviation increased at 1 and 10^{-1} IU/µl calibrator concentration as indicated by the error bar (Fig. 7.3).

7.5.3. Sample influence on RT-PCR calibration plot by Case No. 2

If there is a preanalytical influence on RT-PCR by RNA isolated from plasma sample of patient, then it may be possible to set up an experimental system to reproduce that influence on the HCV 5'UTR templates in the RT-PCR calibrators. The manufacturer's (Qiagen, Germany) validated quantitative HCV RT-PCR calibrators ranged from 10^4 IU/µl to 10^1 IU/µl in the calibrator. To verify this, equal volume (10 µl) of calibrator and RNA sample isolated from an HCV RT-PCR negative cancer

patient before surgery was added to the master mix for RT-PCR. The results showed a consistent increase in Cq on addition of RNA isolated from plasma (Fig. 7.4). These results indicated that even at higher template concentrations (10^4 IU/µl to 10^1 IU/ µl) the quantitative RT-PCR showed influences by nonspecific RNA from the patient's sample.

The wider difference between the calibration plots at lower template concentrations indicate that the preanalytical influences are higher at lower concentrations (Fig. 7.4). The difference between the pairs of Cq values are much greater than the SD of the calibration plot (Fig. 7.3) from 0.4409 to 0.664.

To study the preanalytical influence of the sample of a cancer patient before surgery, RNA was isolated from the sample and equal amounts of the isolated RNA was added to the different concentrations of calibrator. RT-PCR of the calibrators was done with and without the RNA isolated from the HCV negative cancer patient sample. There was increase in Cq value of the calibrators when RNA sample was added to it (Fig. 7.5A and Fig. 7.5B).

Influence on RT-PCR of RNA isolated from an HCV negative cancer patient sample on 10^1 IU/µl and 1 IU/µl calibrator before and 3 days after surgery were studied (Fig. 7.5A and Fig. 7.5B). The influence of the RNA isolated from the patient on the 10^1 IU/µl and 1 IU/µl calibrator before (Fig. 7.5A) and 3 days after surgery (Fig. 7.5B) showed increase in Cq before surgery and a negative result in 1 IU/µl after surgery. The Cq values showing influence on RT-PCR of RNA isolated from an HCV negative cancer patient before and after surgery (Table 7.2).

7.5.4. Quality control data

The Mean ± SD and %CV of calibrators obtained are 10^1 IU/µl= 33.615±0.6099, 1.81; 10^2 IU/µl= 30.118±0.4484, 1.489; 10^3 IU/µl= 26.29±0.664, 2.525 and 10^4 IU/µl= 22.9366±0.4409, 1.92. The Standard deviations Mean ± SD and %CV for the lower concentrations at 1 IU/ µl and 0.1 IU/ µl were 36.7466±0.767, 2.087 and 38.22±1.211, 3.169 respectively (Fig. 7.3).

7.5.5. Comparison of data analysis of RT-PCR amplification plots of calibrator and patient samples

Data analysis was done for HCV standard (10 IU/µl), sample with high, moderate and low plasma viral load. The four-parameter equation gave a fluorescence estimation (F_e or *f*) using the value of Ct at fluorescence (F) at 0.05, slope (b), Ct at inflexion point (Xo), Baseline fluorescence (Yo) and the difference between maximum and baseline fluorescence (a). Of the four parameters characteristic of the sigmoid RT-PCR amplification plots, the fluorescence intensity change and slope showed maximum influence with decrease in template concentrations in both calibrators and patient samples (Table 7.3).

The different parameters of the sigmoid fluorescence amplification plots studied were Cq at a threshold fluorescence of 0.05, slope and Cq at inflection point and difference in fluorescence between maximum fluorescence and baseline fluorescence. When these parameters of the fluorescence amplification plots were examined, maximum influence is on the slope at inflexion point and ΔF.

The Cq of calibration from log 10 IU/µl to log 0.1 IU/µl were plotted against slope at inflection point for the calibrator (Fig. 7.6A) and the patient sample (Fig. 7.6C). It was observed that the slope decreases as Cq values of the calibrators increase. But the Cq versus slope of the patient sample showed a sharper decrease in slope as the Cq value increased. Similarly, ΔF decreased less when the Ct value increased in the calibrators (Fig. 7.6B) and ΔF decreased much more upto near zero change in fluorescence as the Cq increased in the patient sample. These results indicated that slope and ΔF showed a sharper decrease in the slope and ΔF in the patient sample (Fig. 7.6D).

7.5.6. Sample amplification and Internal control amplification

Preanalytical influences on RT-PCR were found to be decreased resulting in decrease in Cq and one sample which became positive. These results confirmed that there are preanalytical influences in these cases. In the case of sample 1, the Cq of HCV RT-PCR and its IC template were found

to decrease after two weeks. In sample 2, PCR negative patient became PCR positive after two weeks. In sample 3, there was a large decrease in Cq in HCV template and in Internal Control (Fig. 7.7A to Fig. 7.7C and Table 7.4).

7.6. DISCUSSION

Common interferences observed in clinical diagnostic RT-PCR are shift in threshold cycle (Cq), decrease in fluorescence intensity, change in slope of the RT-PCR fluorescence amplification plot and PCR inhibition. In this study we are examining the first three influences. The fourth, PCR inhibition, is caused typically in clinical samples by the influence of various drugs, especially heparin. Those conditions were excluded in the study or assays showing RT-PCR inhibition were repeated after decreasing the effect of drugs.

There may be larger amounts of non-HCV RNA contaminating the plasma samples from tissues injury which resulted in the nonspecific amplifications that interfered with the low plasma viral loads in HCV infection. Observational verification of the research hypothesis was done by defining certain case studies for the HCV RT-PCR. An experimental system using calibration plots were designed to support the observational study from these cases. Further experimental evidences were obtained from data analysis of the fluorescence amplification plots.

7.6.1. Observational study for the preanalytical influences

Results from Fig. 7.1 showed that preanalytical influences on samples could affect the diagnostic outcome of RT-PCR, especially when the plasma viral load is low. The possible preanalytical influences may be from the nonspecific RNA or components of plasma co-purified with RNA during RNA isolation procedure, influencing RT-PCR, resulting in shift of the plot to higher Cq values and corresponding lower viral loads two hours after surgery, and then to even an absence of viral load three days after surgery. There may be several explanations given for this phenomenon. But the most reasonable explanation seems to be that the greater quantity of non-HCV RNA isolated from the plasma sample after surgery or tissue injury may bind primers, causing non-specific RT-PCR amplifications. The

resulting non-specific amplification products may consume primers which caused an increase of Cq values. The inflammatory activities associated with tissue repair occurring three days after surgery, may also cause cell and tissue lysis resulting in release of RNA and DNA that may lead to non-specific amplifications, that resulted in the zero Cq values upto the fifty cycles set by the instrument.

The other possible explanation may be that viral load was decreased by the innate immune responses that followed surgical procedures. This may include the acute inflammation at the site of surgery. Inflammation causing decrease in the low viral load below detection limit, or converting to cryptic infection or overcoming the disease by the innate immunity repair mechanisms associated with the inflammation. But the viral load was found to return back or even increase when the tissue damaging condition was overcome. After 2 weeks. The decrease in viral load or a negative RT-PCR result during tissue damage may not be due to overcoming of the infection or due to occult infection

7.6.2. Experimental study for the preanalytical influences:

There were two types of experimental studies done to prove the preanalytical influences. The first was an interventional study on a case with low plasma HCV viral load. An intervention of the diagnostic RT-PCR procedure by a surgical procedure that caused tissue damage was designed to mimic the influence of tissue injury. The surgery caused RT-PCR inhibition resulting in increase in Cq or even converting a positive result to a negative one (Fig. 7.1). The other preanalytical influence resulted in decrease in fluorescence intensity and the slope at inflection point.

The second interventional study was to use validated calibrator concentrations supplied by the manufacturer which includes four calibrator concentrations from 10 IU/µl to 10,000 IU/ µl. The demonstration of preanalytical influences of calibrators showed a consistent shift in Cq value at all concentrations demonstrating the influence of RNA isolated from plasma sample of an HCV negative ovarian cancer patient before surgery. At this point even though the preanalytical influences at higher

concentrations were minimal it could be clearly demonstrated even at higher concentrations.

The increase in Cq of calibrator by the RNA sample isolated from the HCV negative patient sample indicates the possible non-specific amplification that may be leading to shift in Cq values. The data analysis showed increase in variation as the concentration of calibrator decreased.

7.7. CONCLUSIONS

The preanalytical influence on HCV RT-PCR were analysed by selecting HCV RT-PCR positive cases that were to undergo surgery and repeating RT-PCR. Studies were also designed on HCV RT-PCR positive cases that had tissue damaging conditions. In these cases the Cq value decreased or the negative result became positive indicating high viral load when tissue damaging conditions were decreased. These results also indicated that whenever there was a preanalytical influence on the RT-PCR assay, the assay may be repeated after two weeks to obtain a more correct result. The study strongly indicated preanalytical influence were more prominent when HCV viral load was low. Even HCV negative patient samples in the presence of tissue damaging conditions were also found to influence and increase the Cq value of the calibrators.

Fig. 7.1. RT-PCR fluorescence amplification plot of RNA isolated from an HCV infected plasma samples of Case 1 with low viral load, 2 days before surgery (A), 2 hours after surgery (B) and 3 days after surgery (C). Each of these three assay sets has 3 RT-PCR fluorescence amplification plots, standard of 10 IU/µl (S), test (T) and blank (NTC) from left to right with Ct values as follows: **(A)** S = 32.51, T = 36.51, NTC = 0; **(B)** S = 32.38, T = 37.45, NTC = 0; **(C)** S = 32.55, T = 0, NTC = 0.

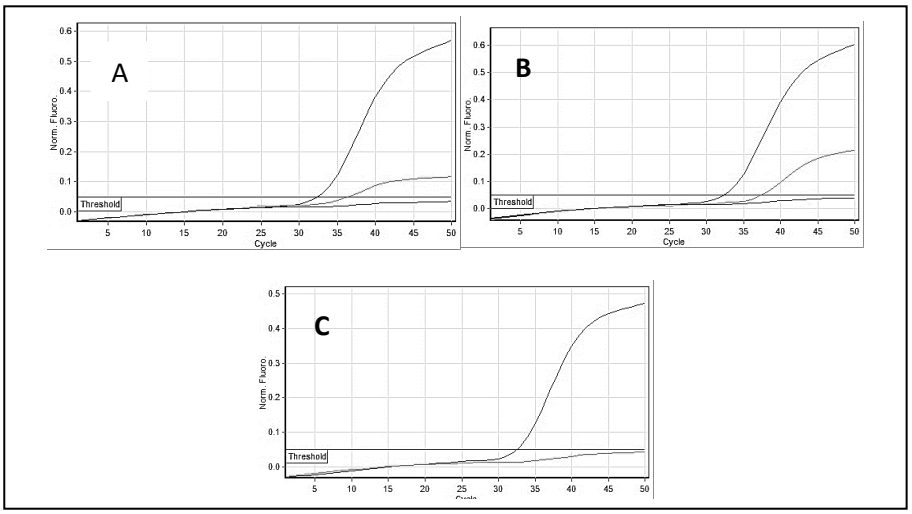

Table 7.1. RT-PCR fluorescence amplification Cq analysis of RNA isolated from an HCV infected plasma samples of Case 1 with low viral load

Sl. No	Name	Type	Cq	Concentration (IU/ ul)
1	Before Surgery			
	QS4 (10 IU/ ul)	Standard	32.51	10
	Case 1	Unknown	36.51	1
	NTC	Non-Template Control		
2	2 hours after surgery			
	QS4 (10 IU/ ul)	Standard	32.38	10
	Case 1	Unknown	37.45	
	NTC	Non-Template Control		
3	3-4 days after surgery			
	QS4 (10 IU/ ul)	Standard	32.55	10
	Case 1	Unknown		
	NTC	Non-Template Control		

Fig. 7.2. Agarose gel electrophoresis of PCR product of Case 1. 100 bp DNA ladder (1), PCR product 5'UTR, ca e 1 (2) and NTC (3)

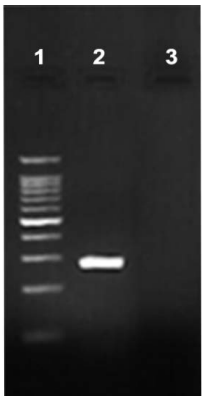

Fig. 7.3. Calibration plot extended to concentrations below the limit of quantitative RT-PCR. The calibration plot validated by the reagent manufacturer (Artus HCV RG RT-PCR Kit of Qiagen, Germany) includes calibrator concentration from 10^1 IU/µl to 10^4 IU/µl of 5' UTR template concentration. Each calibrator assay contains an internal assay control. In addition to the recommended calibrator concentration, the 10^1 IU/µl calibrator was diluted 1 in 10 concentration (1 IU/ µl), which was further diluted 1 in 10 to 0.1 IU/ µl. Six assays was done with each of the calibrators and the Mean ± SD of log calibrator concentration versus Mean ± SD of Ct were plotted.

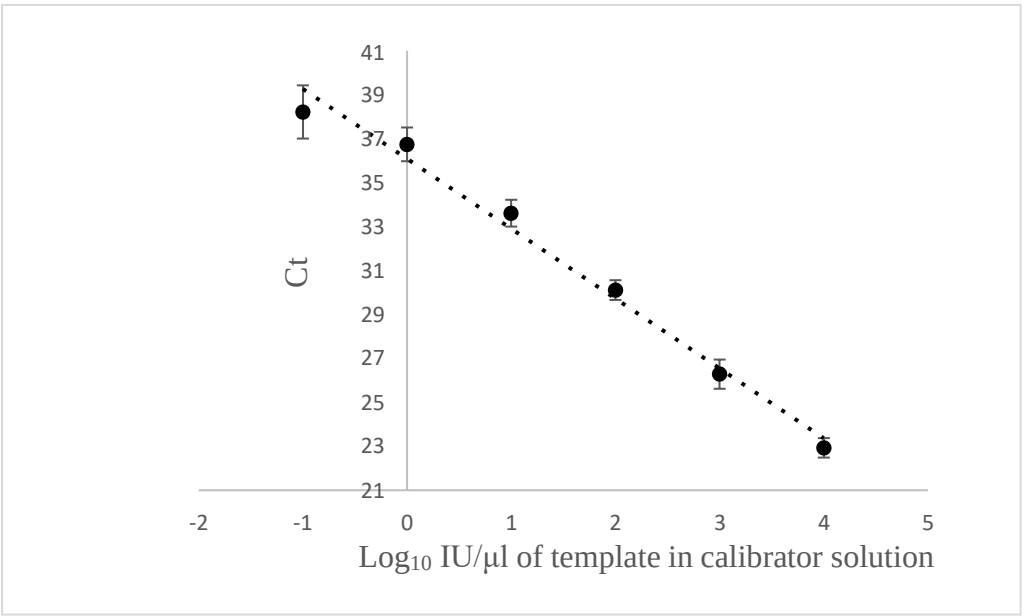

Fig. 7.4. Concentration versus Cq to study preanalytical influence of the sample of a cancer patient (Case 2) before surgery, RNA was isolated from the sample and equal amounts of the isolated RNA was added to the different concentrations of calibrator. RT-PCR of the calibrators was done with and without the RNA isolated from the HCV negative cancer patient sample, increased the Cq value of the different calibrators.

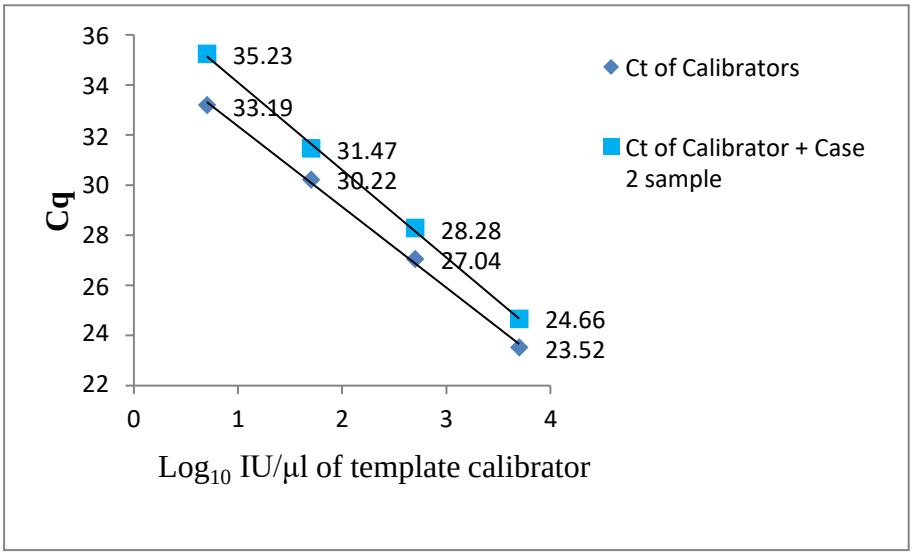

Fig. 7.5. RT-PCR fluorescence amplification plot of RNA isolated from an HCV negative cancer patient sample on 10^1 IU/µl and 1 IU/µl calibrator before (Fig. 7.5A) and 3 days after surgery (Fig. 7.5B) were used to study the influence on RT-PCR. Internal control amplification is seen at the right side.

Fig. 7.5A

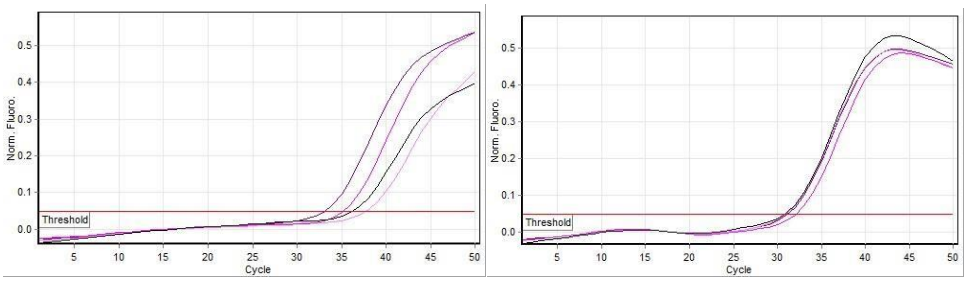

Fig. 7.5B

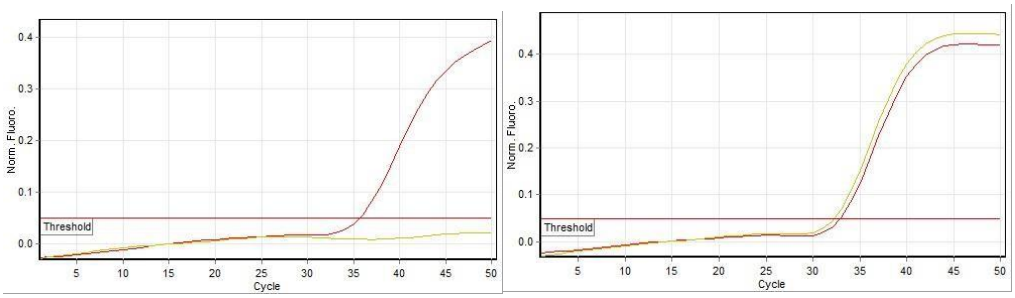

Table 7.2. Influence on RT-PCR of RNA isolated from an HCV negative cancer patient before and after surgery

Sl. No	Name	Cq	IC Cq
1	Before Surgery		
	10 IU/ul QS4	33.19	31.19
	2 IU/ul QS4	37.77	31.06
	10 IU/ul QS4 + 10 ul Case 2	35.23	32.10
	2 ul QS4 + 10 ul Case 2 make up with sterile water	36.29	30.85
2	3-4 days after surgery		
	10 ul QS4 + 10 ul Case 2	35.72	32.93
	2 ul QS4 + 10 ul Case 2 (make up with sterile water)	0	32.29

Table 7.3. Data analysis of RT-PCR amplification plots. Data analysis was done for HCV standard (10 IU/µl), sample with moderate and low plasma viral load. The four-parameter equation gave a fluorescence estimation (F_e or *f*) using the value of Cq at fluorescence (F) at 0.05, slope (b), Cq at inflexion point (Xo), Baseline fluorescence (Yo) and the difference between maximum and baseline fluorescence (a).

Calibrator/ HCV Samples	X	b	Xo	Yo	a	F
Calibrator (10 IU/µl)	33.61	2.035	39.5034	5.84279	12.6829	6.506963
Sample with high viral load	28.28	2.45	35.6542	8.564	24.733	9.7264
Sample with moderate viral load	31.62	1.819	37.0272	4.74647	9.14928	5.19168
Sample with low viral load	37.63	3.477	38.0963	5.03932	1.59964	5.78559

Fig. 7.6. The different parameters of the sigmoid fluorescence amplification plots, Cq versus slope, % relative fluorescence intensity of calibrators and HCV plasma samples.

Fig. 7.6A

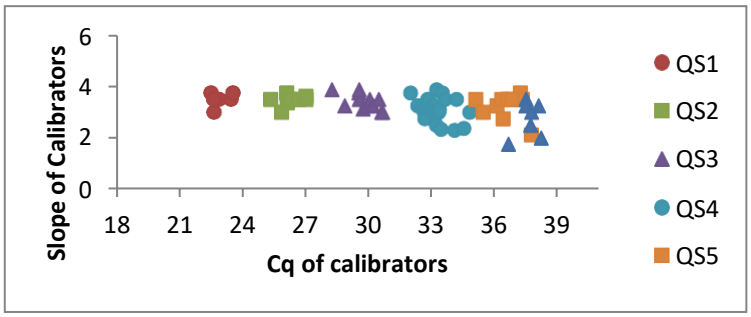

Fig. 7.6B

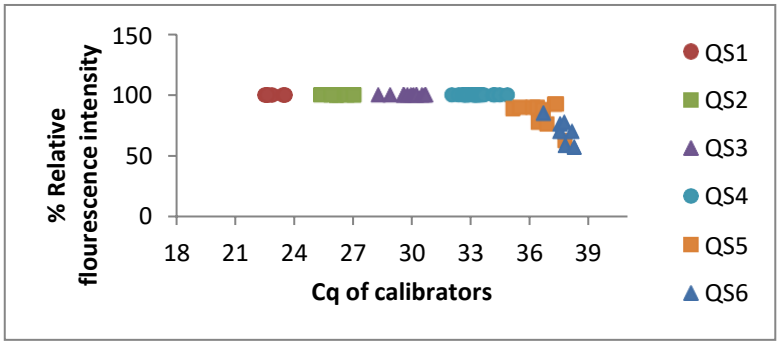

Fig. 7.6C

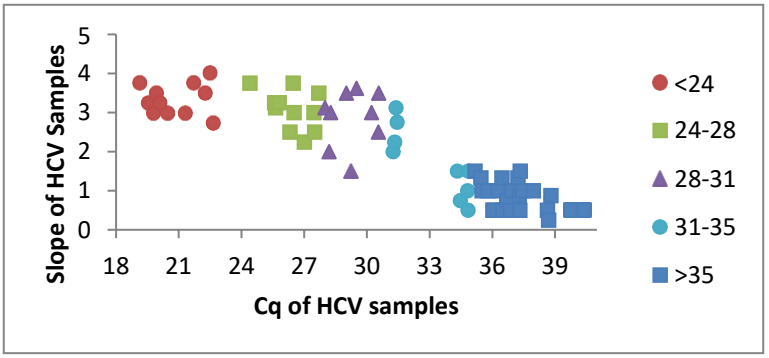

Fig. 7.6D

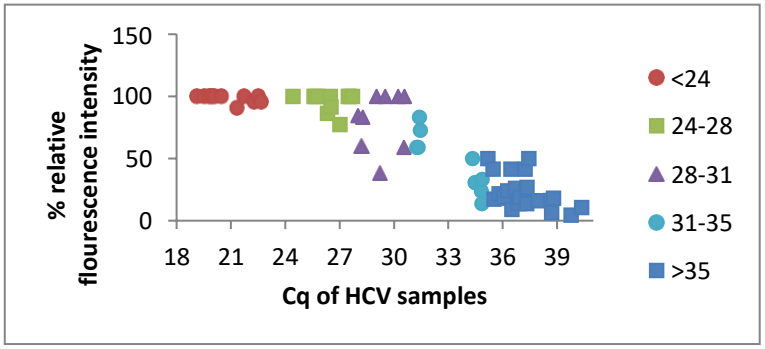

Fig.7.7. Amplification plot and Internal Control amplification plot of the samples that showed inhibition and shift in Cq (Fig. 7.7A to Fig. 7.7C).

Fig. 7.7A - Sample 1

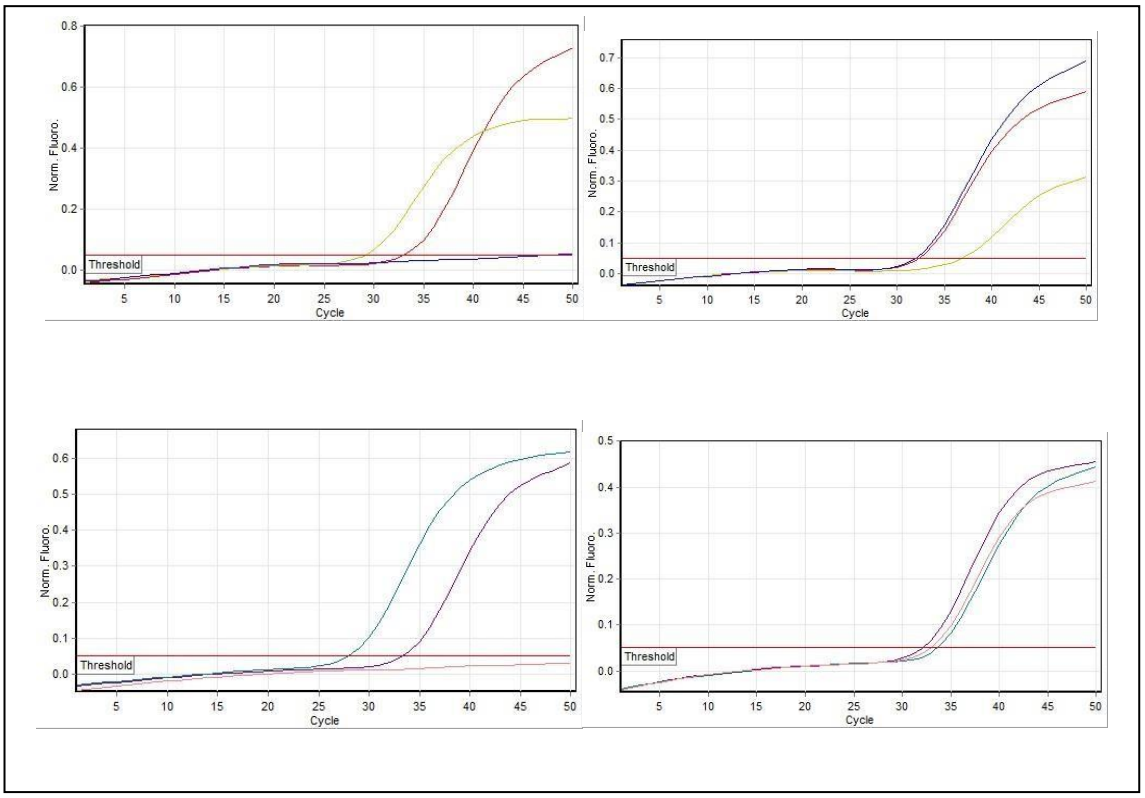

Fig. 7.7B - Sample 2

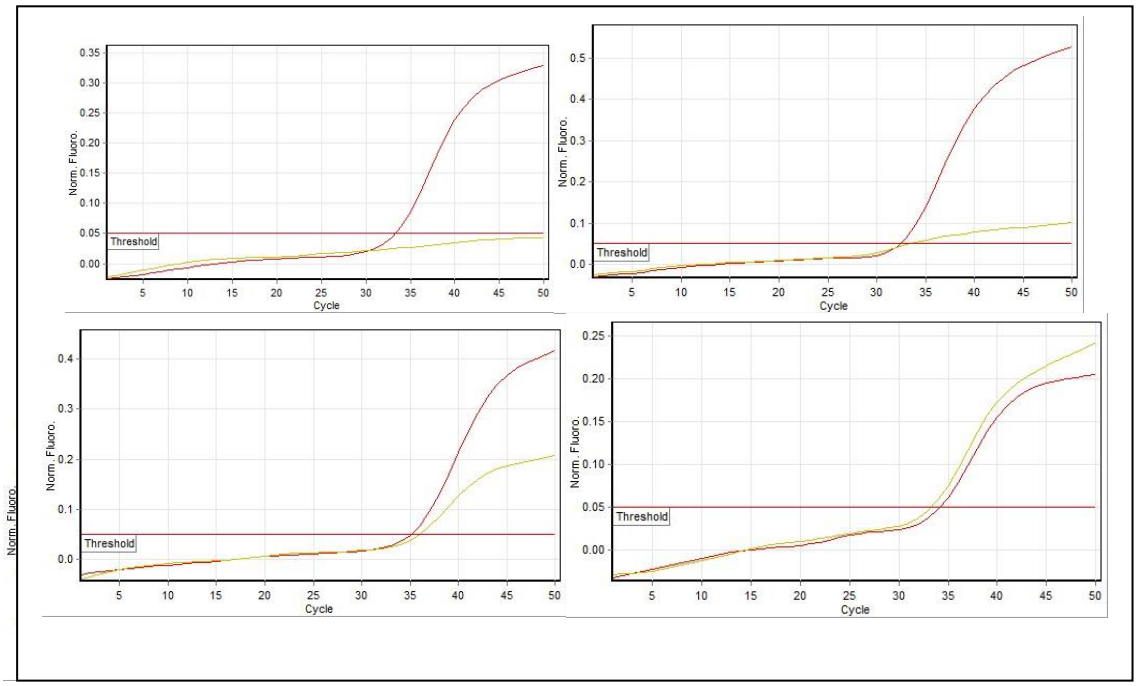

Fig. 7.7C - Sample 3

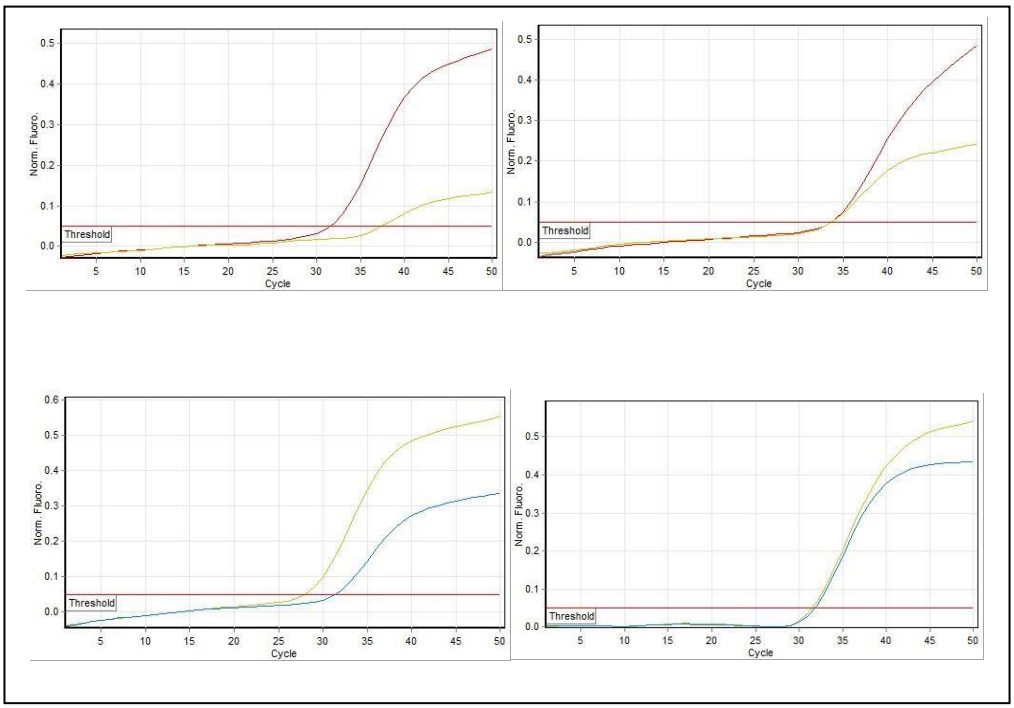

Table 7.4. Cq difference of Sample and Internal control amplification with and without inhibition

	Cq of Sample with Inhibition (Cq without Inhibition)	Cq of Internal Control with Inhibition (Cq without Inhibition)	Relative Fluorescence Intensity
Sample 1	29.23 (27.96)	36.92 (33.62)	50% (no inhibition)
Sample 2	PCR Neg (35.90)	33.31 (33.35)	90% (no inhibition)
Sample 3	37.50 (31.39)	33.80 (31.85)	40% (20% inhibition)

Chapter 8

Reactive concentrations of anti-Hepatitis C Virus antibody distribution in screening assays showed similar bimodal distribution in both qRT-PCR positive and negative samples

8.1. ABSTRACT

Hepatitis C virus (HCV) infection is characterised by low antibody levels, low viral load and almost no symptoms. Diagnosis of HCV infection is done by screening for anti-HCV antibody by the third-generation assay followed by confirmation of the diagnosis by HCV RT-PCR of samples reactive for anti-HCV antibody. The reactive anti-HCV antibody concentrations may be RT-PCR positive or RT-PCR negative. Samples were collected after excluding patients with tissue damaging conditions and influence of drugs, as far as possible. RT-PCR assay was done after preanalytical control of samples to decrease non-specific influences, probably of nucleic acids and drugs, immediate isolation of RNA from EDTA-plasma. Distribution of the concentrations of anti-HCV reactive antibody were plotted as a histogram. There were two distribution clusters for anti-HCV antibody, the lower antibody cluster was between 1.0 and 15.0 and the higher antibody cluster was between 15.0 and 42. Each of the two reactive antibody clusters had HCV RT-PCR positive and negative groups. The two antibody clusters in the antibody distribution of histogram were found to have both RT-PCR negative and positive samples, indicating that both clusters might have occult and positive HCV infection. These results questioned the large number of 'false reactivity' issue with the third generation anti-HCV antibody assays.

8.2. INTRODUCTION

Hepatitis C virus (HCV) infection is a disease in which large number of individuals have low levels anti-HCV antibody, low viral load and with very mild or no symptoms of infection. The low antibody levels and low viral load in circulating plasma were also confirmed in our studies. As the clinical symptoms were absent or low, near to 100% of the detection of infection by screening followed by confirmation of diagnosis of HCV infection was made in the clinical laboratory.

Diagnosis of HCV infection required a 'screening' enzyme immunoassay (EIA) that reported reactive levels of anti-HCV antibody above a cut off, followed by 'confirmation of diagnosis' by real time reverse transcriptase-PCR (real time RT-PCR) or western blotting. A screening EIA may be reactive or non-reactive when the signal level was above or below a cut off, respectively. Increasing the sensitivity of the screening assays for anti-HCV antibody were required to detect

almost all infected samples with near 100% sensitivity. Sensitivity of screening EIAs were increased by use of third generation assays, having high seroconversion detection rates and EIA signal detection by enhanced chemiluminescence or fluorescence (Ritcher, 2002; Vitros ECi procedure manual HCV, 2005). A preliminary screening assay excluded large number of nonreactive samples, thus reducing the number of confirmatory assays which were much more expensive and with long turnaround times.

The third generation anti-HCV screening assay are directed to detect antibody against epitopes located on three different stretches of amino acid sequences on HCV proteins. These three antigenic regions for screening assay are located in the Core (a.a 2-120), NS3-NS4 (a.a 1182- 1931) and NS5 (a.a 2054- 2995) regions (Barrera, 1995). The primers for diagnostic RT-PCR are commonly targeted to 5'UTR conserved sequence (Bukh, J, 1992, Hoffman, Q. Liu, 2011). But the commonly used second-generation anti-HCV antibody screening assays exclude the NS5 epitopes.

A 'false reactive' report is one where the anti-HCV antibody screening assays are reactive and HCV RT-PCR is negative. There were large number of 'false reactive' reports with third generation anti-HCV screening assays. The numbers were too high to be assigned only to cross reactive antibody alone. But the commonly used anti-HCV antibody screening assays are the second-generation assays. This assay excludes the NS5 epitopes, on the suspicion that antibodies against NS5 detects large number of cross-reactive antibodies leading to false reactivity. A curious observation for the third generation anti-HCV screening assays in our preliminary studies, was that large number of "false reactive" screening results were clustered at the low reactivity range which might have provoked 'CDC and Disease Prevention' to raise the cut off level of reactive screening assays to 8.0 from 1.0 (Alter J, 2003, Kamili et al, 2012).

Also, there were interpretation issues with anti HCV antibody screening assay design by manufacturers (2^{nd} and 3^{rd} gen) and guidelines proposed by regulatory authorities (Alter J, 2003, CDC). The WHO-defined diagnostic criteria for HCV infection recommends a third-generation screening assay followed by confirmatory RT-PCR assay (WHO, 2001; Barrera, 1995).

Increasing the sensitivity of screening assays resulted in large increase in the detection of reactive levels of anti-HCV antibody in serum samples. The large increase in reactive screening assays reports and absence of symptoms in HCV infected individuals often lead to questions among clinicians about the usefulness of screening assay with high seroconversion detection rates, dumbed most reports as ‘false reactive’ (personal experience) and even attempted to raise the cut off levels of reactive anti-HCV antibody levels (Kamili et al, 2012) to match it with the cut off levels of absorbance or colour-based, second-generation EIA. This subjective and hypothetical method of branding reactive reports of screening assays with high seroconversion detection rates as ‘false reactive’ was examined in our laboratory and results are reported in this publication.

We hypothesised that the large number of **‘false reactive screening assay’** reports were due to (a) insensitivity of RT-PCR assays and (b) due to occult HCV infections. As the plasma viral loads were low, the issue of lowering the limit of detection for assaying the viral loads by RT-PCR was taken up. The **sensitivity of RT-PCR was increased by controlling the preanalytical procedures of the assay** that involves (a) plasma sample collection, (b) RNA isolation and (c) cDNA preparation from plasma. **Preanalytical control of RT-PCR assays were achieved** by collecting PCR blood samples when tissue damaging conditions were lowest (eg: avoiding PCR in the post-operative state, during acute infection and crush injuries, etc.), avoiding conditions in which there may be PCR inhibition (use of drugs such as heparin), and performing RNA isolation and RT-PCR immediately after blood sample collection in the morning (to avoid RNA degradation). These precautions were taken to reduce contaminating RNA, PCR inhibition and RNA degradation. It was also hypothesised that these precautions increased the sensitivity of RT-PCR and the results are given in this chapter.

This study we analysed the distribution and frequency of distribution of anti-HCV antibody in the non-reactive and reactive screening assays, and in the RT-PCR positive and negative samples after taking the preanalytical precautions for the RT-PCR assay.

8.3. ORIGINAL OBJECTIVES

1. Establishment of the methods for evaluation by data analysis, test validation, quality control and clinical state of the patient for Molecular Diagnostic reporting of Hepatitis C infection.

2. Use of these procedures for confirmatory diagnosis of hepatitis C infection, its plasma viral count determination and genotyping.

8.3.1. Aspects of the original objectives addressed in this chapter

Data analysis of anti-HCV antibody concentrations to understand its distribution, its role in screening for HCV infection, and attempts will be made to evaluate issues of 'false reactivity' and occult infection. Studies also will be attempted to evaluate the relationship of antibody reactivity to HCV RT-PCR results.

8.4. MATERIALS AND METHODS

Research design was observational cross-sectional study with case control. **Institutional research and ethics committee permissions** were obtained (Ref. General Methods).

8.4.1. Sample Collection and Preparation for anti-HCV antibody assay

Collect specimen using standard procedure. 2 – 4 ml of morning blood sample was collected from individuals after describing the details of the project in vernacular language, showing the patient information sheet and getting the signature in the consent form. 4 ml of blood was collected in vacuum tubes with clot activator. Blood sample was centrifuged to prepare serum which was used immediately or stored in aliquots at -20^{o}C. The VITROS Anti HCV assay uses 20 µl serum sample. Mix samples, calibrator and controls by inversion and bring to 15-30^{O}C before use. Blood samples should be completely separated from cellular material or it may lead to erroneous result. Blood samples of patients were routinely screened before surgery or invasive procedures for anti-HCV antibody by a third-generation assay in an immunochemistry autoanalyzer with enhanced chemiluminescence detection method (Ortho Clinical diagnostics, Vitros ECi). When the anti-HCV antibody levels were above a cut off of 1.00, HCV RT-PCR was done to confirm the diagnosis of HCV infection. When the antibody levels were $\leq$0.89, the sample was considered nonreactive for anti-HCV antibody and reported

as negative for HCV infection. When the antibody levels were between ≤0.90 and ≤0.99, the assay was repeated and the antibody levels were reported as borderline reactive. RT-PCR was also done for the borderline reactive samples for confirmation of HCV infection. Refer Details 4.5, 4.9 and 3.5.1.

8.4.1.1. Anti-HCV antibody Screening tests

The VITROS Anti-HCV assay uses 20 µl serum sample. Mix samples, calibrator and controls by inversion and bring to 15-30^{O}C before use. Blood samples should be completely separated from cellular material or it may lead to erroneous result. Blood samples of patients were routinely screened before surgery or invasive procedures for anti-HCV antibody by a third-generation assay in an immunochemistry autoanalyzer with enhanced chemiluminescence detection method (Ortho Clinical diagnostics, Vitros ECi). Samples were incubated in wells containing antigenic epitopes, washed, incubated with anti-antibody linked to peroxidase enzyme. Washed again to remove the unbound antibody and then incubate with signal reagent and chemiluminescence signals were detected.

The VITROS Anti-HCV assay is performed using the VITROS Anti HCV Reagent pack and VITROS Immunodiagnostic Products Anti-HCV calibrator on the VITROS ECi/ECiQ Immunodiagnostic system. An immunometric technique is used. This involves a two-stage reaction. In the first stage, HCV antibody present in the sample binds with HCV recombinant antigens coated on the wells. Unbound sample is removed by washing. In the second stage, horseradish peroxidase (HRP) labelled antibody conjugate (mouse monoclonal anti-human IgG) binds to any human IgG captured on the well in the first stage. Unbound conjugate is removed by washing.

A reagent containing luminogenic substrates (a luminol derivative and a peracid salt) and an electron transfer agent, is added to the wells (Summers M et al, 1995). The HRP in the bound conjugate catalyses the oxidation of the luminol derivative, producing light. The electron transfer agent increases the level and duration of the light produced. The light signals are read by the VITROS immunodiagnostic System. The amount of HRP conjugate bound is indicative of the level of anti-HCV present in the sample.

8.4.2. Sample Collection and Preparation for RNA isolation

8.4.2.1. Inclusion and Exclusion criteria

Inclusion criteria were reactivity to anti-HCV antibody and exposure to HCV infection. **Exclusion criteria** were related to the **preanalytical condition** of the patient, such as acute tissue damaging disease conditions, patients on chemotherapy and who were heparinised were found to influence the RT-PCR. These conditions were avoided as far as possible. Sample collection was delayed till the condition subsides or was overcome, up to a day or two for heparinised patients, or sample was collected before the next intravenous injection. In all emergency and other unavoidable circumstances, all the above preanalytical criteria were overlooked, but the results of RT-PCR were analysed for influences.

2 – 4 ml of EDTA-treated morning blood sample was collected from individuals after describing the details of the project in vernacular language, showing the patient information sheet and getting the signature in the consent form. Samples will be collected in the Clinical Laboratory, Out Patients section or in the wards at Amala Institute of Medical Sciences.

8.4.2.2. RNA isolation and RT –PCR

Real-time RT-PCR technology may provide an accurate and sensitive method to quantify HCV RNA. PCR was based on the amplification of specific regions of the HCV genome in the blood sample 1-3 weeks after infection. In real time RT-PCR the amplified product was detected via fluorescent dyes. These were usually linked to oligonucleotide probes that bind specifically to the amplified product. Monitoring the fluorescence intensities during the PCR run allows the detection and quantitation of the accumulating product.

When the anti-HCV antibody levels were above a cut off of 1.00, RT-PCR (Rotor Gene Q 5 plex HRM, Qiagen), kits and reagents (Artus HCV RG RT-PCR kit reagents and QIAamp viral RNA mini kit) used to confirm the diagnosis of HCV infection.

8.4.3. Statistical Data Analysis

Biostatistical methods used in this study are defined and described below. Statistical data analysis was done mainly by SPSS. Statistical analysis and estimation of the data generated by the screening anti-HCV antibody assay and from the RT-PCR fluorescence amplification data were done. SPSS used for calculating distribution characteristics such as the mean, median, mode, range, standard

deviation, interquartile range, S.E of mean, 95% confidence interval, X-Y scatter plots, Histogram, Distribution frequency, t tests, correlations, etc.

Measures of Central Tendency, Average measures that describe the central aspects of a data are called averages. An average summarizes all the characteristics of entire mass of data. Most of the items of the series are clustered around the average, so it is called as measure of central tendency. **Arithmetic mean** is the sum of all the observations divided by the number of observations

Mean = sum of all the observations/ Total number of observations

Median is the value of the middle item of a given series of data arranged in ascending or descending order of magnitude.

Median = value of the item (n + 1) / 2

Mode is the most frequently occurring value in a sample. A sample with a single mode is referred as unimodal. If it has two mode it is called as bimodal and more modes as polymodal or multimodal. If no mode, it is no modal sample.

A **measure of dispersion** (also called measure of variation, scatter, spread) is to describe the extent of scattering of items around a measure of central tendency. Different types of measure of dispersion used here. **Range** is the minimum and maximum value of the given series of data (Gurumani, 2005). **Standard deviation** is defined as the square root of the arithmetic mean of the squared deviation of the various items from the mean. The mean squared deviation is called the variance. Therefore, the square root of variance is the standard deviation.

Coefficient of variation (CV) is also known as relative standard deviation (RSD). It is a measure of dispersion of a probability distribution or frequency distribution. CV is defined as the ratio of standard deviation to the mean and is expressed as percentage. It is widely used in analytical chemistry to express the precision/bias, and repeatability of an assay.

95% Confidence Interval of Mean is a range of values which can be confident including the true values. A confidence interval for the estimated mean extends to either sides of the mean by a multiple of the standard error. 95% confidence interval was calculated by multiplying standard error by 1.96 and then identifying the range by adding and subtracting the value from mean.

Frequency Graphs, Histogram is the graphical representation of continuous frequency distribution. The X-axis has the true class intervals, and the Y-axis, the frequencies. The bars are of equal width indicating that the class-intervals are of equal width. The height of the bar is proportional to the respective frequency. Therefore, it may be said that the area (length × breadth) of each bar is equal to the total of all the frequencies.

X-Y Scatter diagram is an easy and simple method for studying correlation between two variables. If X and Y are pairs of variables, the values of the variable X are marked in the X – axis and the values of variable Y are marked in the Y axis. A point is plotted against each value of X and the corresponding Y value. A swarm of dots is obtained, and this is called the scatter diagram. From this scatter diagram we can understand about the correlation between the variables whether it is positive correlation or negative correlation.

All other details of Methodology were described under Chapter 4 where the general 'Materials and Methods' were given.

8.4.4. Calculation of frequency distribution

Calculation of frequency distribution of sample per unit chemiluminescence signal range (c) divided by sample number (n). Calculation of anti-HCV antibody reactivity per unit chemiluminescence signal (r) was by dividing the sample number by the chemiluminescence signal range, which gives the sample number per unit chemiluminescence range (r, r=n/c). The frequency distribution of the sample per unit chemiluminescence signal will be r/total sample number (N) (Table 8.3).

8.5. RESULTS

8.5.1. Analysis of the Distribution of Non-reactive, Borderline reactive and Reactive levels of anti-HCV antibody

Distribution of nonreactive and reactive anti-HCV antibody levels may give us information regarding the antibody response to the virus. There were two sets of serum samples collected independently of each other for this study: the non-reactive anti-HCV antibody samples with enhanced chemiluminescence signals between 0.00 to 0.89, with n = 1014, and the reactive anti-HCV antibody samples with signal levels between 0.90 to 42.1, with n = 534 (Fig. 8.1A and 8.1B; Table 1). The non-

reactive range was further split into 0.0 – 0.39 (n = 997) and 0.4 – 0.89 (n = 17). The latter range was again split into 0.4 to 0.64 (n = 10) and 0.65 – 0.89 (n = 7). The non-reactive samples were very large in number, they were collected only for a shorter pre-fixed continuous period of 10 am to 3.30 pm on each day, and the sample collection was independent of the reactive sample collection (Table 8.1 and Table 8.2).

The range ≥0.90 and ≤0.99 (n = 28), were considered as borderline reactive (Vitros ECi, procedure manual), and the reactive range was from 1.0 to 42.1 (n = 506). The reactive and borderline reactive samples were subjected to RT-PCR for HCV from plasma prepared from EDTA-treated blood. All the samples with reactivity ≥0.90, available in our clinical laboratory for a period of four years were collected and subjected to RT-PCR. As the samples with nonreactive and reactive levels of antibody levels were collected independent of each other, the data could not be used to calculate prevalence (Table 8.1 and Table 8.2).

The mean non-reactive antibody level was 0.07, the median was 0.04 and the lowest visually located mode was 0.02 (SPSS output had multiple modes). 95% confidence interval (CI) of mean was 0.0638 to 0.0756. Of the total nonreactive samples between 0.00 to 0.89, 97.14% of samples were falling below 0.30. The nonreactive distribution was positively skewed with very few samples from signal levels 0.4 to 0.89, inclusive of both values (n = 17) (Table 8.1 and 8.2). We propose that the samples between 0.40 to 0.89 (range: 0.89 – 0.40 = 0.49) may be considered as the cross-reactive antibody range (genuinely false reactive), as they were outliers of the non-reactive antibody range from 0.0 to 0.89. The genuinely false reactive sample frequency per unit signal range decreased from range 0.4 – 0.64 (n = 10) to 0.65 – 0.89 (n = 7), and then further decreased in the range 10.0 – 15.0 with RT-PCR negative (n = 12) (Table 8.1 and Table 8.2). This is demonstrated below.

Histogram of the distribution of all antibody reactive samples in the past four years showed a bimodal distribution (Fig. 8.2A and 8.2B), with bulk of the antibody reactive samples between 1.00 and 3.00 and a weaker distribution between 20 and 38 (Fig. 8.1B).

Both the RT-PCR positive samples and PCR negative samples, also showed similar bimodal distribution as described above for the total antibody reactive samples (n = 534). The two clusters of lower (0.4 to 16.0) and higher antibody

reactivities (16.0 to 42.1) were analysed for their distribution in RT-PCR negative (Fig. 8.3A and B) and RT-PCR positive (Fig. 8.3C and 8.3D) groups.

8.5.2. Theoretical calculation of the number of 'genuine' false reactive sample numbers between antibody signal from 0.4 to 42.1

The total number of samples between 0.4 – 0.89 was 17, and that between 0-90 - 42.1 were 534 obtained from Table 1. Of these total numbers, the reactive numbers at various chemiluminescence range were calculated from the data in Table 1 and 2. Among the non-reactive samples, there were very few samples with reactivity between 0.4 - 0.64 (n = 10) and 0.65 – 0.89 (n = 7), and they were decreasing with increase in chemiluminescence signal. These 'weakly reactive' antibodies in the nonreactive range, might be considered as the 'weakly cross reactive' range, as these were outliers of the genuinely nonreactive range, 0.0 – 0.4. Assuming that the values between 0.4 and 0.89 were due to cross reactive antibody, there might be similar reactivity from cross reactive antibodies between 0.90 and 15.0 (Fig. 8.1). The sample distributions were higher between 1.0 – 10.0 and between 15 – 42.1. As the cross-reactive antibodies were decreasing, it was expected that the genuinely false reactive samples would be almost nil between 10.0 and 15.0 in the RT-PCR negative group (Fig. 8.3, Fig. 8.4). The distribution data of the reactive antibody levels at various chemiluminescence signal ranges for RT-PCR positive and RT-PCR negative samples were calculated from Table 8.2 and Fig. 8.3.

Number of samples (n) distributed for specified chemiluminescence signal range (c) and its distribution frequency per unit signal range (r) for the total sample collected (Nonreactive n = 1014 and reactive n = 534) was calculated.

In the non-reactive range, a strong distribution peak was identified between 0.00 and 0.39 (n = 997) (Table 8.2A). The sample distribution from 0.40 to 0.89 might be considered as outliers (n =17) of the strong distribution seen below 0.40. This weak distribution was further split for the chemiluminescence signal range of 0.40 to 0.64 (n = 10) and 0.65 to 0.89 (n = 7).

Calculation of distribution of sample per unit chemiluminescence signal range was done by dividing the sample number by the chemiluminescence signal range (n/c = r). The frequency distribution (F) was calculated by dividing r by the total sample number (1014 or 534) (Table 8.3).

As the sample collection for non-reactive anti-HCV antibody levels (n = 1014) were independent of the reactive antibody sample collection (n = 534), these two samples could not be compared. Comparison was made possible by calculating the distribution of the sample per unit chemiluminescence signal range (r) followed by calculating the frequency distribution (F).

When the frequency distribution of non-reactive samples were calculated per unit chemiluminescence signal range, the frequency, F was high initially at 8.04 at unit chemiluminescence signal range 0.00 – 0.09, as there were large number of non-reactive samples (Table 8.3). The frequency distribution of the non-reactive samples decreased as the chemiluminescence signal increased (Table 8.3).

The frequency distribution of reactive samples from 0.9 to 14.99 were fewer in number. The frequency distribution of samples decreased from 0.524 at the chemiluminescence signal range 0.9 - 0.99 to a low value of 0.034 at the signal range of 10 - 14.99 (Table 8.3).

The above distribution of non-reactive and reactive samples were illustrated in Fig. 8.4A and B. the decrease in the frequency of distribution of samples with increase in chemiluminescence signal for both non-reactive and reactive antibody levels were well illustrated in these two figures.

The proportion of RT-PCR negative to RT-PCR positive sample at various chemiluminescence signal ranges were studied (Table 8.4). As the anti-HCV antibody reactivity increased from 0.90 to 0.99 to a signal level of 15 to 42.1, the proportion or the ratio was found to steadily decrease. This inferred that at lower antibody levels RT-PCR negative samples are more and at higher antibody concentrations, the RT-PCR positive samples were relatively more.

8.5.3. Relationships between anti-HCV antibody levels and Cq of RT-PCR

X-Y scatter of anti-HCV antibody levels with Cq value of HCV RT-PCR positive sample (Fig. 8.5) was constructed. The linear trendline of $R^2 = 0.334$ indicating a negative relationship between the antibody levels and Cq. These results indicate that as viral load increased, antibody levels also increased. Therefore, antibody levels appeared to be dependent on the viral load.

There were large number of RT-PCR positive cases between 0.9 and 15 (Fig. 8.6A). There were also few cases between 0.9 and 0.99 which was the indeterminate

region. Early HCV exposure cases will be RT-PCR positive with non-reactive antibody levels (Fig. 8.7B). These results are due to the long window period required for reactive levels of antibody formation and short periods for detection of RT-PCR positive cases.

As the viral loads were very low too often and were obstructed by preanalytical influence they were missed during RT-PCR assays. The major part of the negative antibody results was for RT-PCR negative samples below the signal level of 0.2. Between 0.2 and 0.4, the reactivity decreased. But between 0.4 to 0.89, the reactivity visually appeared to remain constant (Fig. 8.7A).

In cases of RT-PCR done during the window period, the antibody levels were evaluated. Most of the antibody levels were below 0.2, it remains similar between 0.2 and 0.4. there were 2 out of 41 samples between 0.4 and 0.89 (Fig. 8.7B and Table 8.5)

The Cq distribution of RT-PCR positive samples were found in the low antibody and in the high antibody cluster groups. The distribution appeared to be clustered with a mode at higher Cq value in the low antibody cluster group (Fig. 8.6A). But the Cq distribution appeared to be clustered at a much lower Cq level and mode in the high antibody cluster group (Fig. 8.6B). These results indicated that in the high antibody cluster group, the viral load was higher and in the low antibody cluster group, the viral load was low.

These results indicated that the antibody levels might remain for a long period below 0.2, as interpreted by the frequency of distribution. Following this the antibody levels may increase from below 0.2 to the range of 0.2 – 0.4 for a short duration and may increase faster to 0.9. These results might be arrived at by the frequency distribution upto 0.2. There were 33/41 (31 out of 41) samples below 0.2, 6/41 between 0.2, and 0.4 and 2 samples between 0.4 and 0.89. The range of anti HCV antibody, 0.00 to 0.89, in patients highly susceptible and exposed to HCV infection such as patients undergoing repeated blood transfusion and dialysis.

8.6. DISCUSSION

A preliminary screening assay excluded large number of nonreactive samples, thus reducing the number of confirmatory RT-PCR and Western blotting assays, which were much more expensive and with long turnaround times for clinical reporting. There was a necessity of increasing the sensitivity of screening

assays to detect all infected samples. This increase in sensitivity was associated with increase in reactive assays that were considered as false reactive. RT-PCR was the most sensitive confirmatory test for quantitation of the plasma viral load (Ritcher, 2002). Sensitivity of western blot methods was lower than that of RT-PCR due to low anti-HCV antibody levels.

In this study, it was observed that RT-PCR plasma samples from patients with tissue damaging conditions showed interferences in the RT-PCR assay (Chapters 5, 6 and 7). These interferences were observed as PCR inhibition (decrease in fluorescence intensity of Internal control, eg. Heparin), increase in Cq value and when the viral load was low there was a possibility of a positive result becoming negative. These preanalytical influences became more prominent at low viral load, thus affecting RT-PCR reports. The number of reactive cases with third generation anti-HCV antibody enzyme immune assay showed larger number of reactive samples especially at low antibody levels. They were considered 'false reactive'.

This study analysed the distribution of anti-HCV antibody in the RT-PCR positive and negative samples after increasing the sensitivity of screening assay and RT-PCR. When screening assays with high seroconversion detection rates were used (Ortho Clinical Diagnostics, Procedure manual), a large number of samples with low anti-HCV reactive antibody levels (signal level <12) were detected. These lower levels of anti-HCV antibody were not detected with absorbance-based (colour-based) EIA.

A large majority of non-reactive anti-HCV antibody levels were found to be below 0.2 chemiluminescence signal (Fig. 8.1A). There were lesser number of samples with non-reactive antibody between 0.2 and 0.4. There was a very low and steady decrease in reactivity seen from 0.4 to 0.89. This low steady reactivity was considered as the cross-reactive antibody, which was the genuine false reactivity. Such cross-reactive antibodies were seen in autoimmune disorders or sometimes in tissue damaging conditions. These antibody levels may be considered as false reactive antibody levels. Therefore, the frequency of these antibody between 0.4 and 0.89 as compared to the total non-reactive anti-HCV antibody may give the frequency of false reactivity. This frequency value, 3.42% was used to calculate the possible percentage of false reactivity between reactive antibody levels between 1 and 15. The false reactive values obtained in this range was found to be very much

lower than the antibody reactive RT-PCR negative sample. This observation raised the suspicion, whether the RT-PCR negative samples were genuinely false reactive samples or were due to some other reason such as (a) occult infection or (b) assay done during HCV treatment or (c) due to early HCV infection during window period.

The distribution studies of reactive anti-HCV antibody levels showed two modes in the distribution at 1.08 and 28.7 (Fig. 8.1B). These two modes with the corresponding antibody distribution clusters were observed in the RT-PCR positive samples (Fig. 8.2A). But the RT-PCR negative HCV antibody reactive samples also showed a distribution which was bimodal and with two clusters (Fig. 8.2B). These results indicated that both RT-PCR positive and RT-PCR negative antibody levels were similar and the RT-PCR negative samples may be due to occult infection where the virus may be present in the liver but absent in circulation.

In both non-reactive and in the reactive range, the frequency distribution of samples were highest when the antibody levels were the lowest. The non-reactive antibody peak was between 0.00 and 0.09 and in the reactive range, antibody peak was in the borderline reactive range between 0.9and 0.99. these results indicate that in the non-reactive range between 0.4 and 0.89 there are higher levels of cross-reactive anti-HCV antibody which are genuinely false reactive (Table 8.3 and Fig. 8.4). Similarly, in the reactive range the frequency distribution decreases. But the decrease in frequency distribution in the reactive range is associated with a decrease in the ratio of RT-PCR negative by RT-PCR positive samples (Table 8.4). The high RT-PCR negative samples at lower antibody levels indicated that there may be larger number of occult HCV infection in the patients. This is because it was observed that the genuinely false reactive sample frequency was also decreasing with increase in chemiluminescence signal. These results indicated that at high antibody and at high viral load, the frequency of occult infections is low.

The Cq distribution of RT-PCR positive samples with lower reactive antibody cluster showed lower viral load with Cq between 35 and 40 (Fig. 8.5A). But the cluster with high antibody reactivity showed higher viral load with Cq between 23 and 33 (Fig. 8.5B). These results indicated that higher viral loads generally generate high antibody levels and also indicated that anti-HCV antibody was not protective against the disease.

8.7. CONCLUSIONS

Diagnosis of HCV infection was done by screening for anti-HCV antibody by the third-generation assay followed by HCV RT-PCR of samples reactive for anti-HCV antibody. RT-PCR assay was done after preanalytical control of samples to decrease non-specific influences, probably of nucleic acids and drugs, immediate isolation of RNA from EDTA-plasma. The reactive anti-HCV antibody concentrations were RT-PCR positive or RT-PCR negative. There were two distribution clusters for anti-HCV antibody, the lower antibody cluster was between 1.0 and 15.0 and the higher antibody cluster was between 15.0 and 42. Each of the two reactive antibody clusters in the antibody distribution of histogram were found to have both RT-PCR negative and positive samples. The RT-PCR negative anti-HCV antibody reactive samples may contain samples with occult HCV infection, genuinely false reactive samples and samples with preanalytical influences.

Fig. 8.1. Frequency histogram of the distribution in nonreactive (A) and reactive (B) samples with anti-HCV antibody signal levels between 0.00 – 0.89 (n = 1014) and between 0.90 – 42.1 (n = 534), respectively.

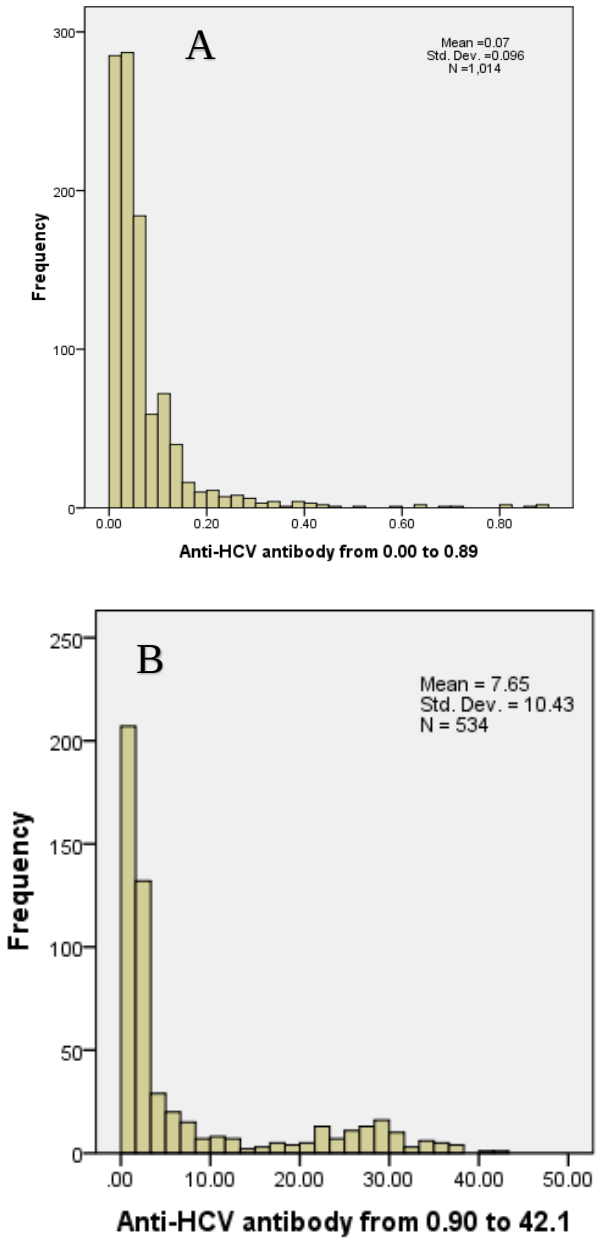

Table 8.1. Characteristics of the data from the non-reactive (n = 1014), borderline reactive (n = 28) and Total reactive samples (n = 534). Nonreactive and reactive samples were collected independent of each other. Total reactive samples included borderline reactive and reactive samples. Reactive samples may be RT-PCR (+ve) and RT-PCR (-ve). Similarly, borderline reactive samples may be RT-PCR (+ve) and (-ve) (Not shown here. Refer Table 8.2).

Sample characteristics	**Non-reactive, <0.89 (n = 1014)**	**Non-reactive, 0.40 – 0.89 (n = 17)**	**Total Reactive, ≥0.90 (n = 534)**	**Borderline reactive, 0.90 – 0.99 (n = 28)**	**Total Reactive (≥0.90) and RT-PCR (+ve) (n = 130)**	**Total Reactive (≥0.90) and RT-PCR(-ve) (n= 404)**
Mean±SD	0.07±0.096	0.62±0.18	7.65±10.42	0.95±0.03	15.45±12.91	5.15±8.04
95% CI mean	0.064 – 0.076	0.527 – 0.713	6.77 – 8.54	0.94 – 0.96	1.42 – 1.73	4.36 – 5.93
Median	0.04	0.63	2.07	0.94	4.82	1.76
Mode (visually detected)	0.02 (lowest mode)	---	1.08	0.94	1.02	1.08
Shapiro-Wilk test, P	<0.001	---	<0.001	---	<0.001	<0.001

Fig. 8.2. Histogram of the distribution of reactive anti-HCV antibody signal levels which were RT-PCR positive from 0.90 to 42.1 (n = 130) **(A)** and RT-PCR negative from 0.90 to 41.00 (n = 404) **(B).**

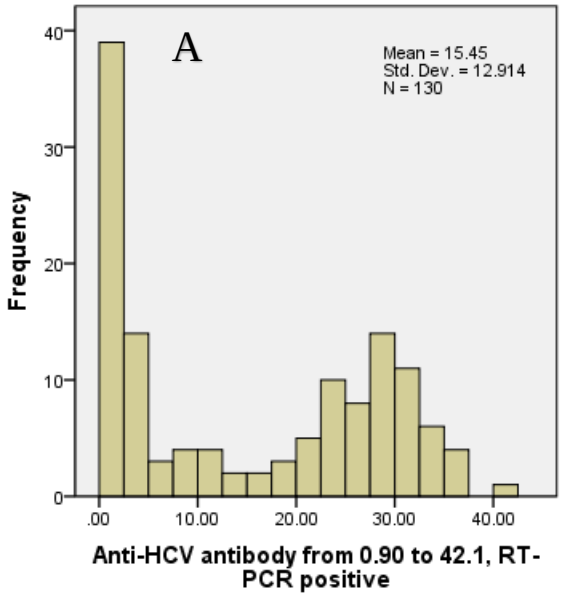

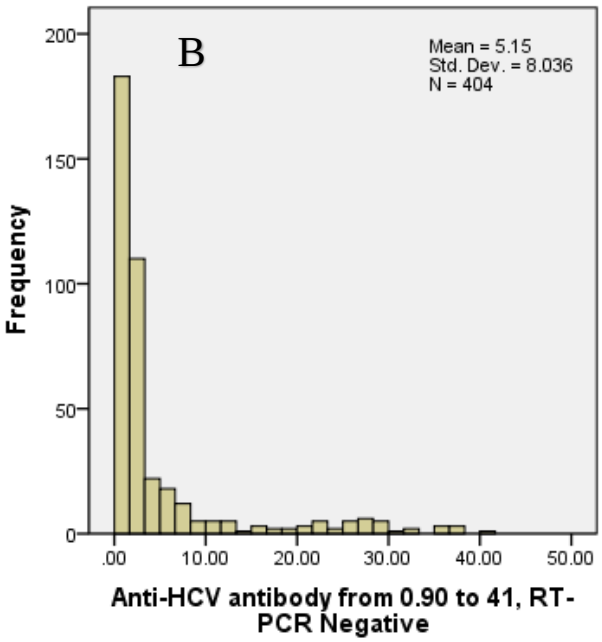

Fig. 8.3. Histogram of the distribution of reactive anti-HCV antibody signal levels from 0.40 to 16.00 (A and C) and from 16.0 to 42.1 (B and D) that were RT-PCR negative (A and B) or RT-PCR positive (C and D).

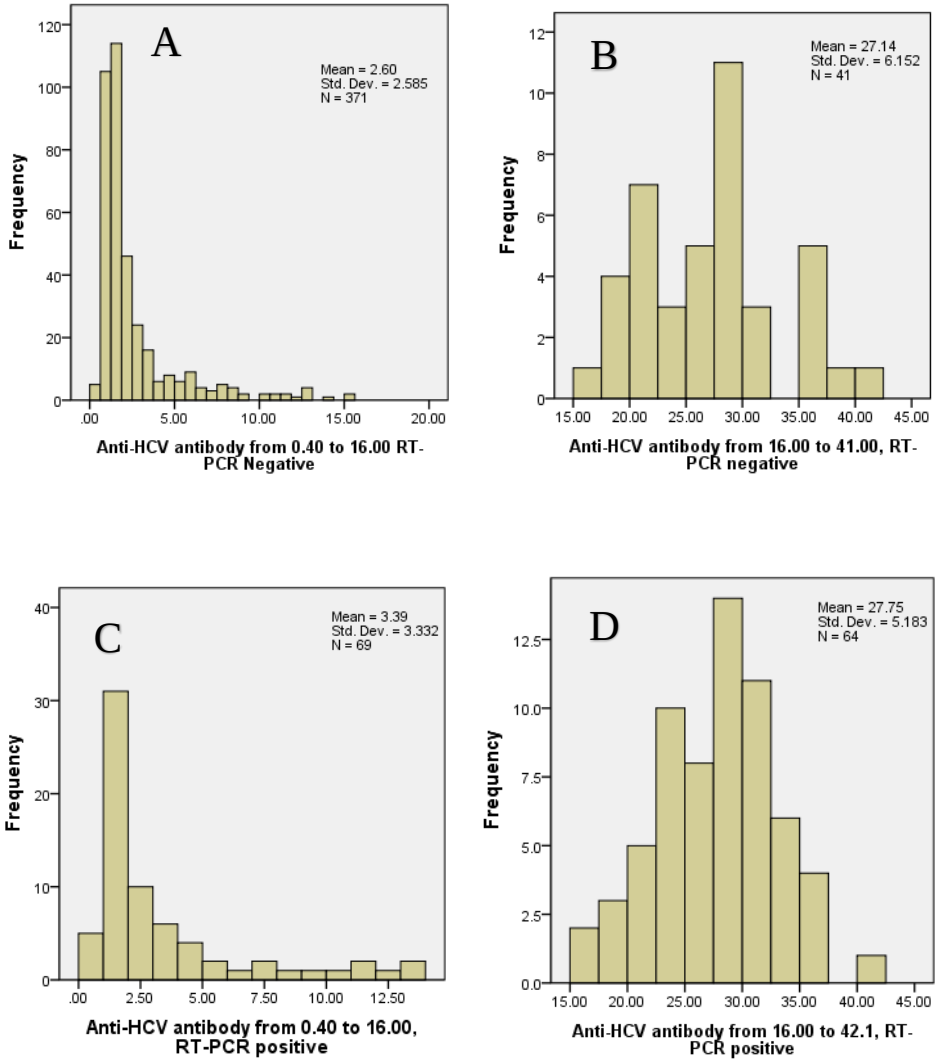

Table 8.2. Sample distribution (n) and the distribution frequency (N) at various anti-HCV antibody chemiluminescence signal levels in the nonreactive (A), borderline reactive (B) and the reactive ranges (C). Sample distribution was expressed as samples frequency / unit chemiluminescence signal range for the number of samples collected.

A. Nonreactive sample frequencies

Non-reactive 0.00 – 0.89 (n = 1014)			
0.00 – 0.39 (n = 997)	0.40 – 0.89 (n = 17)	0.40 - 0.64 (n = 10)	0.65 - 0.89 (n = 7)
N = 2556	N = 34.69	N = 41.67	N = 29.16

B. Borderline Reactive sample frequencies

Borderline Reactive 0.90 – 0.99 (n = 28)	
PCR (+ve) 0.90 – 0.99 (n = 2)	PCR (-ve) 0.90 – 0.99 (n = 26)
22.22	288.88

C. Reactive sample frequencies

Low reactive antibody (1.0 – 4.0) (n = 324)		**Intermediate reactive antibody (10 – 15) (n = 18)**		**High reactive antibody (15 – 42.1) (n = 107)**	
PCR (+ve) 1.00 - 4.0 (n = 47)	PCR (-ve) 1.00 - 4.0 (n = 277)	PCR (+ve) 10.0 - 15.0 (n = 6)	PCR (-ve) 10.0 - 15.0 (n = 12)	PCR (+ve) 15.0 - 42.1 (n = 64)	PCR (-ve) 15.0 - 41.00 (n = 43)
15.66	92.33	1.2	2.4	2.36	0.6

Table 8.3. Calculation of anti-HCV antibody reactivity per unit chemiluminescence signal (r) and frequency distribution of the sample per unit chemiluminescence signal.

Chemiluminescence signal range (c)	**Sample Number (n)**	**Reactive samples / chemiluminescence signal range (r), r = n/c**	**Frequency distribution, F = r / total sample number**
0.00 – 0.09	815	8150	8.04
0.1 – 0.19	138	1380	1.36
0.2 – 0.29	32	320	0.315
0.3 – 0.39	12	120	0.118
0.4 – 0.64	10	41.67	0.041
0.65 – 0.89	7	28	0.027
0.9 – 0.99	28	280	0.524
1 – 1.99	228	228	0.427
2 – 2.99	67	67	0.125
3 – 3.99	29	29	0.054
4 – 4.99	16	16	0.029
10 – 14.99	18	18	0.034

Fig. 8.4. Frequency distribution versus chemiluminescence signal range of Nonreactive samples, 0.2-0.29, 0.3-0.39, 0.4-0.64, 0.65-0.89 (A) and Reactive samples, 0.1.0-1.99 (2), 2.0-2.99 (3), 3-3.99 (4), 4.0-4.99 (5), 10.0-14.99 (6) (B).

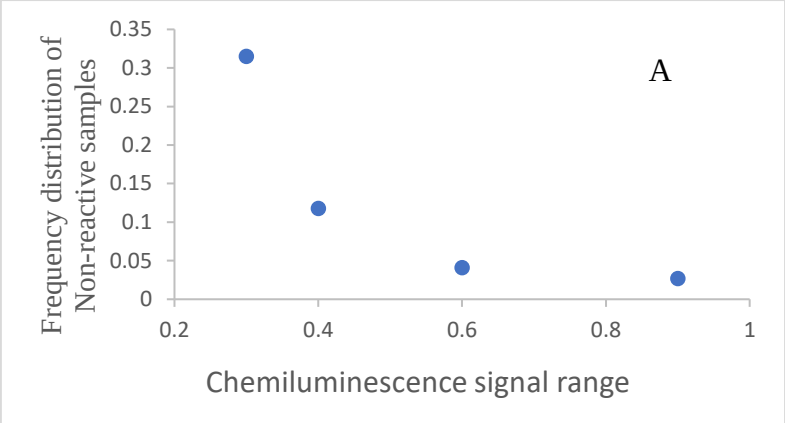

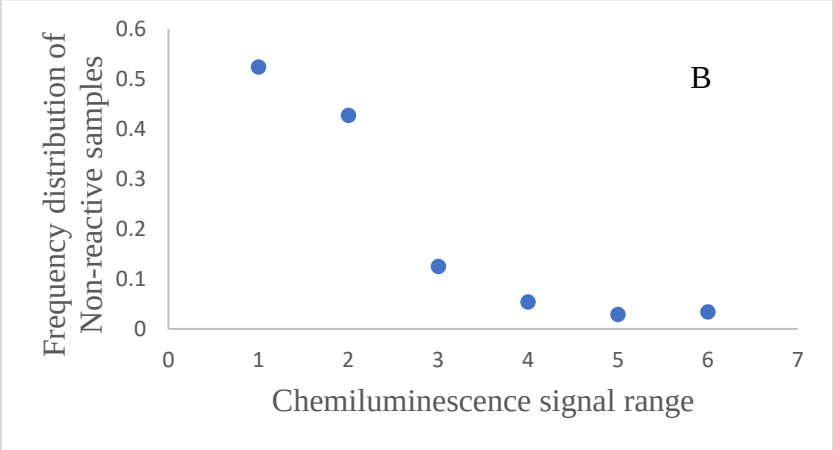

Table 8.4. Proportion of RT-PCR (-ve) / RT-PCR (+ve) at various ranges of anti-HCV antibody reactivity.

Anti-HCV antibody reactivity	RT-PCR (+ve)	RT-PCR (-ve)	Proportion RT-PCR (-ve) / RT-PCR (+ve)
0.90 – 0.99	2	26	13.00
1.00 – 4.00	47	277	5.89
10.00 – 15.00	6	12	2.00
15.00 – 42.1	43	64	0.672

Fig. 8.5. X-Y scatter of anti-HCV antibody levels versus Cq of HCV RT-PCR.

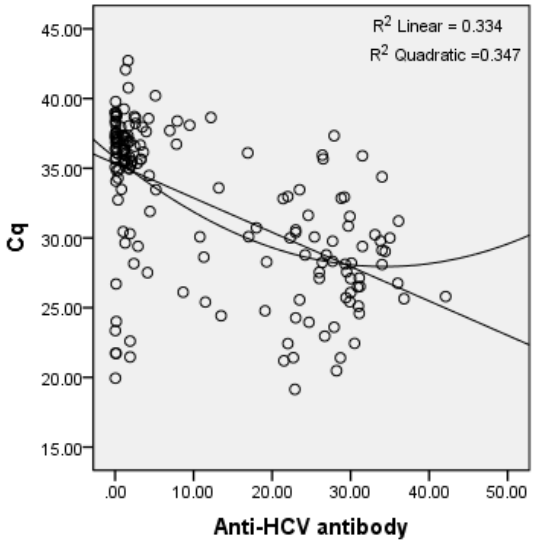

Fig. 8.6. Histogram of the distribution of Cq of samples with reactive anti-HCV antibody signal levels from 0.90 to 15.00 (A) and 15.00 to 42.1 (B).

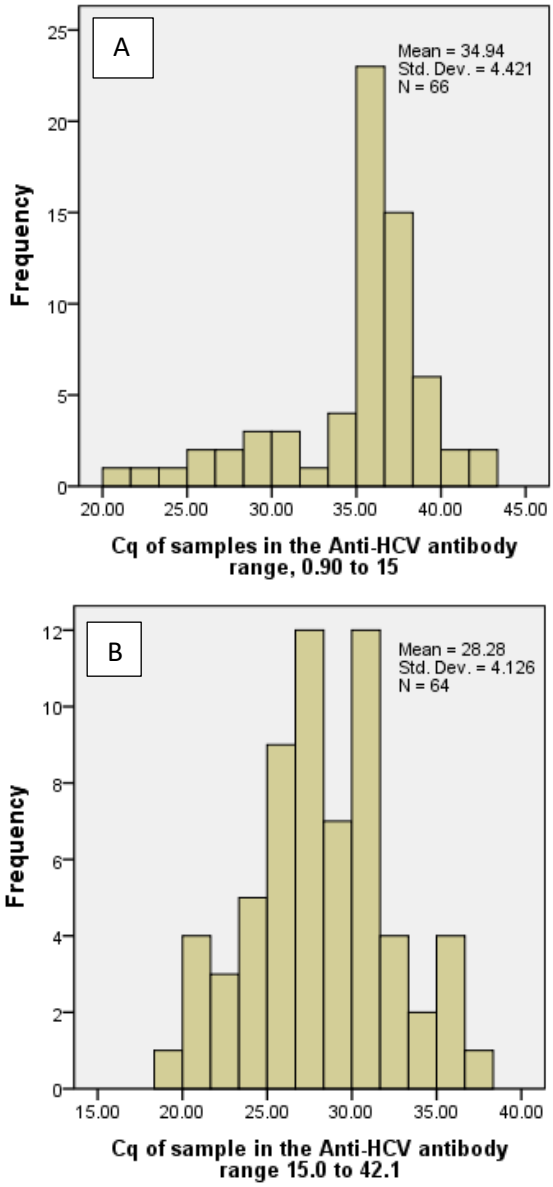

Table 8.5. Frequency of the distribution of RT-PCR positive samples at different anti-HCV antibody chemiluminescence signal ranges.

Anti-HCV antibody range	RT-PCR Positive	RT-PCR Negative	Total (n = 974)
0.00 – 0.89	41	399	440
0.4 - 0.89	3	11	14
0.9 – 0.99 (indeterminate)	2	26	28
1 – 15 (lower reactive range)	64	335	399
15 – 42.1 (higher reactive range)	64	43	107

Fig. 8.7. Histogram of the distribution of reactive anti-HCV antibody signal levels from 0.00 to 0.89, RT-PCR negative (A) and RT-PCR positive (B)

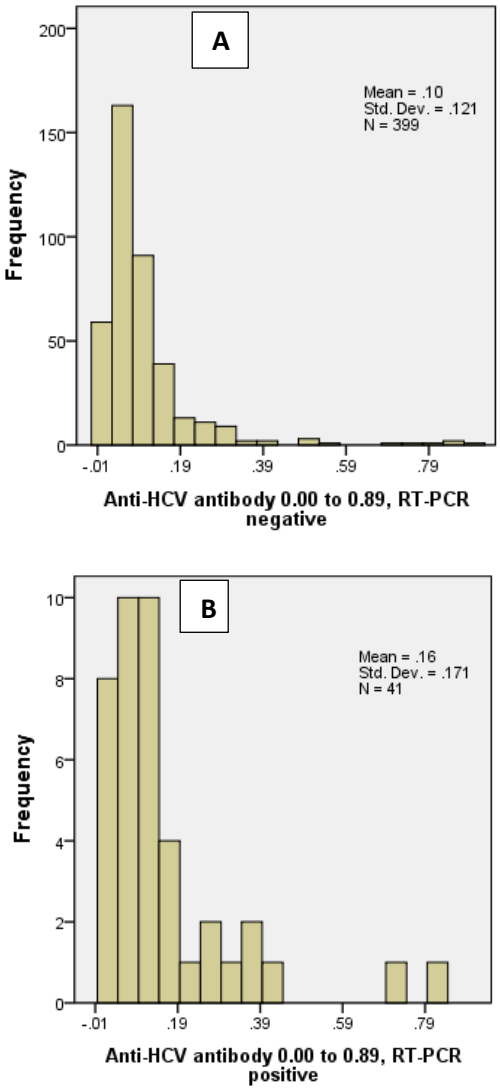

Chapter 9

Sequence and Phylogenetic data analysis of HCV Genotypes of 5'UTR, Core E1 and NS5B

9.1. ABSTRACT

The **5'UTR region** is a highly conserved, 341 bp region with secondary RNA structure that has functional importance. **Graphic representation of 24 sequences** of this region showed >200 alignment score with reference sequence, and percent identity from 96 to 100% for genotype 1. Similar data was obtained for **genotype 3**, with percent identity from 95.57 to 99.57. The major genotypes identified were 1 and 3, and the positions showing nucleotide differences were also studied. There were highly conserved regions of 5'UTR with low entropy, and these sites were used for designing primers that were used for diagnostic purposes. The secondary structure of (5'UTR) showed several sites of stacking interactions between successive base pairs, and predicted energetically most stable structure.

Similar **sequence data analysis** was also done with **Core E1 region**. Six different sequences of **genotype 1** of Core E1 region were submitted to NCBI database and were found to have alignment score >200 and percent identity between 94.59 and 95.46. Due to lack of specific highly conserved sites, primer designing for both CE1 and NS5B were found to be more difficult and less productive. There was one sequence with **genotype 3a** with alignment score >200 and percent identity of 91.53. There were five sequences of core E1 matched with **genotype 3b** with alignment score >200 and percent identity 87.75 to 89.29. One sequence showed >200 alignment score with **genotype 4** with percent identity of 91.67.

Epitope prediction was done for **Core E1** using software (a) Bepipred Linear Epitope Prediction and (b) Kolaskar and Tongaonkar Antigenicity Predicted peptides. B-cell epitopes were used by the former and physicochemical properties were used for the latter. The secondary structure of core E1 were also analysed.

Similar analysis was done with **NS5B** but the PCR product and the data obtained were much less than the other two regions due to larger variations distributed in the NS5B region. There were only **two PCR products** amplified using various primers designed for NS5B. The secondary structure of core E1 and the possible three-dimensional tertiary distribution of the secondary structures were also analysed.

Phylogenetic tree was constructed using reference sequence from the seven genotypes of 5'UTR. These reference sequences were aligned and compared with

the HCV sequences submitted to NCBI from this study. Phylogenetic trees were also constructed for core E1 and NS5B regions with the different reference sequences from NCBI database.

9.2. INTRODUCTION

The high genetic diversity of Hepatitis C Virus (HCV) led to the genotype and subtype classification. HCV also showed varied geographical prevalence. There were seven major genotypes (GTs), the complete genomes of which differ from each other by at least 30% at the nucleotide level (Simmonds P et al, 2005; Smith DB et al, 2014; Murphy et al, 2015; Bukh et al, 1993). The global prevalence of hepatitis C is estimated to be 3% with 12.5 million people in India alone infected with the virus (Roy et al, 2019). Genotype 1 is the most prevalent worldwide (46%) and predominates in Europe, North America, and Australia. It is followed by GT3 (30%), which is primarily distributed in South Asia, particularly the Indian subcontinent (Gower at al, 2014). The estimated prevalence of HCV infection in India is approximately 0.5%–2.0%, with GT3 being most common (Panigrahi et al, 1997; Das et al, 2002). Despite the low prevalence of HCV, India with its large population accounts for a significant proportion of the global HCV burden with approximately 12–18 million people infected. Significant variability in prevalence has been described across Indian geographical regions (Sievert et al, 2011). Investigations on HCV have been conducted mainly through the isolation and sequencing of the virus from infected patients. From the sequence data, it was possible to gather information about the evolution of the virus, variability across geographic locations, and correlations between viral variation and disease progression.

Free energy minimization is an established criteria in computational structural biology which is based on the assumption that, during the equilibrium state, molecular folding problem is unique, and that the molecule folds into the minimum free energy state. It is applicable in RNA folding, protein folding and transmembrane helix packing (Zuker, 1989; Abagyan 1993 and Pappu et al. 1999). There are efficient algorithms for computing the minimum free energy (MFE) structure and other suboptimal structures (Zuker and Stiegler 1981) that are based on free energy parameters. The centroid structures has the minimum total base-pair

distance to the structures in the set. Thus, the centroid structure can be considered as the single structure that best represents the central tendency of the set.

Phylogenetic analysis is important in rapidly changing species like viruses. The purpose of phylogenetic analysis of nucleic acid sequences is to analyse and understand the relationship among group of sequences. Phylogenetic analysis has been used to distinguish viral genotypes and/or subtypes from each other, and for subtyping newly isolated strains by comparing them to existing alignments and trees. However, phylogenetic analysis often cannot distinguish between inter-subtype recombinants and new subtypes, as both can branch out between clusters in a similar way. To reveal the mosaic organization of recombinant viruses, new methods that process the genotype in segments along a sequence were designed (Siepel et al, 1995; Salminen et al, 1995; Lole et al, 1999). These methods rely upon multiple alignments of a query sequence and the reference sequences of known viral subtypes. However, the high variability of viral genomes often makes it impossible to align viral sequences automatically. In these cases, the alignments have to be done laboriously and manually.

When there is a strong sequence similarity between the sequences parsimony or maximum likelihood methods are used. But when there is only a clearly recognizable sequence similarity distance methods are used to construct the phylogenetic tree. In this study, due to a moderate variability between sequences the distance methods were chosen.

Of the numerous phylogenetic distance-based reconstruction methods, two algorithms most often used in population genetics, unweighted pair group mean analysis (UPGMA) and neighbour-joining (Saitou and Nei, 1987) algorithms. UPGMA is one of the most widely used and simplest method of topological reconstruction that assumes a molecular clock which takes into consideration, the rate of change along the branches of the tree and produces a rooted tree. NJ method is one of the minimum evolution methods (Cavalli-Sforza and Edwards, 1967) where the tree with the smallest sum of branch lengths is found and produces a branched tree.

9.3. OBJECTIVES

1. Establishment of the methods for evaluation by data analysis, test validation, quality control and clinical state of the patient for Molecular Diagnostic reporting of Hepatitis C infection.

2. Use of these procedures for confirmatory diagnosis of hepatitis C infection, its plasma viral count determination and genotyping.

9.3.1. Aspects of the original objectives addressed in this chapter

The aspects were sequence data analysis from the first objective and genotyping from the second objective.

9.4. MATERIALS AND METHODS

9.4.1. Sample Collection for RT-PCR:

When screening assays showed anti-HCV antibody levels above cut off limit, **Quantitative RT-PCR was done for confirming the diagnosis of HCV infection**. 4 ml of EDTA blood sample was taken from the patient using EDTA-vacutainers, centrifuged and plasma sample, without hemolysis, jaundice, cloudiness and without clot formation was used for RNA isolation. In the later part of the study preanalytical variables were also taken into consideration before collecting samples for HCV RT-PCR. Plasma and RNA samples were stored immediately at -20^{o}C and -80^{0}C, respectively, in aliquots. Refer Details 4.3.2

9.4.2. Calculation of viral load in plasma

Calculation of plasma viral load from Cq obtained by real time RT-PCR of HCV infected plasma sample, and converted to concentration of the template from the calibration plot.

$$\text{Viral load (IU/ml of plasma)} = \frac{(\text{Patients' result Cq as IU/µl from calibration plot}) \times \text{Elution Volume (60 µl)}}{\text{Sample Volume (0.14 ml)}}$$

Refer Details 4.11.5.

9.4.3. RNA Isolation

HCV viral RNA Isolation was done from 140 µl plasma processed with a QIAamp Viral RNA Mini Kit (QIAGEN, USA) according to manufacturer's

instructions and eluted in 60 µl Elution Buffer. Eluted RNA was stored at -20°C. Refer Details 4.6.

9.4.4. RT-PCR of HCV

Each assay or a set of assays were done in Triplicates, with test sample or several (patients') sample, a standard with a known template concentration (or calibrator) and a non-template control or NTC without template (blank sample). RT PCR was done using Artus HCV RG RT-PCR kit (Qiagen, Germany) based on Taqman probes by One step RT-PCR on Rotor-Gene Q instrument. Master mix is prepared from Hep. C Virus Master A (12 µl) and Hep. C Virus Master B (18 µl) with internal control (2 µl). Add 30 µl of this mix into PCR tube and 20 µl of eluted sample RNA, quantitation standards and Non template control. The cycling conditions were entered as 50°C for 30 minutes when the reverse transcription took place, 95°C for 15 minutes for initial denaturation, 95°C for 30s, 50°C for 60 s and 72°C for 30s repeated for 50 cycles. Fluorescence was measured at annealing step of each cycle.

9.4.5. HCV sequence database and PCR Primer design

Good primer design is one of the major parameters in a Polymerase Chain Reaction. In Real Time PCR the amplicon length should be 50-150 bp in length. Primer should be in the length of 18-24 nucleotides. Primers designed should be specific and be free of internal secondary structures. Compatible annealing temperatures in primer pairs, approximately 50% GC and GC rich 3'end enhances the annealing. For primer designing, primer design software programs such as Oligoperfect designer, Primer Express software or Primer 3 software may be used.

Appropriately validated primers are important in determining the specificity, sensitivity and robustness of a PCR reaction. Primers were synthesised from the conserved region of HCV. The 5' untranslated region (5'UTR) of HCV is the most conserved region. That is the reason for selecting 5'UTR as target by commercial RNA detection kits. The 5'-UTR contains many stem and loop structures. Primer selection is done mainly from the stem part and try to avoid loop structures. The sequences near the 5' end of the 5'-UTR are susceptible to cleavage by 5'-3' exonucleases. 5'UTR sequences of Genotypes 1-7 were aligned and primer was selected from the conserved region. Because the base-pairing structures of the 5'-

UTR might open at increasing temperatures. For validation of qualitative PCR primers were synthesised for 3 regions - UTR, Core/E1 and NS5B.

9.4.6. Amplification of 5'UTR, Core E1 and NS5B

Amplification of HCV RNA sequences by reverse transcription and cDNA Polymerase chain reaction. HCV RNA isolation and Reverse transcription to make cDNA is done using Thermo Verso cDNA synthesis kit at 45^0C for 30 min in Thermal cycler (Applied Biosystem, Veriti model). The pair of primers should hybridise to the sequence and amplify the NS5B region. The primers should correspond to the site in NS5B region. The phylogenetic analysis was done with all the amplified NS5B sequences by the pairs of primers with known NS5B sequences.

9.4.7. DNA sequencing and Sequence analysis

The specific amplified PCR products of 5'UTR, Core E1 and NS5B is sent for sequencing using Sangers method at Aggregenome sequencing Cochin. Chromatograms are checked for the sharpness of peak using FinchTV and analysed for mutation and heterogeneity. The genotype was determined by analysing the sequences using Bioedit and after submitting the sequences at NCBI for BLASTn.

9.4.8. Gel electrophoresis

The amplified viral nucleic acid sample was mixed with loading buffer and loaded on Agarose gel (1.5%) stained with Ethidium bromide. This was added to respective wells, PCR product is electrophoresed at 100V for 30-60 minutes and viewed on gel documentation. Agarose gel was prepared with 1X TAE buffer. The amplified PCR product was analysed by gel electrophoresis, migration is dependent on the size of the PCR product.

9.4.9. NCBI database

BLASTn (Nucleotide BLAST) is used to compare one or more nucleotide query sequences to a reference nucleotide sequence or a database of similar nucleotide sequences. This helps to determine the evolutionary relationships among different organisms.

BLASTx (translated nucleotide sequence searched against protein sequences) compares nucleotide query sequence (first translated to six reading frames that gives six protein sequences) against a database of protein sequences.

tBLASTn (protein sequence searched against translated nucleotide sequences) is used to compare protein query sequence against the six-frame translations nucleotide sequences database. tBLASTn is beneficial for finding homologous protein coding regions in unannotated nucleotide sequences.

BLASTp (Protein BLAST) compares one or more protein query sequences to a subject protein sequence or a database of protein sequences. It is useful in identification of a protein sequence.

Maximum Score is the highest alignment score calculated from the scores provided for matched nucleotides and penalties for mismatches and gaps. **Total Score** is the sum of alignment scores of all segments from the reference sequence. **Query Cover [age] is** the percent of the query length that is covered in the aligned sequences. The **alignment score** has been calculated from the percent identity and the total alignment sequence.

Expect Value is the number of alignments expected by chance with the calculated score. The expect value is a default sorting metric for significant alignments. The E value should be very close to zero. **Identity** is the highest percent identity for a set of aligned segments to the reference sequence.

Accession number is the unique identifier assigned to records in the NCBI databases. **Accession Length** is the number of nucleotides or amino acids in the result sequence identified by the accession number.

Entropy, a thermodynamic quantity representing the unavailability of a system's thermal energy for conversion into mechanical work, often interpreted as the degree of disorder or randomness in the system. In nucleotide sequences, it is a measure of probability of positional homology, lower the entropy higher is the homology.

9.4.10. Hepatitis C Virus Genome Sequencing

Hepatitis C virus RNA was isolated from 140 µL plasma using the QIAamp MinElute Virus spin kit (QIAGEN, Hilden, Germany), and sequencing was performed at AgriGenome Labs, Cochin, Kerala (ABI3730XL, Sanger sequencing). In brief, RNA was reverse transcribed using verso cDNA synthesis kit (Thermoscientific) and amplified using Go Taq, G2 Hot start colourless master mix (Promega). Double-stranded deoxyribonucleic acid was generated and amplified according to the manufacturer’s instructions, with minor modifications. The primers were designed for UTR, Core-E1 and NS5B regions. The amplified PCR

product was sent for Sanger sequencing. The chromatogram of the sequencing result was analysed using Finch TV and BioEdit was used to align the sequence with the reference sequences of respective Genotypes.

9.4.11. Entropy plot

Entropy Plot for 5'UTR region of HCV genotype 1 and genotype 3 calculated and plotted using the Entropy plot tool of BioEdit. It is a measure of probability of positional homology. The entropy in sequence analysis is the measure of the variation of nucleotides in multiple sequences. Entropy plot constructed through multiple sequence alignment, predicted using different types of entropy formulas, namely Shannon's Entropy, Schneider's Entropy, Shenkin's Entropy, Gerstein's Entropy, and Gap normalized Entropy. Prediction of entropy plot consists of two steps: (i) performing multiple sequence alignment and consensus, and (ii) calculation of entropy number for each column through consensus of multiple sequence alignment. The entropy plot is generated by plotting vertical lines in the order of the consensus sequence on the x-axis, and the entropy number on the y-axis.

MEGA software is used for multiple sequence alignment and phylogeny analysis of sequence data. MEGA supports sequence alignment using both the ClustalW and MUSCLE programs. Alignment is done in the Analysis Explorer. With our sequences in the Alignment Explorer, select Alignment from the menu, then do either ClustalW or Muscle. The alignment parameters were set to the values of our requirement. Click Compute/OK.

9.4.12. BepiPred-2.0: Sequential B-Cell Epitope Predictor

The BepiPred-2.0 online tool predicts B-cell epitopes from a protein sequence, using a Random Forest algorithm trained on epitopes and non-epitope amino acids determined from crystal structures. A sequential prediction is performed after that. The residues with scores above the threshold (default value is 0.5) are predicted to be part of an epitope and coloured in yellow on the graph and marked with "E" in the output table. The E values (E) of the scores are not affected by the selected threshold (Jespersen et al, 2017).

This is a semi-empirical method which makes use of physicochemical properties of amino acid residues and their frequencies of occurrence in experimentally known segmental epitopes was developed to predict antigenic

determinants on proteins. Application of this method to a large number of proteins proposed that this method can predict antigenic determinants with about 75% accuracy which is better than most of the other known methods.

9.4.13. Phylogenetic Analysis

The analysis was performed on the Phylogeny.fr platform and sequences were aligned with MUSCLE configured for highest accuracy, after alignment, ambiguous regions (i.e. containing gaps and/or poorly aligned) were removed with Gblocks. The phylogenetic tree was reconstructed using the Maximum Likelihood method implemented in the PhyML program and graphically represented and edited. Finally, the phylogenetic tree was constructed with TreeDyn.

9.5. RESULTS

A. 5'UTR Sequence Data Analysis

9.5.1. General sequence data analysis of HCV Genotype 1 and Genotype 3 5'UTR sequence with query sequences

Sequence data analysis of genomic DNA was important in understanding the significance of various sequences in the gene and their variations. 5'UTR region, a highly conserved site, was also untranslated. The 341 bp sequence, therefore, will have regions that have biological significance, the most important being the intramolecular secondary structures formed from it. Being conserved it was also highly useful for diagnosis of HCV infection. The primers used to perform the diagnostic assay and their nested primers have PCR products of 272 bp and 256 bp, respectively (Fig. 9.1 and Table 9.1). The RT-PCR product of these primers had been subjected to electrophoresis and the size of bands confirm the PCR product (Fig. 9.2). This PCR product has also been used for sequencing.

Graphical representation of the sequences studied and their alignment scores were represented for understanding the query coverage length. The query coverage length was often shortened due to truncated ends of the PCR products which have been the result of low HCV plasma viral load. Most of the sequences had alignment score >200. The alignment score has been calculated from the percentage identity and the total alignment sequence of 272 bp (Fig. 9.3 and Table 9.2). In Table 9.2, the truncated end of sequences had been represented by the accession length and percent query coverage. The percent identity showed the total

alignments for the given accession length. **Maximum Score** is the highest alignment score calculated from the scores provided for matched nucleotides and penalties for mismatches and gaps. **Total Score** was the sum of alignment scores of all segments from the reference sequence.

The relationship of the viral load with anti-HCV antibody levels in Genotype 1 and 3 were studied. When the antibody concentrations were below 0.9, the patients might be from the exposure group such as dialysis or repeated transfusion cases. When the antibody concentrations were increasing from 1 to 36 in genotype 1, the viral load increased (Cq decreased) (Table 9.3). Similar results were also obtained for Genotype 3.

Similar graphic analysis and sequence data analysis were done with query sequence as Genotype 3 (Fig. 9.4 and Table 9.4).

9.5.2. Specific sequence data analysis of HCV Genotype 1 and Genotype 3 sequence with query sequences

Certain genotype characteristics were shared between genotype 1 and genotype 3. Total number of positions for differentiating genotype 1 and genotype 3 in the 5'UTR region was about 13. The dominant characteristic features that are shared with genotypes are given preference in genotyping (Table 9.5). The position numbers 97, 179, 183, 224 and 249 clearly differentiates between Genotype 1 and 3. Sample with Accession number MW970030 was found to have nucleotide positions that overlaps with Genotype 1 and Genotype 3 at positions 175, 220, 243, 247. Sample with accession number MW281562 also overlaps with Genotype 1 and Genotype 3 T position 243.

Just as there are variations between genotypes, there are also conserved regions that are shared between genotype 1 and genotype 3. There were three major conserved regions seen at positions 130 - 175, 185 – 203 and 227 – 245, all with average entropy near to 0.01. The low entropy also indicates large base pairing and sharing of nucleotide sequences (Table 9.6).

Entropy Plot for 5'UTR region of HCV GT1 and GT3 calculated and plotted using the Entropy plot tool of BioEdit using Shannon's entropy formula. It is a measure of probability of positional homology. The entropy in sequence analysis is the measure of the variation of nucleotides in multiple sequences. Entropy plot constructed using multiple sequence alignment predicted sites of low entropy and

high probability of base pairing. There were three such sites demonstrated in Fig. 9.5 which were also found to align with three conserved region sequences.

Free energy minimisation was used to predict the structure of 5'UTR region. This structure prediction gains importance as there are three conserved regions that are resistant to mutation. During the prediction of structure, the molecule forms intramolecular base pairing to form folds that have minimum free energy state. The algorithm used for prediction of the secondary structure involve the free energy minimisation criteria and the centroid secondary structure prediction method.

In comparison with the minimum free energy (MFE) structure using diverse types of structural RNAs, the centroid of the ensemble makes 30.0% fewer prediction errors as measured by the positive predictive value (PPV) with marginally improved sensitivity. Both methods have been used to predict secondary structure of 5'UTR region of the reference sequence of genotype 1 and are given in Fig 9.6A and B. the same methods were also used to predict the secondary structure of genotype sequence submitted to NCBI (Fig. 6C and D). the similarity of the sequence submitted between Fig. 9.6A and C were much better than between B and D. therefore, the method of free energy minimisation in this case may predict the sequences in a more consistent manner between 5'UTR sequences.

B. Core E1 sequence data analysis

9.5.3. General sequence data analysis of Genotype 1 and Genotype 3 Core E1 region of HCV genome with query sequences

There were 6 HCV Core E1 sequences that were compared using BLAST at NCBI site. The total length of the PCR product was 480 bp but most sequences had truncated ends as seen by the accession length and percentage of query coverage. The percent identity with the reference sequence was also high between 94.59 and 95.46 (Fig. 9.7 and Table 9.7). These 6 sequences belong to genotype 1 of HCV Core E1 region.

Of the two BLAST hits of genotype 3a, data for only one sequence was obtained. The alignment of core E1 sequence to the NCBI reference sequence had a percent identity of 91.53 indicating a larger variation with reference sequence (Fig.

9.8 and Table 9.8). The accession length and was 472 bp and the query coverage was 95%.

There were five Core E1 sequences submitted to NCBI with genotype 3 and subtype 3b. the five BLAST hits showed >200 alignment score and some sequences had truncated ends. The general sequence data analysis showed of the five sequences, four had accession length above 400bp and one had 265bp. All the five sequences had percent identity between 87.75 and 89.29. The percent query coverage of 53 % with the sequence with low accession length (Fig. 9.9 and Table 9.9).

There was one core E1 sequence submitted to NCBI with truncated ends and had an alignment score >200. The BLAST hit reported genotype 4 and the accession length was 408 with a lower percent query coverage of 82%. The percent identity was low at 91.67, indicating certain amount of variability or mutation (Fig. 9.10 and Table 9.10).

Comparison of anti-HCV antibody responses with viral load and/or Cq and genotypes (Table 9.11). There were 6 samples with genotype 1 and 5 samples with genotype 3b. There were high and low levels antibody, viral load or Cq in both the genotypes. There was no grouping of levels of antibody with levels of viral load or Cq.

C. Core E1 amino acid sequence data analysis

9.5.4. Core E1 amino acid sequence for epitope, antigenicity and secondary structure prediction

Amino acid sequence data analysis of Core E1 of HCV was used for epitope and antigenicity prediction. The genotype 1 with subtype 1a was selected. The sequence showed high identity of 96.86% to the reference sequence. The stretch of amino acid that are likely to be antigenic epitopes were defined using the software Bepipred linear epitope prediction (Table 9.12A). The software used was Bepipred Linear Epitope Prediction (A) and Kolaskar and Tongaonkar Antigenicity Predicted peptides (B). B-cell epitopes were used by the former and physicochemical properties were used for the latter (Table 9.12B). The stretch of most of the amino acids that are antigenic varied from 9-11 in four cases and two stretches were of short amino acid sequence of four and five. The antigenic epitopes contained very

few amino acids with non-polar side chains but contained large number of amino acids with either polar acidic or basic side chains. Glycine which is known to distort or bend the structure is shown colorless.

The antigenic epitopes generated by Bepipred Linear Epitope Prediction had more number of polar and charged groups (Table 9.12A). The antigenic structure predicted by Kolaskar and Tongaonkar Antigenicity Predicted peptides had more non polar amino acids in their sequence (Table 9.12B).

There were no β sheets demonstrated in the structure. Each anti-paralell βsheet is separated by a β turn. But the number of amino acids in β turn is also very small (Fig. 9.11). the extended strand structures are not interrupted by β turn. Also the extended structures are all unidirectional, also indicating the absence of formation of β sheets from extended structures.

The percentage of secondary structure in the BLAST hit sequence were α helix, extended strand, β turn and random coil were 35.85, 20.75, 9.43 and 33.96%, respectively (Table 9.13). The sequence that falls in the secondary structure were marked in Fig. 9.11. The blue colored α helical region were often flanked by random coil (purple) and extended strand (red). The predicted amino acid mutation and their sites were identified and shown in Table 9.14.

Epitope and antigenicity predicted peptides using the software Bepipred linear epitope prediction of Core E1 sequences, GT3a with MK843925 accession number (Table 9.15A) and Kolaskar and Tongaonkar Antigenicity Predicted peptides (Table 9.15B). The stretch of most of the amino acids that are antigenic varied from 9-23 in three cases and one was a single amino acid. The antigenic epitopes generated by Bepipred Linear Epitope Prediction had more number of polar and charged groups (Table 9.15A). The antigenic structure predicted by Kolaskar and Tongaonkar Antigenicity Predicted peptides had more non polar amino acids in their sequence (Table 9.15B).

The percentage of secondary structure in the BLAST hit sequence were α helix, extended strand, β turn and random coil were 35.26, 21.15, 5.13 and 38.46%, respectively (Table 9.16). The sequence that falls in the secondary structure were marked in Fig. 9.12. The blue colored α helical region were often flanked by random coil (purple) and extended strand (red). Beta sheets were not identified in

the sequence data analysis. The predicted amino acid mutation and their sites are shown in Table 9.17.

Epitope and antigenicity predicted peptides of Core E1 sequences, Genotype 3b with MW970044 accession number, which showed maximum identity of 92.90 % to the reference sequence (Table 9.18A) and Kolaskar and Tongaonkar Antigenicity Predicted peptides (Table 9.18B). The stretch of most of the amino acids that are antigenic varied from 7-13 in all four cases. The antigenic epitopes generated by Bepipred Linear Epitope Prediction had more number of polar and charged groups (Table 9.18A). The antigenic structure predicted by Kolaskar and Tongaonkar Antigenicity Predicted peptides had more non polar amino acids in their sequence (Table 9.18B). The percentage of secondary structure in the BLAST hit sequence were α helix, extended strand, β turn and random coil were 38.06, 21.94, 4.52 and 35.48%, respectively (Table 9.19). The sequence that falls in the secondary structure were marked in Fig. 9.13A and B using SOPMA and Phyre2 web portal. The blue colored α helical region were often flanked by random coil (purple) and extended strand (red). The predicted amino acid mutation and their sites are shown in Table 9.20.

Epitope and antigenicity predicted peptides of Core E1 sequences, GT4d with MW970042 accession number using the software Bepipred linear epitope prediction (Table 9.21A) and Kolaskar and Tongaonkar Antigenicity Predicted peptides (Table 9.21B). The antigenic epitopes generated by Bepipred Linear Epitope Prediction had more number of polar and charged groups (Table 9.21A). The antigenic structure predicted by Kolaskar and Tongaonkar Antigenicity Predicted peptides had more non polar amino acids in their sequence (Table 9.21B). The stretch of most of the amino acids that are antigenic varied from 11-15 in three cases and short stretches of 1-3-amino acids. The percentage of secondary structure in the BLAST hit sequence were α helix, extended strand, β turn and random coil were 24.26, 29.41, 4.41 and 41.91%, respectively (Table 9.22). The sequence that falls in the secondary structure were marked in Fig. 9.14A using SOPMA. The predicted amino acid mutation and their sites are shown in Table 9.23.

D. NS5B sequence data analysis

9.5.6. Sequence data analysis of HCV Genotype 1 NS5B sequence with query sequences

NS5B sequence was found to be difficult for designing primer and to amplify gene sequence for sequencing. These problems arose probably due to the low percent identity resulting from more frequent mutations and less conserved regions. NS5B has also been found to be an epitope for third generation anti-HCV antibody enzyme immune assays. These third-generation assays increase the sensitivity of reactive antibody detection by detecting large number of low levels pf antibodies. Therefore, the samples obtained were only two in number (Fig. 9.15). The percent identity with the reference sequence was also high between 96.23 and 97.7 (Table 9.24). Comparison of anti-HCV antibody with Viral load and Cq of NS5B sequences (Table 9.25).

Epitope and antigenicity predicted peptides of NS5B sequences, Genotype1 with MW281563 accession number using the software Bepipred linear epitope prediction (Table 9.26A) and Kolaskar and Tongaonkar Antigenicity Predicted peptides (Table 9.26B). The stretch of most of the amino acids that are antigenic varied from 8-12 in all four cases. The percentage of secondary structure in the BLAST hit sequence were α helix, extended strand, β turn and random coil of MW281563 were 37.97, 18.99, 7.59 and 35.44% and of MW970050 are 31.51, 17.81, 2.74, and 47.95% respectively (Table 9.27). Domain analysis of Secondary structure prediction of NS5B, Genotype 1a with MW281563 accession number using **Phyre2 web portal** was done in Fig. 9.16A and PDB formatted model of Secondary structure prediction of NS5B, Genotype 1a with MW281563 using Phyre2 web portal in Fig. 9.16B.

Epitope and antigenicity predicted peptides of NS5B sequences, Genotype1 with MW970050 accession number using the software Bepipred linear epitope prediction (Table 9.28A) and Kolaskar and Tongaonkar Antigenicity Predicted peptides (Table 9.28B). The stretch of most of the amino acids that are antigenic varied from 7-12 in all cases. Domain analysis of Secondary structure prediction of NS5B, Genotype 1a with MW970050 accession number using **Phyre2 web portal** was done in Fig. 9.17A and PDB formatted model of Secondary structure prediction of NS5B, Genotype 1a with MW281563 using

Phyre2 web portal in Fig. 9.17B. The predicted amino acid mutation and their sites are shown in Table 9.28.

E. Attempts at predicting the tertiary structure and antigenic epitopes

5.5.7. Protein data bank (PDB) structure of NS5B protein

The region was amplified and translated (amino acid from 141 – 220, Blue) using RCSB PDB tool. From the total NS5B region sequence of 141-220 amino acids, antigenicity predicted regions were 158-170, 175-187 and 202-207 (Fig. 9.18).

This was done as a preliminary attempt to predict antigenic sites. It is extremely difficult to predict tertiary structure of protein as it has contributions from the three-dimensional (3-D) locations and properties of the secondary structure. The 3-D structure should include a polar exterior, non-polar interior and correct 3-D location of the interior salt bridges. These data require crystallographic and protein solution structure data analysis. Therefore, this was an exercise and an attempt to approximately locate the antigenic sites using RCSB PDB software and secondary structure data (Fig. 9.18).

F. Construction of phylogenetic tree

9.5.8. Phylogeny

Phylogenetic tree constructed using the 5'UTR region with data that were available from our study. There were two major branches for genotype 1 and genotype 3. Other genotypes, 2, 4, 5, 6 and 7 are also demonstrated using reference sequences. Three clusters with sequence variation, of these two were major clusters and a single sequence did not align with either genotype 1 or 3 (Fig. 9.19). The following phylogenetic data of 5'UTR region of HCV genome were analysed for Genotype 1 (Red, 11 sequences from this study) and Genotype 3 (Blue, 7 sequences from this study). The reference sequences from NCBI were shown in black.

Phylogenetic tree was constructed using the sequences generated from Core E1 region (Fig. 9.20). Genotypes 1, 3 and 4 from our laboratory are demonstrated. Other genotypes represented are from reference sequences obtained from database.

The phylogenetic data analysis of Core E1 region of HCV genome was done. References sequences for all genotypes (Black) along with Genotype 1 (Red, 7 sequences), Genotype 3a (purple, 1 sequences), Genotype3b (Blue, 5 sequences) and Genotype 4 (Green, 1 sequence) were demonstrated.

Phylogenetic tree was constructed using the sequences generated from NS5B region (Fig. 9.21). Two sequences of genotype 1 obtained by us were demonstrated. The phylogenetic data analysis of NS5B region of HCV genome with two Genotype 1 sequences marked Blue, were done.

9.6. DISCUSSION

There are three major regions of HCV genome, 5'UTR, Core E1 and NS5B, that are structurally and functionally significant. Of the three sites, 5'UTR or the untranslated region was examined for secondary RNA structures using the software RNAfold. in both the reference sequences and in sequences from this study. These secondary RNA structures, with varying stem- loop regions, generate specificity for the 5'UTR functions. Most of the structural proteins were expressed from the Core, E1 and E2 regions. The Core E1 and NS5B were both analysed for nucleic acid sequence and amino acid sequences.

Being highly conserved, the primers designed for the 5'UTR region, generated a large number of PCR products. In this study, there were 24 sequences generated from genotype 1 and genotype 3 of the 5'UTR regions. They had very high 'percent identity' of 92.43 to 99.57 indicating their conserved nature. Despite this large percent identity, it was possible to identify and differentiate genotypes 1 and 3 from this set of 24 sequences (Table 9.5).

There were thirteen sequences generated by primers designed for the Core E1 region. From these thirteen nucleotide sequences of the Core E1 region, it was possible to identify six sequences of genotype 1, one of genotype 3a, five of genotype 3b and one of genotype 4.

Being translated, the Core E1 and NS5B region were also analysed for their amino acid sequences. The amino acid sequences were used for predicting antigenic epitopes by Bepipred linear epitope prediction and antigenicity prediction by Kolasker and Tongaonkar antigenicity prediction methods. The antigenicity prediction by latter method showed more non polar amino acids than by the former

method (Tables 9.12A & B, 9.15A & B, 9.18A & B, 9.21A & B, 9.26A & B, 9.28A & B). The amino acid sequence also showed large percentage of α helical regions followed by extended strand structures or β strands. There were no β sheets, thus resulting in the low percentage of β turn. As expected, there were high percentage of random coils were high for all the sequences predicted (% of secondary structures are in Tables following the above Tables for antigenicity).

There were only two PCR products generated by the primers used to amplify NS5B region. This indicates the variability in this functional protein sequence. The functional protein generated from this region if RNA dependent RNA Polymerase. There were long extended structures in the amino terminal region (blue) (Fig. 9.16B, 17B). the amino terminus also showed a tendency for anti-parallel β strand structure which was seen in both the sequences studied. The carboxy terminal (red) of one sequence had a longer extended structure.

Tertiary structure prediction requires a large database of the secondary structure, detail mapping of polarity-non polarity of amino acids and the location of various internal structure such as salt bridges. The latter data may be available from crystallography database. Therefore, this study might be taken as a preliminary study and an exercise to predict three-dimensional structures and use it to demonstrate the antigenic sites. The predicted antigenic epitopes fall in the α helical regions.

Genotype 3 was found to have higher prevalence in South Asia and India, in our study there were large number of genotype 1 (14 numbers) and genotype 3 (10 numbers) in the 5'UTR region. Similarly, in the Core E1 region there were six sequences from genotype 1, five sequences from genotype 3b and one each from genotype 3a and 4d. Both the sequence from the NS5B region were assigned genotype 1. In the rooted phylogenetic trees constructed (Fig. 9.19, 9.20, 9.21), all the above sequences were found to be aligning correctly with the corresponding genotypes described earlier (Tables 9.5, 9.14, 9.20, 9.23, 9.29).

Final Decision criteria for differentiation quantitative and qualitative real time RT-PCR. Data from the fluorescence amplification plots by (a) visual observation, (b) calibration plots, (c) four-parameter data from SigmaStat, (d) log fluorescence intensity from LinRegPCR and (e) validation of PCR product by sequence analysis (Table 9.30).

9.8. CONCLUSIONS

There were seven major genotypes (GTs), the complete genomes of which differ from each other by at least 30% at the nucleotide level. Genotype 1 is the most prevalent worldwide (46%) and predominates in Europe, North America, and Australia. It is followed by GT3 (30%), which is primarily distributed in South Asia, particularly the Indian subcontinent. GT3 is the most common genotype in India followed by GT1.

The major genotypes identified in this study were 1 and 3. The **5'UTR region** was highly conserved, 341 bp region with secondary RNA structure that has functional importance. **Graphic representation of 24 sequences of genotype 1** of 5'UTR showed >200 alignment score with reference sequence, and percent identity from 96 to 100% for genotype 1. Similar data was obtained for **genotype 3**, with percent identity from 95.57 to 99.57. There were highly conserved regions of 5'UTR with low entropy, and these sites were used for designing primers that were used for diagnostic purposes. The secondary RNA structure of (5'UTR) showed several sites of stacking interactions between successive base pairs, and predicted energetically most stable structure.

Similar **sequence data analysis** was also done with **Core E1 region**. Six different sequences of **genotype 1** of Core E1 region were submitted to NCBI database and were found to have alignment score >200 and percent identity between 94.59 and 95.46. Due to lack of specific highly conserved sites, primer designing for both CE1 and NS5B were found to be more difficult and less productive. There was one sequence with **genotype 3a** with alignment score >200 and percent identity of 91.53. There were five sequences of core E1 matched with **genotype 3b** with alignment score >200 and percent identity 87.75 to 89.29. One sequence showed >200 alignment score with **genotype 4** with percent identity of 91.67.

Epitope prediction was done for **Core E1** using software (a) Bepipred Linear Epitope Prediction and (b) Kolaskar and Tongaonkar Antigenicity Predicted peptides. B-cell epitopes were used by the former and physicochemical properties were used for the latter. The secondary structure of core E1 were also analysed.

Similar analysis was done with **NS5B** but the PCR product and the data obtained were much less than the other two regions due to larger variations distributed in the NS5B region. There were only **two PCR products** amplified using various primers designed for NS5B. The **secondary structure of NS5B and the possible three-dimensional tertiary distribution** of the secondary structures were also analysed.

Phylogenetic tree was constructed using reference sequence from the **seven genotypes of 5'UTR**. These reference sequences were aligned and compared with the HCV sequences that we had submitted to NCBI from this study.

Phylogenetic tree construction was also done for **Core E1 and NS5B** regions with our sequences and the reference sequences from NCBI database.

9.5.1. 5'UTR Sequence Data Analysis

Fig. 9.1. Sequence data analysis of 341 bp 5'UTR region of HCV reference sequence (Accession NC_004102, Genotype 1). The external (yellow-ended) and nested (green-ended) primers are highlighted.

5'GCCAGCCCCCTGATGGGGGCGACACTCCACCATGAATCACTCCCCTGTGAGGAACTA
CTGTCTTCACGCAGAAAGCGTCTAGCCATGGCGTTAGTATGAGTGTCGTGCAGCCTCCA
GGACCCCCCCTCCCGGGAGAGCCATAGTGGTCTGCGGAACCGGTGAGTACACCGGAAT
TGCCAGGACGACCGGGTCCTTTCTTGGATAAACCCGCTCAATGCCTGGAGATTTGGGCG
TGCCCCCGCAAGACTGCTAGCCGAGTAGTGTTGGGTCGCGAAAGGCCTTGTGGTACTGC
CTGATAGGGTGCTTGCGAGTGCCCCGGGAGGTCTCGTAGACCGTGCACC-3'

Table 9.1. Table showing the list of primers used to amplify the 5'UTR region of Hepatitis C virus genome as in Fig. 9.1.

Primers	Primer sequences synthesised (5' – 3')	Nucleotide position 5' to 3'	PCR product size
External Sense Forward Primer	ACTGTCTTCACGCAGAAAGCGTCTAGCCAT	-285 to -256, Tm- 64.3	272 bp
External Sense Reverse Primer	GGGTGCTTGCGAGTGCCCCGGGAGGTCTCG	-14 t o -43 Tm-72.9	
Nested Sense Forward Primer	ACGCAGAAAGCGTCTAGCCATGGCGTTAGT	-276 - -247	256 bp
Nested Sense Reverse Primer	CCTGATAGGGTGCTTGCGAGTGCCCCGGGA	-21 - -50	

Fig. 9.2. Agarose gel electrophoresis of PCR amplification of 5'UTR region with external primers (lane 2) and internal primers (lane 3). Lane 1 is the 100 bp DNA ladder

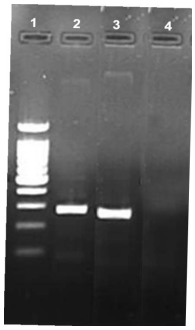

Fig. 9.2. 5'UTR Amplification using External and Nested Primers
Lane 1: 100 bp DNA Ladder
Lane 2: Amplification with External Primer (272 bp)
Lane 3: Amplification with Nested Primer (256 bp)
ane 4 NTC

Fig. 9.3. Graphic summary of 5'UTR sequences submitted at NCBI database, BLAST with **Reference Sequence NC_004102 (Genotype 1).** Truncated ends of some PCR products in the lower part of the figure indicate the errors in sequencing by Sanger's method due to low HCV plasma viral load of pure PCR products. The alignment score has been calculated from the percent identity and the total alignment sequence of 272 bp.

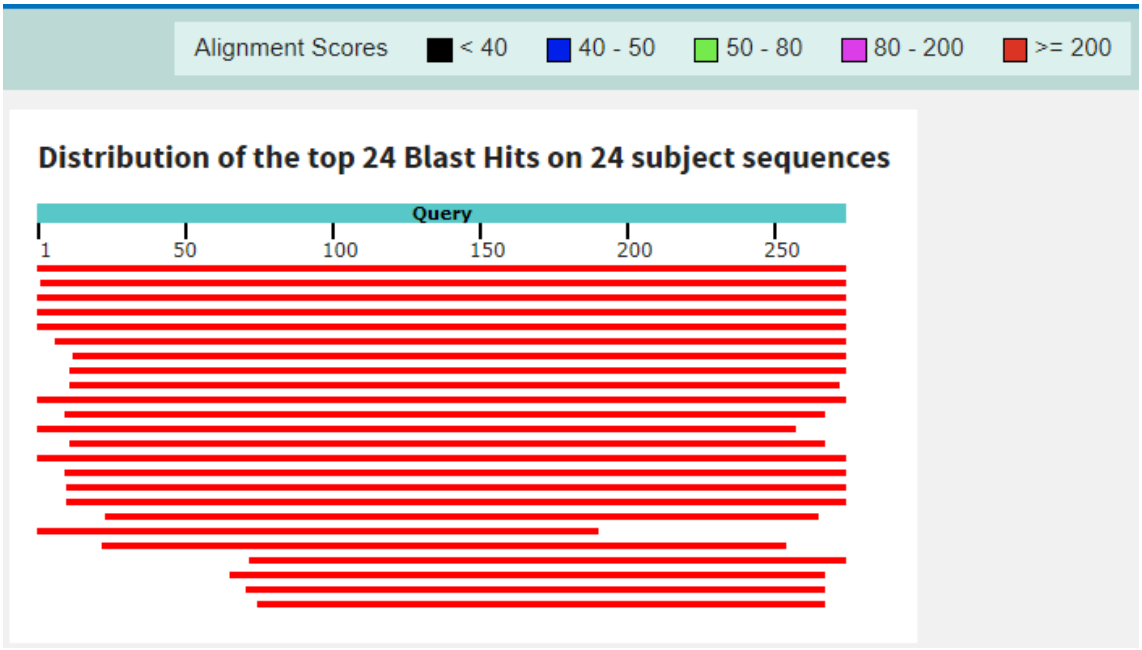

Table 9.2. Description of the alignment of 5'UTR sequences submitted at NCBI database nBLAST (nucleotide BLAST) done with Reference Sequence NC_004102 (Genotype 1). Query sequence is the sequence submitted to NCBI with BLAST. Query Cover(age): the percent of the query length that is included in the aligned segments. **Max**imum **Score:** the highest alignment score calculated from the matched nucleotides and penalties for mismatches and gaps. **Total Score:** the sum of alignment scores of all segments from the same subject sequence. **Query Cover**age: the percent of the query length that is included in the aligned segments. **Ident**ity: the highest percent identity for a set of aligned segments to the same subject sequence. **Acc**ession **Len**gth: the number of nucleotides in the result sequence identified by the accession number.

Serial No.	Description (Accession number)	Max. Score	Total Score	Query Cover	Per. Ident	Acc. Len
1.	MW970038.1	505	505	80%	100	273
2.	MW970033.1	501	501	79%	100	271
3.	MK843928.1	481	481	76%	100	261
4.	MK561494.1	350	350	55%	100	190
5.	MW970034.1	499	499	80%	99.63	273
6.	MW970031.1	499	499	80%	99.63	274
7.	MK133357.1	499	499	80%	99.63	276
8.	MW281560.1	486	486	78%	99.62	266
9.	MW281562.1	477	477	76%	99.62	261
10.	MW970040.1	473	473	75%	99.61	259
11.	MW970039.1	468	468	75%	99.61	256
12.	MT258412.1	468	468	75%	99.61	256
13.	MW281561.1	464	464	74%	99.61	254
14.	MW970030.1	472	472	80%	97.8	273
15.	MW970036.1	440	440	80%	95.62	274
16.	MW970041.1	420	420	77%	95.44	263
17.	MW970032.1	412	412	76%	95.04	262
18.	KX424960.1	377	377	70%	95	240
19.	MW970037.1	407	407	76%	94.66	262
20.	MW970035.1	311	311	58%	94.53	201
21.	KX455812.1	292	292	56%	94.24	192
22.	KX455813.1	303	303	58%	94	200
23.	KX455811.1	294	294	57%	93.85	196
24.	MK625193.1	337	337	67%	93.04	231

Table 9.3. Description of Anti HCV antibody, viral load and Cq of 5'UTR sequences amplified and submitted at NCBI database. Plasma viral load from the calibration plot could be validated upto 1 IU/µl, below 1 IU/µl the quantitation was not valid, therefore, it is represented as Cq.

NCBI Acc. No.	Anti-HCV Ab	Viral load (IU/µl)	Cq	Genotype
MW970030	0.03	0	38.99	1
MW281562	0.06	112468	20.07	1
MW281561	0.31	1	36.85	1
MW281560	1.26	1	35.5	1
MW970039	2.54	0	38.91	1
MT258412	3.96	0	37.63	1
MW970038	4.13	1367	27	1
MK561494	10.8	22	30.08	1
MK133357	28.2	72038	20.48	1
MW970031	30	1325	26.08	1
MW970040	30.9	2522	26.48	1
MW970034	31.2	1753	26.52	1
MK843928	33.8	337	29.78	1
MW970033	36.1	108	31.21	1
MW970035	1.11	1	36.37	3
KX455811	1.28	643	29.64	3
MW970037	6.96	0	37.7	3
MW970036	7.29	0	37.89	3
KX455813	16.9	1	36.1	3
KX424960	26.8	14,929	28.78	3
KX455812	29	6005	24.28	3
MW970041	30	1102	27.09	3
MK843929	34	414	29.34	3
MK625193	34	414	29.12	3
MW970032	36.8	3437	25.64	3

Fig. 9.4. Graphic summary of 5'UTR sequences submitted at NCBI database, BLAST with **Reference Sequence NC_009824 (Genotype 3).** The alignment score has been calculated from the percent identity and the total alignment sequence of 272 bp.

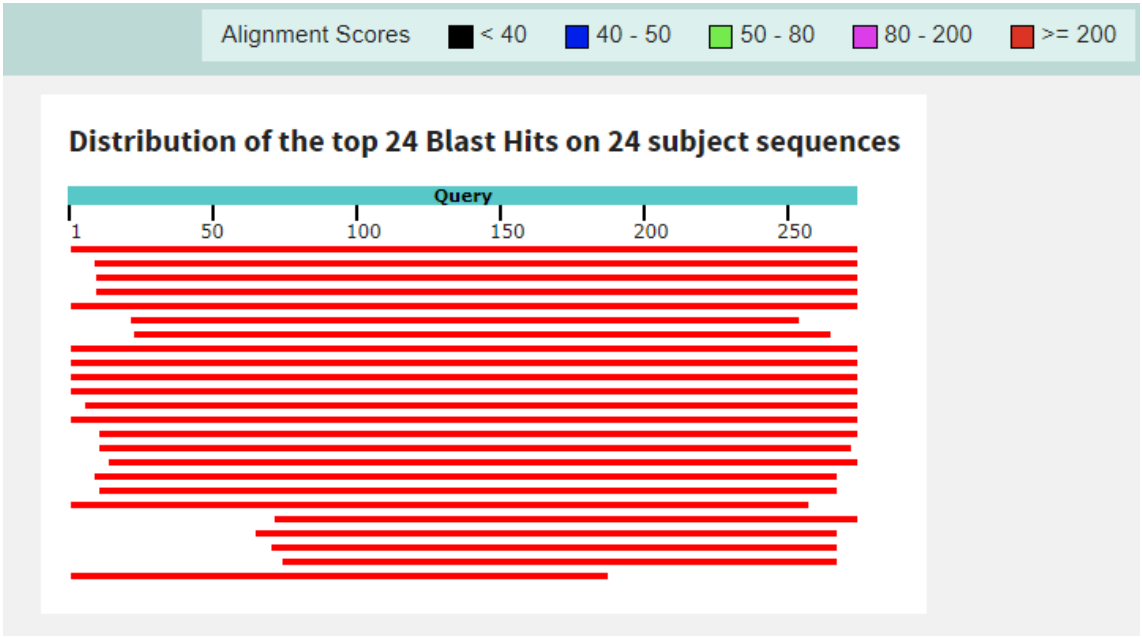

Table 9.4. Description of the alignment of 5'UTR sequences submitted at NCBI database nBLAST (nucleotide BLAST) done with Reference Sequence of Genotype 3, NC_009824. Details of the data are given in Table 9.2.

Serial No.	Description	Max Score	Total Score	Query Cover	Per. ident	Acc. Len
1.	MK625193.1	420	420	84%	99.57	231
2.	KX424960	416	416	88%	97.92	240
3.	MW970035.1	344	344	73%	97.51	201
4.	MW970036.1	462	462	99%	97.42	272
5.	KX455812.1	326	326	70%	97.38	192
6.	MW970041.1	448	448	96%	97.34	263
7.	MW970037.1	446	446	96%	97.33	262
8.	KX455813.1	337	337	73%	97	200
9.	MW970032.1	440	440	96%	96.95	262
10.	KX455811	327	327	71%	96.92	196
11.	MW970030.1	435	435	99%	95.57	272
12.	MW970034.1	407	407	99%	93.73	272
13.	MW970031.1	407	407	99%	93.73	272
14.	MW281560.1	398	398	97%	93.61	266
15.	MW281562.1	388	388	95%	93.49	261
16.	MW970040.1	385	385	95%	93.44	259
17.	MK843928.1	383	383	94%	93.41	260
18.	MW970038.1	401	401	99%	93.36	272
19.	MW970033.1	401	401	99%	93.36	271
20.	MW970039.1	379	379	94%	93.36	256
21.	MW281561.1	375	375	93%	93.31	254
22.	MT258412.1	375	375	93%	93.31	255
23.	MK133357.1	396	396	99%	92.99	272
24.	MK561494.1	265	265	68%	92.43	189

Table 9.5. Table with 5'UTR sequences of HCV showing nucleotide changes in various positions.

	Positions showing Nucleotide difference																	
	97	119	165	175	178	179	182	183	203	204	217	220	221	224	243	247	248	249
Genotype 1																		
NC_004102	T	A	A	T	C	A	A	C	T	A	G	T	G	G	A	C	T	G
MT258412	.	.	.	.	.	.	.	.	.	C	.	.	.	.	.	.	.	.
MW970039	.	.	.	.	.	.	.	.	.	C	.	.	.	.	.	.	.	.
MW281561	.	.	.	.	.	.	.	.	.	C	.	.	.	.	.	.	.	.
MW281560	.	.	.	.	.	.	.	.	.	C	.	.	.	.	.	.	.	.
MW970034	.	.	.	.	.	.	.	.	.	C	.	.	.	.	.	.	.	.
MW970031	.	.	.	.	.	.	.	.	.	C	.	.	.	.	.	.	.	.
MW970038	.	.	.	.	.	.	.	.	.	.	.	.	.	.	.	.	.	.
MK561494	.	.	.	.	.	.	.	.	.	.	.	.	.	.	.	.	.	.
MW970040	.	.	.	.	.	.	.	.	.	.	.	.	.	.	.	.	C	.
MW970033	.	.	.	.	.	.	.	.	.	.	.	.	.	.	.	.	.	.
MK133357	.	.	.	.	.	.	.	.	.	.	.	.	.	.	.	.	.	.
MK843928	.	.	.	.	.	.	.	.	.	.	.	.	.	.	.	.	.	.
MW281562	.	.	.	.	.	.	.	.	.	.	.	.	.	.	G	.	.	.
MW970030				C	.	.	.	.	.	.	.	C	.	.	G	T	C	.
Genotype 3																		
NC009824	C	.	·	C	T	G	G	T	G	C	A	C	A	A	G	T	C	A
MK625193	C	.	·	C	T	G	G	T	.	C	A	C	A	A	G	T	C	A
KX424960	C	.	·	C	T	G	.	T	.	C	.	C	.	A	G	T	C	A
KX455812	C	.	·	C	.	G	.	T	.	C	.	C	.	A	G	T	C	A
MW970035	C	.	·	C	.	G	.	T	.	C	.	C	.	A	G	T	C	A
MW970037	C	C	·	C	.	G	.	T	.	C	.	C	.	A	G	T	C	A
KX455811	C	.	T	C	.	G	.	T	G	T	.	C	.	A	G	T	C	A
KX455813	C	.	T	C	.	G	.	T	G	T	.	C	.	A	G	T	C	A
MW970032	C	C	·	C	.	G	.	T	.	C	.	C	.	A	G	T	C	A
MW970041	C	.	·	C	.	G	.	T	.	C	.	C	.	A	G	T	C	A
MW970036	C	.	·	C	.	G	.	T	.	C	.	C	.	A	G	T	C	A

Table 9.6. Conserved regions of 5'UTR identified

Sl. No.	Conserved region	Average entropy
1	130 CCGGGAGAGCCATAGTGGTCTGCGGAACCGGTGAGTACACCGGAAT 175	0.0077
2	185 GACCGGGTCCTTTCTTGGA 203	0.0118
3	227 ATTTGGGCGTGCCCCCGC 245	0.0118

Fig. 9.5. Entropy Plot for 5'UTR region of HCV Genotype 1 and Genotype 3, **Entropy Plot** for 5'UTR region of HCV GT1 and GT3 calculated and plotted using the Entropy plot tool of BioEdit using Shannon's entropy formula. It is a measure of probability of positional homology. The entropy in sequence analysis is the measure of the variation of nucleotides in multiple sequences.

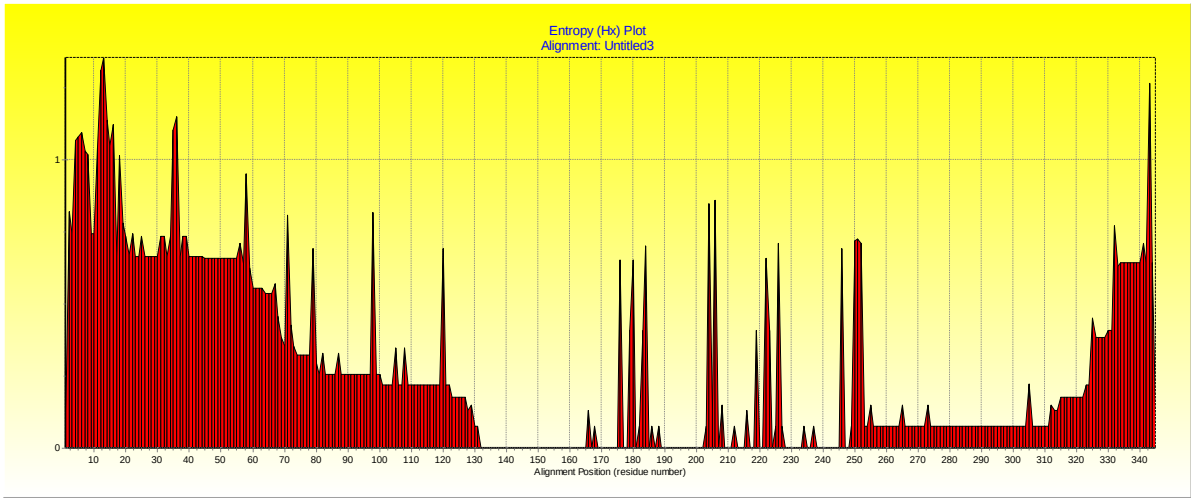

Fig. 9.6. Minimum Free Energy (MFE) secondary structure and centroid secondary structure of Reference Sequence of 5'UTR (NC_004102) (A and B) and HCV 5'UTR sequence submitted to NCBI (MW970038) (C and D) using **RNA*fold* webserver**.

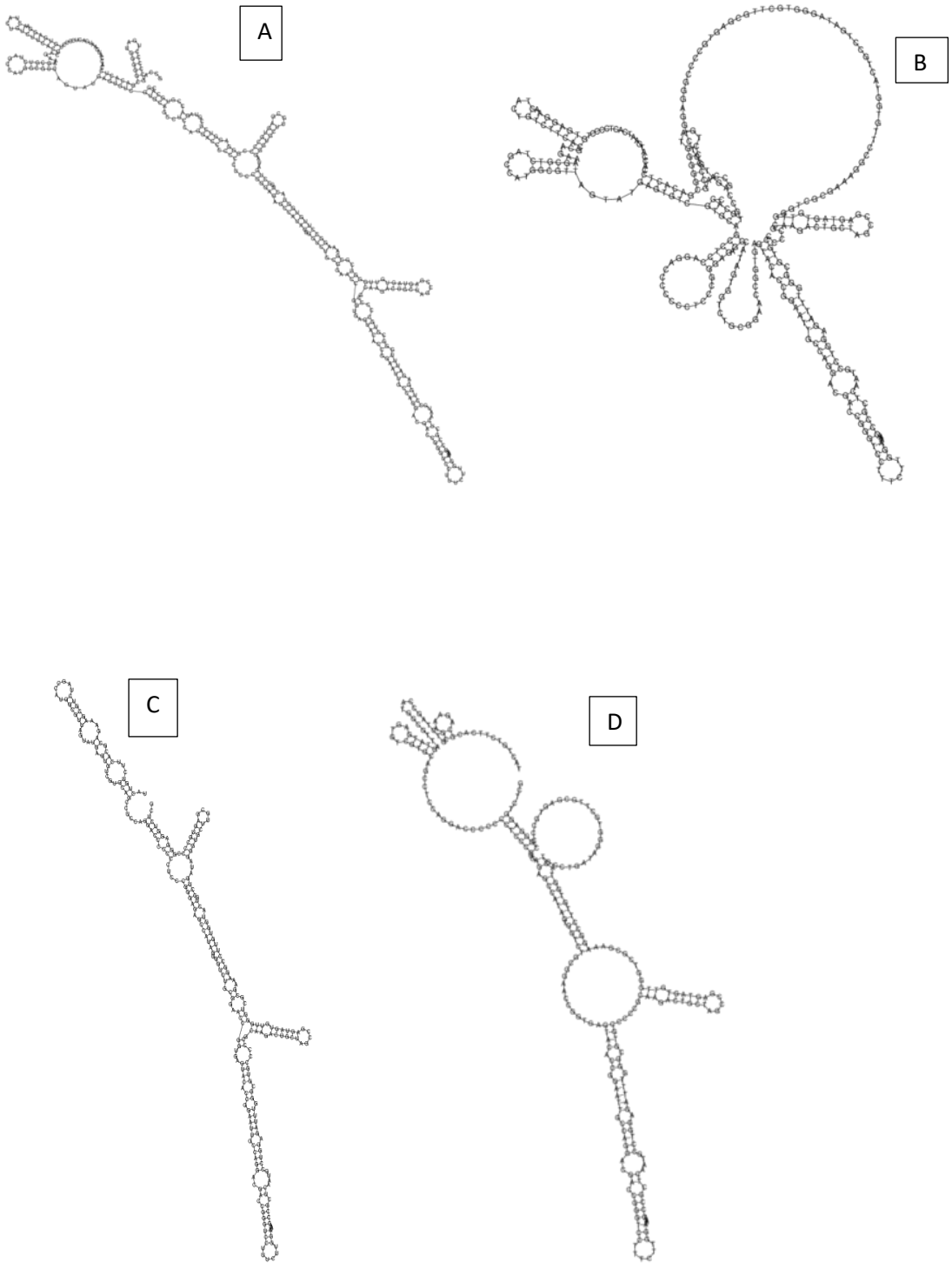

9.5.2. Core E1 sequence data analysis

Fig. 9.7. Graphic summary of Core E1 sequences submitted at NCBI database, BLAST with Reference Sequence NC_004102 (Genotype 1)

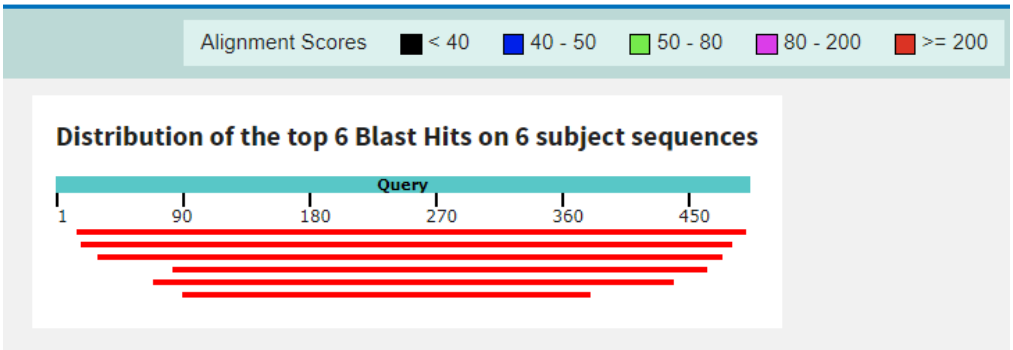

Table 9.7. Description of the alignment of Core E1 sequences submitted at NCBI database BLAST done with Reference Sequence NC_004102 (Genotype 1).

Accession No.	Max Score	Total Score	Query Cover	Per. ident	Acc. Len
MK133356	739	739	93%	95.46	463
MK561495	758	758	96%	95.38	477
MK843926	459	459	58%	95.17	290
MW970047	586	586	75%	95.15	371
MK843927	597	597	76%	95	381
MW970045	688	688	89%	94.59	444

Fig. 9.8. Graphic summary of Core E1 sequences submitted at NCBI database, BLAST with Reference Sequence **NC_009824 (Genotype 3a)**

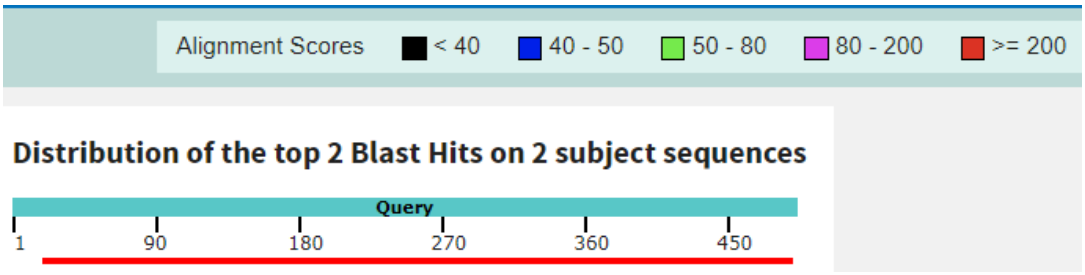

Table 9.8. Description of the alignment of Core E1 sequences submitted at NCBI database BLAST done with Reference Sequence **NC_009824 (Genotype 3a).**

Accession No.	Max Score	Total Score	Query Cover	Per. ident	Acc. Len
MK843925	651	651	95%	91.53	472

Fig. 9.9. Graphic summary of Core E1 sequences submitted at NCBI database, BLAST with Reference Sequence **Genotype 3b, KY620871**.

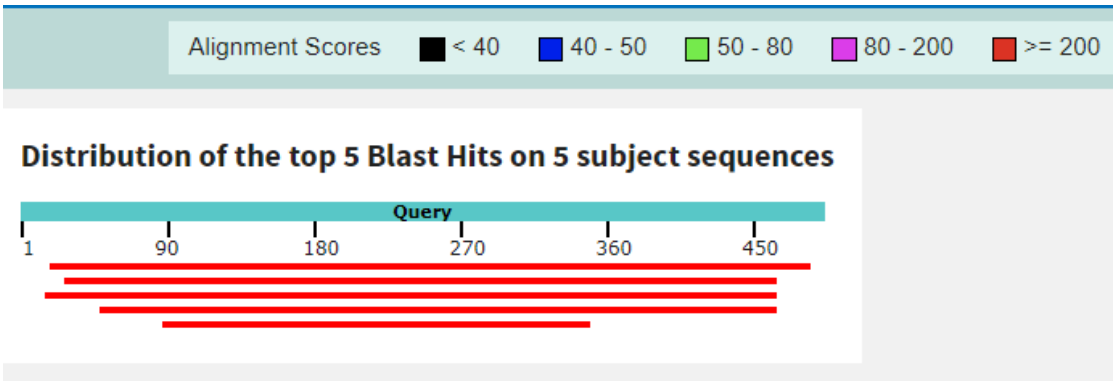

Table 9.9. Description of the alignment of Core E1 sequences submitted at NCBI database BLAST done with **Genotype 3b, KY620871**.

Accession	Max Score	Total Score	Query Cover	Per. ident	Acc. Len
MW970044.1	586	586	94%	89.29	467
MW970046.1	547	547	88%	89.24	437
MW970043.1	492	492	84%	87.98	416
MW970049.1	309	309	53%	87.83	265
MW970048.1	525	525	90%	87.75	449

Fig. 9.10. Graphic summary of Core E1 sequences submitted at NCBI database, BLAST with Reference Sequence **Genotype 4, FJ462437**.

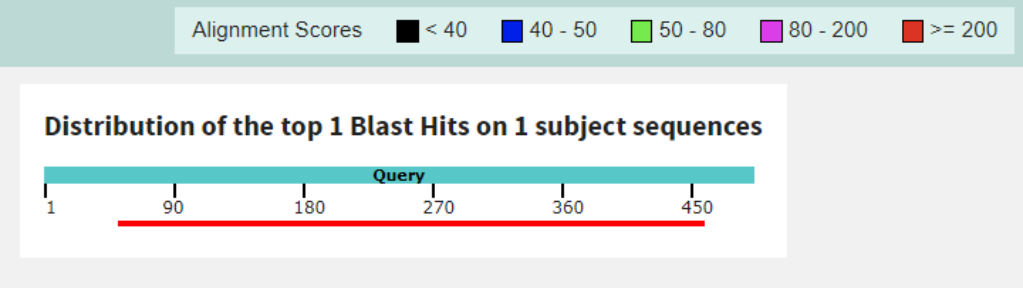

Table 9.10. Description of the alignment of Core E1 sequences submitted at NCBI database BLAST done with **Genotype 4, FJ462437**.

Accession No.	Max Score	Total Score	Query Cover	Per. ident	Acc. Len
MW970042	566	566	82%	91.67	408

Table 9.11. Comparison of anti-HCV antibody responses with viral load/ Cq and genotypes.

Core E1 sequence submitted	Anti-HCV Antibody	Viral load (IU/µl)	Cq	Genotype
MK133356	28.2	72038	20.48	1
MK561495	10.8	22	30.08	1
MK843926	33.8	337	29.78	1
MW970047	30.9	2522	26.48	1
MK843927	29.5	988	27.56	1
MW970045	31.2	1753	26.52	1
MK843925	29.2	10	31.78	3a
MW970044.1	36.1	108	31.21	3b
MW970046.1	1.11	1	36.37	3b
MW970043.1	36.8	3437	25.64	3b
MW970049.1	6.96	0	37.7	3b
MW970048.1	30	1102	27.09	3b
MW970042	30	1325	26.08	4

9.5.3. Core E1 amino acid sequence data analysis

Table 9.12A. Epitope and antigenicity predicted peptides of Core E1 amino acid sequences, Genotype 1a with MK561495 accession number. The software used was Bepipred Linear Epitope Prediction (A) and Kolaskar and Tongaonkar Antigenicity Predicted peptides (B). B-cell epitopes were used by the former (A) and physicochemical properties were used for the latter (B). Amino acid sequences were colored as Blue (charged amino acids), Yellow (Polar amino acids) and Green (Non-polar amino acids).

No.	Start	End	Peptide	Length a.a.
1	24	33	QVRNSTGLYH	10
2	39	43	PNSSI	5
3	63	66	EGNA	4
4	77	87	VATRDGRLPTT	11
5	126	135	PRRHWTTQDC	10
6	140	148	YPGEITGHR	9

Table 9.12B. Kolaskar and Tongaonkar Antigenicity Predicted peptides of Core E1 amino acid sequences, Genotype 1a with MK561495 accession number.

No.	Start	End	Peptide	Length a a
1	4	23	SFSIFLLALLSCLTVPASAY	20
2	31	36	LYHVTN	6
3	54	61	TPGCVPCV	8
4	69	76	CWVAVTPT	8
5	94	121	DLLVGSATLCSALYVGDLCGSVFLVGQL	28

Table 9.13. Percentage of secondary structures in Core E1 of sequence with MK561495 (Genotype 1a) accession number. 'H' was the total number of amino acids in the secondary structure (alpha helix) and 'h' was the percentage of the secondary structure (alpha helix) compared to the total number amino acids.

Genomic Region	Alpha Helix (H, h%)	Extended strand (E, e%)	Beta Turn (T, t%)	Random Coil (C, c%)
Core E1	57, 35.85%	33, 20.75%	15, 9.43%	54, 33.96%

Fig. 9.11. Secondary structure prediction of Core E1 sequence MK561495 (Genotype 1a) using SOPMA. **Red** region is Extended strand, **Blue** is the alpha helix, **Green** is Beta turn and **Purple** is the Random coil.

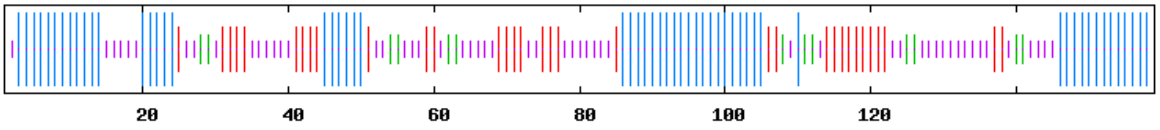

Table 9.14. Predicted amino acid mutation sites of Core E1 sequence submissions of Genotype 1. Reference sequence (NC..) and sequences submitted from our laboratory (M..).

	Amino Acid positions										
	198	**218**	**219**	**234**	**237**	**241**	**243**	**249**	**252**	**284**	**312**
NC_004102	S	D	A	N	R	A	T	R	K	V	H
MK561495	T	E	T	.	.	.	.	.	R	.	E
MK843926	T	E	T	G	.	P	.	.	R	.	.
MK133356	T	.	T	.	.	.	.	K	R	.	E
MK843927	T	.	T	.	.	.	.	.	R	I	E
MW970045	T	.	.	.	K	.	S	K	R	I	E
MW970047	T	.	.	.	K	.	.	.	R	.	.

Table 9.15A. Epitope and antigenicity predicted peptides of Core E1 sequences, GT3a with MK843925 accession number. The software used was Bepipred Linear Epitope Prediction (A) and Kolaskar and Tongaonkar Antigenicity Predicted peptides (B). B-cell epitopes were used by the former (A) and physicochemical properties were used for the latter (B).

No.	Start	End	Peptide	Length
1	19	29	ASLEWRNTSGL	11
2	63	63	N	1
3	76	84	AVRYVGATT	9
4	123	145	RPRHHQTVQTCNCSLYPGHLTGH	23

Table 9.15B. Kolaskar and Tongaonkar Antigenicity Predicted peptides of Core E1 amino acid sequences, GT3a with MK843925 accession number.

No.	Start	End	Peptide	Length
1	4	18	SIFLLALFSCLIHPA	15
2	29	34	LYVLTN	6
3	48	59	VILHAPGCVPCV	12
4	72	80	TPTVAVRYV	9
5	90	96	HVDLLVG	7
6	101	118	CSALYVGDVCGAIFLVGQ	18
7	132	140	TCNCSLYPG	9

Table 9.16. Percentage of secondary structures in Core E1, Genotype 3a with MK843925 accession number. 'H' was the total number of amino acids in the secondary structure (alpha helix) and 'h' was the percentage of the secondary structure (alpha helix) compared to the total number amino acids.

Genomic region	Alpha Helix (H, h%)	Extended strand (E, e%)	Beta Turn (T, t%)	Random Coil (C, c%)
Core E1	55, 35.26%	33, 21.15%	8, 5.13%	60, 38.46%

Fig. 9.12. Secondary structure prediction of Core E1 of Genotype 3a with MK843925 using SOPMA. **Red** region is Extended strand, **Blue** is the alpha helix, **Green** is Beta turn and **Purple** is the Random coil.

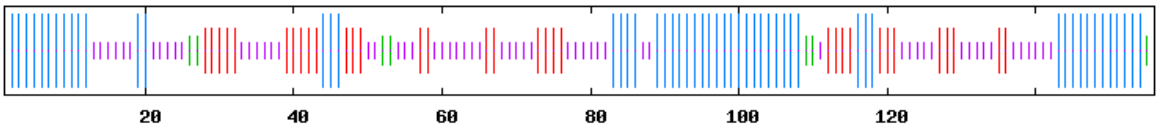

Table 9.17. Predicted amino acid mutation sites seen in Core E1, MK843925 accession number compared with the reference sequence NC_009824.

	Amino Acid positions							
	223	**233**	**237**	**260**	**280**	**284**	**297**	**314**
NC_009824	T	G	T	S	M	V	R	S
MK843925	A	N	K	G	V	I	H	T

Table 9.18A. Epitope and antigenicity predicted peptides of Core E1 sequences, Genotype 3b with MW970044 accession number, which showed maximum identity of 92.90 % to the reference sequence used GT3b. The software used was Bepipred Linear Epitope Prediction (A) and Kolaskar and Tongaonkar Antigenicity Predicted peptides (B). B-cell epitopes were used by the former (A) and physicochemical properties were used for the latter (B).

No.	Start	End	Peptide	Length
1	22	29	LEYRNTSG	8
2	77	85	AVKHPGATT	9
3	125	131	PRRHMTV	7
4	138	150	LYPGHISGHRMAW	13

Table 9.18B. Kolaskar and Tongaonkar Antigenicity Predicted peptides of Core E1 amino acid sequences, GT3b with MW970044 accession number.

No.	**Start**	**End**	**Peptide**	**Length**
1	4	20	FSIFLLALFSCLTCPAS	17
2	49	62	VILHLPGCVPCVAA	14
3	73	79	SPTVAVK	7
4	98	114	AATLCSALYVGDLCGAV	17
5	133	141	TCNCSLYPG	9

Table 9.19. Percentage of secondary structures in Core E1, GT3b with MW970044 accession number. 'H' was the total number of amino acids in the secondary structure (alpha helix) and 'h' was the percentage of the secondary structure (alpha helix) compared to the total number amino acids.

Accession No.	Alpha Helix (H, h%)	Extended strand (E, e%)	Beta Turn (T, t%)	Random Coil (C, c%)
MW970044	59, 38.06%	34, 21.94%	7, 4.52%	55, 35.48%

Fig. 13A. Secondary structure prediction of Core E1, GT3b with MW970044 accession number using **SOPMA (A)**. **Red** region is Extended strand, **Blue** is the alpha helix, **Green** is Beta turn and **Purple** is the Random coil.

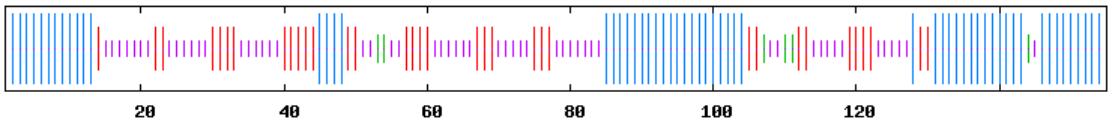

Fig. 9.13B. Domain analysis of Secondary structure prediction of Core E1 of Genotype 3b with MW970044 accession number using **Phyre2 web portal (B).**

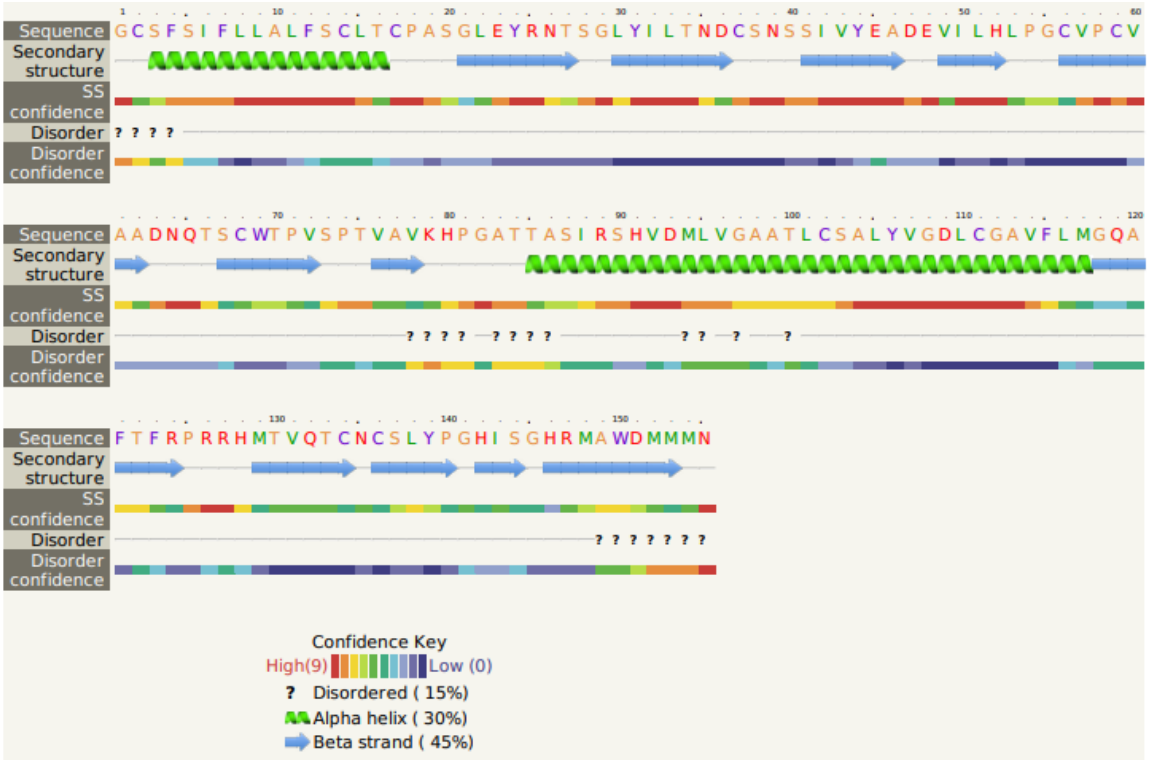

Table 9.20. Predicted amino acid mutation sites seen in Core E1 of Genotype 3b in reference with KY620871

Acc. No.	Amino Acid positions												
	189	**191**	**202**	**210**	**218**	**231**	**232**	**233**	**237**	**250**	**264**	**280**	**287**
KY620871	A	T	L	K	E	T	T	G	L	Y	L	L	M
MW970044	-	G	I	S	-	A	A	D	S	H	M	-	-
MW970043	-	S	I	N	-	A	A	D	S	H	M	-	-
MW970046	-	S	I	N	-	A	A	D	S	H	M	-	-
MW970049	-	-	I	S	-	A	A	D	S	H	M	-	-
MW970048	T	G	I	R	D	N	-	D	S		V	V	V

Table 9.21A. Epitope and antigenicity predicted peptides of Core E1 sequences, GT4d with MW970042 accession number. The software used was Bepipred Linear Epitope Prediction (A) and Kolaskar and Tongaonkar Antigenicity Predicted peptides (B). B-cell epitopes were used by the former (A) and physicochemical properties were used for the latter (B).

No.	Start	End	Peptide	Length
1	7	21	PPPAYNYRNSSGVYH	15
2	27	28	PN	2
3	30	31	SI	2
4	34	34	E	1
5	66	76	AAPYLNAPLES	11
6	113	122	RPRRHWTTQE	10
7	130	132	GHI	3

Table 9.21B. Kolaskar and Tongaonkar Antigenicity Predicted peptides sequences, GT4d with MW970042 accession number.

No.	Start	End	Peptide	Length
1	4	9	LTVPPP	6
2	38	51	HILHLPGCVPCVKV	14
3	88	94	ATLCSAL	7
4	100	109	CGGVFLVGQL	10

Table 9.22. Percentage of secondary structures in Core E1 of GT4d with MW970042 accession number. 'H' was the total number of amino acids in the secondary structure (alpha helix) and 'h' was the percentage of the secondary structure (alpha helix) compared to the total number amino acids.

Genomic region	Alpha Helix (H, h%)	Extended strand (E, e%)	Beta Turn (T, t%)	Random Coil (C, c%)
Core E1	33, 24.26%	40, 29.41%	6, 4.41%	57, 41.91%

Fig. 9.14. Secondary structure prediction of Core E1 using **SOPMA of** Genotype 4d (MW970042). **Red** region is Extended strand, **Blue** is the alpha helix, **Green** is Beta turn and **Purple** is the Random coil.

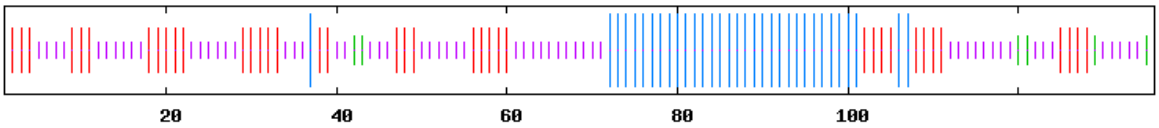

Table 9.23. Predicted amino acid mutation sites of MW970042 with reference to FJ462437, Genotype 4d.

Accession No.	Amino Acid positions										
	189	**190**	**203**	**231**	**235**	**241**	**268**	**280**	**284**	**294**	**303**
FJ462437	A	S	V	R	K	S	A	V	A	Q	D
MW970042	P	P	I	K	T	A	S	L	V	R	E

9.5.4. NS5B sequence data analysis

Fig. 9.15. Graphic summary of NS5B sequences submitted at NCBI database nBLAST (nucleotide BLAST) done with Reference Sequence NC_004102 (Genotype 1).

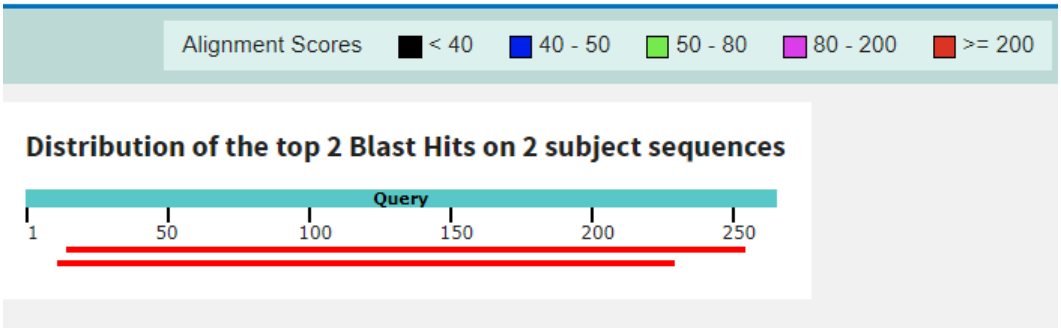

Table 9.24. Description of the alignment of NS5B sequences submitted at NCBI database nBLAST (nucleotide BLAST) done with Reference Sequence NC_004102 (Genotype 1).

Accession No.	Max Score	Total Score	Query Cover	Per. Ident	Acc. Len
MW281563	392	392	90%	96.23	239
MW970050	374	374	82%	97.7	220

Table 9.25. Comparison of anti-HCV antibody with Viral load and Cq of NS5B sequences

Accession No.	Anti-HCV Antibody	Viral load (IU/µl)	Cq	Genotype
MW281563	0.06	112468	20.07	1
MW970050	31.2	1753	26.52	1

Table 9.26A. Epitope and antigenicity predicted peptides of NS5B sequences, Genotype1 with MW281563 accession number. The software used was Bepipred Linear Epitope Prediction (A) and Kolaskar and Tongaonkar Antigenicity Predicted peptides (B). B-cell epitopes were used by the former (A) and physicochemical properties were used for the latter (B).

No.	Start	End	Peptide	Length
1	6	15	VQPEKGGRKP	10
2	33	40	ALYDVVSK	8
3	50	61	YGFQYSPGQRVE	12
4	67	75	WKSKKTPMG	9

Table 9.26B. Kolaskar and Tongaonkar Antigenicity Predicted peptides for NS5B, Genotype 1 with **MW281563** accession number.

No.	Start	End	Peptide	Length
1	17	29	RLIVFPDLGVRVC	13
2	34	46	LYDVVSKLPLAVM	13
3	61	66	EFLVRA	6

Table 9.27. Percentage of secondary structures in NS5B sequences. 'H' was the total number of amino acids in the secondary structure (alpha helix) and 'h' was the percentage of the secondary structure (alpha helix) compared to the total number amino acids.

Accession No.	Alpha Helix (H, h%)	Extended strand (E, e%)	Beta Turn (T, t%)	Random Coil (C, c%)
MW281563	30, 37.97%	15, 18.99%	6, 7.59%	28, 35.44%
MW970050	23, 31.51%	13, 17.81%	2, 2.74%	35, 47.95%

Fig. 9.16A. Domain analysis of Secondary structure prediction of NS5B, Genotype 1a with MW281563 accession number using **Phyre2 web portal.**

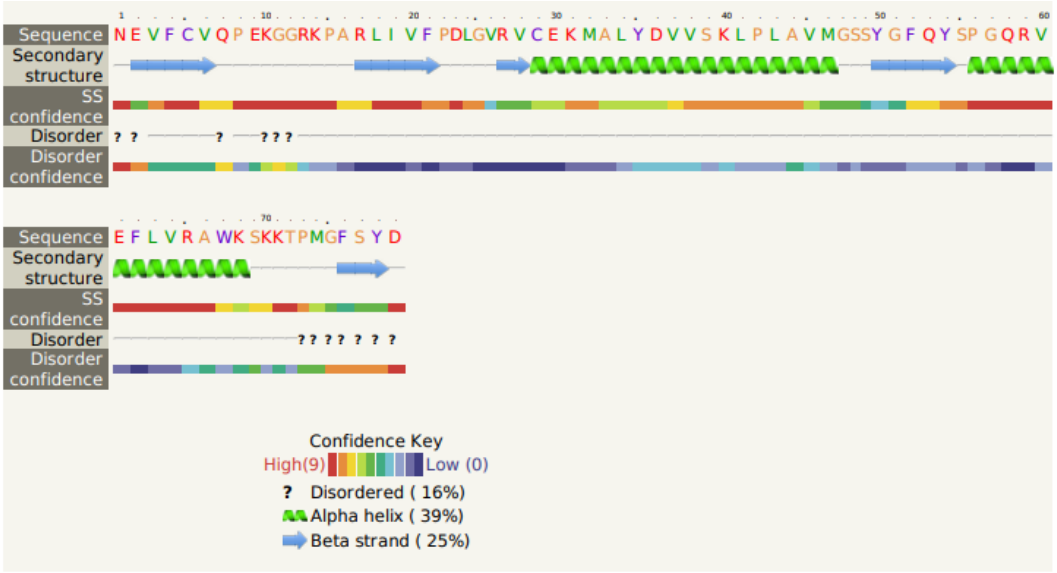

Fig. 16B. PDB formatted model of Secondary structure prediction of NS5B, Genotype 1a with MW281563 using Phyre2 web portal.

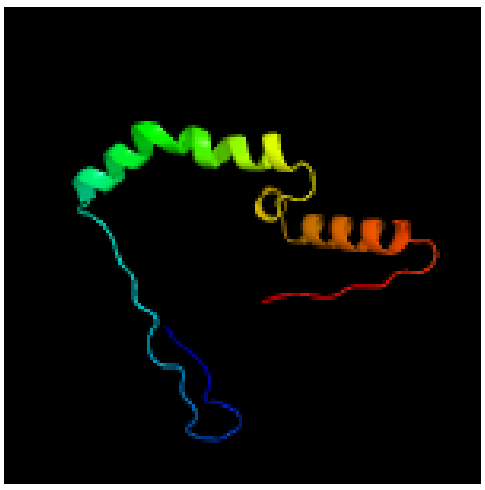

Table 9.28A. Epitope and antigenicity predicted peptides of NS5B sequences, Genotype 1 with MW970050 accession number.

No.	Start	End	Peptide	Length
1	6	16	CVQPEKGGRKP	11
2	35	41	LYDVVSK	7
3	51	62	YGFQYSPGQRVE	12

Table 9.28B. Kolaskar and Tongaonkar Antigenicity Predicted peptides for NS5B sequences, Genotype 1 with MW970050 accession number.

No.	Start	End	Peptide	Length
1	4	9	VFCVQP	6
2	18	24	RLIVFPD	7
3	35	46	LYDVVSKLPLAV	12

Fig. 17A. Domain analysis of Secondary structure prediction of NS5B, Genotype 1a with MW970050 accession number using **Phyre2 web portal**

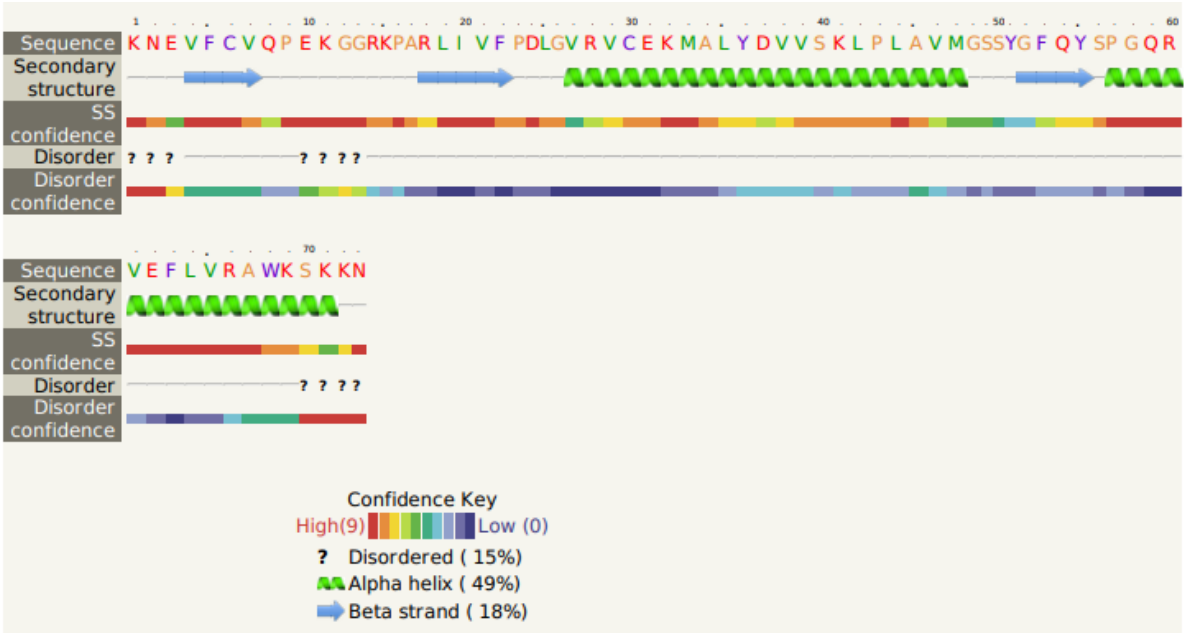

Fig. 17B. PDB formatted model of Secondary structure prediction of NS5B, Genotype 1a with MW970050 using Phyre2 web portal.

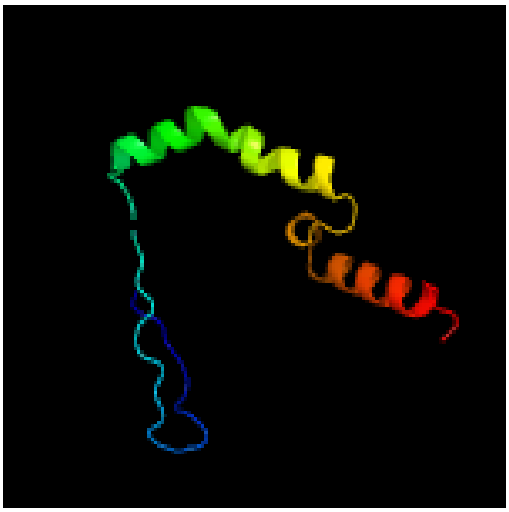

Table 9.29. Predicted amino acid mutation sites of genotype 1a of NS5B

Accession No.	205	212
NC_004102	Q	T
MW281563	R	
MW970050	R	N

Table 9.30. Final Decision criteria for differentiation quantitative and qualitative real time RT-PCR. Data from the fluorescence amplification plots by (a) visual observation, (b) calibration plots, (c) four-parameter data from SigmaStat, (d) log fluorescence intensity from LinRegPCR and (e) validation of PCR product by sequence analysis.

Parameter	Quantitative range	Qualitative range	Sources of the Data and Comments
A. Graphical observation from fluorescence amplification plot			
Normalised fluorescence intensity, 'a'	Near 100%	<90%	Manually measured; Data from Fig. 5.1 and Table 5.3
Slope at inflection point, b	1.65 – 1.50	1.50 – 1.08	Manually measured; Data from Fig. 5.1 and Table 5.3
Cq or Concentration of Calibrator	<33.20 or >10 IU/µl	33.20 to 39.90 or <10 IU/µl	Data from Fig. 8.1, Table 5.1. 10 IU/µl calibrator may be used as a reference data point in RT-PCR assays
B. Four-parameter data from calibrators and plasma RNA by SigmaStat software			
Fluorescence intensity (normalised), 'a'	28.35 – 21.93 (100%)	21.74 – 15.39 (decreased)	Data from Table 5.2
Slope at inflection point, b	2.55 – 1.95 (100%)	≤1.90 (decreased)	Data from Table 5.2
C. Log fluorescence intensity from LinRegPCR software			
Slope	0.301 - 0.255	<0.255	Data from Fig. 5.3. and Table 5.3
Efficiency, E	2.0 – 1.80	<1.80	Data from Fig. 5.3. and Table 5.3
D. Data analysis of Calibration plots			
Slope, M	-3.1 to -3.6	>-3.1 or <-3.6 (outside numerical value of 3.1 to 3.6)	Data from Fig. 5.1B
Efficiency	110% - 90%	>110% and < 90%	Data from Fig. 5.1B
Acceptable calibration Sensitivity, Cq at 1 IU/µl	33 – 37	33 – 37	<33 or >37 unacceptable calibration plot sensitivity.
%CV of calibrator and diluted calibrator, Cq	<7%	<7%	>7% Unacceptable calibrator RT-PCR Cq performance. Data from Table 5.1.
E. Validation of PCR product by Sequencing			
Sequencing (Sanger's Method)	-	272 bp amplified (5' UTR)	Fig. 9.2, validated by submitting the sequence to NCBI which should report highest percent identity with 5'UTR region of HCV

9.5.5. Attempts at predicting the tertiary structure and antigenic epitopes

Fig. 9.18. PDB structure of NS5B protein – The region amplified and translated was assigned blue color from 141 – 220 using RCSB PDB tool. In the blue range, red, yellow and purple are the antigenic epitopes.

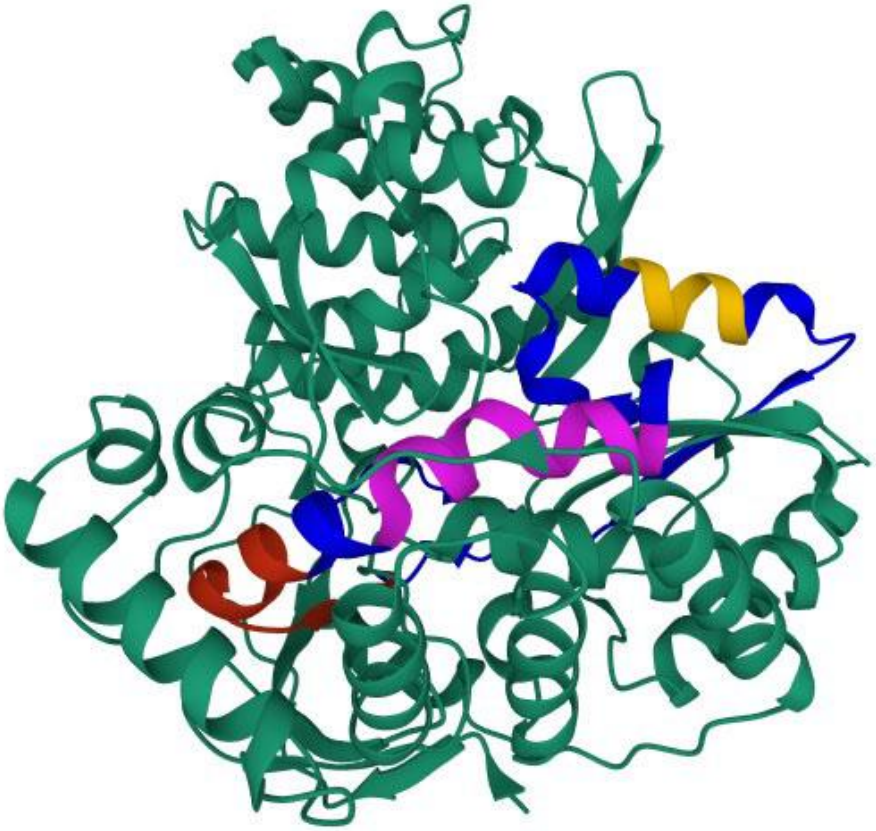

Translated NS5B region (Blue) : 141 - 220
Antigenicity Predicted peptides positions: 158 - 170 (Red),
175 - 187 (Purple) and 202 - 207 (Yellow).

9.5.6. Construction of phylogenetic tree

Fig. 9.19. Phylogenetic data analysis of 5'UTR region of HCV genome, Genotype 1 (Red, 11 sequences from this study) and Genotype 3 (Blue, 7 sequences from this study). The reference and other sequences from NCBI are shown in black.

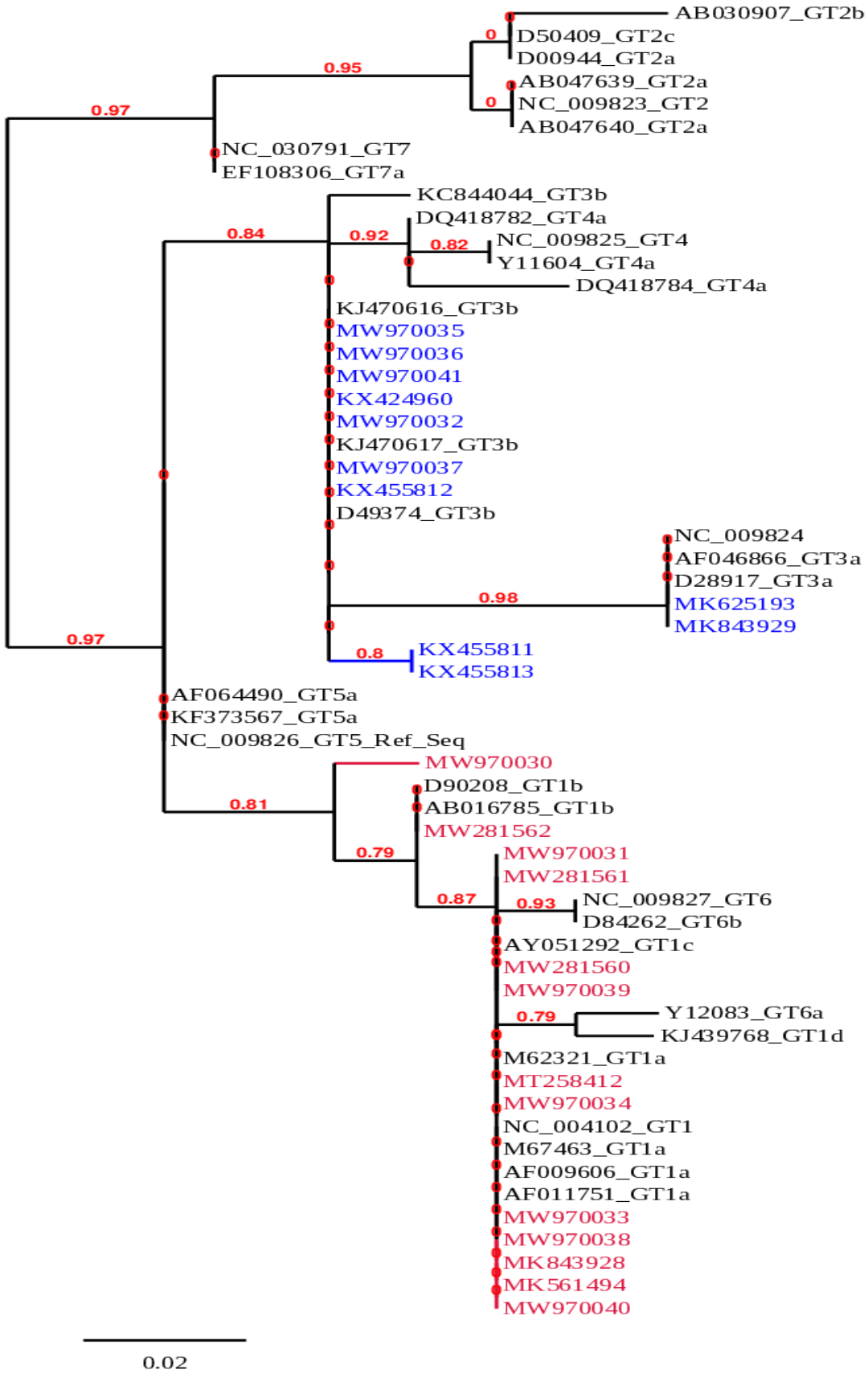

Fig. 9.20. Phylogenetic data analysis of Core E1 region of HCV genome. References sequences and other sequences from NCBI database (Black). Rest of the sequences were from this study. Genotype 1 (Red, 7 sequences), Genotype 3a (purple, 1 sequences), Genotype3b (Blue, 5 sequences), Genotype 4 (Green, 1 sequence).

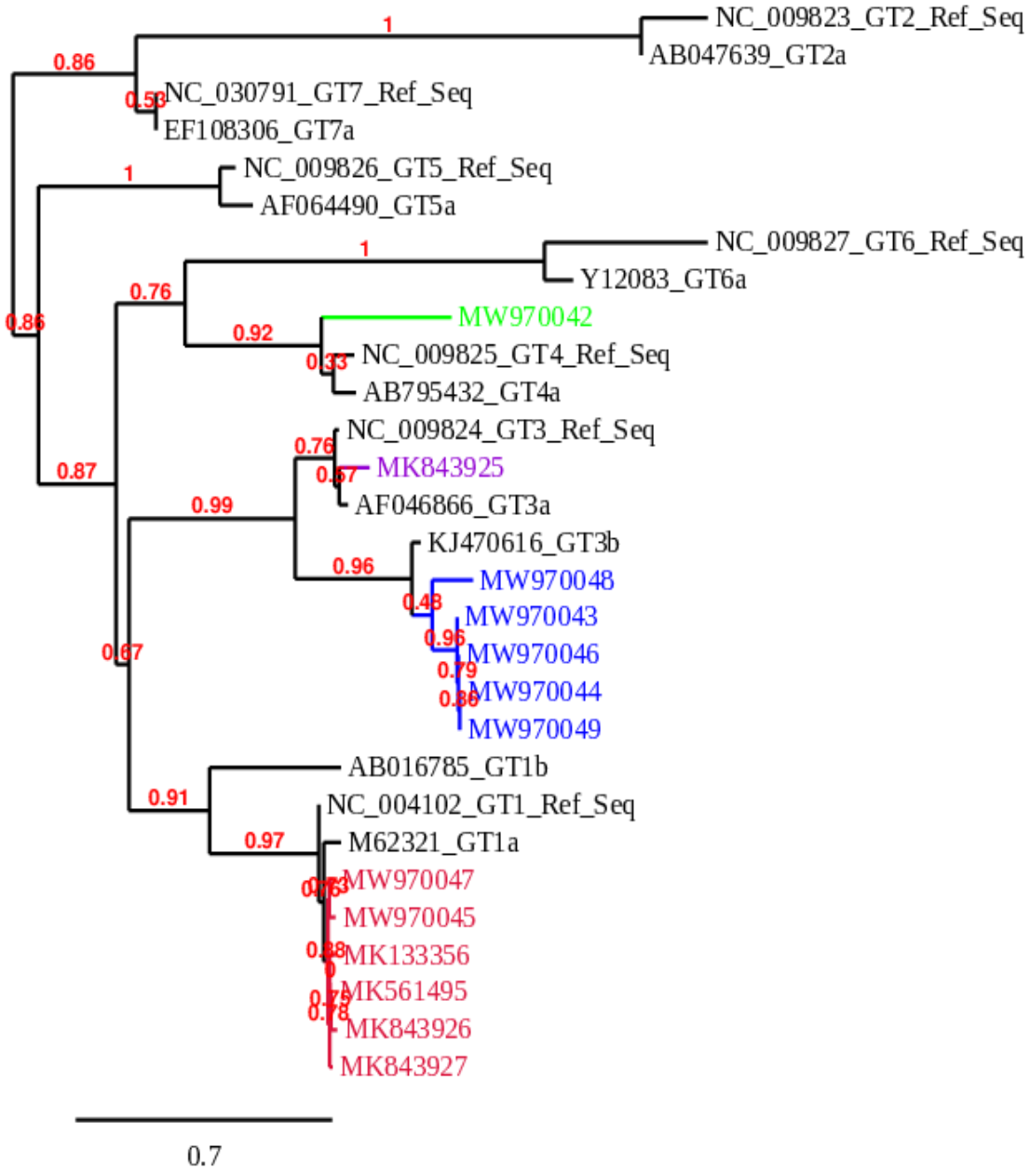

Fig. 9.21. Phylogenetic data analysis of NS5B region of HCV genome with two Genotype 1 sequences from this study marked Blue. Rest of the sequences were from NCBI database.

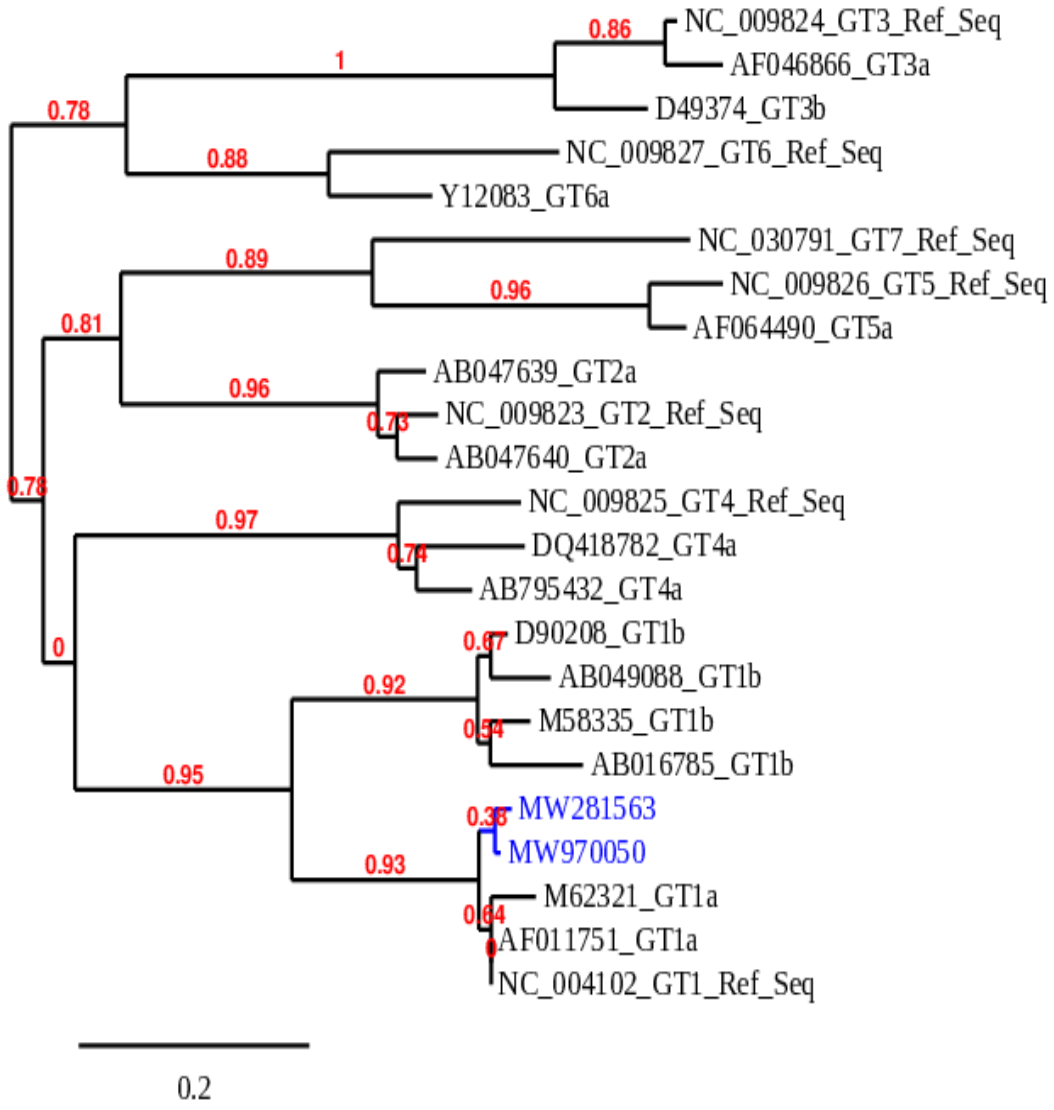

Summary and Conclusions

Chapter-wise summary from the results chapters 5 to 9.

Data analysis of calibration plot and HCV RT-PCR fluorescence amplification plots were analysed to differentiate between qualitative and quantitative RT-PCR and to establish validation criteria for qualitative RT-PCR. In qualitative RT-PCR, the fluorescence intensity and slope at inflection point were decreased in qualitative PCR. The lower analytical limit of quantitative PCR calibration plot was at 10 IU/µl calibrator concentration which was equivalent to Cq of about 33. The calibration plot of qualitative RT-PCR concentrations showed unacceptable performance outside the acceptable limits: Cq range 33.2 to 39.9; slope at inflection point from 1.50 – 1.08; four-parameter slope at inflection point ≤1.90; log fluorescence intensity slope <0.255 and efficiency <1.80; calibration plot slope >-3.1 or <-3.6, efficiency >110% and < 90% and acceptable calibration sensitivity 33 – 37.

Internal control (IC) was added to HCV RT-PCR assays with patients' plasma RNA, calibrators, QC RNA and non-template control (NTC). All IC additions were from the same lot for a set of calculations. The IC fluorescence emission of ROX dye at 610±5 nm, was independent of the HCV template amplification with FAM dye having emission at 510±5 nm. The average IC Cq was lowest for NTC, followed by the calibrators, QC samples and the HCV infected patients' plasma RNA sample. The average %CV was the same for NTC, calibrators and QC sample, but was increased for patients' sample. The results showed that the analytical influences might be due to HCV RT-PCR products which could be attributed to the IC Cq difference between the calibrator and NTC. The preanalytical influences might be contributed by IC Cq difference between patients' (or QC) sample, and the calibrator. QC and patients' sample contained non-specific RNA from plasma which might contribute to the pre-analytical influences. The patients' samples were from different patients' contributing to higher average patients' %CV, unlike that of QC sample and calibrators which were a single sample. Slope, normalised fluorescence intensity and efficiency **of the fluorescence amplification plot** decrease**d** with decrease in viral load both in calibrators and with patient samples. when concentration is

expressed as Cq, the relationship of Cq, fluorescence intensity and efficiency become inversely related.

The preanalytical influence on HCV RT-PCR were analysed by selecting HCV RT-PCR positive cases that were to undergo surgery and then repeating HCV RT-PCR after surgery. Studies were also designed on HCV RT-PCR positive cases that had tissue damaging conditions. In these cases, the Cq value decreased or the negative result became positive indicating high viral load when tissue damaging conditions were decreased. These results also indicated that whenever there was a preanalytical influence on the RT-PCR assay, the assay may be repeated after two weeks to obtain a more correct result. The study strongly indicated preanalytical influence were more prominent when HCV viral load was low. Even HCV negative patient samples in the presence of tissue damaging conditions were also found to influence and increase the Cq value of the calibrators.

Diagnosis of HCV infection was done by screening for anti-HCV antibody using the third-generation assay followed by HCV RT-PCR of samples reactive for anti-HCV antibody. RT-PCR assay was done after preanalytical control of samples to decrease non-specific influences, probably of nucleic acids and drugs, immediate isolation of RNA from EDTA-plasma. The reactive anti-HCV antibody concentrations were RT-PCR positive or RT-PCR negative. There were two distribution clusters for anti-HCV antibody, the lower antibody cluster was between 1.0 and 15.0 and the higher antibody cluster was between 15.0 and 42. Each of the two reactive antibody clusters in the antibody distribution of histogram were found to have both RT-PCR negative and positive samples. The RT-PCR negative, anti-HCV antibody reactive samples may contain samples with occult HCV infection, very few genuinely false reactive samples and samples with preanalytical influences.

There were seven major genotypes (GTs), the complete genomes of which differ from each other by at least 30% at the nucleotide level. Genotype 1 is the most prevalent worldwide (46%) and predominates in Europe, North America, and Australia. It is followed by GT3 (30%), which is primarily distributed in South Asia, particularly the Indian subcontinent.

GT3 is the most common genotype in India followed by GT1. The major genotypes identified in this study were 1 and 3. The **5'UTR region** was highly conserved, 341 bp region with secondary RNA structure that has functional importance. **Graphic representation of 24 sequences of genotype 1** of 5'UTR showed >200 alignment score with reference sequence, and percent identity from 96 to 100% for genotype 1. Similar data was obtained for **genotype 3**, with percent identity from 95.57 to 99.57. There were highly conserved regions of 5'UTR with low entropy, and these sites were used for designing primers that were used for diagnostic purposes. The secondary RNA structure of (5'UTR) showed several sites of stacking interactions between successive base pairs, and predicted energetically most stable structure.

Similar **sequence data analysis** was also done with **Core E1 region**. Six different sequences of **genotype 1** of Core E1 region were submitted to NCBI database and were found to have alignment score >200 and percent identity between 94.59 and 95.46. Due to lack of specific highly conserved sites, primer designing for both CE1 and NS5B were found to be more difficult and less productive. There was one sequence with **genotype 3a** with alignment score >200 and percent identity of 91.53. There were five sequences of core E1 matched with **genotype 3b** with alignment score >200 and percent identity 87.75 to 89.29. One sequence showed >200 alignment score with **genotype 4** with percent identity of 91.67. **Epitope prediction** was done for **Core E1** using software (a) Bepipred Linear Epitope Prediction and (b) Kolaskar and Tongaonkar Antigenicity Predicted peptides. B-cell epitopes were used by the former and physicochemical properties were used for the latter. The secondary structure of core E1 were also analysed.

Similar analysis was done with **NS5B** but the PCR product and the data obtained were much less than the other two regions due to larger variations distributed in the NS5B region. There were only **two PCR products** amplified using various primers designed for NS5B. The **secondary structure of NS5B and the possible three-dimensional tertiary distribution** of the secondary structures were also analysed.

Phylogenetic tree was constructed using reference sequence from the **seven genotypes of 5'UTR**. These reference sequences were aligned and compared with the HCV sequences that we had submitted to NCBI from this study. **Phylogenetic tree** construction was also done for **Core E1 and NS5B** regions with our sequences and the reference sequences from NCBI database.

Final Conclusions:

Data analysis and analysis of the performance characteristics were done with HCV RT-PCR 1) fluorescence amplification plots of calibrators and patients' sample, 2) calibration plots and 3) internal control fluorescence amplification plots from NTC, calibrators and patients' samples. Data analysis and performance characteristics showed analytical and preanalytical influences that can influence HCV RT-PCR results and the clinical reports. Performance characteristics such as analytical sensitivity, bias/imprecision and %CV also showed preanalytical influences on the RT-PCR. Verification and validation of the RT-PCR products were done using agarose gel electrophoresis for the product size and by sequencing the PCR products with Sanger's method. HCV RT-PCR product sequence data analysis was done for the three functionally important regions of the HCV genome, 5'UTR, Core E1 and NS5B. 5'UTR showed three regions with very low entropy and with least variability between sequences. Productive primers were designed from these regions. Core E1 and NS5B regions showed higher variability, and PCR products with primers designed to these sites were less. 40 sequences were submitted to NCBI from out study and accession number obtained. Genotypes of these sequences were as follows: 5'UTR – GT1 and 3; Core E1: GT 1, 3a, 3b and 4; NS5B: GT 1. Phylogenetic tree was also constructed with these sequences and with the reference sequences obtained from NCBI.

Chapter 10

Recommendations

Clinical Molecular Biology is not done systematically in many cases. There are many influences of sample and PCR products on the RT-PCR system. There can be several pre-analytical, analytical and post-analytical influences. Most of the influences become prominent when the template concentrations are low and these influences may not be evident when the template concentrations are high. The major preanalytical influences are due to the presence of nonspecific interfering plasma RNA/ DNA which can result from tissue damaging conditions. Drugs can cause inhibition of RT-PCR enzymes, thus interfering with RT-PCR results.

It was not possible to differentiate between analytical and preanalytical influences in the earlier report of studies. There are also postanalytical interpretation issues related to PCR product sequences such as in cancer molecular biology.

There are also issues related to defining and validating the qualitative PCR especially at the Limit of Detection. These are the major issues which are clinically important for molecular biology diagnosis developed in the study. There were also postanalytical issues related to large sample number in the case of SARS CoV-2 infection resulting in serious problem associated with report.

The most important analytical problem was associated with SARS CoV-2 was very high viral load leading to issues of contamination. Due to the large number of samples the issues of contamination were overlooked. This led to repeated decrease of Cq value for defining the negative RT-PCR levels from above 36 to Cq 34. Therefore, the high viral load results in overlooking the diagnosis of carrier state infection. Neither was it possible to develop a dependable quantitative RT-PCR with a dependable calibration plot. These are the problems faced in the preanalytical, analytical and post analytical stages of RT-PCR and has to be improved upon. Given below are some of the suggestions that may be incorporated in future studies and for clinical diagnosis using RT-PCR.

The approach to a diagnostic molecular biology lab should be quite different from that of experimental clinical molecular biology laboratory.

A diagnostic molecular biology lab should produce a result that is correct, each and every time a patient sample is run. There should be room for repetition if RT-PCR influences that are seen both in qualitative and quantitative results.

But in experimental works there is always room for repetition, even later, when some of it results are not consistent with the other data. The results become final only after a set of data become consistent for the conclusion of the research problem.

Future Direction

1. There should be dedicated RT-PCR rooms and instruments for high template, low template concentration assays and non-symptomatic carrier states

2. There should be a regular evaluation of systematic internal controls for pre-analytical and analytical influences

3. For RT-PCR assays at low template concentration and at high template concentration, NTC should be made compulsory for detection.

4. When sequencing studies are required, there should be agarose gel electrophoresis and gel documentation system available in laboratory to carefully detect and carefully do the semi quantitation of the band before sequencing.

l

Bibliography

Abdel Nour AM, Pfaffl MW. MIQE & QPCR Ibook How to Apply the MIQE Guidelines - a Visual, Interactive and Practical QPCR Guide! bioMCC; 2015.

Abdel-Hakeem MS and Shoukry NH. Protective immunity against hepatitis C: many shades of gray. *Front. Immunol.* 2014. **5**:274. doi: 10.3389/fimmu.2014.00274

Adams PS. Data analysis and reporting. In: Dorak MT, editor. Real-Time PCR. Taylor and Francis, USA; 2006. p.39-62.

Adinolfi LE, Utili R, Andreana A, et al. Serum HCV RNA levels correlate with histological liver damage and concur with steatosis in progression of chronic hepatitis C. Dig Dis Sci. 2001;46(8):1677-1683. doi:10.1023/a:1010697319589

Afdhal N, Reddy KR, Nelson DR, et al. Ledipasvir and Sofosbuvir for Previously Treated HCV Genotype 1 Infection. New England Journal of Medicine. 2014a;370(16):1483-1493. doi:10.1056/NEJMoa1316366

Afdhal N, Zeuzem S, Kwo P, et al. Ledipasvir and Sofosbuvir for Untreated HCV Genotype 1 Infection. N Engl J Med. 2014b;370(20):1889-1898. doi:10.1056/NEJMoa1402454

Agnello V, Abel G, Elfahal M, Knight GB, Zhang QX. Hepatitis C virus and other flaviviridae viruses enter cells via low density lipoprotein receptor. Proc Natl Acad Sci U S A. 1999;96(22):12766-12771. doi:10.1073/pnas.96.22.12766

Agnello V, Abel G, Elfahal M, Knight GB, Zhang QX. Hepatitis C virus and other flaviviridae viruses enter cells via low density lipoprotein receptor. Proc Natl Acad Sci U S A. 1999;96(22):12766-12771. doi:10.1073/pnas.96.22.12766

Ago H, Adachi T, Yoshida A, et al. Crystal structure of the RNA-dependent RNA polymerase of hepatitis C virus. Structure. 1999;7(11):1417-1426. doi:10.1016/s0969-2126(00)80031-3

Akane A, Matsubara K, Nakamura H, Takahashi S, Kimura K. Identification of the heme compound copurified with deoxyribonucleic acid (DNA) from bloodstains, a major inhibitor of polymerase chain reaction (PCR) amplification. J Forensic Sci. 1994;39(2):362-372.

Al-Quaiz MN, Madani TA, Karawi MA. The natural history of hepatitis C virus infection. Saudi Med J. 2003;24 Suppl 2:S67-70.

Al-Soud WA, Rådström P. Purification and characterization of PCR-inhibitory components in blood cells. J Clin Microbiol. 2001;39(2):485-493. doi:10.1128/JCM.39.2.485-493.2001

Alter HJ, Seeff LB. Recovery, persistence, and sequelae in hepatitis C virus infection: a perspective on long-term outcome. Semin Liver Dis. 2000;20(1):17-35. doi:10.1055/s-2000-9505

Alter MJ, Gerety RJ, Smallwood LA, et al. Sporadic non-A, non-B hepatitis: frequency and epidemiology in an urban U.S. population. J Infect Dis. 1982;145(6):886-893. doi:10.1093/infdis/145.6.886

Alter MJ, Margolis HS, Krawczynski K, et al. The Natural History of Community-Acquired Hepatitis C in the United States. New England Journal of Medicine. 1992;327(27):1899-1905. doi:10.1056/NEJM199212313272702

Alter MJ, Margolis HS, Krawczynski K, et al. The natural history of community-acquired hepatitis C in the United States. The Sentinel Counties Chronic non-A, non-B Hepatitis Study Team. N Engl J Med. 1992;327(27):1899-1905. doi:10.1056/NEJM199212313272702

Amid C, Alako BTF, Balavenkataraman Kadhirvelu V, et al. The European Nucleotide Archive in 2019. Nucleic Acids Res. 2020;48(D1):D70-D76. doi:10.1093/nar/gkz1063

André P, Komurian-Pradel F, Deforges S, et al. Characterization of low- and very-low-density hepatitis C virus RNA-containing particles. J Virol. 2002;76(14):6919-6928. doi:10.1128/jvi.76.14.6919-6928.2002

Antaki N, Craxi A, Kamal S, et al. The neglected hepatitis C virus genotypes 4, 5 and 6: an international consensus report. Liver International. 2010;30(3):342-355. doi:10.1111/j.1478-3231.2009.02188.x

Arora DR. Quality assurance in microbiology. Indian J Med Microbiol. 2004;22(2):81-86.

Artus HCV RG RT-PCR Kit Handbook. Version 1. Qiagen, Germany. 2012.

Atrah HI, Hutchinson F, Gough D, Ala FA, Ahmed MM. Hepatitis C virus seroconversion rate in established blood donors. J Med Virol. 1995;46(4):329-333. doi:10.1002/jmv.1890460407

Bacon BR, Gordon SC, Lawitz E, et al. Boceprevir for previously treated chronic HCV genotype 1 infection. N Engl J Med. 2011;364(13):1207-1217. doi:10.1056/NEJMoa1009482

Baltimore D. RNA-dependent DNA polymerase in virions of RNA tumour viruses. Nature. 1970;226(5252):1209-1211. doi:10.1038/2261209a0

Baril M, Brakier-Gingras L. Translation of the F protein of hepatitis C virus is initiated at a non-AUG codon in a +1 reading frame relative to the polyprotein. Nucleic Acids Res. 2005;33(5):1474-1486. doi:10.1093/nar/gki292

Barreiro P, Labarga P, Fernandez-Montero JV, et al. Rate and predictors of serum HCV-RNA >6 million IU/mL in patients with chronic hepatitis C. J Clin Virol. 2015;71:63-66. doi:10.1016/j.jcv.2015.08.001

Barrera JM, Bruguera M, Ercilla MG, et al. Persistent hepatitis C viremia after acute self-limiting posttransfusion hepatitis C. Hepatology. 1995;21(3):639-644. doi:10.1002/hep.1840210306

Barrera JM, Francis B, Ercilla G, et al. Improved detection of anti-HCV in post-transfusion hepatitis by a third-generation ELISA. Vox Sang. 1995;68(1):15-18. doi:10.1111/j.1423-0410.1995.tb02538.x

Barría MI, González A, Vera-Otarola J, et al. Analysis of natural variants of the hepatitis C virus internal ribosome entry site reveals that primary sequence plays a key role in cap-independent translation. Nucleic Acids Res. 2009;37(3):957-971. doi:10.1093/nar/gkn1022

Bartenschlager R, Frese M, Pietschmann T. Novel insights into hepatitis C virus replication and persistence. Adv Virus Res. 2004;63:71-180. doi:10.1016/S0065-3527(04)63002-8

Bartenschlager R, Lohmann V, Wilkinson T, Koch JO. Complex formation between the NS3 serine-type proteinase of the hepatitis C virus and NS4A and its importance for polyprotein maturation. J Virol. 1995;69(12):7519-7528.

Barth H, Cerino R, Arcuri M, et al. Scavenger Receptor Class B Type I and Hepatitis C Virus Infection of Primary Tupaia Hepatocytes. J Virol. 2005;79(9):5774-5785. doi:10.1128/JVI.79.9.5774-5785.2005

Barth H, Schafer C, Adah MI, et al. Cellular binding of hepatitis C virus envelope glycoprotein E2 requires cell surface heparan sulfate. J Biol Chem. 2003;278(42):41003-41012. doi:10.1074/jbc.M302267200

Bartlett RC, Mazens-Sullivan M, Tetreault JZ, Lobel S, Nivard J. Evolving approaches to management of quality in clinical microbiology. Clin Microbiol Rev. 1994;7(1):55-88. doi:10.1128/CMR.7.1.55

Bartosch B, Dubuisson J, Cosset FL. Infectious hepatitis C virus pseudo-particles containing functional E1-E2 envelope protein complexes. J Exp Med. 2003a;197(5):633-642. doi:10.1084/jem.20021756

Bartosch B, Vitelli A, Granier C, et al. Cell entry of hepatitis C virus requires a set of co-receptors that include the CD81 tetraspanin and the SR-B1 scavenger receptor. J Biol Chem. 2003b;278(43):41624-41630. doi:10.1074/jbc.M305289200

Basic Method Validation, 4th Edition - Westgard. Accessed June 24, 2022. https://www.westgard.com/basic-method-validation-4th-edition.htm

Beguiristain N, Robertson HD, Gómez J. RNase III cleavage demonstrates a long range RNA: RNA duplex element flanking the hepatitis C virus internal

ribosome entry site. Nucleic Acids Res. 2005;33(16):5250-5261. doi:10.1093/nar/gki822

Beld M, Penning M, McMorrow M, Gorgels J, van den Hoek A, Goudsmit J. Different Hepatitis C Virus (HCV) RNA Load Profiles Following Seroconversion among Injecting Drug Users without Correlation with HCV Genotype and Serum Alanine Aminotransferase Levels. J Clin Microbiol. 1998;36(4):872-877.

Benson DA, Cavanaugh M, Clark K, et al. GenBank. Nucleic Acids Res. 2013;41(Database issue):D36-D42. doi:10.1093/nar/gks1195

Benson DA, Clark K, Karsch-Mizrachi I, Lipman DJ, Ostell J, Sayers EW. GenBank. Nucleic Acids Research. 2015;43(D1):D30-D35. doi:10.1093/nar/gku1216

Beutler E, Gelbart T, Kuhl W. Interference of heparin with the polymerase chain reaction. Biotechniques. 1990;9(2):166.

Bilofsky HS, Burks C, Fickett JW, et al. The GenBank genetic sequence databank. Nucleic Acids Res. 1986;14(1):1-4. doi:10.1093/nar/14.1.1

Blackard JT, Shata MT, Shire NJ, Sherman KE. Acute Hepatitis C Virus Infection: A Chronic Problem. Hepatology. 2008;47(1):321-331. doi:10.1002/hep.21902

Boone DJ, Hansen HJ, Hearn TL, Lewis DS, Dudley D. Laboratory evaluation and assistance efforts: mailed, on-site and blind proficiency testing surveys conducted by the Centers for Disease Control. Am J Public Health. 1982;72(12):1364-1368. doi:10.2105/ajph.72.12.1364

Brass V, Bieck E, Montserret R, et al. An amino-terminal amphipathic alpha-helix mediates membrane association of the hepatitis C virus nonstructural protein 5A. J Biol Chem. 2002;277(10):8130-8139. doi:10.1074/jbc.M111289200

Bressanelli S, Tomei L, Roussel A, et al. Crystal structure of the RNA-dependent RNA polymerase of hepatitis C virus. Proc Natl Acad Sci U S A. 1999;96(23):13034-13039. doi:10.1073/pnas.96.23.13034

Brown EA, Zhang H, Ping LH, Lemon SM. Secondary structure of the 5' nontranslated regions of hepatitis C virus and pestivirus genomic RNAs. Nucleic Acids Res. 1992;20(19):5041-5045. doi:10.1093/nar/20.19.5041

Bukh J, Miller RH, Purcell RH. Genetic heterogeneity of hepatitis C virus: quasispecies and genotypes. Semin Liver Dis. 1995;15(1):41-63. doi:10.1055/s-2007-1007262

Bukh J, Purcell RH, Miller RH. At least 12 genotypes of hepatitis C virus predicted by sequence analysis of the putative E1 gene of isolates collected worldwide. Proc Natl Acad Sci U S A. 1993;90(17):8234-8238.

Bukh J, Purcell RH, Miller RH. Importance of primer selection for the detection of hepatitis C virus RNA with the polymerase chain reaction assay. Proc Natl Acad Sci U S A. 1992;89(1):187-191. doi:10.1073/pnas.89.1.187

Bukh J, Purcell RH, Miller RH. Sequence analysis of the 5' noncoding region of hepatitis C virus. Proc Natl Acad Sci U S A. 1992;89(11):4942-4946.

Bulteel N, Partha Sarathy P, Forrest E, et al. Factors associated with spontaneous clearance of chronic hepatitis C virus infection. J Hepatol. 2016;65(2):266-272. doi:10.1016/j.jhep.2016.04.030

Burkardt HJ. Standardization and quality control of PCR analyses. Clin Chem Lab Med. 2000;38(2):87-91. doi:10.1515/CCLM.2000.014

Busch MP, Glynn SA, Stramer SL, et al. A new strategy for estimating risks of transfusion-transmitted viral infections based on rates of detection of recently infected donors. Transfusion. 2005;45(2):254-264. doi:10.1111/j.1537-2995.2004.04215.x

Busch MP, Kleinman SH, Jackson B, Stramer SL, Hewlett I, Preston S. Committee report. Nucleic acid amplification testing of blood donors for transfusion-transmitted infectious diseases: Report of the Interorganizational Task Force on Nucleic Acid Amplification Testing of Blood Donors. Transfusion. 2000;40(2):143-159. doi:10.1046/j.1537-2995.2000.40020143.x

Bustin S, Wittwer C. MIQE: A Step Toward More Robust and Reproducible Quantitative PCR. Clinical Chemistry. 2017;63:clinchem.2016.268953. doi:10.1373/clinchem.2016.268953

Bustin SA, Benes V, Garson J, et al. The need for transparency and good practices in the qPCR literature. Nat Methods. 2013;10(11):1063-1067. doi:10.1038/nmeth.2697

Bustin SA, Benes V, Garson JA, et al. The MIQE Guidelines: Minimum Information for Publication of Quantitative Real-Time PCR Experiments. Clinical Chemistry. 2009;55(4):611-622. doi:10.1373/clinchem.2008.112797

Bustin SA. Absolute quantification of mRNA using real-time reverse transcription polymerase chain reaction assays. J Mol Endocrinol. 2000;25(2):169-193. doi:10.1677/jme.0.0250169

Byrnes JJ, Downey KM, Esserman L, So AG. Mechanism of hemin inhibition of erythroid cytoplasmic DNA polymerase. Biochemistry. 1975;14(4):796-799. doi:10.1021/bi00675a023

Candotti D, Richetin A, Cant B, et al. Evaluation of a transcription-mediated amplification-based HCV and HIV-1 RNA duplex assay for screening individual blood donations: a comparison with a minipool testing system. Transfusion. 2003;43(2):215-225. doi:10.1046/j.1537-2995.2003.00308.x

Candotti D, Sarkodie F, Allain JP. Residual risk of transfusion in Ghana. Br J Haematol. 2001;113(1):37-39. doi:10.1046/j.1365-2141.2001.02679.x

Cantaloube JF, Laperche S, Gallian P, Bouchardeau F, de Lamballerie X, de Micco P. Analysis of the 5' noncoding region versus the NS5b region in genotyping hepatitis C virus isolates from blood donors in France. J Clin Microbiol. 2006;44(6):2051-2056. doi:10.1128/JCM.02463-05

Carithers RL, Emerson SS. Therapy of hepatitis C: meta-analysis of interferon alfa-2b trials. Hepatology. 1997;26(3 Suppl 1):83S-88S. doi:10.1002/hep.510260715

Carreño V, Bartolomé J, Castillo I, Quiroga JA. Occult hepatitis B virus and hepatitis C virus infections. Rev Med Virol. 2008;18(3):139-157. doi:10.1002/rmv.569

Carrère-Kremer S, Montpellier-Pala C, Cocquerel L, Wychowski C, Penin F, Dubuisson J. Subcellular Localization and Topology of the p7 Polypeptide of Hepatitis C Virus. J Virol. 2002;76(8):3720-3730. doi:10.1128/JVI.76.8.3720-3730.2002

Cashman SB, Marsden BD, Dustin LB. The Humoral Immune Response to HCV: Understanding is Key to Vaccine Development. Front Immunol. 2014;5:550. doi:10.3389/fimmu.2014.00550

Castillo I, Rodríguez-Iñigo E, Bartolomé J, et al. Hepatitis C virus replicates in peripheral blood mononuclear cells of patients with occult hepatitis C virus infection. Gut. 2005;54(5):682-685. doi:10.1136/gut.2004.057281

Cavalli-Sforza LL, Edwards AW. Phylogenetic analysis. Models and estimation procedures. Am J Hum Genet. 1967;19(3 Pt 1):233-257.

CDC, Updated U.S. Public Health Service Guidelines for the Management of Occupational Exposures to HBV, HCV, and HIV and Recommendations for Postexposure Prophylaxis.

Cha TA, Kolberg J, Irvine B, et al. Use of a signature nucleotide sequence of hepatitis C virus for detection of viral RNA in human serum and plasma. J Clin Microbiol. 1991;29(11):2528-2534. doi:10.1128/jcm.29.11.2528-2534.1991

Chang SC, Yen JH, Kang HY, Jang MH, Chang MF. Nuclear localization signals in the core protein of hepatitis C virus. Biochem Biophys Res Commun. 1994;205(2):1284-1290. doi:10.1006/bbrc.1994.2804

Chen Z, Weck KE. Hepatitis C virus genotyping: interrogation of the 5' untranslated region cannot accurately distinguish genotypes 1a and 1b. J Clin Microbiol. 2002;40(9):3127-3134. doi:10.1128/JCM.40.9.3127-3134.2002

Cheng JC, Chang MF, Chang SC. Specific interaction between the hepatitis C virus NS5B RNA polymerase and the 3' end of the viral RNA. J Virol. 1999;73(8):7044-7049. doi:10.1128/JVI.73.8.7044-7049.1999

Chevaliez S. Virological tools to diagnose and monitor hepatitis C virus infection. Clin Microbiol Infect. 2011;17(2):116-121. doi:10.1111/j.1469-0691.2010.03418.x

Chinchai T, Labout J, Noppornpanth S, et al. Comparative study of different methods to genotype hepatitis C virus type 6 variants. J Virol Methods. 2003;109(2):195-201. doi:10.1016/s0166-0934(03)00071-5

Choo QL, Kuo G, Weiner AJ, Overby LR, Bradley DW, Houghton M. Isolation of a cDNA clone derived from a blood-borne non-A, non-B viral hepatitis genome. Science. 1989;244(4902):359-362. doi:10.1126/science.2523562

Choo QL, Richman KH, Han JH, et al. Genetic organization and diversity of the hepatitis C virus. Proc Natl Acad Sci U S A. 1991;88(6):2451-2455.

Clarke B. Molecular virology of hepatitis C virus. J Gen Virol. 1997;78 (Pt 10):2397-2410. doi:10.1099/0022-1317-78-10-2397

Clemens JM, Taskar S, Chau K, et al. IgM antibody response in acute hepatitis C viral infection. Blood. 1992;79(1):169-172.

CLSI/NCCLS. 2003. Evaluation of the linearity of quantitative measurement procedures: a statistical approach. Approved guideline. CLSI document EP6-A. Clinical and Laboratory Standards Institute, Wayne, PA.

CLSI/NCCLS. 2003. Quantitative molecular methods for infectious diseases. Approved guideline. CLSI document MM06-A. Clinical and Laboratory Standards Institute, Wayne, PA.

CLSI/NCCLS. 2004. Protocols for determination for limits of detection and limits of quantitation. Approved guideline. CLSI document EP17-A. Clinical and Laboratory Standards Institute, Wayne, PA.

CLSI/NCCLS. 2008. Verification and validation of multiplex nucleic acid assays. Approved guideline. CLSI document MM17-A. Clinical and Laboratory Standards Institute, Wayne, PA.

Cobb BR, Vaks JE, Do T, Vilchez RA. Evolution in the sensitivity of quantitative HIV-1 viral load tests. J Clin Virol. 2011;52 Suppl 1:S77-82. doi:10.1016/j.jcv.2011.09.015

Cocquerel L, Meunier JC, Pillez A, Wychowski C, Dubuisson J. A retention signal necessary and sufficient for endoplasmic reticulum localization maps to the transmembrane domain of hepatitis C virus glycoprotein E2. J Virol. 1998;72(3):2183-2191. doi:10.1128/JVI.72.3.2183-2191.1998

Cocquerel L, Wychowski C, Minner F, Penin F, Dubuisson J. Charged residues in the transmembrane domains of hepatitis C virus glycoproteins play a major

role in the processing, subcellular localization, and assembly of these envelope proteins. J Virol. 2000;74(8):3623-3633. doi:10.1128/jvi.74.8.3623-3633.2000

Code of Federal Regulations. 2009. Title 42. Public health, vol. 4, chapter V. Health Care Financing Administration, Department of Health and Human Services, part 493. Laboratory requirements, section 493.1253. Standard: establishment and verification of performance specifications. U.S. Government Printing Office, Washington, DC.

Code of Federal Regulations. 2009. Title 42. Public health, vol. 4, chapter V. Health Care Financing Administration, Department of Health and Human Services, part 493. Laboratory requirements, section 493.2. Definitions. U.S. Government Printing Office, Washington, DC.

Code of Federal Regulations. 2010. Title 21. Food and drugs, vol. 8, chapter 1. Food and Drug Administration, Department of Health and Human Services, part 809. In vitro diagnostic products for human use, section 809.30. Restrictions on the sale, distribution and use of analyte specific reagents. U.S. Government Printing Office, Washington, DC.

Code of Federal Regulations. 2010. Title 21. Food and drugs, vol. 8, chapter 1. Food and Drug Administration, Department of Health and Human Services, part 820. Quality system regulation. U.S. Government Printing Office, Washington, DC.

Colin C, Lanoir D, Touzet S, et al. Sensitivity and specificity of third-generation hepatitis C virus antibody detection assays: an analysis of the literature. J Viral Hepat. 2001;8(2):87-95. doi:10.1046/j.1365-2893.2001.00280.x

Cooke GS, Lemoine M, Thursz M, et al. Viral hepatitis and the Global Burden of Disease: a need to regroup. J Viral Hepat. 2013;20(9):600-601. doi:10.1111/jvh.12123

Corbet S, Bukh J, Heinsen A, Fomsgaard A. Hepatitis C Virus Subtyping by a Core-Envelope 1-Based Reverse Transcriptase PCR Assay with Sequencing and Its Use in Determining Subtype Distribution among Danish Patients. J Clin Microbiol. 2003;41(3):1091-1100. doi:10.1128/JCM.41.3.1091-1100.2003

Cronin M, Ghosh K, Sistare F, Quackenbush J, Vilker V, O'Connell C. Universal RNA Reference Materials for Gene Expression. Clinical Chemistry. 2004;50(8):1464-1471. doi:10.1373/clinchem.2004.035675

D'Ambrosio R, Degasperi E, Colombo M, Aghemo A. Direct-acting antivirals: the endgame for hepatitis C? Curr Opin Virol. 2017;24:31-37. doi:10.1016/j.coviro.2017.03.017

D'Oliveira A, Voirin N, Allard R, et al. Prevalence and sexual risk of hepatitis C virus infection when human immunodeficiency virus was acquired through sexual intercourse among patients of the Lyon University Hospitals, France,

1992-2002. J Viral Hepat. 2005;12(3):330-332. doi:10.1111/j.1365-2893.2005.00583.x

Das BR, Kundu B, Khandapkar R, Sahni S. Geographical distribution of hepatitis C virus genotypes in India. Indian J Pathol Microbiol. 2002;45(3):323-328.

David MW, Theo PS. Clinical Virology. In: Dorak MT, editor. Real-Time PCR. Taylor and Francis, USA; 2006. p. 39-62.

Davidson F, Simmonds P, Ferguson JC, et al. Survey of major genotypes and subtypes of hepatitis C virus using RFLP of sequences amplified from the 5' non-coding region. J Gen Virol. 1995;76 (Pt 5):1197-1204. doi:10.1099/0022-1317-76-5-1197

Davis GL. Hepatitis C virus genotypes and quasispecies. The American Journal of Medicine. 1999;107(6):21-26. doi:10.1016/S0002-9343(99)00376-9

De Marco L, Gillio-Tos A, Fiano V, et al. Occult HCV Infection: An Unexpected Finding in a Population Unselected for Hepatic Disease. PLoS One. 2009;4(12):e8128. doi:10.1371/journal.pone.0008128

Deleersnyder V, Pillez A, Wychowski C, et al. Formation of native hepatitis C virus glycoprotein complexes. J Virol. 1997;71(1):697-704. doi:10.1128/JVI.71.1.697-704.1997

Dhiman RK, Satsangi S, Grover GS, Puri P. Tackling the Hepatitis C Disease Burden in Punjab, India. J Clin Exp Hepatol. 2016;6(3):224-232. doi:10.1016/j.jceh.2016.09.005

Dhiman RK. Future of therapy for Hepatitis C in India: A Matter of Accessibility and Affordability? J Clin Exp Hepatol. 2014;4(2):85-86. doi:10.1016/j.jceh.2014.06.011

Di Bisceglie AM, Goodman ZD, Ishak KG, Hoofnagle JH, Melpolder JJ, Alter HJ. Long-term clinical and histopathological follow-up of chronic posttransfusion hepatitis. Hepatology. 1991;14(6):969-974. doi:10.1016/0270-9139(91)90113-a

Di Marco S, Volpari C, Tomei L, et al. Interdomain communication in hepatitis C virus polymerase abolished by small molecule inhibitors bound to a novel allosteric site. J Biol Chem. 2005;280(33):29765-29770. doi:10.1074/jbc.M505423200

Díaz-Toledano R, Ariza-Mateos A, Birk A, Martínez-García B, Gómez J. In vitro characterization of a miR-122-sensitive double-helical switch element in the 5′ region of hepatitis C virus RNA. Nucleic Acids Res. 2009;37(16):5498-5510. doi:10.1093/nar/gkp553

Didenko VV. DNA probes using fluorescence resonance energy transfer (FRET): designs and applications. Biotechniques. 2001;31(5):1106-1116, 1118, 1120-1121. doi:10.2144/01315rv02

Dijkstra J, van Kempen L, Nagtegaal I, Bustin S. Critical appraisal of quantitative PCR results in colorectal cancer research: Can we rely on published qPCR results? Molecular oncology. 2014;8. doi:10.1016/j.molonc.2013.12.016

Dooms M, Chango A, Abdel-Nour A. Quantitative PCR (qPCR) and the Guide to good practices MIQE: adapting and relevance in the clinical biology context. Annales de biologie clinique. 2014;72(3):265-269. doi:10.1684/abc.2014.0955

Dorak MT. Real-Time PCR.; 2007. Accessed June 27, 2022. https://public.ebookcentral.proquest.com/choice/publicfullrecord.aspx?p=292841

Drexler JF, Kupfer B, Petersen N, et al. A Novel Diagnostic Target in the Hepatitis C Virus Genome. PLOS Medicine. 2009;6(2):e1000031. doi:10.1371/journal.pmed.1000031

Dustin LB, Cashman SB, Laidlaw SM. Immune control and failure in HCV infection—tipping the balance. J Leukoc Biol. 2014;96(4):535-548. doi:10.1189/jlb.4RI0214-126R

Efron B, Gong G. A Leisurely Look at the Bootstrap, the Jackknife, and Cross-Validation. The American Statistician. 1983;37(1):36-48. doi:10.2307/2685844

Egger D, Wölk B, Gosert R, et al. Expression of hepatitis C virus proteins induces distinct membrane alterations including a candidate viral replication complex. J Virol. 2002;76(12):5974-5984. doi:10.1128/jvi.76.12.5974-5984.2002

Elazar M, Cheong KH, Liu P, Greenberg HB, Rice CM, Glenn JS. Amphipathic helix-dependent localization of NS5A mediates hepatitis C virus RNA replication. J Virol. 2003;77(10):6055-6061. doi:10.1128/jvi.77.10.6055-6061.2003

Elazar M, Liu P, Rice CM, Glenn JS. An N-Terminal Amphipathic Helix in Hepatitis C Virus (HCV) NS4B Mediates Membrane Association, Correct Localization of Replication Complex Proteins, and HCV RNA Replication. J Virol. 2004;78(20):11393-11400. doi:10.1128/JVI.78.20.11393-11400.2004

El-Zanaty F. Egypt Demographic and Health Survey 2008. :463.

Enomoto N, Takada A, Nakao T, Date T. There are two major types of hepatitis C virus in Japan. Biochemical and Biophysical Research Communications. 1990;170(3):1021-1025. doi:10.1016/0006-291X(90)90494-8

Espy MJ, Uhl JR, Sloan LM, et al. Real-Time PCR in Clinical Microbiology: Applications for Routine Laboratory Testing. Clin Microbiol Rev. 2006;19(1):165-256. doi:10.1128/CMR.19.1.165-256.2006

Eyster ME, Alter HJ, Aledort LM, Quan S, Hatzakis A, Goedert JJ. Heterosexual co-transmission of hepatitis C virus (HCV) and human immunodeficiency virus (HIV). Ann Intern Med. 1991;115(10):764-768. doi:10.7326/0003-4819-115-10-764

Farci P, Alter HJ, Wong D, et al. A long-term study of hepatitis C virus replication in non-A, non-B hepatitis. N Engl J Med. 1991;325(2):98-104. doi:10.1056/NEJM199107113250205

Feeney ER, Chung RT. Antiviral treatment of hepatitis C. BMJ. 2014;348:g3308. doi:10.1136/bmj.g3308

Felsenstein J. Confidence Limits on Phylogenies: An Approach Using the Bootstrap. Evolution. 1985;39(4):783-791. doi:10.2307/2408678

Flint M, McKeating JA. The role of the hepatitis C virus glycoproteins in infection. Reviews in Medical Virology. 2000;10(2):101-117. doi:10.1002/(SICI)1099-1654(200003/04)10:2<101::AID-RMV268>3.0.CO;2-W

Florese RH, Nagano-Fujii M, Iwanaga Y, Hidajat R, Hotta H. Inhibition of protein synthesis by the nonstructural proteins NS4A and NS4B of hepatitis C virus. Virus Res. 2002;90(1-2):119-131. doi:10.1016/s0168-1702(02)00146-6

Franck N, Le Seyec J, Guguen-Guillouzo C, Erdtmann L. Hepatitis C Virus NS2 Protein Is Phosphorylated by the Protein Kinase CK2 and Targeted for Degradation to the Proteasome. J Virol. 2005;79(5):2700-2708. doi:10.1128/JVI.79.5.2700-2708.2005

Frank C, Mohamed MK, Strickland GT, et al. The role of parenteral antischistosomal therapy in the spread of hepatitis C virus in Egypt. Lancet. 2000;355(9207):887-891. doi:10.1016/s0140-6736(99)06527-7

Freiman JM, Tran TM, Schumacher SG, et al. Hepatitis C Core Antigen Testing for Diagnosis of Hepatitis C Virus Infection: A Systematic Review and Meta-analysis. Ann Intern Med. 2016;165(5):345-355. doi:10.7326/M16-0065

Friebe P, Bartenschlager R. Genetic analysis of sequences in the 3' nontranslated region of hepatitis C virus that are important for RNA replication. J Virol. 2002;76(11):5326-5338. doi:10.1128/jvi.76.11.5326-5338.2002

Fytili P, Tiemann C, Wang C, et al. Frequency of very low HCV viremia detected by a highly sensitive HCV-RNA assay. J Clin Virol. 2007;39(4):308-311. doi:10.1016/j.jcv.2007.05.007

Gale MJ, Korth MJ, Katze MG. Repression of the PKR protein kinase by the hepatitis C virus NS5A protein: a potential mechanism of interferon resistance. Clin Diagn Virol. 1998;10(2-3):157-162. doi:10.1016/s0928-0197(98)00034-8

Gao L, Aizaki H, He JW, Lai MMC. Interactions between Viral Nonstructural Proteins and Host Protein hVAP-33 Mediate the Formation of Hepatitis C Virus RNA Replication Complex on Lipid Raft. J Virol. 2004;78(7):3480-3488. doi:10.1128/JVI.78.7.3480-3488.2004

Gardner JP, Durso RJ, Arrigale RR, et al. L-SIGN (CD 209L) is a liver-specific capture receptor for hepatitis C virus. Proc Natl Acad Sci U S A. 2003;100(8):4498-4503. doi:10.1073/pnas.0831128100

Garson JA, Tedder RS, Briggs M, et al. Detection of hepatitis C viral sequences in blood donations by "nested" polymerase chain reaction and prediction of infectivity. The Lancet. 1990;335(8703):1419-1422. doi:10.1016/0140-6736(90)91446-H

Germer JJ, Rys PN, Thorvilson JN, Persing DH. Determination of Hepatitis C Virus Genotype by Direct Sequence Analysis of Products Generated with the Amplicor HCV Test. J Clin Microbiol. 1999;37(8):2625-2630.

Global hepatitis report, 2017. Accessed June 17, 2022. https://www.who.int/publications-detail-redirect/9789241565455

Glynn SA, Wright DJ, Kleinman SH, et al. Dynamics of viremia in early hepatitis C virus infection. Transfusion. 2005;45(6):994-1002. doi:10.1111/j.1537-2995.2005.04390.x

Golemba MD, Culasso ACA, Villamil FG, et al. Hepatitis C Virus Diversification in Argentina: Comparative Analysis between the Large City of Buenos Aires and the Small Rural Town of O'Brien. PLOS ONE. 2013;8(12):e84007. doi:10.1371/journal.pone.0084007

Gowans EJ. Distribution of markers of hepatitis C virus infection throughout the body. Semin Liver Dis. 2000;20(1):85-102. doi:10.1055/s-2000-9503

Gower E, Estes C, Blach S, Razavi-Shearer K, Razavi H. Global epidemiology and genotype distribution of the hepatitis C virus infection. J Hepatol. 2014;61(1 Suppl):S45-57. doi:10.1016/j.jhep.2014.07.027

Grakoui A, McCourt DW, Wychowski C, Feinstone SM, Rice CM. A second hepatitis C virus-encoded proteinase. Proc Natl Acad Sci U S A. 1993c;90(22):10583-10587.

Grakoui A, Wychowski C, Lin C, Feinstone SM, Rice CM. Expression and identification of hepatitis C virus polyprotein cleavage products. J Virol. 1993;67(3):1385-1395. doi:10.1128/JVI.67.3.1385-1395.1993

Grebely J, Conway B, Raffa JD, Lai C, Krajden M, Tyndall MW. Hepatitis C virus reinfection in injection drug users. Hepatology. 2006;44(5):1139-1145. doi:10.1002/hep.21376

Greub G, Sahli R, Brouillet R, Jaton K. Ten years of R&D and full automation in molecular diagnosis. Future Microbiol. 2016;11(3):403-425. doi:10.2217/fmb.15.152

Guidelines for Laboratory Testing and Result Reporting of Antibody to Hepatitis C Virus. Accessed June 27, 2022. https://www.cdc.gov/mmwr/preview/mmwrhtml/rr5203a1.htm

Gwack Y, Kim DW, Han JH, Choe J. DNA helicase activity of the hepatitis C virus nonstructural protein 3. Eur J Biochem. 1997;250(1):47-54. doi:10.1111/j.1432-1033.1997.00047.x

Hagan LM, Schinazi RF. Best strategies for global HCV eradication. Liver Int. 2013;33 Suppl 1:68-79. doi:10.1111/liv.12063

Hajarizadeh B, Grebely J, Dore GJ. Epidemiology and natural history of HCV infection. Nat Rev Gastroenterol Hepatol. 2013;10(9):553-562. doi:10.1038/nrgastro.2013.107

Han JH, Shyamala V, Richman KH, et al. Characterization of the terminal regions of hepatitis C viral RNA: identification of conserved sequences in the 5' untranslated region and poly(A) tails at the 3' end. Proc Natl Acad Sci U S A. 1991;88(5):1711-1715.

Harada S, Watanabe Y, Takeuchi K, et al. Expression of processed core protein of hepatitis C virus in mammalian cells. J Virol. 1991;65(6):3015-3021.

Hartwell D, Jones J, Baxter L, Shepherd J. Peginterferon alfa and ribavirin for chronic hepatitis C in patients eligible for shortened treatment, re-treatment or in HCV/HIV co-infection: a systematic review and economic evaluation. Health Technol Assess. 2011;15(17):i-xii, 1-210. doi:10.3310/hta15170

Hedskog C, Doehle B, Chodavarapu K, et al. Characterization of hepatitis C virus intergenotypic recombinant strains and associated virological response to sofosbuvir/ribavirin. Hepatology. 2015;61(2):471-480. doi:10.1002/hep.27361

Heid CA, Stevens J, Livak KJ, Williams PM. Real time quantitative PCR. Genome Res. 1996;6(10):986-994. doi:10.1101/gr.6.10.986

Hepatitis C Guidance 2018 Update: AASLD-IDSA Recommendations for Testing, Managing, and Treating Hepatitis C Virus Infection. Clin Infect Dis. 2018;67(10):1477-1492. doi:10.1093/cid/ciy585

Higuchi R, Dollinger G, Walsh PS, Griffith R. Simultaneous amplification and detection of specific DNA sequences. Biotechnology (N Y). 1992;10(4):413-417. doi:10.1038/nbt0492-413

Higuchi R, Fockler C, Dollinger G, Watson R. Kinetic PCR Analysis: Real-time Monitoring of DNA Amplification Reactions. Bio/Technology. 1993;11(9):1026-1030. doi:10.1038/nbt0993-1026

Higuchi R, Fockler C, Dollinger G, Watson R. Kinetic PCR analysis: real-time monitoring of DNA amplification reactions. Biotechnology (N Y). 1993;11(9):1026-1030. doi:10.1038/nbt0993-1026

Hijikata M, Kato N, Mori S, et al. Frequent Detection of Hepatitis C Virus US Strain in Japanese Hemophiliacs. Japanese Journal of Cancer Research. 1990;81(12):1195-1197. doi:10.1111/j.1349-7006.1990.tb02676.x

Hijikata M, Kato N, Ootsuyama Y, Nakagawa M, Ohkoshi S, Shimotohno K. Hypervariable regions in the putative glycoprotein of hepatitis C virus. Biochemical and Biophysical Research Communications. 1991;175(1):220-228. doi:10.1016/S0006-291X(05)81223-9

Hijikata M, Shimizu YK, Kato H, et al. Equilibrium centrifugation studies of hepatitis C virus: evidence for circulating immune complexes. J Virol. 1993;67(4):1953-1958.

Hisada M, Chatterjee N, Kalaylioglu Z, Battjes RJ, Goedert JJ. Hepatitis C virus load and survival among injection drug users in the United States. Hepatology. 2005;42(6):1446-1452. doi:10.1002/hep.20938

Hoefs JC, Aulakh VS, Ilagan BJ. Very low viral load (VLVL) relapse following treatment of naïve patients with chronic hepatitis C. Dig Dis Sci. 2012;57(1):243-249. doi:10.1007/s10620-011-1973-7

Hofer H, Watkins-Riedel T, Janata O, et al. Spontaneous viral clearance in patients with acute hepatitis C can be predicted by repeated measurements of serum viral load. Hepatology. 2003;37(1):60-64. doi:10.1053/jhep.2003.50019

Hoffman B, Liu Q. Hepatitis C viral protein translation: mechanisms and implications in developing antivirals. Liver Int. 2011;31(10):1449-1467. doi:10.1111/j.1478-3231.2011.02543.x

Holland PM, Abramson RD, Watson R, Gelfand DH. Detection of specific polymerase chain reaction product by utilizing the 5'----3' exonuclease activity of Thermus aquaticus DNA polymerase. Proc Natl Acad Sci U S A. 1991;88(16):7276-7280. doi:10.1073/pnas.88.16.7276

Honda M, Beard MR, Ping LH, Lemon SM. A phylogenetically conserved stem-loop structure at the 5' border of the internal ribosome entry site of hepatitis C virus is required for cap-independent viral translation. J Virol. 1999a;73(2):1165-1174. doi:10.1128/JVI.73.2.1165-1174.1999

Honda M, Brown EA, Lemon SM. Stability of a stem-loop involving the initiator AUG controls the efficiency of internal initiation of translation on hepatitis C virus RNA. RNA. 1996a;2(10):955-968.

Honda M, Ping LH, Rijnbrand RC, et al. Structural requirements for initiation of translation by internal ribosome entry within genome-length hepatitis C virus RNA. Virology. 1996;222(1):31-42. doi:10.1006/viro.1996.0395

Hoofnagle JH. Hepatitis C: the clinical spectrum of disease. Hepatology. 1997;26(3 Suppl 1):15S-20S. doi:10.1002/hep.510260703

Hsu M, Zhang J, Flint M, et al. Hepatitis C virus glycoproteins mediate pH-dependent cell entry of pseudotyped retroviral particles. Proc Natl Acad Sci U S A. 2003;100(12):7271-7276. doi:10.1073/pnas.0832180100

Huggett J, Dheda K, Bustin S, Zumla A. Real-time RT-PCR normalisation; strategies and considerations. Genes Immun. 2005;6(4):279-284. doi:10.1038/sj.gene.6364190

Huggett JF, Foy CA, Benes V, et al. The digital MIQE guidelines: Minimum Information for Publication of Quantitative Digital PCR Experiments. Clin Chem. 2013;59(6):892-902. doi:10.1373/clinchem.2013.206375

Hügle T, Fehrmann F, Bieck E, et al. The hepatitis C virus nonstructural protein 4B is an integral endoplasmic reticulum membrane protein. Virology. 2001;284(1):70-81. doi:10.1006/viro.2001.0873

Hwang SB, Park KJ, Kim YS, Sung YC, Lai MM. Hepatitis C virus NS5B protein is a membrane-associated phosphoprotein with a predominantly perinuclear localization. Virology. 1997;227(2):439-446. doi:10.1006/viro.1996.8357

Ijaz B, Ahmad W, Javed FT, et al. Association of laboratory parameters with viral factors in patients with hepatitis C. Virology Journal. 2011;8(1):361. doi:10.1186/1743-422X-8-361

International Organization for Standardization. 2006. Statistics—vocabulary and symbols, part 1. Probability and general statistical terms. ISO 3534-1. International Organization for Standardization, Geneva, Switzerland

International Organization for Standardization. 2007. Medical laboratories—particular requirements for quality and competence. ISO 15189, 2nd ed. International Organization for Standardization, Geneva, Switzerland.

Ito T, Lai MM. Determination of the secondary structure of and cellular protein binding to the 3'-untranslated region of the hepatitis C virus RNA genome. J Virol. 1997;71(11):8698-8706.

Jafari S, Copes R, Baharlou S, Etminan M, Buxton J. Tattooing and the risk of transmission of hepatitis C: a systematic review and meta-analysis. Int J Infect Dis. 2010;14(11):e928-940. doi:10.1016/j.ijid.2010.03.019

Ji H, Fraser CS, Yu Y, Leary J, Doudna JA. Coordinated assembly of human translation initiation complexes by the hepatitis C virus internal ribosome entry site RNA. Proc Natl Acad Sci U S A. 2004;101(49):16990-16995. doi:10.1073/pnas.0407402101

Johnson G, Nolan T, Bustin SA. Real-time quantitative PCR, pathogen detection and MIQE. Methods Mol Biol. 2013;943:1-16. doi:10.1007/978-1-60327-353-4_1

José M, Gajardo R, Jorquera JI. Stability of HCV, HIV-1 and HBV nucleic acids in plasma samples under long-term storage. Biologicals. 2005;33(1):9-16. doi:10.1016/j.biologicals.2004.10.003

Joseph AM, Yathi KK, Jacob J. Analysis of Internal Controls in the matrix of HCV RT-PCR assays showed analytical and pre-analytical influences independent of template concentrations. 2022;13:11.

Kadoya H, Nagano-Fujii M, Deng L, Nakazono N, Hotta H. Nonstructural proteins 4A and 4B of hepatitis C virus transactivate the interleukin 8 promoter. Microbiol Immunol. 2005;49(3):265-273. doi:10.1111/j.1348-0421.2005.tb03728.x

Kalra J. Medical errors: impact on clinical laboratories and other critical areas. Clin Biochem. 2004;37(12):1052-1062. doi:10.1016/j.clinbiochem.2004.08.009

Kamili S, Drobeniuc J, Araujo AC, Hayden TM. Laboratory diagnostics for hepatitis C virus infection. Clin Infect Dis. 2012;55 Suppl 1:S43-48. doi:10.1093/cid/cis368

Kaminuma E, Kosuge T, Kodama Y, et al. DDBJ progress report. Nucleic Acids Res. 2011;39(Database issue):D22-27. doi:10.1093/nar/gkq1041

Kanehisa M, Fickett JW, Goad WB. A relational database system for the maintenance and verification of the Los Alamos sequence library. Nucleic Acids Res. 1984;12(1 Pt 1):149-158.

Kao JH, Lai MY, Hwang YT, et al. Chronic hepatitis C without anti-hepatitis C antibodies by second-generation assay. A clinicopathologic study and demonstration of the usefulness of a third-generation assay. Dig Dis Sci. 1996;41(1):161-165. doi:10.1007/BF02208599

Karsch-Mizrachi I, Nakamura Y, Cochrane G. The International Nucleotide Sequence Database Collaboration. Nucleic Acids Res. 2012;40(Database issue):D33-D37. doi:10.1093/nar/gkr1006

Karsch-Mizrachi I, Takagi T, Cochrane G, International Nucleotide Sequence Database Collaboration. The international nucleotide sequence database collaboration. Nucleic Acids Res. 2018;46(D1):D48-D51. doi:10.1093/nar/gkx1097

Karuru JW, Lule GN, Joshi M, Anzala O. Prevalence of HCV and HCV/HIV co-infection among in-patients at the Kenyatta National Hospital. East Afr Med J. 2005;82(4):170-172. doi:10.4314/eamj.v82i4.9276

Kato J, Kato N, Yoshida H, Ono-Nita SK, Shiratori Y, Omata M. Hepatitis C virus NS4A and NS4B proteins suppress translation in vivo. J Med Virol. 2002;66(2):187-199. doi:10.1002/jmv.2129

Kato N, Yokosuka O, Omata M, Hosoda K, Ohto M. Detection of hepatitis C virus ribonucleic acid in the serum by amplification with polymerase chain reaction. J Clin Invest. 1990;86(5):1764-1767.

Kato N. Genome of human hepatitis C virus (HCV): gene organization, sequence diversity, and variation. Microb Comp Genomics. 2000;5(3):129-151. doi:10.1089/omi.1.2000.5.129

Kelley LA, Mezulis S, Yates CM, Wass MN, Sternberg MJE. The Phyre2 web portal for protein modeling, prediction and analysis. Nat Protoc. 2015;10(6):845-858. doi:10.1038/nprot.2015.053

Khan AG, Whidby J, Miller MT, et al. Structure of the core ectodomain of the hepatitis C virus envelope glycoprotein 2. Nature. 2014;509(7500):381-384. doi:10.1038/nature13117

Klein D. Quantification using real-time PCR technology: applications and limitations. Trends Mol Med. 2002;8(6):257-260. doi:10.1016/s1471-4914(02)02355-9

Kleppe K, Ohtsuka E, Kleppe R, Molineux I, Khorana HG. Studies on polynucleotides. XCVI. Repair replications of short synthetic DNA's as catalyzed by DNA polymerases. J Mol Biol. 1971;56(2):341-361. doi:10.1016/0022-2836(71)90469-4

Klevens RM, Hu DJ, Jiles R, Holmberg SD. Evolving epidemiology of hepatitis C virus in the United States. Clin Infect Dis. 2012;55 Suppl 1:S3-9. doi:10.1093/cid/cis393

Kolaskar AS, Tongaonkar PC. A semi-empirical method for prediction of antigenic determinants on protein antigens. *FEBS Lett*. 1990;276(1-2):172-174.

Kolykhalov AA, Feinstone SM, Rice CM. Identification of a highly conserved sequence element at the 3’ terminus of hepatitis C virus genome RNA. J Virol. 1996;70(6):3363-3371. doi:10.1128/JVI.70.6.3363-3371.1996

Kong L, Giang E, Nieusma T, et al. Hepatitis C virus E2 envelope glycoprotein core structure. Science. 2013;342(6162):1090-1094. doi:10.1126/science.1243876

Krajden M. Hepatitis C Virus Diagnosis and Testing. Can J Public Health. 2000;91(Suppl 1):S36-S42. doi:10.1007/BF03405108

Kralik P, Ricchi M. A Basic Guide to Real Time PCR in Microbial Diagnostics: Definitions, Parameters, and Everything. Frontiers in Microbiology. 2017;8.

Kubista M, Andrade JM, Bengtsson M, et al. The real-time polymerase chain reaction. Mol Aspects Med. 2006;27(2-3):95-125. doi:10.1016/j.mam.2005.12.007

Kubo Y, Takeuchi K, Boonmar S, et al. A cDNA fragment of hepatitis C virus isolated from an implicated donor of post-transfusion non-A, non-B hepatitis in Japan. Nucleic Acids Res. 1989;17(24):10367-10372.

Kuiken C, Hraber P, Thurmond J, Yusim K. The hepatitis C sequence database in Los Alamos. Nucleic Acids Res. 2008;36(Database issue):D512-D516. doi:10.1093/nar/gkm962

Kuiken C, Simmonds P. Nomenclature and numbering of the hepatitis C virus. Methods Mol Biol. 2009;510:33-53. doi:10.1007/978-1-59745-394-3_4

Kumasaka K, Kawano K, Yamaguchi K, et al. A study of quality assessment in clinical microbiology performance of independent laboratories in Tokyo: 18-year participation in the Tokyo Metropolitan Government External Quality Assessment Program. Journal of Infection and Chemotherapy. 2001;7(2):102-109. doi:10.1007/s101560100016

Kuo G, Choo QL, Alter HJ, et al. An assay for circulating antibodies to a major etiologic virus of human non-A, non-B hepatitis. Science. 1989;244(4902):362-364. doi:10.1126/science.2496467

Laperche S, Lunel F, Izopet J, et al. Comparison of Hepatitis C Virus NS5b and 5′ Noncoding Gene Sequencing Methods in a Multicenter Study. J Clin Microbiol. 2005;43(2):733-739. doi:10.1128/JCM.43.2.733-739.2005

Larghi A, Zuin M, Crosignani A, et al. Outcome of an outbreak of acute hepatitis C among healthy volunteers participating in pharmacokinetics studies. Hepatology. 2002;36(4 Pt 1):993-1000. doi:10.1053/jhep.2002.36129

Larsen JE, Lund O, Nielsen M. Improved method for predicting linear B-cell epitopes. *Immunome Res*. 2006;2:2. Published 2006 Apr 24. doi:10.1186/1745-7580-2-2

Laskus T, Radkowski M, Piasek A, et al. Hepatitis C virus in lymphoid cells of patients coinfected with human immunodeficiency virus type 1: evidence of active replication in monocytes/macrophages and lymphocytes. J Infect Dis. 2000;181(2):442-448. doi:10.1086/315283

Lavanchy D. Evolving epidemiology of hepatitis C virus. Clin Microbiol Infect. 2011;17(2):107-115. doi:10.1111/j.1469-0691.2010.03432.x

Lavanchy D. The global burden of hepatitis C. Liver Int. 2009;29 Suppl 1:74-81. doi:10.1111/j.1478-3231.2008.01934.x

Lee H, Shin H, Wimmer E, Paul AV. cis-Acting RNA Signals in the NS5B C-Terminal Coding Sequence of the Hepatitis C Virus Genome. J Virol. 2004;78(20):10865-10877. doi:10.1128/JVI.78.20.10865-10877.2004

Leinonen R, Akhtar R, Birney E, et al. The European Nucleotide Archive. Nucleic Acids Res. 2011;39(Database issue):D28-31. doi:10.1093/nar/gkq967

Lesburg CA, Cable MB, Ferrari E, Hong Z, Mannarino AF, Weber PC. Crystal structure of the RNA-dependent RNA polymerase from hepatitis C virus reveals a fully encircled active site. Nat Struct Biol. 1999;6(10):937-943. doi:10.1038/13305

Li Y, Masaki T, Lemon SM. miR-122 and the Hepatitis C RNA genome. RNA Biol. 2013;10(6):919-923. doi:10.4161/rna.25137

Lievens A, Van Aelst S, Van den Bulcke M, Goetghebeur E. Enhanced analysis of real-time PCR data by using a variable efficiency model: FPK-PCR. Nucleic Acids Res. 2012;40(2):e10. doi:10.1093/nar/gkr775

Lifetechnologies. Real-time PCR handbook. https://www.thermofischer.com/in/en/home/india/molecular-biology-start-to-end-solutions/handbook-downlod.html

Lin C, Thomson JA, Rice CM. A central region in the hepatitis C virus NS4A protein allows formation of an active NS3-NS4A serine proteinase complex in vivo and in vitro. J Virol. 1995;69(7):4373-4380.

Lin C, Wu JW, Hsiao K, Su MS. The hepatitis C virus NS4A protein: interactions with the NS4B and NS5A proteins. J Virol. 1997;71(9):6465-6471.

Lin CC, Hwang SJ, Chiou ST, et al. The prevalence and risk factors analysis of serum antibody to hepatitis C virus in the elders in northeast Taiwan. J Chin Med Assoc. 2003;66(2):103-108.

Lindenbach BD, Rice CM. The ins and outs of hepatitis C virus entry and assembly. Nat Rev Microbiol. 2013;11(10):688-700. doi:10.1038/nrmicro3098

Lindenbach BD, Rice CM. Unravelling hepatitis C virus replication from genome to function. Nature. 2005;436(7053):933-938. doi:10.1038/nature04077

Liu W, Saint DA. Validation of a quantitative method for real time PCR kinetics. Biochem Biophys Res Commun. 2002;294(2):347-353. doi:10.1016/S0006-291X(02)00478-3

Lohmann V. Hepatitis C virus RNA replication. Curr Top Microbiol Immunol. 2013;369:167-198. doi:10.1007/978-3-642-27340-7_7

Lole KS, Bollinger RC, Paranjape RS, et al. Full-length human immunodeficiency virus type 1 genomes from subtype C-infected seroconverters in India, with evidence of intersubtype recombination. J Virol. 1999;73(1):152-160. doi:10.1128/JVI.73.1.152-160.1999

Lozach P yves, Lortat-Jacob H, de Lacroix de Lavalette A, et al. DC-SIGN and L-SIGN are high affinity binding receptors for hepatitis C virus glycoprotein E2. Journal of Biological Chemistry. 2003;278(22):20358-20366. doi:10.1074/jbc.M301284200

Lozach PY, Amara A, Bartosch B, et al. C-type lectins L-SIGN and DC-SIGN capture and transmit infectious hepatitis C virus pseudotype particles. J Biol Chem. 2004;279(31):32035-32045. doi:10.1074/jbc.M402296200

Lundin M, Monné M, Widell A, von Heijne G, Persson MAA. Topology of the Membrane-Associated Hepatitis C Virus Protein NS4B. J Virol. 2003;77(9):5428-5438. doi:10.1128/JVI.77.9.5428-5438.2003

Ly KN, Hughes EM, Jiles RB, Holmberg SD. Rising Mortality Associated With Hepatitis C Virus in the United States, 2003-2013. Clin Infect Dis. 2016;62(10):1287-1288. doi:10.1093/cid/ciw111

Maaroufi Y, de Bruyne JM, Duchateau V, Scheen R, Crokaert F. Development of a multiple internal control for clinical diagnostic real-time amplification assays. FEMS Immunology & Medical Microbiology. 2006;48(2):183-191. doi:10.1111/j.1574-695X.2006.00125.x

Maggi F, Focosi D, Pistello M. How Current Direct-Acting Antiviral and Novel Cell Culture Systems for HCV are Shaping Therapy and Molecular Diagnosis of Chronic HCV Infection? Curr Drug Targets. 2017;18(7):811-825. doi:10.2174/1389450116666150806123119

Manns MP, McHutchison JG, Gordon SC, et al. Peginterferon alfa-2b plus ribavirin compared with interferon alfa-2b plus ribavirin for initial treatment of chronic hepatitis C: a randomised trial. Lancet. 2001;358(9286):958-965. doi:10.1016/s0140-6736(01)06102-5

Manns MP, Wedemeyer H, Cornberg M. Treating viral hepatitis C: efficacy, side effects, and complications. Gut. 2006;55(9):1350-1359. doi:10.1136/gut.2005.076646

Marx MA, Murugavel KG, Sivaram S, et al. The association of health-care use and hepatitis C virus infection in a random sample of urban slum community residents in southern India. Am J Trop Med Hyg. 2003;68(2):258-262.

Mason G, Provero P, Vaira AM, Accotto GP. Estimating the number of integrations in transformed plants by quantitative real-time PCR. BMC Biotechnology. 2002;2(1):20. doi:10.1186/1472-6750-2-20

Mast EE, Hwang LY, Seto DSY, et al. Risk factors for perinatal transmission of hepatitis C virus (HCV) and the natural history of HCV infection acquired in infancy. J Infect Dis. 2005;192(11):1880-1889. doi:10.1086/497701

Mateescu RB, Rimbaş M, Stăniceanu F, et al. Histological and nonhistological criteria in the evaluation of liver involvement in chronic hepatitis C. Rom J Intern Med. 2006;44(2):117-130.

McCaughan GW, McGuinness PH, Bishop GA, et al. Clinical assessment and incidence of hepatitis C RNA in 50 consecutive RIBA-positive volunteer blood donors. Med J Aust. 1992;157(4):231-233. doi:10.5694/j.1326-5377.1992.tb137124.x

McGovern BH, Birch CE, Bowen MJ, et al. Improving the diagnosis of acute hepatitis C virus infection with expanded viral load criteria. Clin Infect Dis. 2009;49(7):1051-1060. doi:10.1086/605561

McHutchison JG, Gordon SC, Schiff ER, et al. Interferon alfa-2b alone or in combination with ribavirin as initial treatment for chronic hepatitis C. Hepatitis Interventional Therapy Group. N Engl J Med. 1998;339(21):1485-1492. doi:10.1056/NEJM199811193392101

Micallef JM, Kaldor JM, Dore GJ. Spontaneous viral clearance following acute hepatitis C infection: a systematic review of longitudinal studies. Journal of Viral Hepatitis. 2006;13(1):34-41. doi:10.1111/j.1365-2893.2005.00651.x

Miller RH, Purcell RH. Hepatitis C virus shares amino acid sequence similarity with pestiviruses and flaviviruses as well as members of two plant virus supergroups. Proc Natl Acad Sci U S A. 1990;87(6):2057-2061.

MIQE Guidelines: Minimum Information for Publication of Quantitative Real-Time PCR Experiments | Clinical Chemistry | Oxford Academic.

Mocellin S, Rossi CR, Pilati P, Nitti D, Marincola FM. Quantitative real-time PCR: a powerful ally in cancer research. Trends Mol Med. 2003;9(5):189-195. doi:10.1016/s1471-4914(03)00047-9

Mohamadnejad M, Pourshams A, Malekzadeh R, et al. Healthy ranges of serum alanine aminotransferase levels in Iranian blood donors. World J Gastroenterol. 2003;9(10):2322-2324. doi:10.3748/wjg.v9.i10.2322

Mohd Hanafiah K, Groeger J, Flaxman AD, Wiersma ST. Global epidemiology of hepatitis C virus infection: new estimates of age-specific antibody to HCV seroprevalence. Hepatology. 2013;57(4):1333-1342. doi:10.1002/hep.26141

Moradpour D, Brass V, Bieck E, et al. Membrane Association of the RNA-Dependent RNA Polymerase Is Essential for Hepatitis C Virus RNA Replication. J Virol. 2004;78(23):13278-13284. doi:10.1128/JVI.78.23.13278-13284.2004

Morikawa K, Lange CM, Gouttenoire J, et al. Nonstructural protein 3-4A: the Swiss army knife of hepatitis C virus. J Viral Hepat. 2011;18(5):305-315. doi:10.1111/j.1365-2893.2011.01451.x

Morin TJ, Broering TJ, Leav BA, et al. Human Monoclonal Antibody HCV1 Effectively Prevents and Treats HCV Infection in Chimpanzees. PLOS Pathogens. 2012;8(8):e1002895. doi:10.1371/journal.ppat.1002895

Muerhoff AS, Leary TP, Simons JN, et al. Genomic organization of GB viruses A and B: two new members of the Flaviviridae associated with GB agent hepatitis. J Virol. 1995;69(9):5621-5630. doi:10.1128/JVI.69.9.5621-5630.1995

Mullis K, Faloona F, Scharf S, Saiki R, Horn G, Erlich H. Specific enzymatic amplification of DNA in vitro: the polymerase chain reaction. Cold Spring Harb Symp Quant Biol. 1986;51 Pt 1:263-273. doi:10.1101/sqb.1986.051.01.032

Murphy DG, Sablon E, Chamberland J, Fournier E, Dandavino R, Tremblay CL. Hepatitis C virus genotype 7, a new genotype originating from central Africa. J Clin Microbiol. 2015;53(3):967-972. doi:10.1128/JCM.02831-14

N. Gurumani, "An Introduction to Biostatistics," MJP Publishers, Chennai, 2005

Nafishah A, Asiah MN, Syimah ATN, et al. Rate of Seroconversion in Repeat Blood Donors at The National Blood Centre, Kuala Lumpur. Indian J Hematol Blood Transfus. 2014;30(2):105-110. doi:10.1007/s12288-012-0213-4

Nakano T, Lau GMG, Lau GML, Sugiyama M, Mizokami M. An updated analysis of hepatitis C virus genotypes and subtypes based on the complete coding region. Liver Int. 2012;32(2):339-345. doi:10.1111/j.1478-3231.2011.02684.x

Narberhaus F, Waldminghaus T, Chowdhury S. RNA thermometers. FEMS Microbiol Rev. 2006;30(1):3-16. doi:10.1111/j.1574-6976.2005.004.x

NCBI Resource Coordinators. Database resources of the National Center for Biotechnology Information. Nucleic Acids Res. 2013;41(Database issue):D8-D20. doi:10.1093/nar/gks1189

Ndongo N, Berthillon P, Pradat P, et al. Association of anti-E1E2 antibodies with spontaneous recovery or sustained viral response to therapy in patients infected with hepatitis C virus. Hepatology. 2010;52(5):1531-1542. doi:10.1002/hep.23862

Nelson PK, Mathers BM, Cowie B, et al. Global epidemiology of hepatitis B and hepatitis C in people who inject drugs: results of systematic reviews. Lancet. 2011;378(9791):571-583. doi:10.1016/S0140-6736(11)61097-0

Neumaier M, Braun A, Wagener C. Fundamentals of quality assessment of molecular amplification methods in clinical diagnostics. International Federation of Clinical Chemistry Scientific Division Committee on Molecular Biology Techniques. Clin Chem. 1998;44(1):12-26.

Neumann AU, Lam NP, Dahari H, et al. Hepatitis C viral dynamics in vivo and the antiviral efficacy of interferon-alpha therapy. Science. 1998;282(5386):103-107. doi:10.1126/science.282.5386.103

Nielsen SU, Bassendine MF, Burt AD, Bevitt DJ, Toms GL. Characterization of the genome and structural proteins of hepatitis C virus resolved from infected human liver. J Gen Virol. 2004;85(Pt 6):1497-1507. doi:10.1099/vir.0.79967-0

NIH, Management of Hepatitis C: 2002, June 10-12, 2002

nMaster software - https://www.cmc-biostatistics.ac.in/nmaster/

Noiri E, Nakao A, Oya A, Fujita T, Kimura S. Hepatitis C Virus in Blood and Dialysate in Hemodialysis. American Journal of Kidney Diseases. 2001;37(1):38-42. doi:10.1053/ajkd.2001.20630

Nolte FS. Hepatitis C virus genotyping: clinical implications and methods. Mol Diagn. 2001;6(4):265-277. doi:10.1054/modi.2001.29157

Ogasawara O, Kodama Y, Mashima J, Kosuge T, Fujisawa T. DDBJ Database updates and computational infrastructure enhancement. Nucleic Acids Research. 2020;48(D1):D45-D50. doi:10.1093/nar/gkz982

Okamoto H, Okada S, Sugiyama Y, et al. Detection of hepatitis C virus RNA by a two-stage polymerase chain reaction with two pairs of primers deduced from the 5'-noncoding region. Jpn J Exp Med. 1990;60(4):215-222.

Orland JR, Wright TL, Cooper S. Acute hepatitis C. Hepatology. 2001;33(2):321-327. doi:10.1053/jhep.2001.22112

Ortho Clinical Diagnostics. aHCV reagent pack, Procedure manual, Version 4.0. Vitros ECi Immunochemistry autoanalyzer, USA, 2005.

Osburn WO, Snider AE, Wells BL, et al. Clearance of hepatitis C infection is associated with the early appearance of broad neutralizing antibody responses. Hepatology. 2014;59(6):2140-2151. doi:10.1002/hep.27013

Ottiger C, Gygli N, Huber AR. Detection limit of architect hepatitis C core antigen assay in correlation with HCV RNA, and renewed confirmation algorithm for reactive anti-HCV samples. J Clin Virol. 2013;58(3):535-540. doi:10.1016/j.jcv.2013.08.028

Otto GA, Puglisi JD. The pathway of HCV IRES-mediated translation initiation. Cell. 2004;119(3):369-380. doi:10.1016/j.cell.2004.09.038

Panigrahi AK, Panda SK, Dixit RK, et al. Magnitude of hepatitis C virus infection in India: prevalence in healthy blood donors, acute and chronic liver diseases. J Med Virol. 1997;51(3):167-174.

Papatheodoridis GV, Tsochatzis E, Hardtke S, Wedemeyer H. Barriers to care and treatment for patients with chronic viral hepatitis in Europe: a systematic review. Liver Int. 2014;34(10):1452-1463. doi:10.1111/liv.12565

Park JS, Yang JM, Min MK. Hepatitis C virus nonstructural protein NS4B transforms NIH3T3 cells in cooperation with the Ha-ras oncogene. Biochem Biophys Res Commun. 2000;267(2):581-587. doi:10.1006/bbrc.1999.1999

Paul D, Madan V, Bartenschlager R. Hepatitis C virus RNA replication and assembly: living on the fat of the land. Cell Host Microbe. 2014;16(5):569-579. doi:10.1016/j.chom.2014.10.008

Pawlotsky JM, Bouvier-Alias M, Hezode C, Darthuy F, Remire J, Dhumeaux D. Standardization of hepatitis C virus RNA quantification. Hepatology. 2000;32(3):654-659. doi:10.1053/jhep.2000.16603

Pawlotsky JM, McHutchison JG. Hepatitis C. Development of new drugs and clinical trials: Promises and pitfalls. Summary of an AASLD hepatitis single topic conference, Chicago, IL, February 27–March 1, 2003. Hepatology. 2004;39(2):554-567. doi:10.1002/hep.20065

Pawlotsky JM. Molecular diagnosis of viral hepatitis. Gastroenterology. 2002;122(6):1554-1568. doi:10.1053/gast.2002.33428

Pawlotsky JM. New hepatitis C therapies: the toolbox, strategies, and challenges. Gastroenterology. 2014;146(5):1176-1192. doi:10.1053/j.gastro.2014.03.003

Pawlotsky JM. Therapy of hepatitis C: from empiricism to eradication. Hepatology. 2006;43(2 Suppl 1):S207-220. doi:10.1002/hep.21064

Pearlman BL, Ehleben C. Hepatitis C genotype 1 virus with low viral load and rapid virologic response to peginterferon/ribavirin obviates a protease inhibitor. Hepatology. 2014;59(1):71-77. doi:10.1002/hep.26624

Peccoud J, Jacob C. Theoretical uncertainty of measurements using quantitative polymerase chain reaction. Biophys J. 1996;71(1):101-108. doi:10.1016/S0006-3495(96)79205-6

Peirson SN, Butler JN, Foster RG. Experimental validation of novel and conventional approaches to quantitative real-time PCR data analysis. Nucleic Acids Res. 2003;31(14):e73. doi:10.1093/nar/gng073

Pellerin M, Lopez-Aguirre Y, Penin F, Dhumeaux D, Pawlotsky JM. Hepatitis C Virus Quasispecies Variability Modulates Nonstructural Protein 5A Transcriptional Activation, Pointing to Cellular Compartmentalization of Virus-Host Interactions. J Virol. 2004;78(9):4617-4627. doi:10.1128/JVI.78.9.4617-4627.2004

Penin F, Dubuisson J, Rey FA, Moradpour D, Pawlotsky JM. Structural biology of hepatitis C virus. Hepatology. 2004a;39(1):5-19. doi:10.1002/hep.20032

Pfaffl MW, Hageleit M. Validities of mRNA quantification using recombinant RNA and recombinant DNA external calibration curves in real-time RT-PCR. Biotechnology Letters. 2001;23(4):275-282. doi:10.1023/A:1005658330108

Pfaffl MW, Horgan GW, Dempfle L. Relative expression software tool (REST) for group-wise comparison and statistical analysis of relative expression results in real-time PCR. Nucleic Acids Res. 2002;30(9):e36. doi:10.1093/nar/30.9.e36

Pfaffl MW. A new mathematical model for relative quantification in real-time RT-PCR. Nucleic Acids Res. 2001;29(9):e45. doi:10.1093/nar/29.9.e45

Piccininni S, Varaklioti A, Nardelli M, Dave B, Raney KD, McCarthy JEG. Modulation of the hepatitis C virus RNA-dependent RNA polymerase activity by the non-structural (NS) 3 helicase and the NS4B membrane

protein. J Biol Chem. 2002;277(47):45670-45679. doi:10.1074/jbc.M204124200

Pileri P, Uematsu Y, Campagnoli S, et al. Binding of hepatitis C virus to CD81. Science. 1998;282(5390):938-941. doi:10.1126/science.282.5390.938

Piñeiro D, Martinez-Salas E. RNA Structural Elements of Hepatitis C Virus Controlling Viral RNA Translation and the Implications for Viral Pathogenesis. Viruses. 2012;4(10):2233-2250. doi:10.3390/v4102233

Plebani M. Errors in clinical laboratories or errors in laboratory medicine? Clin Chem Lab Med. 2006;44(6):750-759. doi:10.1515/CCLM.2006.123

Pöhlmann S, Zhang J, Baribaud F, et al. Hepatitis C virus glycoproteins interact with DC-SIGN and DC-SIGNR. J Virol. 2003;77(7):4070-4080. doi:10.1128/jvi.77.7.4070-4080.2003

Poordad F, McCone J, Bacon BR, et al. Boceprevir for untreated chronic HCV genotype 1 infection. N Engl J Med. 2011;364(13):1195-1206. doi:10.1056/NEJMoa1010494

Powell KE, Thompson PD, Caspersen CJ, Kendrick JS. Physical activity and the incidence of coronary heart disease. Annu Rev Public Health. 1987;8:253-287. doi:10.1146/annurev.pu.08.050187.001345

Poynard T, Leroy V, Cohard M, et al. Meta-analysis of interferon randomized trials in the treatment of viral hepatitis C: effects of dose and duration. Hepatology. 1996;24(4):778-789. doi:10.1002/hep.510240405

Prati D, Taioli E, Zanella A, et al. Updated definitions of healthy ranges for serum alanine aminotransferase levels. Ann Intern Med. 2002;137(1):1-10. doi:10.7326/0003-4819-137-1-200207020-00006

Price H, Gilson R, Mercey D, et al. Hepatitis C in men who have sex with men in London – a community survey. HIV Med. 2013;14(9):578-580. doi:10.1111/hiv.12050

Puoti C, Castellacci R, Montagnese F. Hepatitis C virus carriers with persistently normal aminotransferase levels: healthy people or true patients? Dig Liver Dis. 2000;32(7):634-643. doi:10.1016/s1590-8658(00)80850-6

QIAamp viral RNA mini handbook. Third edition. Qiagen, Germany. 2012.

Quaranta JF, Delaney SR, Alleman S, Cassuto JP, Dellamonica P, Allain JP. Prevalence of antibody to hepatitis C virus (HCV) in HIV-1-infected patients (nice SEROCO cohort). J Med Virol. 1994;42(1):29-32. doi:10.1002/jmv.1890420106

Rådström P, Knutsson R, Wolffs P, Dahlenborg M, Löfström C. Pre-PCR processing of samples. Methods in molecular biology (Clifton, NJ). 2003;216:31-50.

Rådström P, Knutsson R, Wolffs P, Lövenklev M, Löfström C. Pre-PCR processing: strategies to generate PCR-compatible samples. Mol Biotechnol. 2004;26(2):133-146. doi:10.1385/MB:26:2:133

Ramakers C, Ruijter JM, Deprez RHL, Moorman AFM. Assumption-free analysis of quantitative real-time polymerase chain reaction (PCR) data. Neurosci Lett. 2003;339(1):62-66. doi:10.1016/s0304-3940(02)01423-4

Rao X, Lai D, Huang X. A New Method for Quantitative Real-Time Polymerase Chain Reaction Data Analysis. J Comput Biol. 2013;20(9):703-711. doi:10.1089/cmb.2012.0279

Rasmussen R. Quantification on the LightCycler. In: Meuer S, Wittwer C, Nakagawara KI, eds. Rapid Cycle Real-Time PCR: Methods and Applications. Springer; 2001:21-34. doi:10.1007/978-3-642-59524-0_3

Rauch A, Rickenbach M, Weber R, et al. Unsafe sex and increased incidence of hepatitis C virus infection among HIV-infected men who have sex with men: the Swiss HIV Cohort Study. Clin Infect Dis. 2005;41(3):395-402. doi:10.1086/431486

Recommendations for Testing, Managing, and Treating Hepatitis C | HCV Guidance. Accessed June 18, 2022. https://www.hcvguidelines.org/

Reilly AA, Salkin IF, McGinnis MR, et al. Evaluation of mycology laboratory proficiency testing. J Clin Microbiol. 1999;37(7):2297-2305. doi:10.1128/JCM.37.7.2297-2305.1999

Reiter M, Kirchner B, Muller H, Holzhauer C, Mann W, Pfaffl MW. Quantification noise in single cell experiments. Nucleic Acids Research. 2011;39(18):e124-e124. doi:10.1093/nar/gkr505

Remans T, Keunen E, Bex GJ, Smeets K, Vangronsveld J, Cuypers A. Reliable Gene Expression Analysis by Reverse Transcription-Quantitative PCR: Reporting and Minimizing the Uncertainty in Data Accuracy. The Plant Cell. 2014;26(10):3829-3837. doi:10.1105/tpc.114.130641

Reynolds JE, Kaminski A, Carroll AR, Clarke BE, Rowlands DJ, Jackson RJ. Internal initiation of translation of hepatitis C virus RNA: the ribosome entry site is at the authentic initiation codon. RNA. 1996;2(9):867-878.

Reynolds JE, Kaminski A, Kettinen HJ, et al. Unique features of internal initiation of hepatitis C virus RNA translation. EMBO J. 1995;14(23):6010-6020.

Richter SS. Laboratory Assays for Diagnosis and Management of Hepatitis C Virus Infection. J Clin Microbiol. 2002;40(12):4407-4412. doi:10.1128/JCM.40.12.4407-4412.2002

Richter SS. Laboratory Assays for Diagnosis and Management of Hepatitis C Virus Infection. J Clin Microbiol. 2002;40(12):4407-4412. doi:10.1128/JCM.40.12.4407-4412.2002

Rijnbrand R, Bredenbeek P, van der Straaten T, et al. Almost the entire 5' non-translated region of hepatitis C virus is required for cap-independent translation. FEBS Lett. 1995;365(2-3):115-119. doi:10.1016/0014-5793(95)00458-l

Roy P, Patel A, Lole K, Gupta RM, Kumar A, Hazra S. Prevalence and genotyping pattern of hepatitis C virus among patients on maintenance hemodialysis at five centers in Pune, India. Med J Armed Forces India. 2019;75(1):74-80. doi:10.1016/j.mjafi.2018.08.001

Ruijter JM, Pfaffl MW, Zhao S, et al. Evaluation of qPCR curve analysis methods for reliable biomarker discovery: bias, resolution, precision, and implications. Methods. 2013;59(1):32-46. doi:10.1016/j.ymeth.2012.08.011

Ruijter JM, Ramakers C, Hoogaars W, et al. Amplification Efficiency: Linking Baseline and Bias in the Analysis Of Quantitative PCR Data. Nucleic acids research. 2009;37:e45. doi:10.1093/nar/gkp045

Rutledge RG, Côté C. Mathematics of quantitative kinetic PCR and the application of standard curves. Nucleic Acids Res. 2003;31(16):e93. doi:10.1093/nar/gng093

Rutledge RG, Stewart D. Critical evaluation of methods used to determine amplification efficiency refutes the exponential character of real-time PCR. BMC Molecular Biology. 2008;9(1):96. doi:10.1186/1471-2199-9-96

Rutledge RG. Sigmoidal curve-fitting redefines quantitative real-time PCR with the prospective of developing automated high-throughput applications. Nucleic Acids Res. 2004;32(22):e178. doi:10.1093/nar/gnh177

Saiki RK, Gelfand DH, Stoffel S, et al. Primer-directed enzymatic amplification of DNA with a thermostable DNA polymerase. Science. 1988;239(4839):487-491. doi:10.1126/science.2448875

Saiki RK, Scharf S, Faloona F, et al. Enzymatic amplification of beta-globin genomic sequences and restriction site analysis for diagnosis of sickle cell anemia. Science. 1985;230(4732):1350-1354. doi:10.1126/science.2999980

Saito I, Miyamura T, Ohbayashi A, et al. Hepatitis C virus infection is associated with the development of hepatocellular carcinoma. Proc Natl Acad Sci U S A. 1990;87(17):6547-6549. doi:10.1073/pnas.87.17.6547

Saitou N, Nei M. The neighbor-joining method: a new method for reconstructing phylogenetic trees. Mol Biol Evol. 1987;4(4):406-425. doi:10.1093/oxfordjournals.molbev.a040454

Salminen MO, Carr JK, Burke DS, McCutchan FE. Identification of breakpoints in intergenotypic recombinants of HIV type 1 by bootscanning. AIDS Res Hum Retroviruses. 1995;11(11):1423-1425. doi:10.1089/aid.1995.11.1423

Sambrook J, Fritsch EF, Maniatis T. Molecular cloning: a laboratory manual. Molecular cloning: a laboratory manual. 1989;(Ed. 2). Accessed June 26, 2022. https://www.cabdirect.org/cabdirect/abstract/19901616061

Sanger F, Nicklen S, Coulson AR. DNA sequencing with chain-terminating inhibitors. Proc Natl Acad Sci U S A. 1977;74(12):5463-5467. doi:10.1073/pnas.74.12.5463

Santolini E, Migliaccio G, La Monica N. Biosynthesis and biochemical properties of the hepatitis C virus core protein. J Virol. 1994;68(6):3631-3641.

Santolini E, Pacini L, Fipaldini C, Migliaccio G, Monica N. The NS2 protein of hepatitis C virus is a transmembrane polypeptide. J Virol. 1995;69(12):7461-7471. doi:10.1128/JVI.69.12.7461-7471.1995

Satsangi J, Jewell DP, Welsh K, Bunce M, Bell JI. Effect of heparin on polymerase chain reaction. Lancet. 1994;343(8911):1509-1510. doi:10.1016/s0140-6736(94)92622-0

Saxena R, Thakur V, Sood B, Guptan RC, Gururaja S, Sarin SK. Transfusion-associated hepatitis in a tertiary referral hospital in India. A prospective study. Vox Sang. 1999;77(1):6-10. doi:31067

Sayers EW, Beck J, Brister JR, et al. Database resources of the National Center for Biotechnology Information. Nucleic Acids Res. 2020;48(D1):D9-D16. doi:10.1093/nar/gkz899

Scarselli E, Ansuini H, Cerino R, et al. The human scavenger receptor class B type I is a novel candidate receptor for the hepatitis C virus. EMBO J. 2002;21(19):5017-5025. doi:10.1093/emboj/cdf529

Scheinmann R, Hagan H, Lelutiu-Weinberger C, et al. Non-injection drug use and Hepatitis C Virus: a systematic review. Drug Alcohol Depend. 2007;89(1):1-12. doi:10.1016/j.drugalcdep.2006.11.014

Schmidt-Mende J, Bieck E, Hugle T, et al. Determinants for membrane association of the hepatitis C virus RNA-dependent RNA polymerase. J Biol Chem. 2001;276(47):44052-44063. doi:10.1074/jbc.M103358200

Schrader C, Schielke A, Ellerbroek L, Johne R. PCR inhibitors - occurrence, properties and removal. J Appl Microbiol. 2012;113(5):1014-1026. doi:10.1111/j.1365-2672.2012.05384.x

Schreiber J, McNally J, Chodavarapu K, Svarovskaia E, Moreno C. Treatment of a patient with genotype 7 hepatitis C virus infection with sofosbuvir and velpatasvir. Hepatology. 2016;64(3):983-985. doi:10.1002/hep.28636

Schwer B, Ren S, Pietschmann T, et al. Targeting of Hepatitis C Virus Core Protein to Mitochondria through a Novel C-Terminal Localization Motif. J Virol. 2004;78(15):7958-7968. doi:10.1128/JVI.78.15.7958-7968.2004

Scott JD, McMahon BJ, Bruden D, et al. High rate of spontaneous negativity for hepatitis C virus RNA after establishment of chronic infection in Alaska Natives. Clin Infect Dis. 2006;42(7):945-952. doi:10.1086/500938

Seeff LB. Natural history of hepatitis C. Hepatology. 1997;26(S3):21S-28S. doi:10.1002/hep.510260704

Selby MJ, Choo QL, Berger K, et al. Expression, identification and subcellular localization of the proteins encoded by the hepatitis C viral genome. J Gen Virol. 1993;74 (Pt 6):1103-1113. doi:10.1099/0022-1317-74-6-1103

Shahangian S. Proficiency testing in laboratory medicine: uses and limitations. Arch Pathol Lab Med. 1998;122(1):15-30.

Shepard CW, Finelli L, Alter MJ. Global epidemiology of hepatitis C virus infection. Lancet Infect Dis. 2005;5(9):558-567. doi:10.1016/S1473-3099(05)70216-4

Sherman KE, Rouster SD, Chung RT, Rajicic N. Hepatitis C Virus prevalence among patients infected with Human Immunodeficiency Virus: a cross-sectional analysis of the US adult AIDS Clinical Trials Group. Clin Infect Dis. 2002;34(6):831-837. doi:10.1086/339042

Sherman M. Chronic Hepatitis C and Screening for Hepatocellular Carcinoma. Clinics in Liver Disease. 2006;10(4):735-752. doi:10.1016/j.cld.2006.08.010

Shiffman ML, Diago M, Tran A, et al. Chronic hepatitis C in patients with persistently normal alanine transaminase levels. Clin Gastroenterol Hepatol. 2006;4(5):645-652. doi:10.1016/j.cgh.2006.02.002

Shimakami T, Hijikata M, Luo H, et al. Effect of interaction between hepatitis C virus NS5A and NS5B on hepatitis C virus RNA replication with the hepatitis C virus replicon. J Virol. 2004;78(6):2738-2748. doi:10.1128/jvi.78.6.2738-2748.2004

Shindoh J, Hasegawa K, Matsuyama Y, et al. Low hepatitis C viral load predicts better long-term outcomes in patients undergoing resection of hepatocellular carcinoma irrespective of serologic eradication of hepatitis C virus. J Clin Oncol. 2013;31(6):766-773. doi:10.1200/JCO.2012.44.3234

Siepel AC, Halpern AL, Macken C, Korber BT. A computer program designed to screen rapidly for HIV type 1 intersubtype recombinant sequences. AIDS Res Hum Retroviruses. 1995;11(11):1413-1416. doi:10.1089/aid.1995.11.1413

Sievert W, Altraif I, Razavi HA, et al. A systematic review of hepatitis C virus epidemiology in Asia, Australia and Egypt. Liver Int. 2011;31 Suppl 2:61-80. doi:10.1111/j.1478-3231.2011.02540.x

Sievert W. Management issues in chronic viral hepatitis: hepatitis C. J Gastroenterol Hepatol. 2002;17(4):415-422. doi:10.1046/j.1440-1746.2002.02725.x

Simmonds P, Bukh J, Combet C, et al. Consensus proposals for a unified system of nomenclature of hepatitis C virus genotypes. Hepatology. 2005;42(4):962-973. doi:10.1002/hep.20819

Simmonds P, McOmish F, Yap PL, et al. Sequence variability in the 5′ non-coding region of hepatitis C virus: identification of a new virus type and restrictions on sequence diversity. Journal of General Virology. 74(4):661-668. doi:10.1099/0022-1317-74-4-661

Simmonds P. Genetic diversity and evolution of hepatitis C virus--15 years on. J Gen Virol. 2004;85(Pt 11):3173-3188. doi:10.1099/vir.0.80401-0

Singh S, Dwivedi SN, Sood R, Wali JP. Hepatitis B, C and human immunodeficiency virus infections in multiply-injected kala-azar patients in Delhi. Scand J Infect Dis. 2000;32(1):3-6. doi:10.1080/00365540050164137

Smith BD, Morgan RL, Beckett GA, et al. Recommendations for the identification of chronic hepatitis C virus infection among persons born during 1945-1965. MMWR Recomm Rep. 2012;61(RR-4):1-32.

Smith DB, Bukh J, Kuiken C, et al. Expanded classification of hepatitis C virus into 7 genotypes and 67 subtypes: updated criteria and genotype assignment web resource. Hepatology. 2014;59(1):318-327. doi:10.1002/hep.26744

Smith DB, McAllister J, Casino C, Simmonds P. Virus “quasispecies”: making a mountain out of a molehill? J Gen Virol. 1997;78 (Pt 7):1511-1519. doi:10.1099/0022-1317-78-7-1511

Smith RM, Walton CM, Wu CH, Wu GY. Secondary structure and hybridization accessibility of hepatitis C virus 3’-terminal sequences. J Virol. 2002;76(19):9563-9574. doi:10.1128/jvi.76.19.9563-9574.2002

Somi MH, Etemadi J, Ghojazadeh M, et al. Risk Factors of HCV Seroconversion in Hemodialysis Patients in Tabriz, Iran. Hepat Mon. 2014;14(6):e17417. doi:10.5812/hepatmon.17417

Soriano V, Labarga P, Fernández-Montero JV, et al. The changing face of hepatitis C in the new era of direct-acting antivirals. Antiviral Res. 2013;97(1):36-40. doi:10.1016/j.antiviral.2012.10.011

Souazé F, Ntodou-Thomé A, Tran CY, Rostène W, Forgez P. Quantitative RT-PCR: limits and accuracy. Biotechniques. 1996;21(2):280-285. doi:10.2144/96212rr01

Spahn CM, Kieft JS, Grassucci RA, et al. Hepatitis C virus IRES RNA-induced changes in the conformation of the 40s ribosomal subunit. Science. 2001;291(5510):1959-1962. doi:10.1126/science.1058409

Spiess AN, Feig C, Ritz C. Highly accurate sigmoidal fitting of real-time PCR data by introducing a parameter for asymmetry. BMC Bioinformatics. 2008;9(1):221. doi:10.1186/1471-2105-9-221

Strader DB, Wright T, Thomas DL, Seeff LB. Diagnosis, management, and treatment of hepatitis C. Hepatology. 2004;39(4):1147-1171. doi:10.1002/hep.20119

Stuyver L, Wyseur A, van Arnhem W, Hernandez F, Maertens G. Second-generation line probe assay for hepatitis C virus genotyping. J Clin Microbiol. 1996;34(9):2259-2266.

Sulkowski MS, Gardiner DF, Rodriguez-Torres M, et al. Daclatasvir plus Sofosbuvir for Previously Treated or Untreated Chronic HCV Infection. New England Journal of Medicine. 2014;370(3):211-221. doi:10.1056/NEJMoa1306218

Summers M, Booth T, Brockas T, et al. Luminogenic reagent using 3-chloro 4-hydroxy acetanilide to enhance peroxidase/luminol chemiluminescence. Clinical Chemistry 41(S6 Part. 1995;2:73.

Suzuki R, Matsuura Y, Suzuki T, et al. Nuclear localization of the truncated hepatitis C virus core protein with its hydrophobic C terminus deleted. J Gen Virol. 1995;76 (Pt 1):53-61. doi:10.1099/0022-1317-76-1-53

Suzuki R, Sakamoto S, Tsutsumi T, et al. Molecular Determinants for Subcellular Localization of Hepatitis C Virus Core Protein. J Virol. 2005;79(2):1271-1281. doi:10.1128/JVI.79.2.1271-1281.2005

Svec D, Tichopad A, Novosadova V, Pfaffl MW, Kubista M. How good is a PCR efficiency estimate: Recommendations for precise and robust qPCR efficiency assessments. Biomol Detect Quantif. 2015;3:9-16. doi:10.1016/j.bdq.2015.01.005

Tai CL, Chi WK, Chen DS, Hwang LH. The helicase activity associated with hepatitis C virus nonstructural protein 3 (NS3). J Virol. 1996;70(12):8477-8484. doi:10.1128/JVI.70.12.8477-8484.1996

Takamizawa A, Mori C, Fuke I, et al. Structure and organization of the hepatitis C virus genome isolated from human carriers. J Virol. 1991;65(3):1105-1113. doi:10.1128/JVI.65.3.1105-1113.1991

Tamalet C, Colson P, Tissot-Dupont H, et al. Genomic and phylogenetic analysis of hepatitis C virus isolates: a survey of 535 strains circulating in southern France. J Med Virol. 2003;71(3):391-398. doi:10.1002/jmv.10505

Tan SL, Katze MG. How hepatitis C virus counteracts the interferon response: the jury is still out on NS5A. Virology. 2001;284(1):1-12. doi:10.1006/viro.2001.0885

Tanaka T, Kato N, Cho MJ, Shimotohno K. A novel sequence found at the 3' terminus of hepatitis C virus genome. Biochem Biophys Res Commun. 1995;215(2):744-749. doi:10.1006/bbrc.1995.2526

Tanaka T, Kato N, Cho MJ, Sugiyama K, Shimotohno K. Structure of the 3' terminus of the hepatitis C virus genome. J Virol. 1996;70(5):3307-3312. doi:10.1128/JVI.70.5.3307-3312.1996

Tanji Y, Hijikata M, Satoh S, Kaneko T, Shimotohno K. Hepatitis C virus-encoded nonstructural protein NS4A has versatile functions in viral protein processing. J Virol. 1995;69(3):1575-1581.

Taylor LE, Swan T, Mayer KH. HIV coinfection with hepatitis C virus: evolving epidemiology and treatment paradigms. Clin Infect Dis. 2012;55 Suppl 1:S33-42. doi:10.1093/cid/cis367

Tellinghuisen TL, Marcotrigiano J, Gorbalenya AE, Rice CM. The NS5A protein of hepatitis C virus is a zinc metalloprotein. J Biol Chem. 2004;279(47):48576-48587. doi:10.1074/jbc.M407787200

Tellinghuisen TL, Rice CM. Interaction between hepatitis C virus proteins and host cell factors. Curr Opin Microbiol. 2002;5(4):419-427. doi:10.1016/s1369-5274(02)00341-7

TEMIN HM, MIZUTANI S. Viral RNA-dependent DNA Polymerase: RNA-dependent DNA Polymerase in Virions of Rous Sarcoma Virus. Nature. 1970;226(5252):1211-1213. doi:10.1038/2261211a0

Teoh NC, Farrell GC. Management of chronic hepatitis C virus infection: a new era of disease control. Intern Med J. 2004;34(6):324-337. doi:10.1111/j.1445-5994.2004.00615.x

Terrault NA, Dodge JL, Murphy EL, et al. Sexual transmission of hepatitis C virus among monogamous heterosexual couples: the HCV partners study. Hepatology. 2013;57(3):881-889. doi:10.1002/hep.26164

Thakur V, Guptan RC, Arankale V, Sarin SK. Low Specificity of the Third Generation Elisa for HCV Detection in Voluntary Blood Donors in India. EJIFCC. 2003;14(1):27-30.

Thimme R, Oldach D, Chang KM, Steiger C, Ray SC, Chisari FV. Determinants of viral clearance and persistence during acute hepatitis C virus infection. J Exp Med. 2001;194(10):1395-1406. doi:10.1084/jem.194.10.1395

Thomas DL, Astemborski J, Rai RM, et al. The natural history of hepatitis C virus infection: host, viral, and environmental factors. JAMA. 2000;284(4):450-456. doi:10.1001/jama.284.4.450

Thomas DL, Thio CL, Martin MP, et al. Genetic variation in IL28B and spontaneous clearance of hepatitis C virus. Nature. 2009;461(7265):798-801. doi:10.1038/nature08463

Thomas DL, Villano SA, Riester KA, et al. Perinatal transmission of hepatitis C virus from human immunodeficiency virus type 1-infected mothers. Women and Infants Transmission Study. J Infect Dis. 1998;177(6):1480-1488. doi:10.1086/515315

Thomas DL. Global control of hepatitis C: where challenge meets opportunity. Nat Med. 2013;19(7):850-858. doi:10.1038/nm.3184

Thurner C, Witwer C, Hofacker IL, Stadler PF. Conserved RNA secondary structures in Flaviviridae genomes. J Gen Virol. 2004;85(Pt 5):1113-1124. doi:10.1099/vir.0.19462-0

Tichopad A, Didier A, Pfaffl MW. Inhibition of real-time RT-PCR quantification due to tissue-specific contaminants. Mol Cell Probes. 2004;18(1):45-50. doi:10.1016/j.mcp.2003.09.001

Tichopad A, Dilger M, Schwarz G, Pfaffl MW. Standardized determination of real-time PCR efficiency from a single reaction set-up. Nucleic Acids Res. 2003;31(20):e122. doi:10.1093/nar/gng122

Tine' F, Magrin S, Craxi' A, Pagliaro L. Interferon for non-A, non-B chronic hepatitis: A meta-analysis of randomised clinical trials. Journal of Hepatology. 1991;13(2):192-199. doi:10.1016/0168-8278(91)90814-R

Tohme RA, Holmberg SD. Is sexual contact a major mode of hepatitis C virus transmission? Hepatology. 2010;52(4):1497-1505. doi:10.1002/hep.23808

Tong L, Yu W, Chen L, et al. Discovery of Ruzasvir (MK-8408): A Potent, Pan-Genotype HCV NS5A Inhibitor with Optimized Activity against Common Resistance-Associated Polymorphisms. J Med Chem. 2017;60(1):290-306. doi:10.1021/acs.jmedchem.6b01310

Trucchi C, Orsi A, Alicino C, Sticchi L, Icardi G, Ansaldi F. State of the Art, Unresolved Issues, and Future Research Directions in the Fight against Hepatitis C Virus: Perspectives for Screening, Diagnostics of Resistances, and Immunization. J Immunol Res. 2016;2016:1412840. doi:10.1155/2016/1412840

Tseng YT, Sun HY, Chang SY, et al. Seroprevalence of hepatitis virus infection in men who have sex with men aged 18–40 years in Taiwan. Journal of the Formosan Medical Association. 2012;111(8):431-438. doi:10.1016/j.jfma.2011.06.022

Tsukiyama-Kohara K, Iizuka N, Kohara M, Nomoto A. Internal ribosome entry site within hepatitis C virus RNA. J Virol. 1992;66(3):1476-1483. doi:10.1128/JVI.66.3.1476-1483.1992

Tu H, Gao L, Shi ST, et al. Hepatitis C virus RNA polymerase and NS5A complex with a SNARE-like protein. Virology. 1999;263(1):30-41. doi:10.1006/viro.1999.9893

Uyttendaele S, Claeys H, Mertens W, Verhaert H, Vermylen C. Evaluation of Third-Generation Screening and Confirmatory Assays for HCV Antibodies. Vox Sanguinis. 1994;66(2):122-129. doi:10.1111/j.1423-0410.1994.tb00293.x

Valadez JJ, Berendes S, Jeffery C, et al. Filling the Knowledge Gap: Measuring HIV Prevalence and Risk Factors among Men Who Have Sex with Men and Female Sex Workers in Tripoli, Libya. PLoS One. 2013;8(6):e66701. doi:10.1371/journal.pone.0066701

Van der Graaf PH, Schoemaker RC. Analysis of asymmetry of agonist concentration-effect curves. J Pharmacol Toxicol Methods. 1999;41(2-3):107-115. doi:10.1016/s1056-8719(99)00026-x

van der Helm J, Geskus R, Sabin C, et al. Effect of HCV infection on cause-specific mortality after HIV seroconversion, before and after 1997. Gastroenterology. 2013;144(4):751-760.e2. doi:10.1053/j.gastro.2012.12.026

van der Poel CL, Cuypers HT, Reesink HW. Hepatitis C virus six years on. Lancet. 1994;344(8935):1475-1479. doi:10.1016/s0140-6736(94)90293-3

Vandelli C, Renzo F, Romanò L, et al. Lack of evidence of sexual transmission of hepatitis C among monogamous couples: results of a 10-year prospective follow-up study. Am J Gastroenterol. 2004;99(5):855-859. doi:10.1111/j.1572-0241.2004.04150.x

Walewski JL, Keller TR, Stump DD, Branch AD. Evidence for a new hepatitis C virus antigen encoded in an overlapping reading frame. RNA. 2001;7(5):710-721.

Walker CM, Grakoui A. Hepatitis C virus: why do we need a vaccine to prevent a curable persistent infection? Curr Opin Immunol. 2015;35:137-143. doi:10.1016/j.coi.2015.06.010

Walker CM. Designing an HCV vaccine: a unique convergence of prevention and therapy? Curr Opin Virol. 2017;23:113-119. doi:10.1016/j.coviro.2017.03.014

Wallace P, McCulloch E. Quality Assurance in the Clinical Virology Laboratory. Encyclopedia of Virology. Published online 2021:64-81. doi:10.1016/B978-0-12-814515-9.00132-6

Wang C, Gale M, Keller BC, et al. Identification of FBL2 as a geranylgeranylated cellular protein required for hepatitis C virus RNA replication. Mol Cell. 2005a;18(4):425-434. doi:10.1016/j.molcel.2005.04.004

Wang C, Le SY, Ali N, Siddiqui A. An RNA pseudoknot is an essential structural element of the internal ribosome entry site located within the hepatitis C virus 5’ noncoding region. RNA. 1995;1(5):526-537.

Wang C, Sarnow P, Siddiqui A. Translation of human hepatitis C virus RNA in cultured cells is mediated by an internal ribosome-binding mechanism. J Virol. 1993;67(6):3338-3344. doi:10.1128/JVI.67.6.3338-3344.1993

Wasley A, Alter MJ. Epidemiology of hepatitis C: geographic differences and temporal trends. Semin Liver Dis. 2000;20(1):1-16. doi:10.1055/s-2000-9506

Watashi K, Ishii N, Hijikata M, et al. Cyclophilin B is a functional regulator of hepatitis C virus RNA polymerase. Mol Cell. 2005;19(1):111-122. doi:10.1016/j.molcel.2005.05.014

Weck K. Molecular methods of hepatitis C genotyping. Expert Rev Mol Diagn. 2005;5(4):507-520. doi:10.1586/14737159.5.4.507

Weiner AJ, Brauer MJ, Rosenblatt J, et al. Variable and hypervariable domains are found in the regions of HCV corresponding to the flavivirus envelope and NS1 proteins and the pestivirus envelope glycoproteins. Virology. 1991;180(2):842-848. doi:10.1016/0042-6822(91)90104-J

Weiner AJ, Kuo G, Bradley DW, et al. Detection of hepatitis C viral sequences in non-A, non-B hepatitis. Lancet. 1990;335(8680):1-3. doi:10.1016/0140-6736(90)90134-q

Welker MW, Zeuzem S. Occult hepatitis C: How convincing are the current data? Hepatology. 2009;49(2):665-675. doi:10.1002/hep.22706

Welzel TM, Nelson DR, Morelli G, et al. Effectiveness and safety of sofosbuvir plus ribavirin for the treatment of HCV genotype 2 infection: results of the real-world, clinical practice HCV-TARGET study. Gut. 2017;66(10):1844-1852. doi:10.1136/gutjnl-2016-311609

West J, Atherton J, Costelloe SJ, Pourmahram G, Stretton A, Cornes M. Preanalytical errors in medical laboratories: a review of the available methodologies of data collection and analysis. Ann Clin Biochem. 2017;54(1):14-19. doi:10.1177/0004563216669384

Westgard JO. Use and interpretation of common statistical tests in method comparison studies. Clin Chem. 2008;54(3):612. doi:10.1373/clinchem.2007.094060

Westgard, J. O. 2008. Basic method validation, 3rd ed. Westgard QC, Inc., Madison, WI.

Wittwer CT, Herrmann MG, Moss AA, Rasmussen RP. Continuous fluorescence monitoring of rapid cycle DNA amplification. Biotechniques. 1997;22(1):130-131, 134-138. doi:10.2144/97221bi01

World Health Organization Expert Committee on Biological Standardization. 1995. Glossary of terms for biological substances used for texts of the requirements. WHO unpublished document BS/95.1793. World Health Organization, Geneva, Switzerland.

World Health Organization; 2012. Blood donor selection: guidelines on assessing donor suitability for blood donation. Geneva.

World Health Organization; 2013.Consolidated guidelines on the use of antiretroviral drugs for treating and preventing HIV infection: recommendations for a public health approach. Geneva.

World Health Organization; 2013. Global policy report on the prevention and control of viral hepatitis in WHO Member States. Geneva.

World Health Organization; 2012. Guidance on prevention of viral hepatitis B and C among people who inject drugs. Geneva.

World Health Organization; 2012. Handbook for guidelines development. Geneva.

World Health Organization; 2001. Hepatitis C test kit evaluations. Geneva.

World Health Organization; 2010. mhGAP intervention guide for mental, neurological and substance use disorders in non-specialized health settings. Geneva.

World Health Organization; 2008. Universal access to safe blood transfusion. Geneva.

WHO guidelines for the psychosocially assisted pharmacological treatment of opioid dependence. Geneva: World Health Organization; 2009

WHO guidelines on drawing blood: best practices in phlebotomy. Geneva: World Health Organization; 2010.

WHO guidelines on hand hygiene in health care. Geneva: World Health Organization; 2009

World Health Organization. Guidelines for the Screening, Care and Treatment of Persons with Chronic Hepatitis C Infection. World Health Organization; 2016. Accessed June 18, 2022. https://apps.who.int/iris/handle/10665/205035

World Health Organization. Rapid Diagnostic Tests to Detect Hepatitis C Antibody or Antigen. World Health Organization; 2019.

Yamaga AK, Ou JH. Membrane topology of the hepatitis C virus NS2 protein. J Biol Chem. 2002;277(36):33228-33234. doi:10.1074/jbc.M202304200

Yang S, Rothman RE. PCR-based diagnostics for infectious diseases: uses, limitations, and future applications in acute-care settings. Lancet Infect Dis. 2004;4(6):337-348. doi:10.1016/S1473-3099(04)01044-8

Ye J, Wang C, Sumpter R, Brown MS, Goldstein JL, Gale M. Disruption of hepatitis C virus RNA replication through inhibition of host protein geranylgeranylation. Proceedings of the National Academy of Sciences. 2003;100(26):15865-15870. doi:10.1073/pnas.2237238100

Yedidag EN, Koffron AJ, Mueller KH, et al. Acyclovir triphosphate inhibits the diagnostic polymerase chain reaction for cytomegalovirus. Transplantation. 1996;62(2):238-242. doi:10.1097/00007890-199607270-00015

Yi M, Lemon SM. 3′ Nontranslated RNA Signals Required for Replication of Hepatitis C Virus RNA. J Virol. 2003a;77(6):3557-3568. doi:10.1128/JVI.77.6.3557-3568.2003

Yi M, Lemon SM. Structure-function analysis of the 3' stem-loop of hepatitis C virus genomic RNA and its role in viral RNA replication. RNA. 2003b;9(3):331-345. doi:10.1261/rna.2144203

Yokota M, Tatsumi N, Nathalang O, Yamada T, Tsuda I. Effects of heparin on polymerase chain reaction for blood white cells. J Clin Lab Anal. 1999;13(3):133-140. doi:10.1002/(sici)1098-2825(1999)13:3<133::aid-jcla8>3.0.co;2-0

Zambenedetti MR, Pavoni DP, Dallabona AC, et al. Internal control for real-time polymerase chain reaction based on MS2 bacteriophage for RNA viruses diagnostics. Mem Inst Oswaldo Cruz. 2017;112(5):339-347. doi:10.1590/0074-02760160380

Zer Y, Karaoğlan I, Ciçek H, Karağoz ID, Sağlam M. [Evaluation of the patients with low levels of anti-HCV positivity]. Mikrobiyol Bul. 2009;43(1):133-139.

Zeuzem S, Andreone P, Pol S, et al. Telaprevir for retreatment of HCV infection. N Engl J Med. 2011;364(25):2417-2428. doi:10.1056/NEJMoa1013086

Zeuzem S, Buti M, Ferenci P, et al. Efficacy of 24 weeks treatment with peginterferon alfa-2b plus ribavirin in patients with chronic hepatitis C infected with genotype 1 and low pretreatment viremia. J Hepatol. 2006;44(1):97-103. doi:10.1016/j.jhep.2005.10.003

Zeuzem S, Franke A, Lee JH, Herrmann G, Ruster B, Roth WK. Phylogenetic analysis of hepatitis C virus isolates and their correlation to viremia, liver function tests, and histology. Hepatology. 1996;24(5):1003-1009. doi:10.1002/hep.510240505

Zhao S, Fernald RD. Comprehensive algorithm for quantitative real-time polymerase chain reaction. J Comput Biol. 2005;12(8):1047-1064. doi:10.1089/cmb.2005.12.1047

Zhu YZ, Qian XJ, Zhao P, Qi ZT. How hepatitis C virus invades hepatocytes: the mystery of viral entry. World J Gastroenterol. 2014;20(13):3457-3467. doi:10.3748/wjg.v20.i13.3457

Zonaro A, Puoti M, Fiordalisi G, et al. Detection of Serum Hepatitis C Virus RNA in Acute Non-A, Non-B Hepatitis. Journal of Infectious Diseases. 1991;163(4):923-924. doi:10.1093/infdis/163.4.923a

Zuker M, Stiegler P. Optimal computer folding of large RNA sequences using thermodynamics and auxiliary information. Nucleic Acids Res. 1981;9(1):133-148.

Food and Drug Administration. 2001. FDA guidance for industry: bioanalytical method validation. Center for Drug Evaluation and Research, U.S. Department of Health and Human Services, Rockville, MD.

LIST OF PUBLICATIONS

1. Ann M. Joseph, Krishna K. Yathi, Jose Jacob. Analysis of Internal Controls in the matrix of HCV RT-PCR assays showed analytical and pre-analytical influences independent of template concentration. Adv. Biores. Vol 13 [2] March 2022: 36-46**.**